Corrosion Basics in Primary and Secondary Systems of LWRs

Presented at

ATR NSUF User Week June 1, 2009

by Roger W. Staehle

Staehle Consulting
22 Red Fox Road
North Oaks, Minnesota, 55127
USA 55127

E mail: rwstaehle@gmail.com

Office: 651 482 9493
Telefax: 651 484 5735
Mobile: 651 261 9482

Preamble

In order to predict and understand the performance of structural materials, it is necessary to recognize that all materials are chemicals--the surprise is not that they fail, the surprise is that they work.

This presentation is based on the approach that the principal features of chemistry, thermodynamics and kinetics, should underlie the design and operation of nuclear power plants. While configurational design is necessary for achieving functions, this does not assure long life nor freedom from accidental degradation. Responsible design requires sophistication in the integration of both configuration and chemical integrity of materials of construction.

Main concerns in corrosion

1. Release of activated species from surfaces in the primary systems
2. Formation of oxidizing species in primary system due to radiolysis
3. SCC in vessels, piping, tubing
4. FAC in secondary systems
5. Concentration in superheat locations, transformations, boric acid at leaks, hydrazine forms low valence sulfur
6. Deposit accumulation in secondary system

Early failures in nuclear plants in steam generators

Steam generators replaced due to corrosion

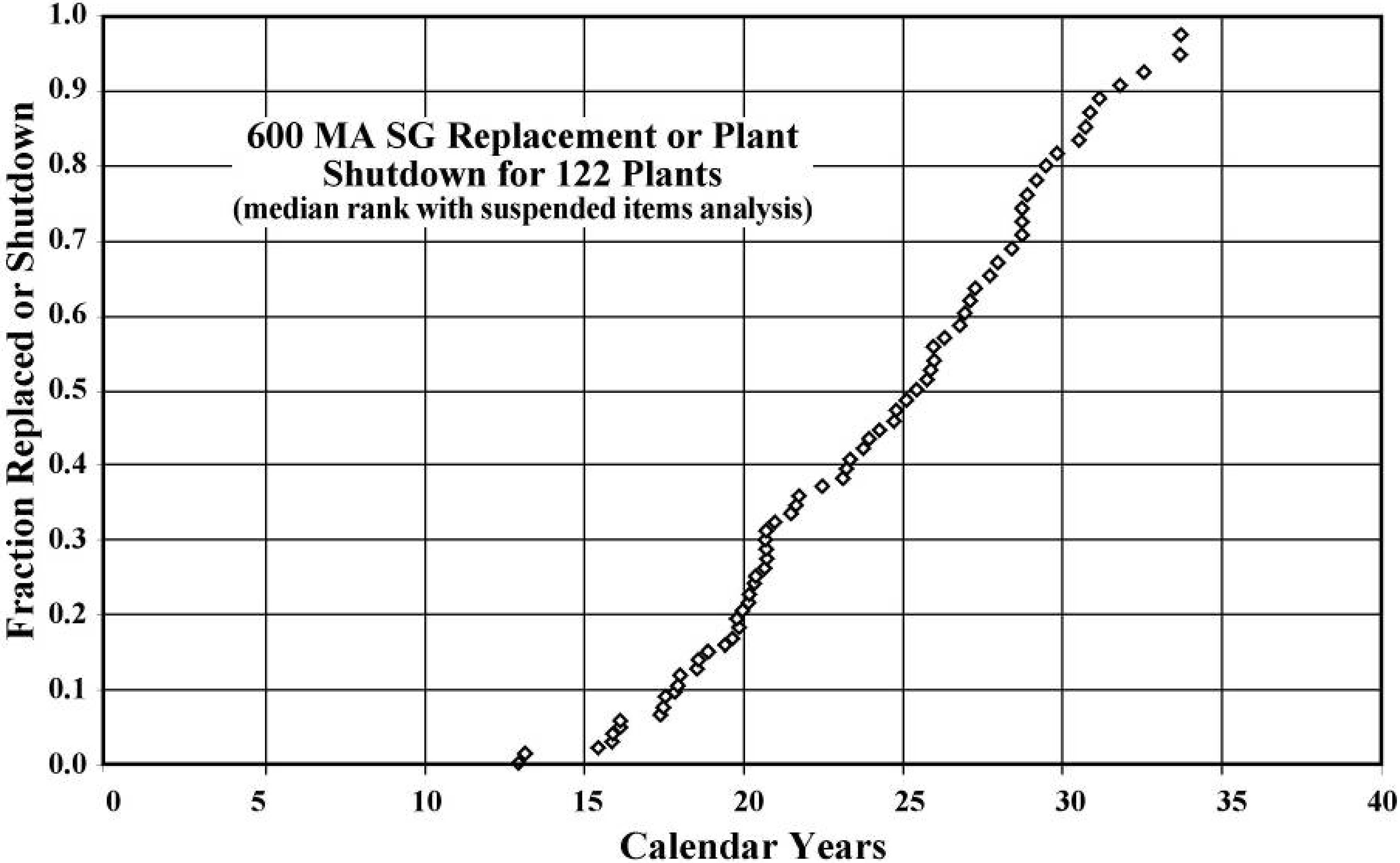

25 mode-location cases of corrosion in steam generators using Alloy 600 with drilled holes

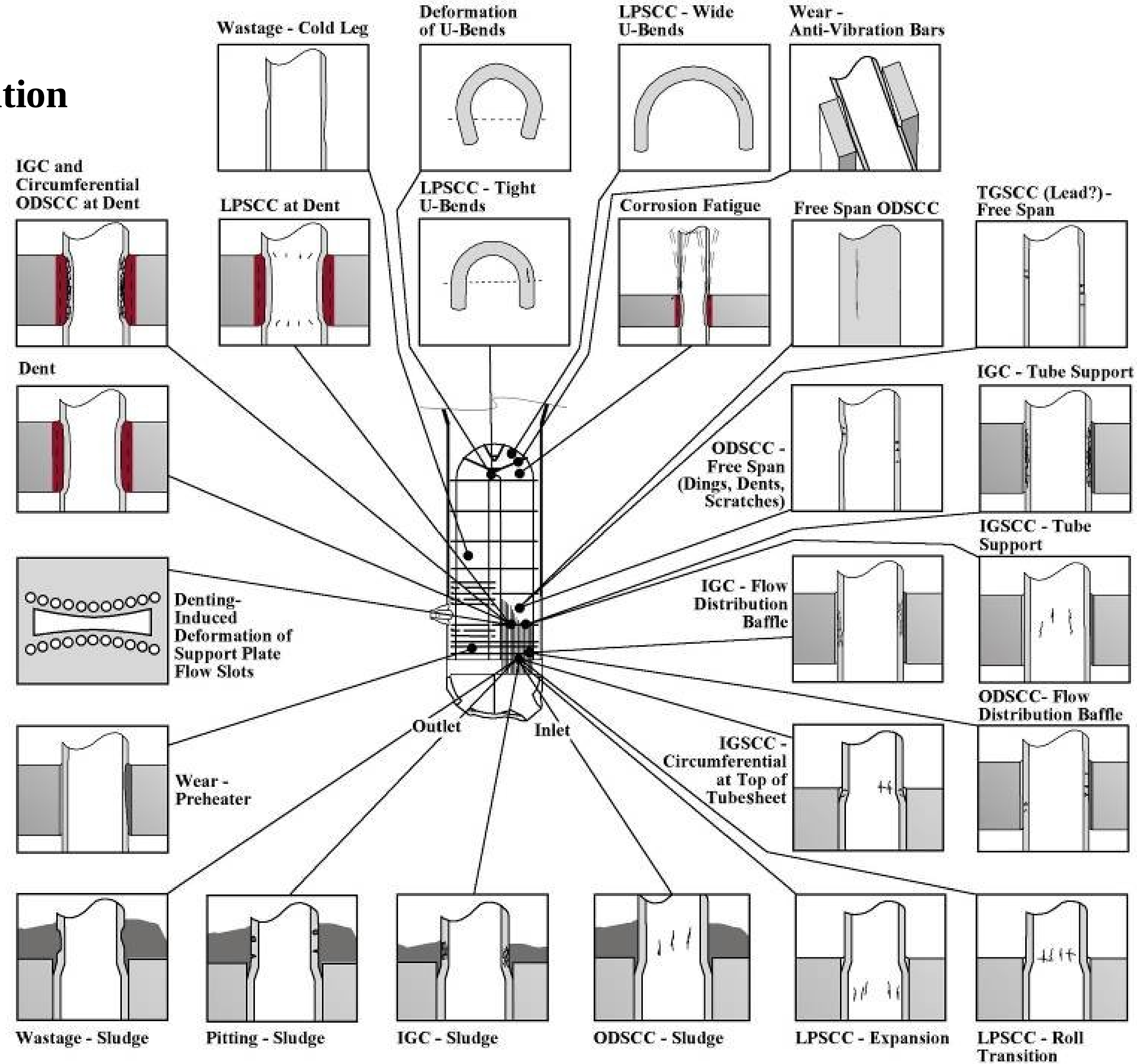

Undetected failure of bi-metallic weldin primary system at nozzle and pipe intersection

SCC at weld of V.C. Summer plant found in 2000

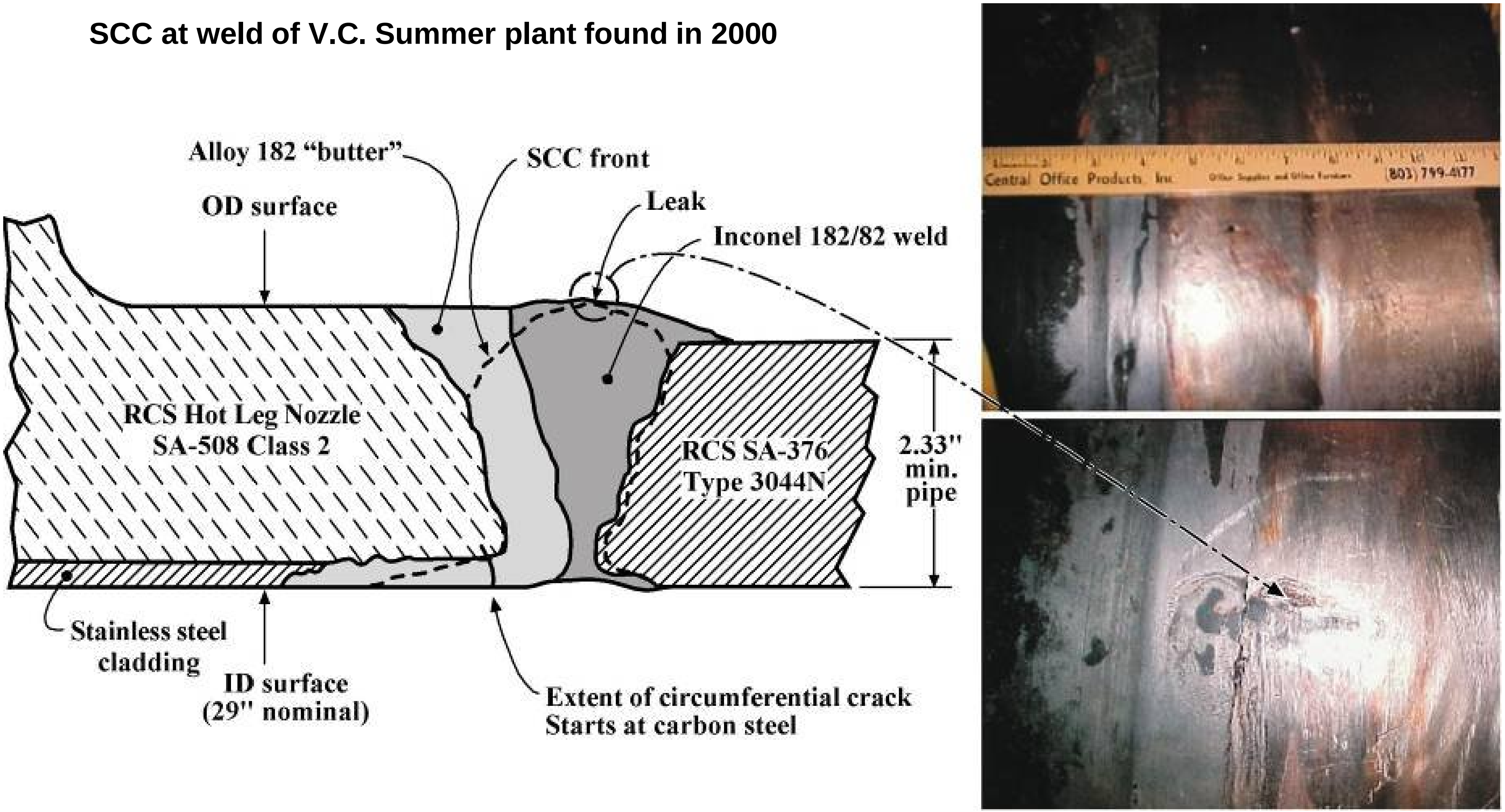

Davis Besse corrosion of pressure vessel head, 2002

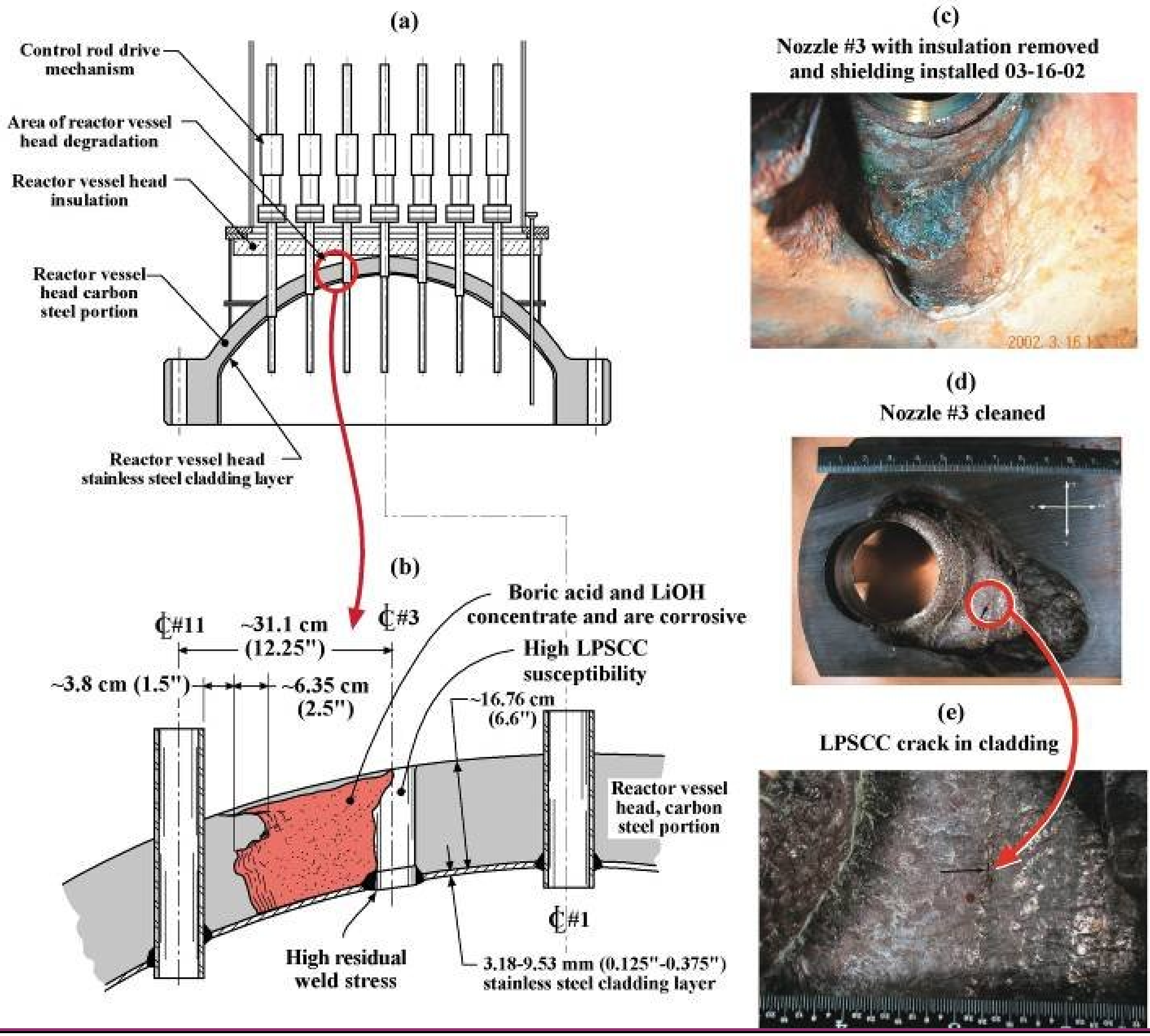

Fewer but larger failures with time

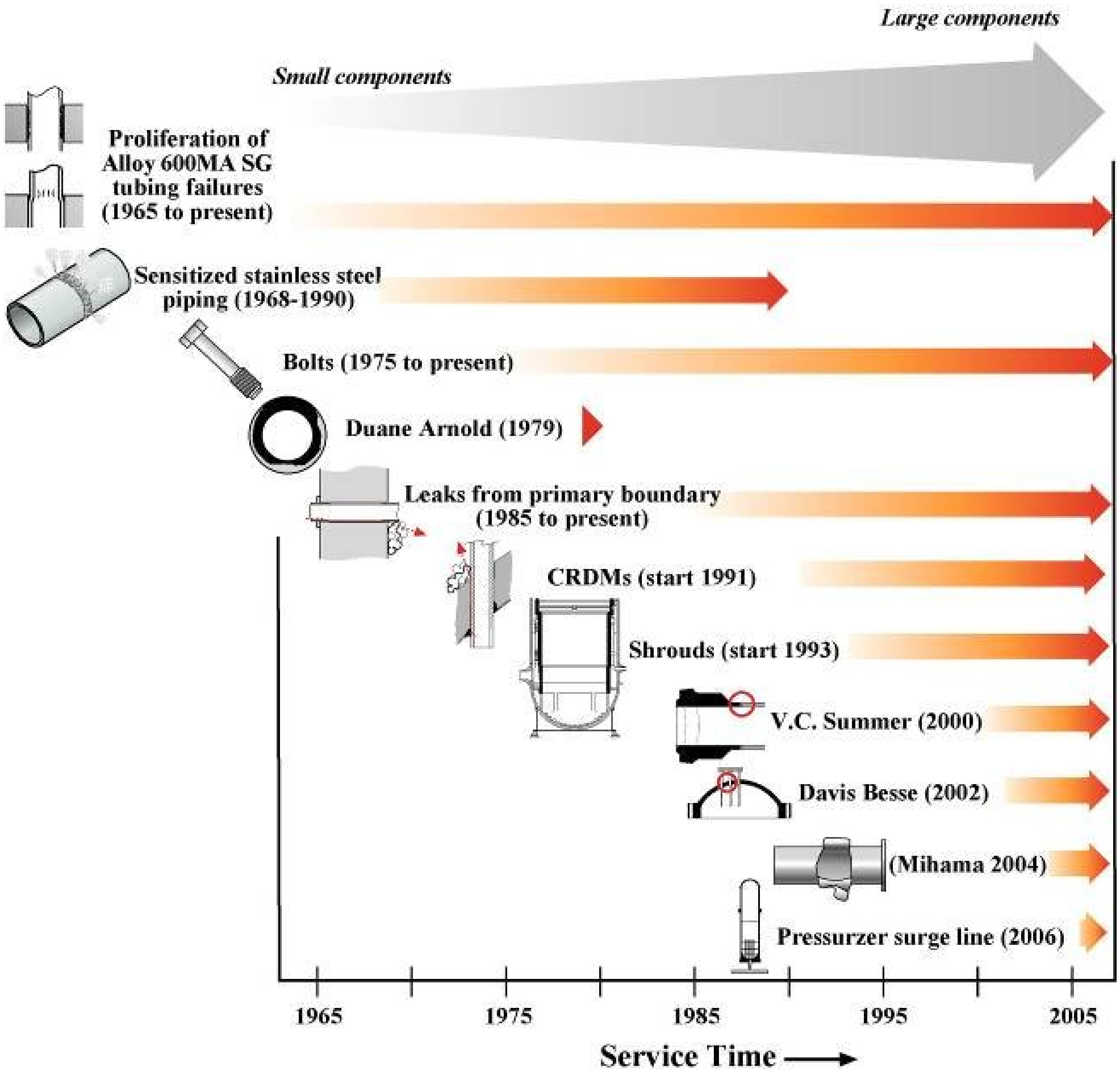

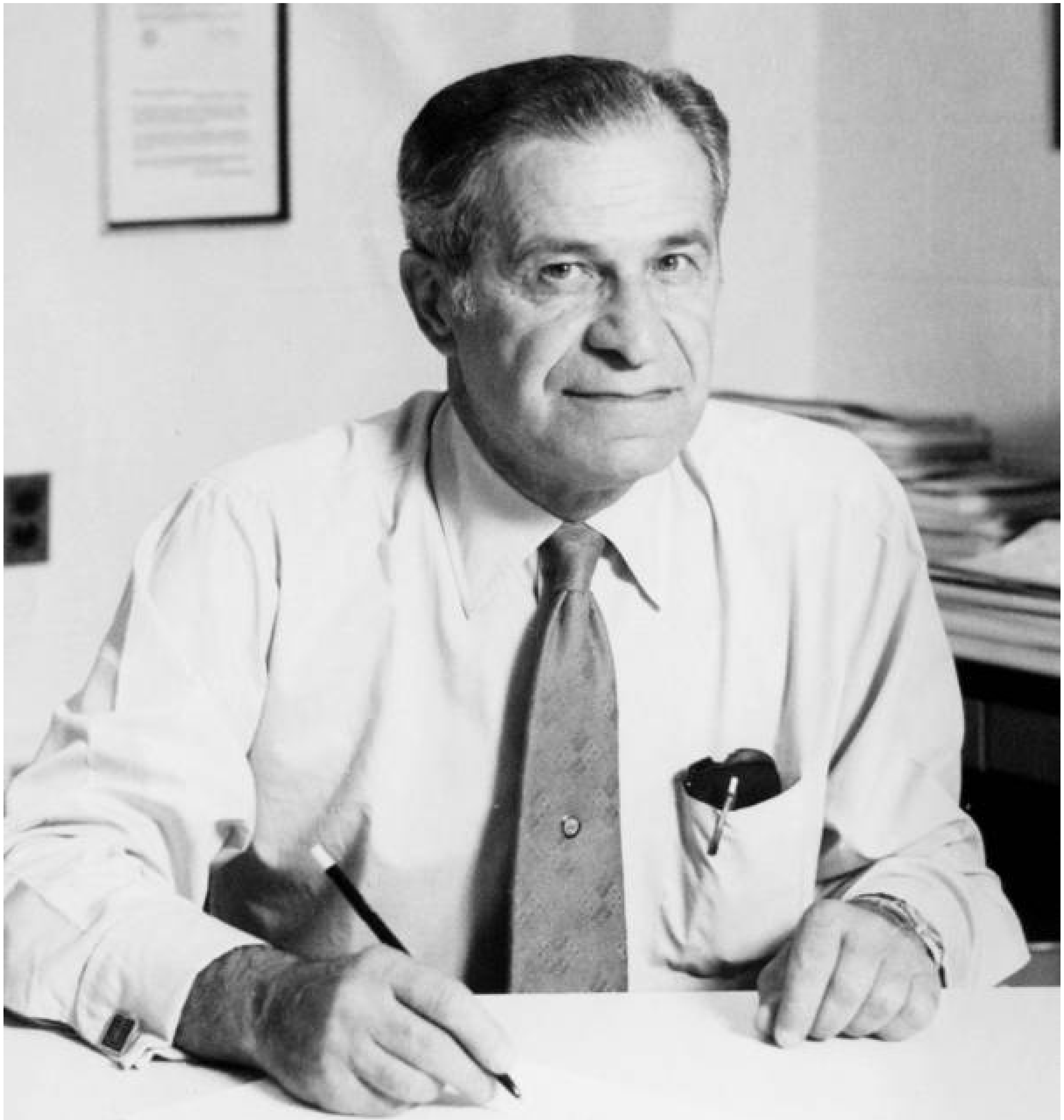

Mars Fontana, Professor and Chairman,
Metallurgical Engineering, The Ohio State University, 1945-1975

Family Tree

John Chipman
(Michigan,
then to MIT)

↓

Mars Fontana, NAE
(Ohio State)

↓

Roger Staehle, NAE
(Ohio State)

↓

Ron Latanision, NAE
(MIT)

↓

Gary Was
(Michigan)

↓

LWR Systems, Materials, Environments

Materials and components in PWRs

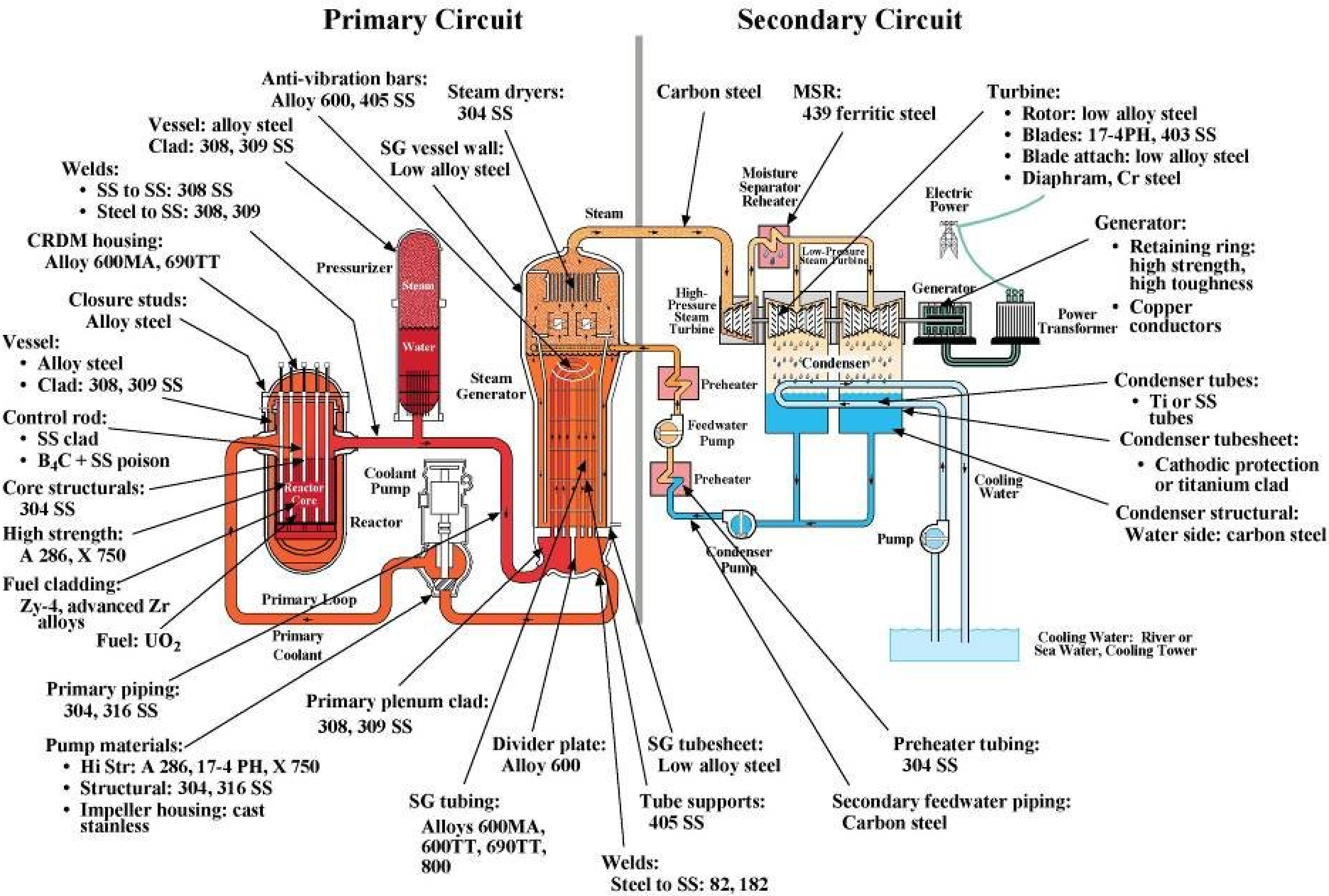

Bulk water chemistry in PWRs

Primary Water Chemistry

Role	Species	Concentration
Burnable poison	H_3BO_3	1500 ppm to zero
pH adjust	LiOH	Adjust to meet 7.1-7.4 pH_T
Minimize radiolytic oxygen	H_2	25-50 STP cc/kg
Oxygen	O_2	< 5 ppb
Corrosion product	Fe, Ni, Co	No spec.
Contaminant	Cl, SO_4, F	Each < 0.15 ppb

Secondary Water Chemistry

Role	Species	Conc., ppb
pH control	NH_3	≈ X
O_2 decrease	N_2H_4	≤ 8xO_2
Leaks	O_2	< 10
Boil off remnant	H_2	≈ 1
Corrosion product	Cu	< 1
	Fe	< 5
Contaminant	Na	< 5
	Cl_2	< 10
	SO_4	< 10

Bulk PWR Environments:
Water Chemistry, Stress, Thermal, Radiation

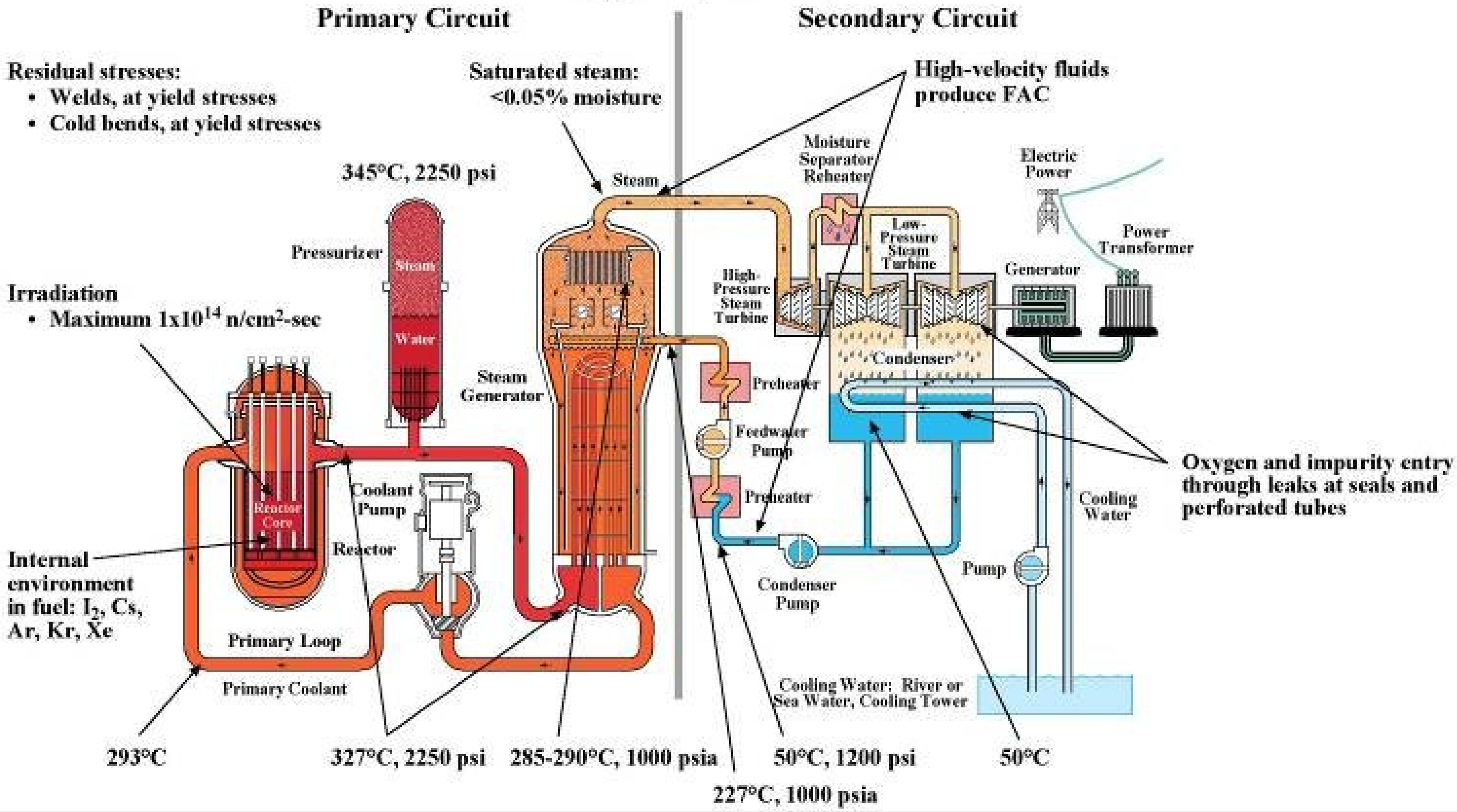

BWR Components and Materials

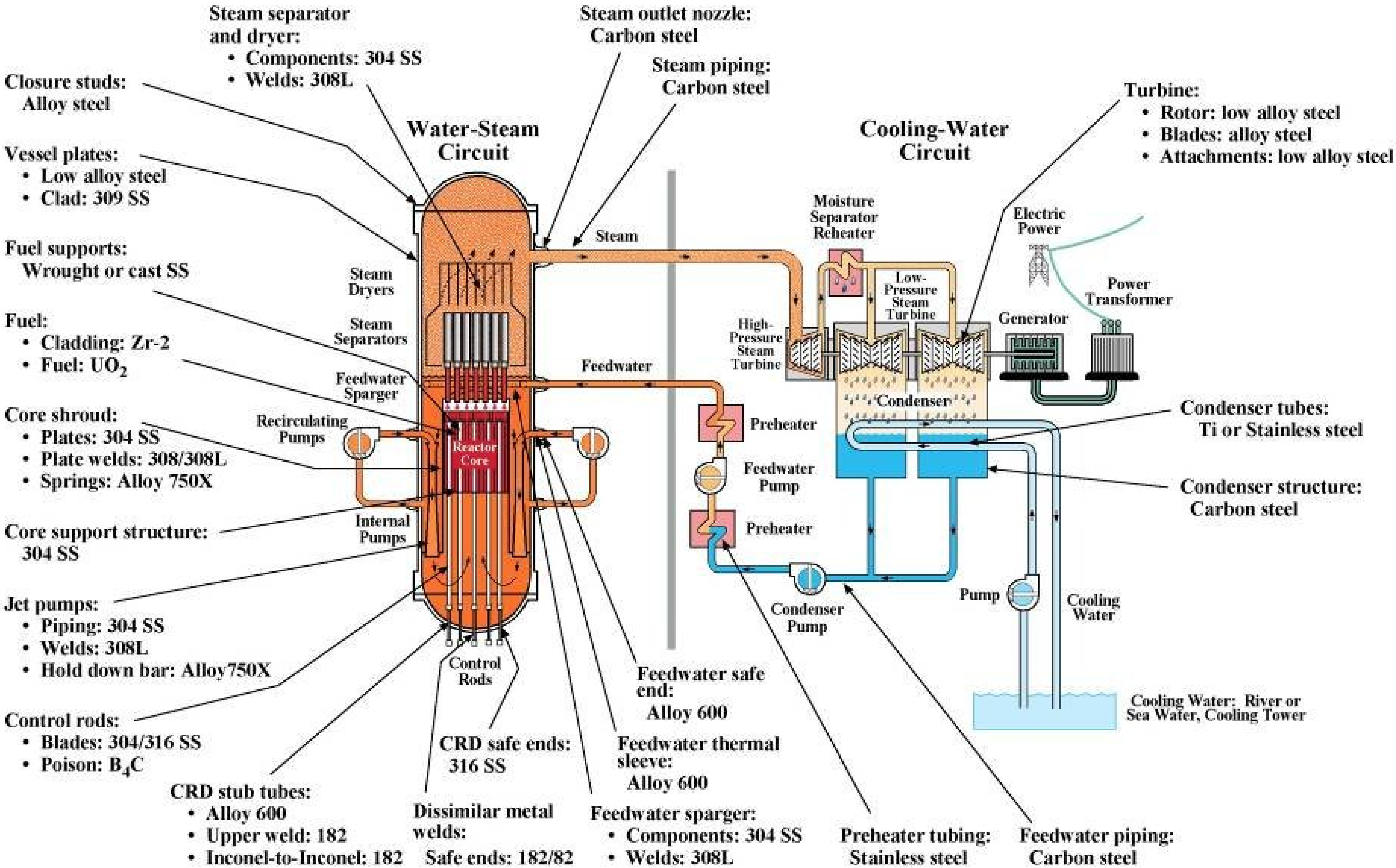

BWR Bulk Environments

BWR Water Chemistry

Role	Species	Conc., ppb or other
Radiolytic oxygen, hydrogen peroxide	O_2, H_2O_2	< 200
Corrosion impurity	Fe	< 5
	Cu	< 0.20
Contamination impurity	$Cl^- + SO_4^{2-}$	< 5
Conductivity		> 0.15 µS/cm

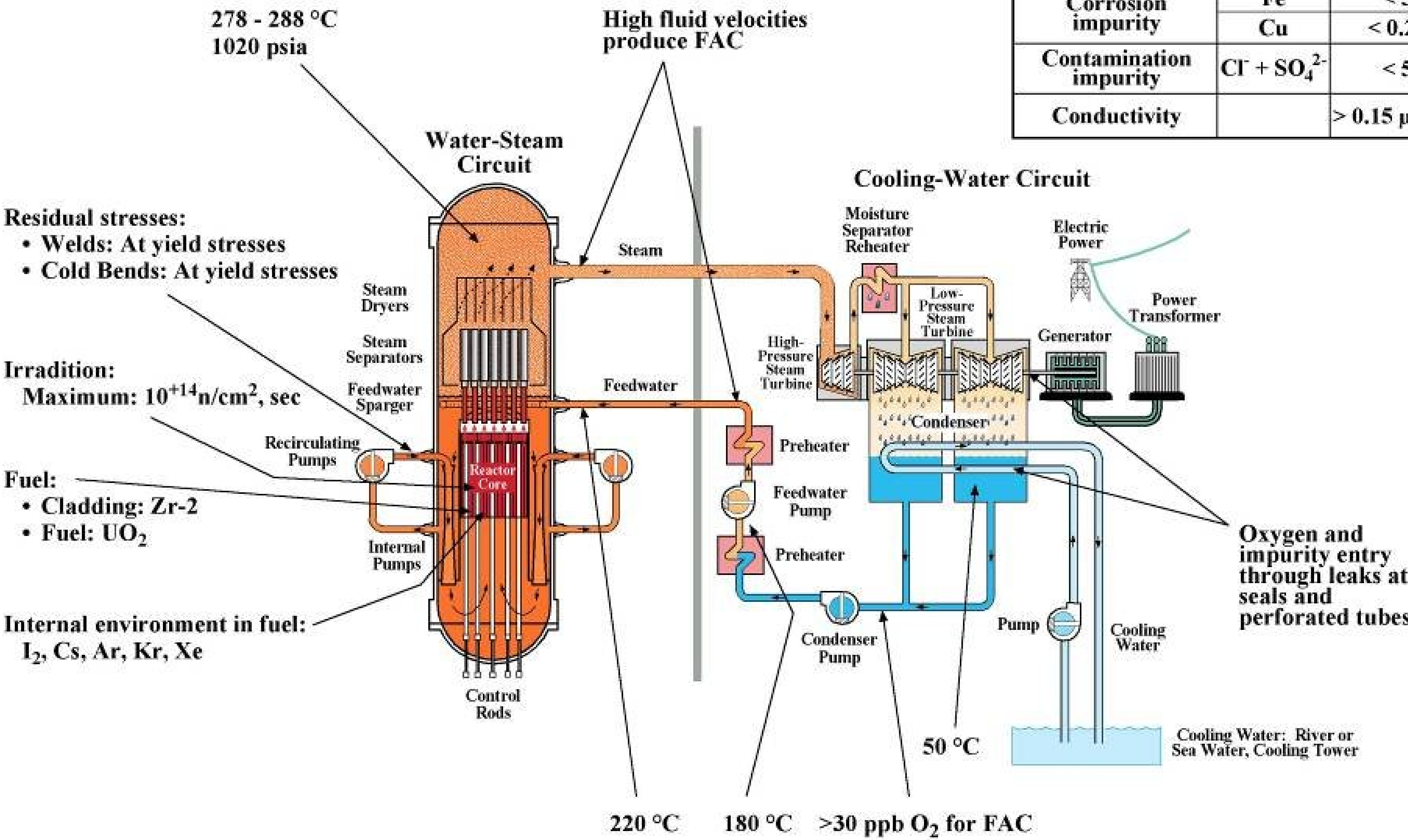

General view of damages in PWRs

SCC both primary, secondary

- SCC and CF
- Cold work accelerates SCC
- Weld structures with high cold work and residual stresses

Primary Chemistry

- Boric acid additions to water as neutron poisons
- Boric acid leaks concentrate boric acid on outer surfaces and produce concentrated boric acid on outside
- Lithium hydroxide additions counteract acidity of boric acid
- Radiolytic oxygen and hydrogen products
- Hydrogen added to counteract radiolytic oxygen

Physical in Primary

- High velocity flows produce vibration
- Single phase water
- About 320°C outlet primary temperatures
- About 340°C in pressurizer

Secondary Chemistry and Corrosion

- Amines to raise pH and reduce iron deposits.
- Hydrazine added to minimize oxygen
- Low hydrogen in steam raises potential
- Hydrazine reduces +6 sulfur impurities to -2 sulfur
- Lead from feedwater and other impurities accumulate (resins) in superheated crevices
- Shutdown impurities
- Flow assisted corrosion, hydrogen produced

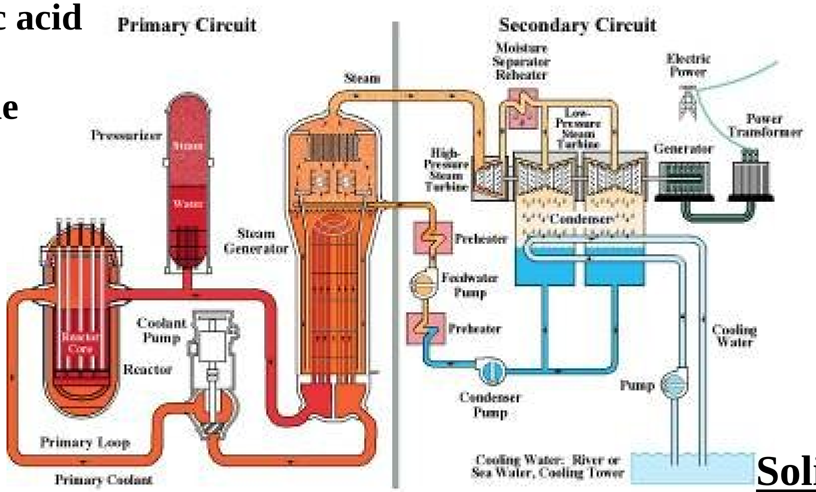

Radiation and Flux

- Neutron flux produces displacement reactions, vacancies, interstitials
- Gamma flux produces local heating
- (n,α) reactions with nickel produce He bubbles and increase volume
- Release of activated chemical species from corrosion, accumulate
- Axial offset anomaly from deposit of boron compound on fuel

Solids, Damage on Secondary

- Deposits on free surfaces reduces flow and increases corrosion in superheated crevices
- Superheated crevices at TSP
- Superheated crevices at TTS
- Tube vibration due to high flows

BWR Components

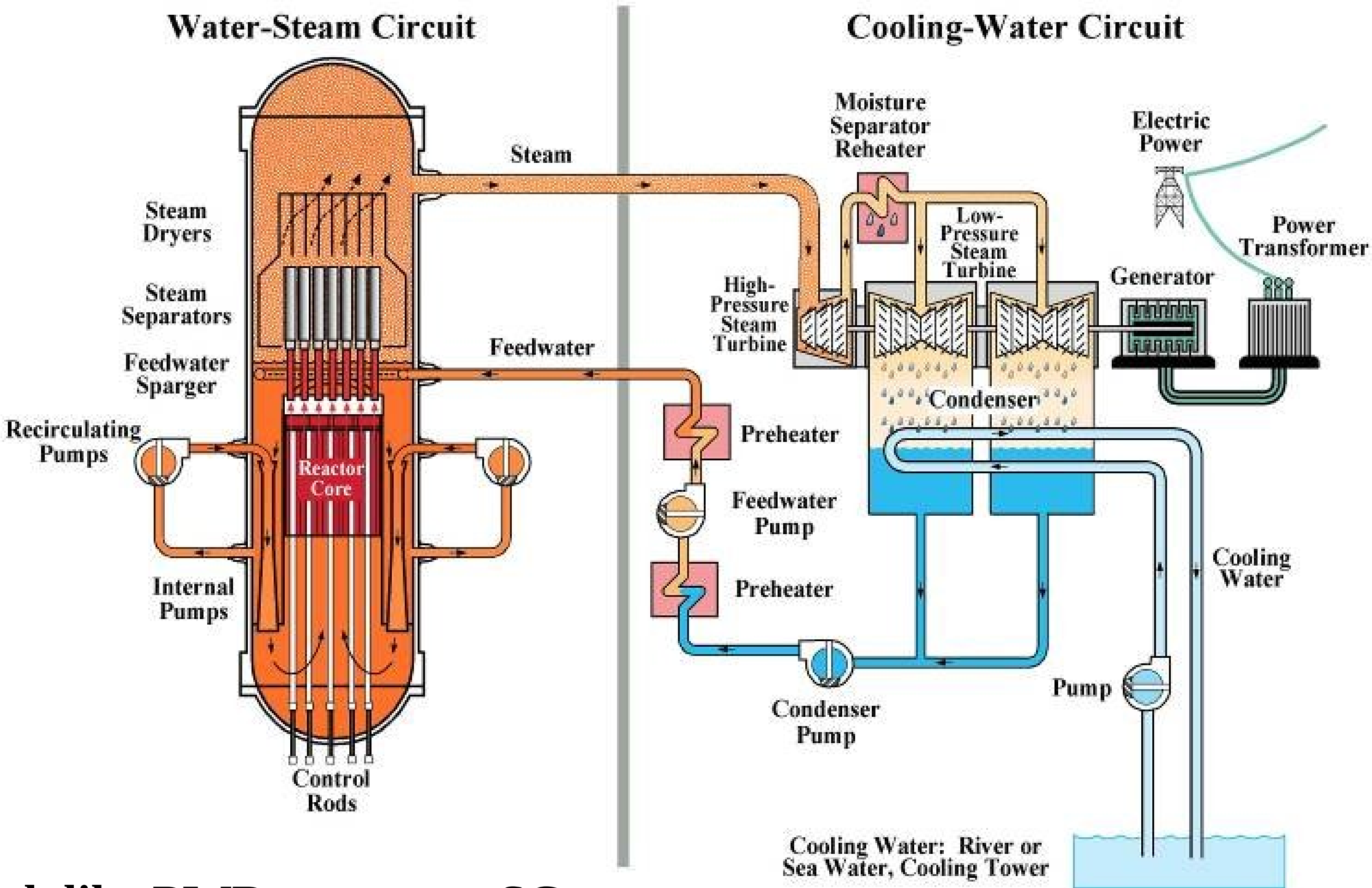

Much like PWRs except to SG and boiling on fuel surfaces

- **Noble metal additions**
- **Hydrogen additions**

The Fe-Cr-Ni alloy system--backbone of nuclear power except for fuels and condensers

Materials basis for nuclear power structural materials

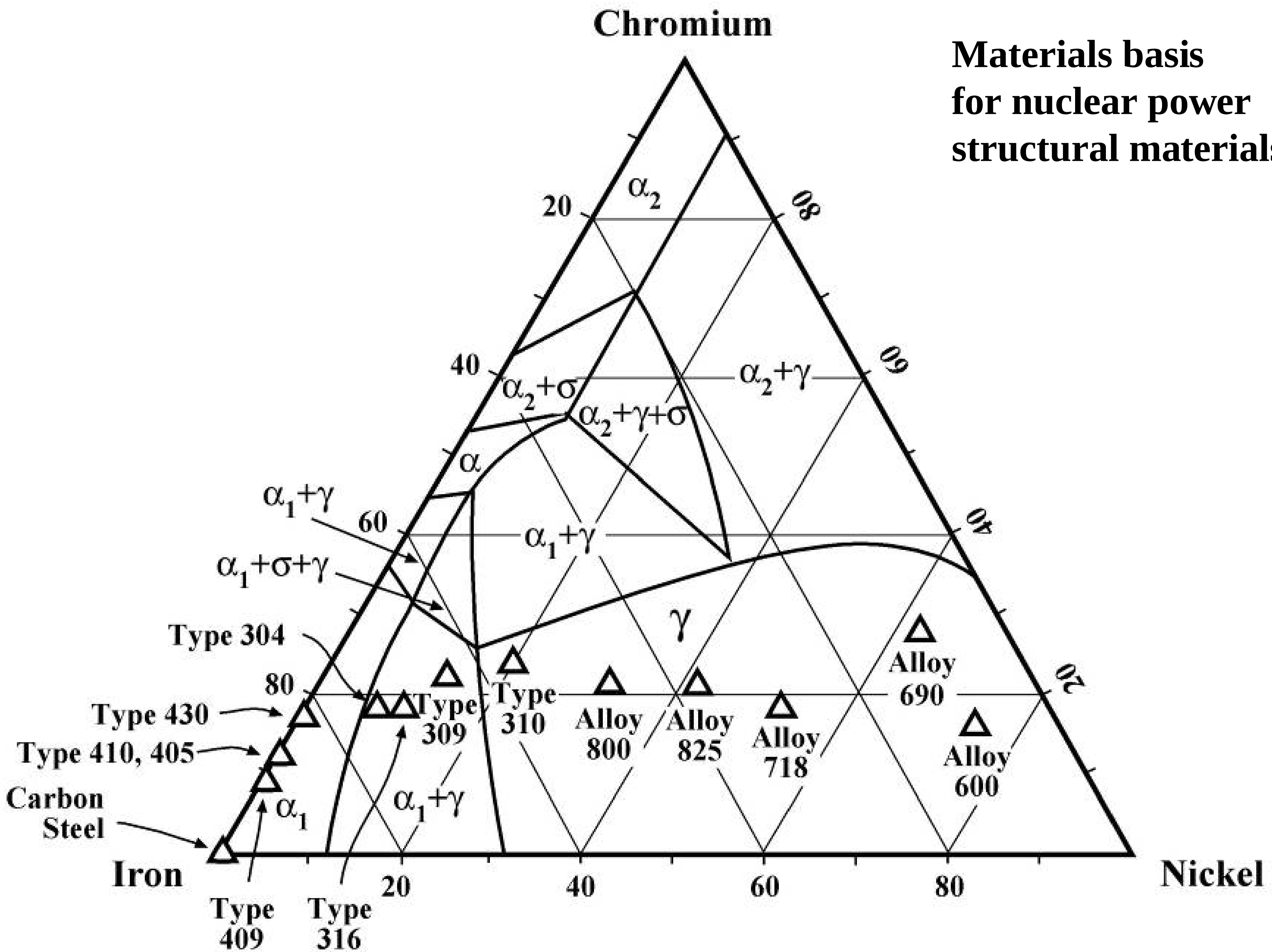

Aqueous Thermodynamics--
potential/pH diagrams
or "Pourbaix Diagrams"

- **Dominates all of corrosion and water chemistry treatment in LWRs**
- **Provides unquestioning framework for kinetics**

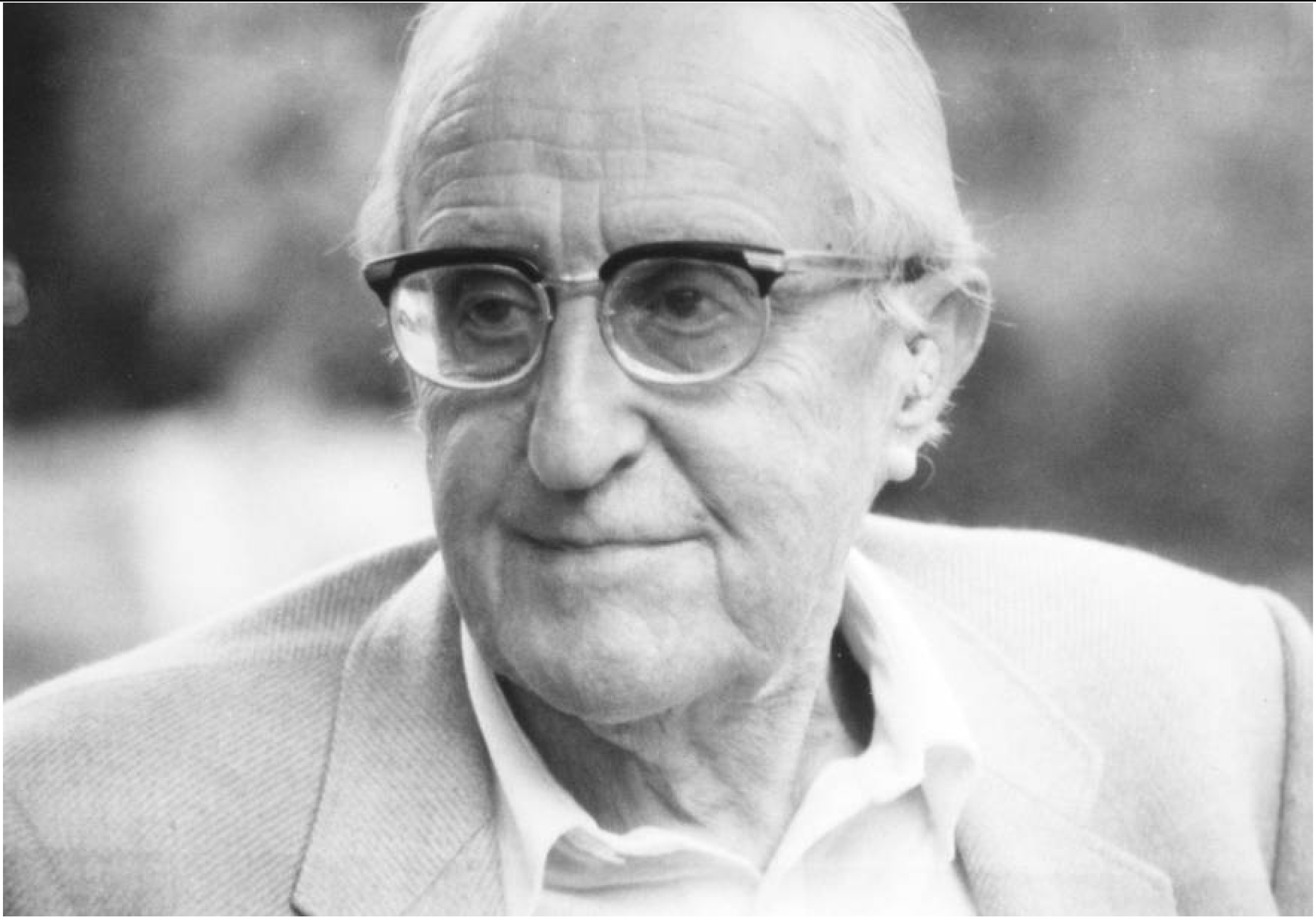

Marcel Pourbaix--developer of the E-pH diagram and other thermodynamic correlations

E-pH (Pourbaix) Diagrams

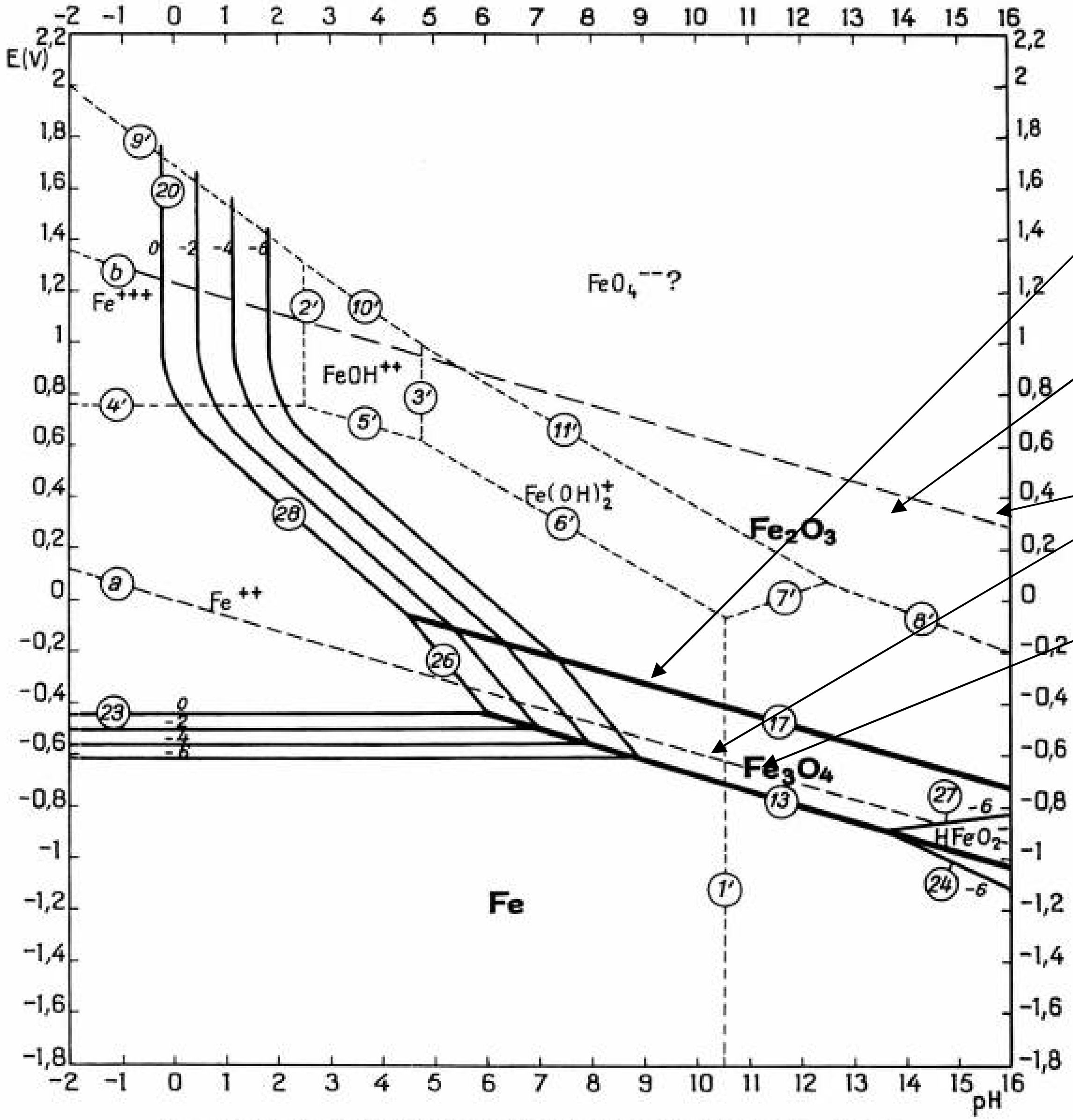

FIG. 4. Potential–pH equilibrium diagram for the system iron–water, at 25°C (considering as solid substances only Fe, Fe_3O_4 and Fe_2O_3).

- **Connect chemistry of reactor with stability of materials**
- **Provide bases for selecting corrosion resistant materials**
- **Provide criteria for roles of oxygen and hydrogen**
- **Provide bases for minimizing release and deposition of corrosion products at low solubility locations**
- **Provide bases for superposition of E-pH diagrams for various alloying additions to assess probable effects of additions**
- **Provide bases for expected reactions of metals with environments**

The E and pH coordinates for E-pH Diagrams

Potential:

- The potential is a measure of the force required to remove electrons from atoms and lead to soluble ions.
- The electrochemical potential of interest is in the range of about -2.5 to +2.0 volts.
- The potential is defined relative to the H_2O/H_2 equilibrium half cell
- Laboratory measurements of potential are often obtained with reference to Ag/AgCl or Hg/Hg_2Cl_2 . These reference cells are ionically connected to the specimens but no current flows in this circuit owing to its high impedance.

pH:

- The pH affects mainly the stability of surface oxides or other protective compounds.
- Often surface oxides are unstable in both acidic and alkaline directions but the regions of stability of these oxides may vary from small, e.g. Zn or Pb, or very broad, e.g. Sn, Ti.
- pH basically affects the solubility of the compounds the log of which is linear with pH with slopes in the range of ± 2.0 or ±3.0
- The solubility which is conventionally taken as the boundary for corrosion purposes is 10^{-6} M.

Superposition of E-pH diagrams for Fe with water

E-pH diagram for Fe

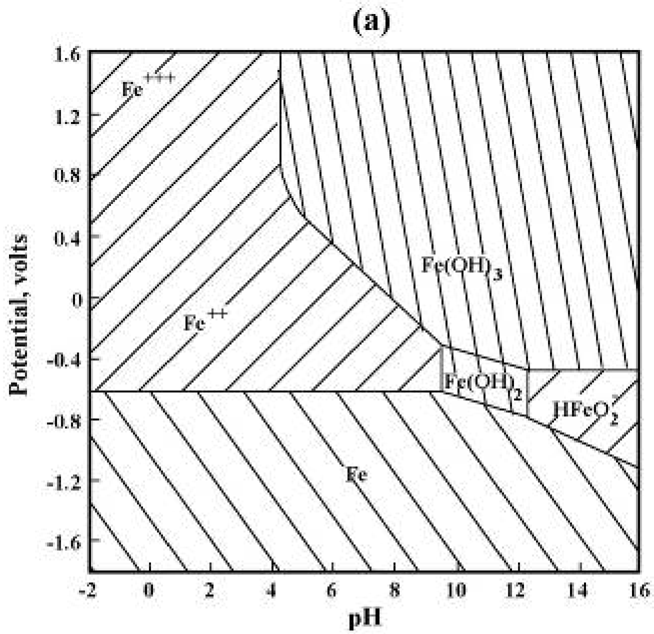

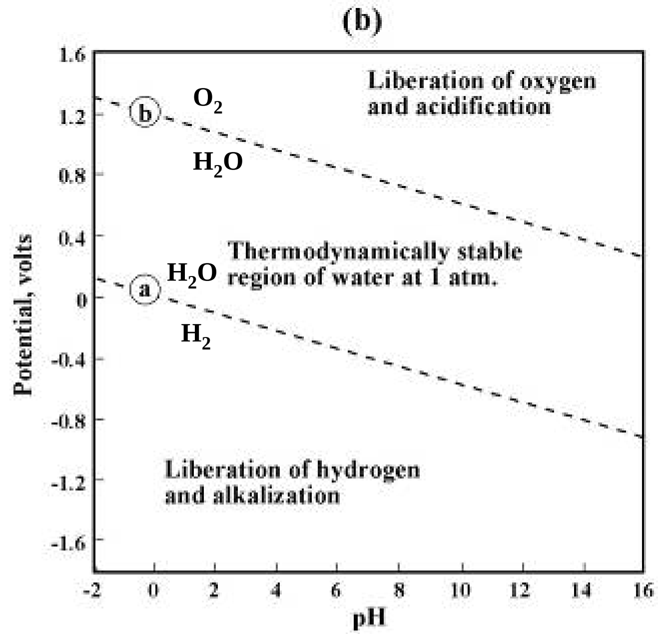

E-pH diagram for water

E-pH diagrams for Fe and water superimposed

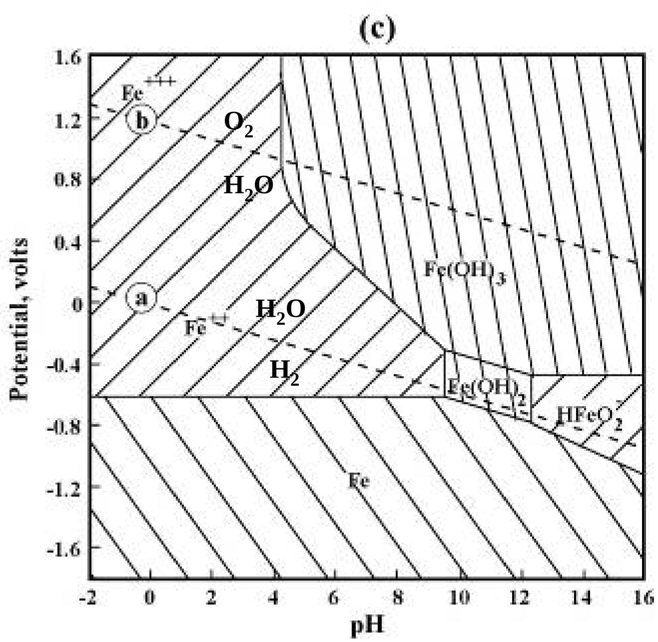

Fundamental bases for half cell reactions in E-pH diagrams

Oxidation half reactions for Fe and H

$$Fe = Fe^{2+} + 2e^-$$

$$H_2 = 2H^+ + 2e^-$$

Whole cell reaction for reactions of Fe and H

$$Fe + 2H^+ + 2e^- = Fe^{2+} + H_2 + 2e^-$$

Use the chemical potential, μ_i , for evaluating the total chemical potentials

$$\mu_i = \mu_i^o + RT \ln a_i$$

$$\Delta G = \sum_i \mu_i = \sum_i \mu_i^o + RT \sum_i \ln a_i = \Delta G^o + RT \sum_i \ln a_i$$

Where:

- μ_i **= chemical potential of 'i"**
- μ_i^o **= standard chemical potential of "i"**
- a_i **= activity of "i"**
- R **= gas constant**
- T **= absolute temperature**

- ΔG **= free energy change**
- ΔG^o **= standard free energy change**
- E_o **= electrochemical potential in equilibrium with activity of species**
- E_o^o **= standard electrochemical potential**
- F **= Faraday constant**
- n **= number of electrical equivalents**

Iron half cell

$$Fe = Fe^{2+} + 2e^{-}_{Fe}$$

Hydrogen half cell

$$H_2 = 2H^{+} + 2e^{-}_{H}$$

Whole cell for iron/hydrogen equilibrium

$$Fe + 2H^{+} + 2e^{-}_{H} = Fe^{2+} + H_2 + 2e^{-}_{Fe}$$

Chemical potential of the ith species

$$\mu_i = \mu_i^o + RT\ln a_i$$

Gibbs free energy change for chemical and electron species

$$\Delta G_T = \Delta G_{chem} + \Delta G_{elect}$$

Gibbs free energy change for chemical species

$$\Delta G_{chem} = \sum_i \mu_{i,c} = \sum_i \mu^o_{i,c} + RT\sum_i \ln a_{i,c} = \Delta G^o_c + RT\sum_i \ln a_{i,c}$$

Gibbs free energy change for electrons

$$\Delta G_{elect} = \sum_i \mu_{i,e} = \sum_i \mu^o_{i,e} + RT\sum_i \ln a_{i,e} = \Delta G^o_e + RT\sum_i \ln a_{i,e}$$

Standard chemical Gibbs free energy change

$$\Delta G_c^o = \mu^o_{Fe^{2+}} + \mu^o_{H_2} - \left(\mu^o_{Fe} + 2\mu^o_{H^+}\right)$$

Free energy for electrons

$$\Delta G_e = 2\mu^o_{e,Fe} - 2\mu^o_{e,H} + RT\ln\frac{[a_{e,Fe}]}{[a_{e,H}]}$$

Taking the Gibbs free energy change to be zero at equilibrium

$$-2\mu^o_{e,Fe} + 2\mu^o_{e,H} - RT\ln\frac{[a_{e,Fe}]}{[a_{e,H}]} = \mu^o_{Fe^{2+}} + \mu^o_{H_2} - \left(\mu^o_{Fe} + 2\mu^o_{H^+}\right) + RT\ln\frac{[a_{Fe^{2+}}][a_{H_2}]}{[a_{Fe}][a_{H^+}]^2}$$

$$0 = 2\mu^o_{e,Fe} - 2\mu^o_{e,H} + RT\ln\frac{[a_{e,Fe}]}{[a_{e,H}]} + \mu^o_{Fe^{2+}} + \mu^o_{H_2} - \left(\mu^o_{Fe} + 2\mu^o_{H^+}\right) + RT\ln\frac{[a_{Fe^{2+}}][a_{H_2}]}{[a_{Fe}][a_{H^+}]^2}$$

Dividing by Faraday's constant, calories/volt, and converting to base 10 logs

$$E_o = E_o^o + \frac{2.3RT}{nF}\log\frac{[a_{Fe^{2+}}][a_{H_2}]}{[a_{Fe}][a_{H^+}]^2}$$

By definition, taking the activity of hydrogen as one atmosphere and the activity of hydrogen ions as unity, an equilibrium expression for the iron half cell is:

$$E_o = E_o^o + \frac{2.3RT}{nF}\log[a_{Fe^{2+}}]$$

Physical Meaning of Potential

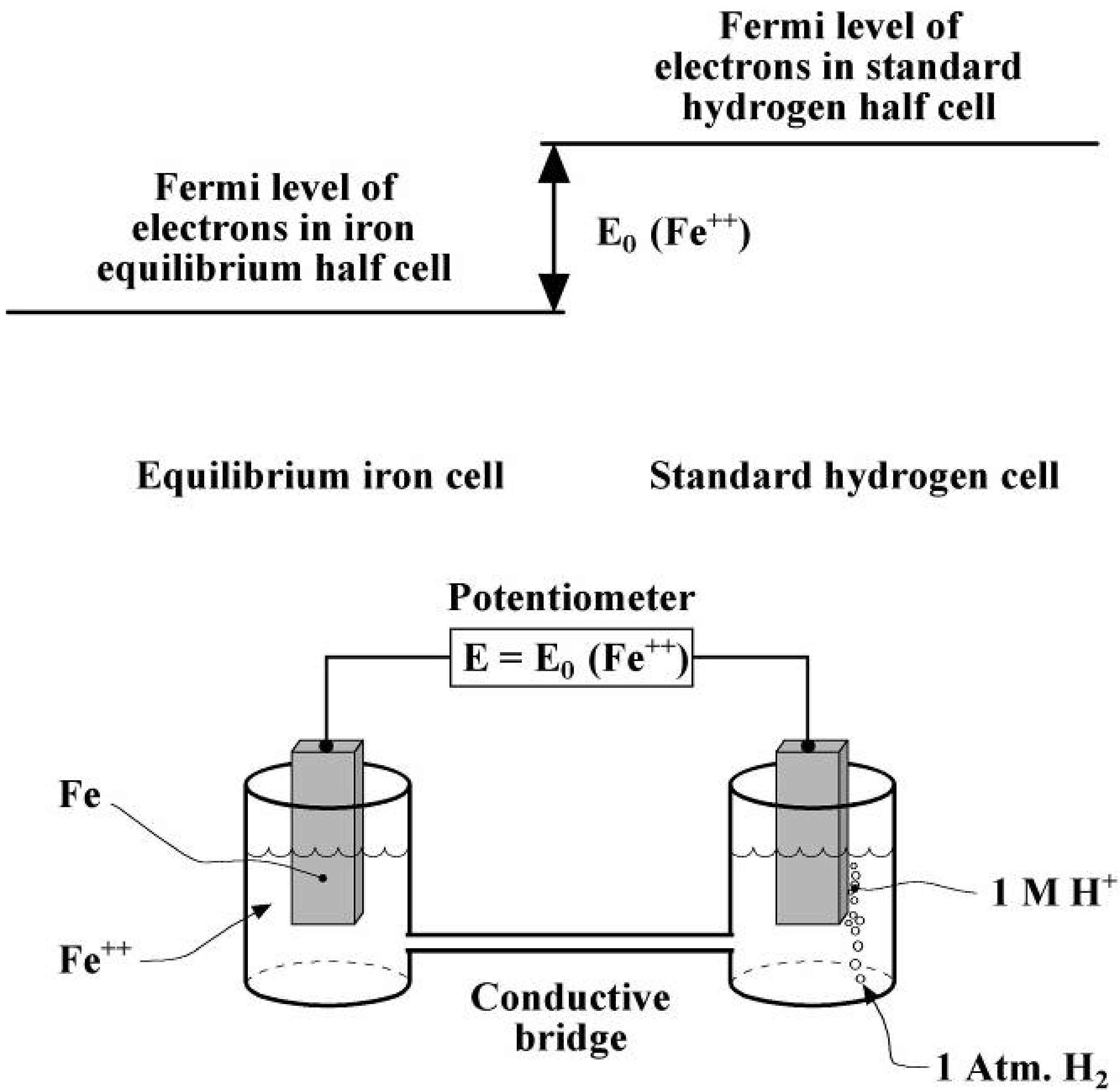

The thermodynamic map of corrosion: potential (E) and pH

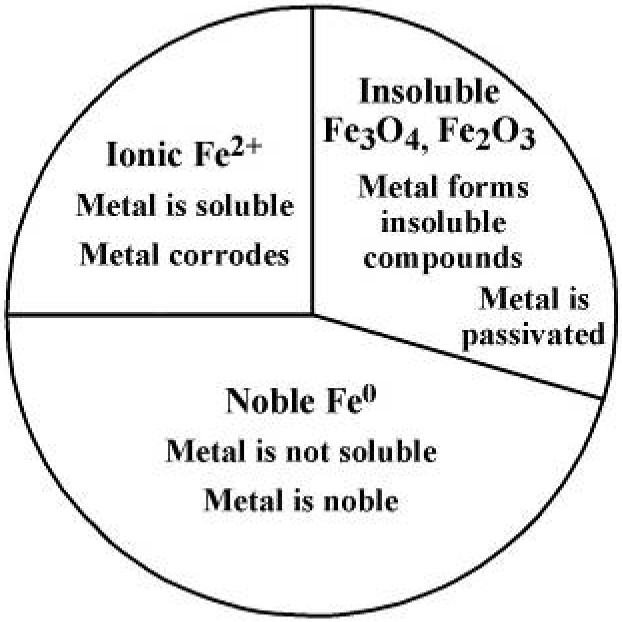

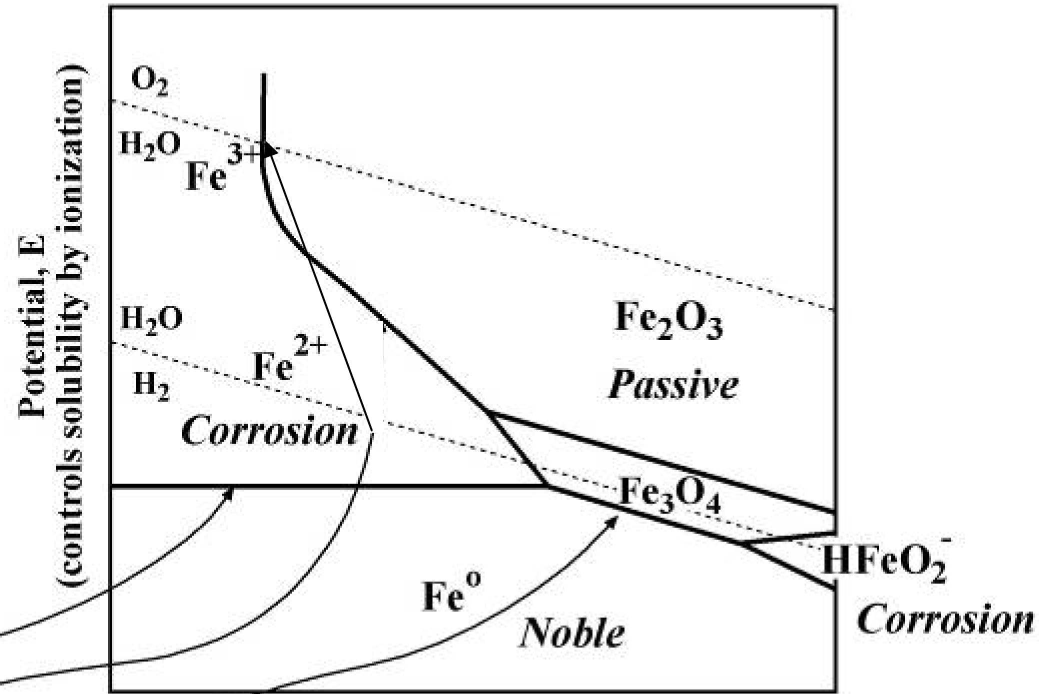

pH
(controls solubility by breaking M-O bonds in oxides and deposits)

Horizontal line depends only on potential

Vertical line depends only on pH

Sloping line involve reactions depending on both pH and E

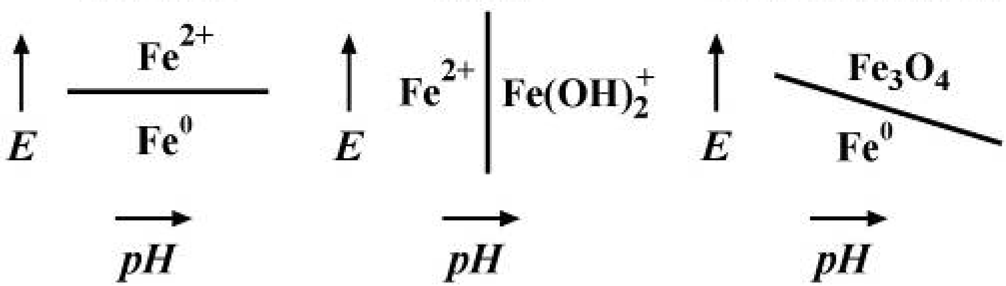

- **Potential, E, removes or adds electrons**
- **pH solubilizes or insolubizes surface deposits**

Approach to calculating and organizing diagrams of potential and pH

Procedure for establishment of E-pH diagrams

1. SUBSTANCES CONSIDERED AND SUBSTANCES NOT CONSIDERED

	Oxidation number (Z)	Considered	Not considered	μ^0(cal.)	Name, colour, crystalline system
Solid substances	0	**Fe**	–	0	α-Iron, light grey, f.c.cub.
	+2	**FeO** hydr.	–	— 58 880 (2)	Ferrous hydroxide $Fe(OH)_2$, white, rhomb.
	»	–	**FeO** anh.	–	Ferrous oxide, black, cub.
	+2.67	**Fe_3O_4** anh.	–	—242 400	Magnetite, black, cub.
	»	–	**Fe_3O_4**$.xH_2O$	–	Hydrated magnetite, green–black
	+3	**Fe_2O_3** anh.	–	*a.* —177 100	Haematite, red–brown, rhomb. or cub.
	»	» hydr.	–	*b.* —161 930 (3)	Ferric hydroxide $Fe(OH)_3$, red-brown, f.c.cub.
Dissolved substances	+2	Fe^{++}	–	— 20 300	Ferrous ion, green
	»	$HFeO_2^-$	–	— 90 627 (*)	Dihypoferrite ion, green
	»	–	FeO_2^{--}	–	Hypoferrite ion
	+3	Fe^{+++}	–	— 2 530	Ferric ion, colourless
	»	$FeOH^{++}$	–	— 55 910	Ferric ion, colourless
	»	$Fe(OH)_2^+$	–	—106 200	Ferric ion, colourless
	»	–	FeO_2^-	–	Ferrite ion
	+4	–	FeO^{++}	–	Ferryl ion
	»	–	FeO_3^{--}	–	Perferrite ion
	+5	–	FeO_2^+	–	Perferryl ion
	+6	FeO_4^{--} ?	–	—111 685 ? (*)	Ferrate ion, violet

2.1. TWO DISSOLVED SUBSTANCES

2.1.1. *Relative stability of the dissolved substances*

$Z = +2$

1. $Fe^{++} + 2H_2O = HFeO_2^- + 3H^+$ $\qquad \log \frac{(HFeO_2^-)}{(Fe^{++})} = -31.58 + 3\,pH$

$Z = +3$

2. $Fe^{+++} + H_2O = FeOH^{++} + H^+$ $\qquad \log \frac{(FeOH^{++})}{(Fe^{+++})} = -\ 2.43 + \ pH$

3. $FeOH^{++} + H_2O = Fe(OH)_2^+ + H^+$ $\qquad \log \frac{(Fe(OH)_2^+)}{(FeOH^{++})} = -\ 4.69 + \ pH$

$+2 \rightarrow +3$

4. $Fe^{++} = Fe^{+++} + e^-$ $\qquad E_0 = 0.771 + 0.0591 \log \frac{(Fe^{+++})}{(Fe^{++})}$

5. $Fe^{++} + H_2O = FeOH^{++} + H^+ + e^-$ $\qquad E_0 = 0.914 - 0.0591\,pH + 0.0591 \log \frac{(FeOH^{++})}{(Fe^{++})}$

6. $Fe^{++} + 2H_2O = Fe(OH)_2^+ + 2H^+ + e^-$ $\qquad E_0 = 1.191 - 0.1182\,pH + 0.0591 \log \frac{(Fe(OH)_2^+)}{(Fe^{++})}$

7. $HFeO_2^- + H^+ = Fe(OH)_2^+ + e^-$ $\qquad E_0 = -0.675 + 0.0591\,pH + 0.0591 \log \frac{(Fe(OH)_2^+)}{(HFeO_2^-)}$

$+2 \rightarrow +6$

8. $HFeO_2^- + 2H_2O = FeO_4^{--} + 5H^+ + 4e^-$ $\qquad E_0 = 1.001 - 0.0738\,pH + 0.0148 \log \frac{(FeO_4^{--})}{(HFeO_2^-)}$

$+3 \rightarrow +6$

9. $Fe^{+++} + 4H_2O = FeO_4^{--} + 8H^+ + 3e^-$ $\qquad E_0 = 1.700 - 0.1580\,pH + 0.0197 \log \frac{(FeO_4^{--})}{(Fe^{+++})}$

10. $FeOH^{++} + 3H_2O = FeO_4^{--} + 7H^+ + 3e^-$ $\qquad E_0 = 1.652 - 0.1379\,pH + 0.0197 \log \frac{(FeO_4^{--})}{(FeOH^{++})}$

11. $Fe(OH)_2^+ + 2H_2O = FeO_4^{--} + 6H^+ + 3e^-$ $\qquad E_0 = 1.559 - 0.1182\,pH + 0.0197 \log \frac{(FeO_4^{--})}{(Fe(OH)_2^+)}$

2.1.2. *Limits of the domains of relative predominance of the dissolved substances*

1'.	Fe^{++} / $HFeO_2^-$	$pH = 10.53$
2'.	Fe^{+++} / $FeOH^{++}$	$pH = 2.43$
3'.	$FeOH^{++}$ / $Fe(OH)_2^+$	$pH = 4.69$
4'.	Fe^{++} / Fe^{+++}	$E_0 = 0.771$
5'.	Fe^{++} / $FeOH^{++}$	$E_0 = 0.914 - 0.0591\,pH$
6'.	Fe^{++} / $Fe(OH)_2^+$	$E_0 = 1.191 - 0.1182\,pH$
7'.	$HFeO_2^-$ / $Fe(OH)_2^+$	$E_0 = -0.675 + 0.0591\,pH$
8'.	$HFeO_2^-$ / FeO_4^{--}	$E_0 = 1.001 - 0.0738\,pH$
9'.	Fe^{+++} / FeO_4^{--}	$E_0 = 1.700 - 0.1580\,pH$
10'.	$FeOH^{++}$ / FeO_4^{--}	$E_0 = 1.652 - 0.1379\,pH$
11'.	$Fe(OH)_2^+$ / FeO_4^{--}	$E_0 = 1.559 - 0.1182\,pH$

2.2. TWO SOLID SUBSTANCES [5]

Limits of the domains of relative stability of iron and its oxides and hydroxides

$0 \rightarrow +2$

12. $Fe + H_2O = FeO + 2H^+ + 2e^-$ $\qquad E_0 = -0.047 - 0.0591\,pH$

$0 \rightarrow +2.67$

13. $3Fe + 4H_2O = Fe_3O_4 + 8H^+ + 8e^-$ $\qquad E_0 = -0.085 - 0.0591\,pH$

$0 \rightarrow +3$

14. $2Fe + 3H_2O = Fe_2O_3 + 6H^+ + 6e^-$ $\qquad$ a. $E_0 = -0.051 - 0.0591\,pH$
    b. $\quad = 0.059 - 0.0591\,pH$

$+2 \rightarrow 2.67$

15. $3FeO + H_2O = Fe_3O_4 + 2H^+ + 2e^-$ $\qquad E_0 = -0.197 - 0.0591\,pH$

$+2 \rightarrow +3$

16. $2FeO + H_2O = Fe_2O_3 + 2H^+ + 2e^-$ $\qquad$ a. $E_0 = -0.057 - 0.0591\,pH$
    b. $\quad = 0.271 - 0.0591\,pH$

$+2.67 \rightarrow +3$

17. $2Fe_3O_4 + H_2O = 3Fe_2O_3 + 2H^+ + 2e^-$ $\qquad$ a. $E_0 = 0.221 - 0.0591\,pH$
    b. $\quad = 1.208 - 0.0591\,pH$

2.3. ONE SOLID SUBSTANCE AND ONE DISSOLVED SUBSTANCE [5]

Solubility of iron and its oxides and hydroxides

$Z = +2$

18.	$Fe^{++} + H_2O = \mathbf{FeO} + 2H^+$		$\log(Fe^{++}) = 13.29 - 2\,pH$
19.	$\mathbf{FeO} + H_2O = HFeO_2^- + H^+$		$\log(HFeO_2^-) = -18.30 + pH$

$Z = +3$

20.	$2Fe^{+++} + 3H_2O = \mathbf{Fe_2O_3} + 6H^+$	a.	$\log(Fe^{+++}) = -0.72 - 3\,pH$
		b.	$= 4.84 - 3\,pH$
21.	$2FeOH^{++} + H_2O = \mathbf{Fe_2O_3} + 4H^+$	a.	$\log(FeOH^{++}) = -3.15 - 2\,pH$
		b.	$= 2.41 - 2\,pH$
22.	$2Fe(OH)_2^+ = \mathbf{Fe_2O_3} + H_2O + 2H^+$	a.	$\log(Fe(OH)_2^+) = -7.84 - pH$
		b.	$= -2.28 - pH$

$0 \rightarrow +2$

23.	$\mathbf{Fe} = Fe^{++} + 2e^-$		$E_0 = -0.440 + 0.0295\log(Fe^{++})$
24.	$\mathbf{Fe} + 2H_2O = HFeO_2^- + 3H^+ + 2e^-$		$E_0 = 0.493 - 0.0886\,pH + 0.0295\log(HFeO_2^-)$

$0 \rightarrow +3$

25.	$\mathbf{Fe} = Fe^{+++} + 3e^-$		$E_0 = -0.037 + 0.0197\log(Fe^{+++})$

$+2 \rightarrow +2.67$

26.	$3Fe^{++} + 4H_2O = \mathbf{Fe_3O_4} + 8H^+ + 2e^-$		$E_0 = 0.980 - 0.2364\,pH - 0.0886\log(Fe^{++})$
27.	$3HFeO_2^- + H^+ = \mathbf{Fe_3O_4} + 2H_2O + 2e^-$		$E_0 = -1.819 + 0.0295\,pH - 0.0886\log(HFeO_2^-)$

$+2 \rightarrow +3$

28.	$2Fe^{++} + 3H_2O = \mathbf{Fe_2O_3} + 6H^+ + 2e^-$	a.	$E_0 = 0.728 - 0.1773\,pH - 0.0591\log(Fe^{++})$
		b.	$= 1.057 - 0.1773\,pH - 0.0591\log(Fe^{++})$
29.	$2HFeO_2^- = \mathbf{Fe_2O_3} + H_2O + 2e^-$	a.	$E_0 = -1.139 - 0.0591\log(HFeO_2^-)$
		b.	$= -0.810 - 0.0591\log(HFeO_2^-)$

Solubility

Important to

- **Release of radioactive species**
- **Accumulation of deposits on SG surfaces**
- **Flow assisted corrosion**
- **Preferential release of alloy species**

Solubility of iron at RT in water.

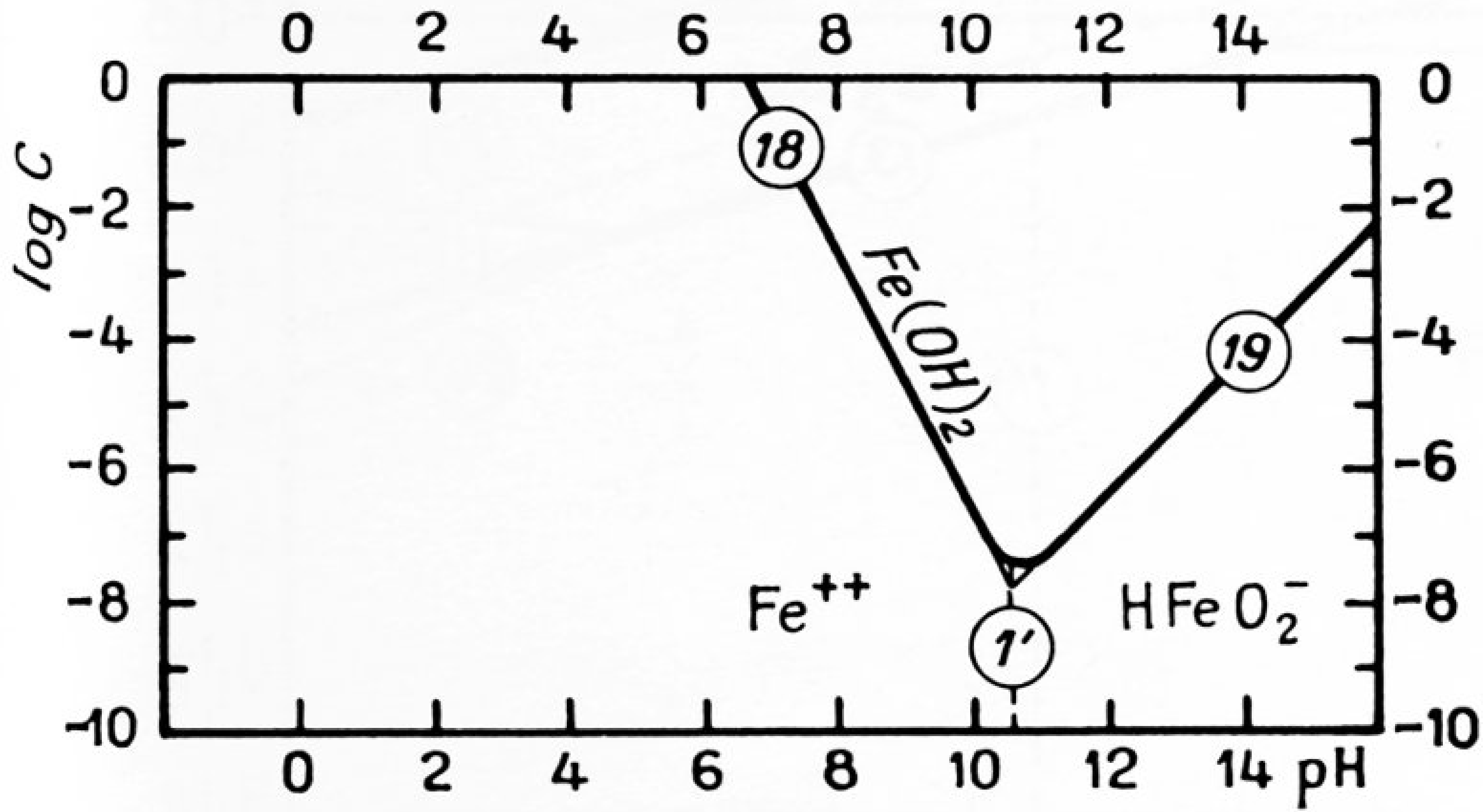

FIG. 2. Influence of pH on the solubility of $Fe(OH)_2$.

Minimum solubility is the goal of water chemistry treatments in nuclear plants to minimize both the deposition of iron on secondary surfaces and the deposition of radioactive species on the primary side. Minimizing solubility is important to minimize flow assisted corrosion (FAC).

Solubility and corrosion for aluminum

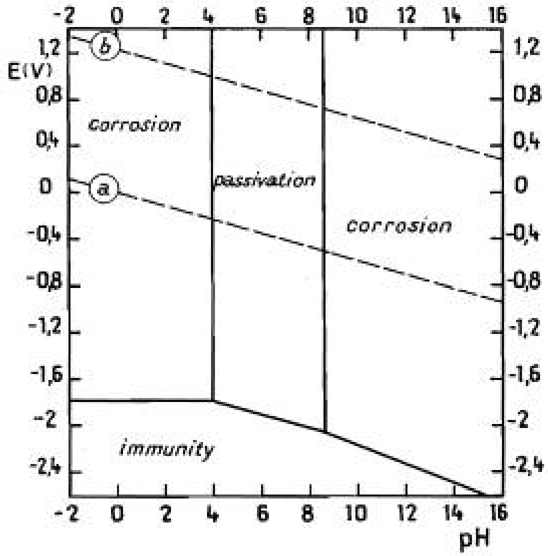

(*a*) Passivation by a film of hydrargillite $Al_2O_3 \cdot 3H_2O$.

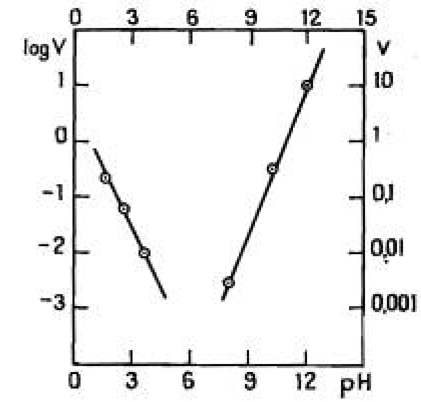

(*a*) log V as a function of pH.
(V, corrosion rate in mg/dm² h).
FIG. 3. Influence of pH on the corrosion rate of aluminium (Chatalov).

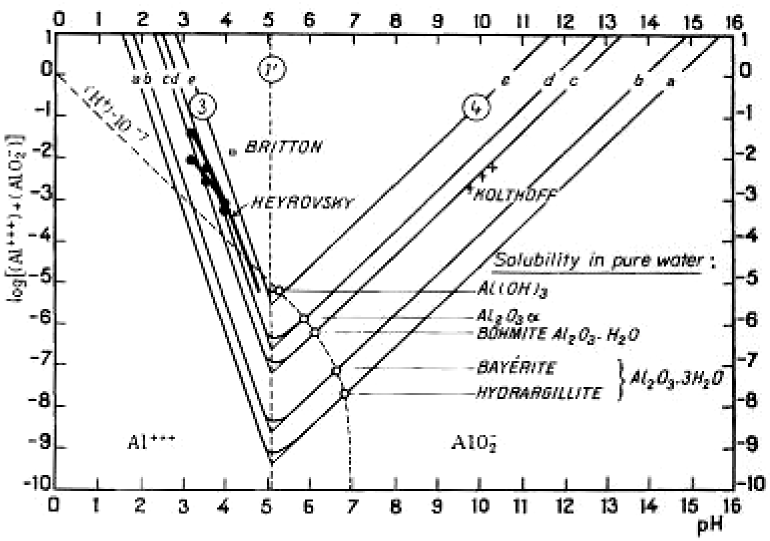

FIG. 4. Influence of pH on the solubility of Al_2O_3 and its hydrates, at 25°C.

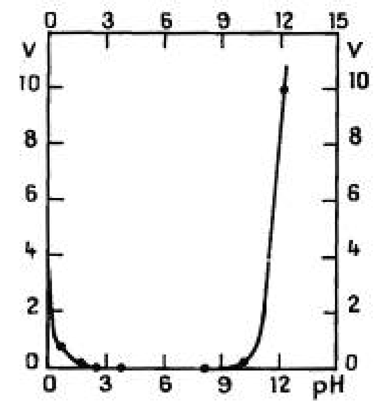

(*b*) log V as a function of pH.
(V, corrosion rate in mg/dm² h).
FIG. 3. Influence of pH on the corrosion rate of aluminium (Chatalov).

Preferential dissolution of Cr

Solubility of Fe, Cr, Ni at 300°C

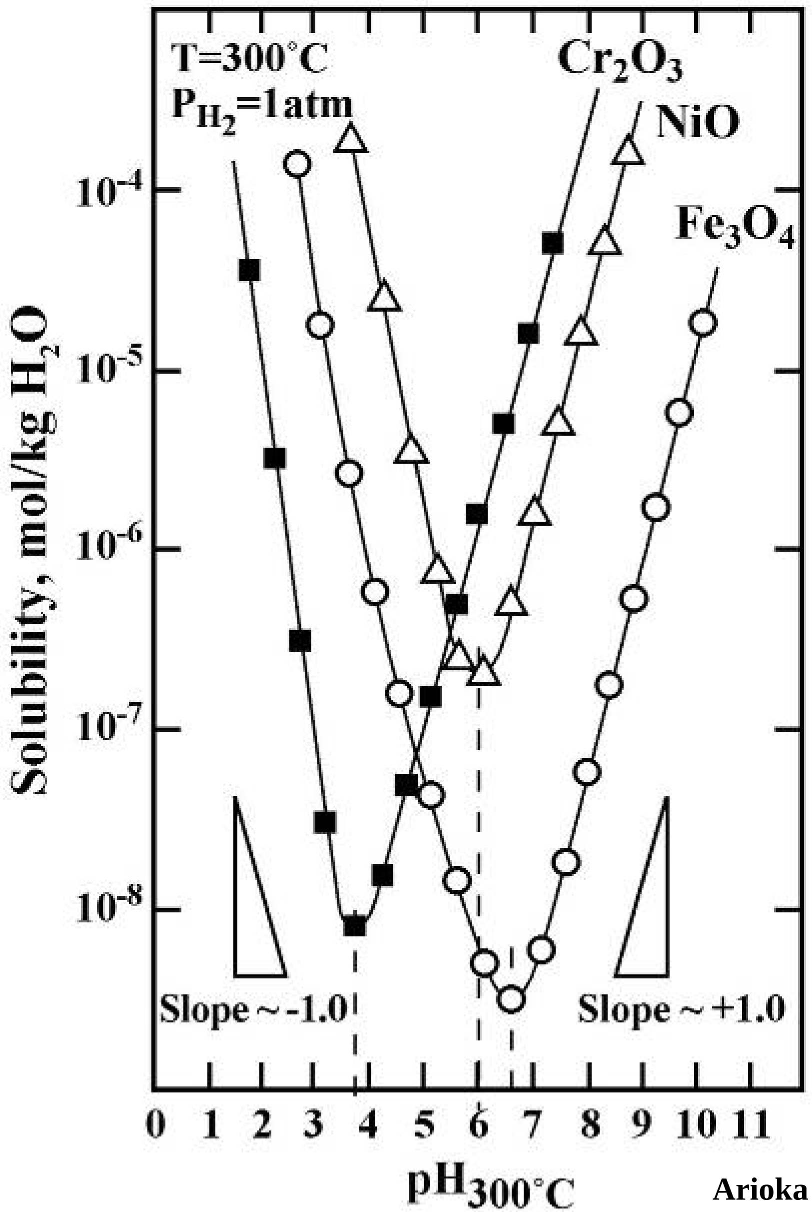

Arioka

Preferential dissolution of Cr by AES

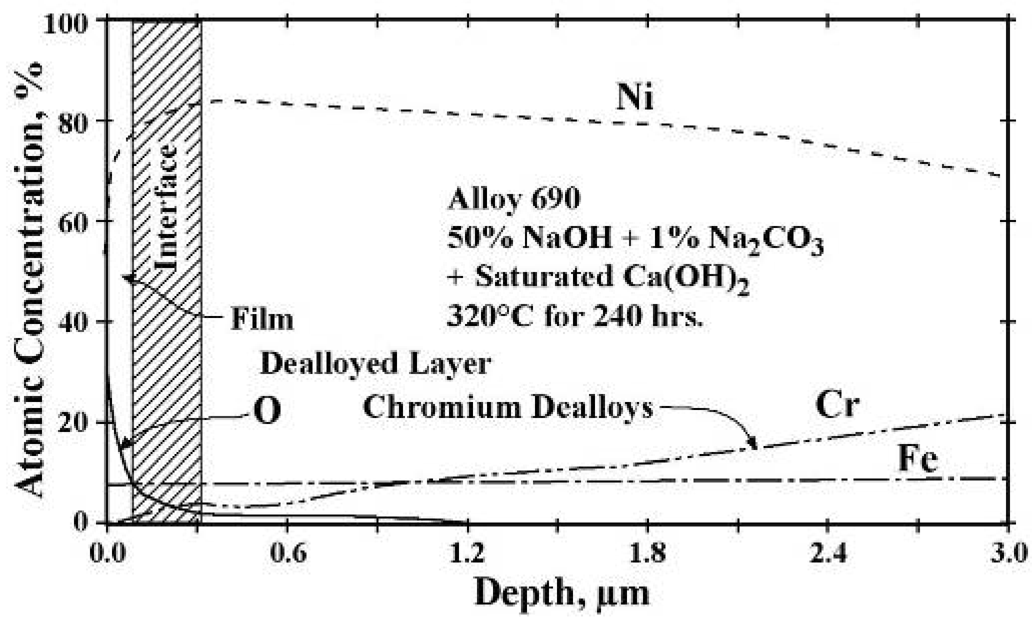

Lumsden

Different solubilities means that, at one pH, some species will dissolve preferentially leaving the surface enriched in other species.

The surface of Alloy 690 changes as Cr dissolves

Cr preferentially soluble

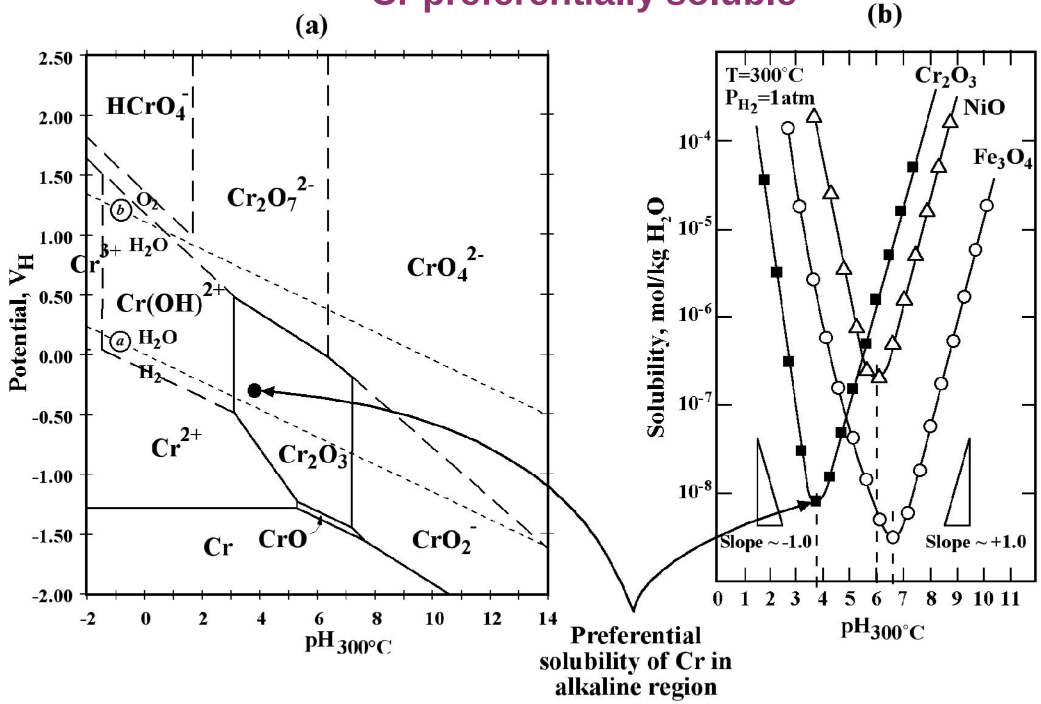

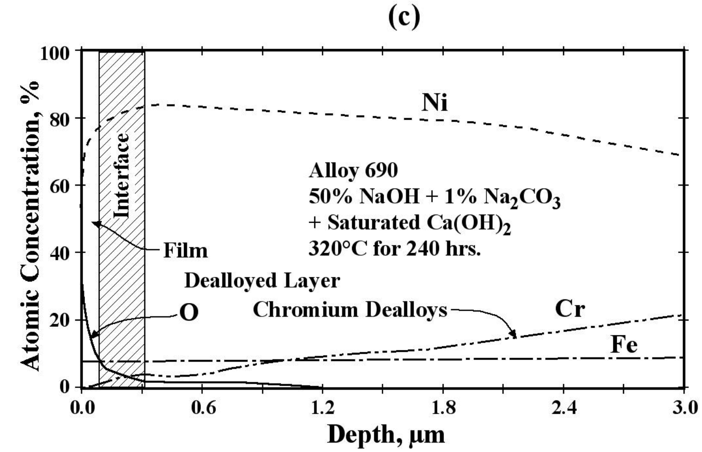

Cr dissolves preferentially

Loss of Cr increases SCC

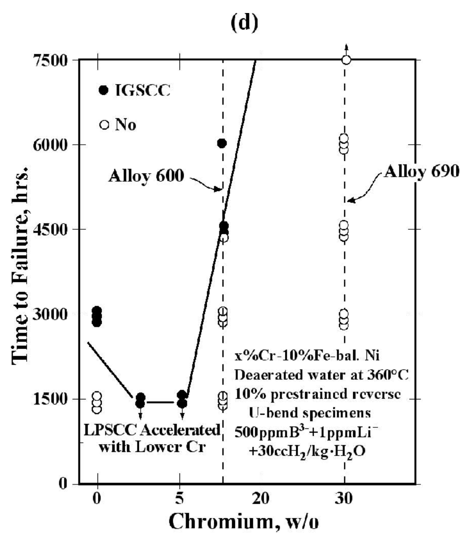

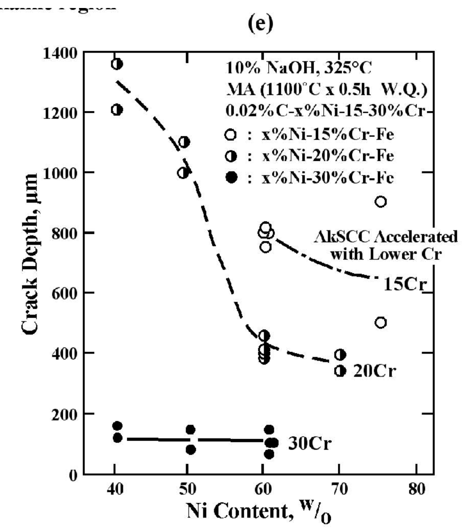

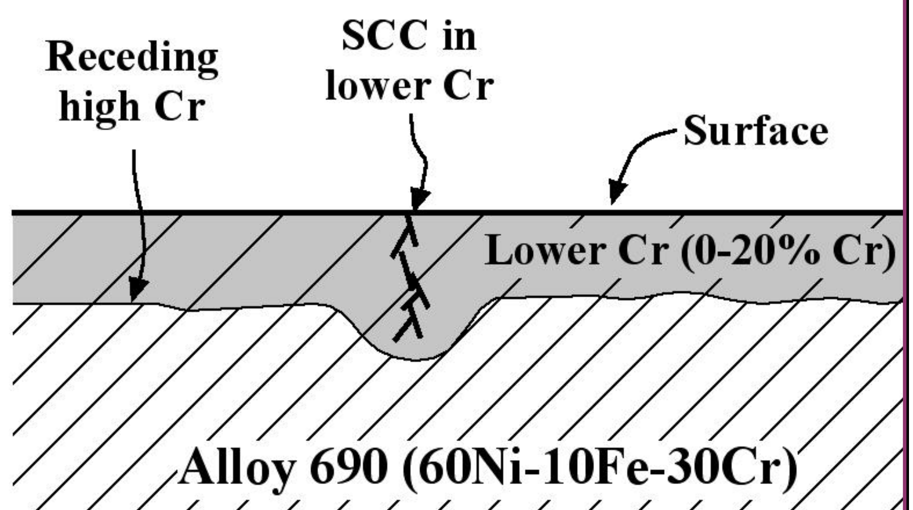

Loss of Cr from Alloy 690
produces Alloy 600 then SCC

Applications of E-pH Diagrams

The superposition of half cell equilibria predicts what reactions can occur

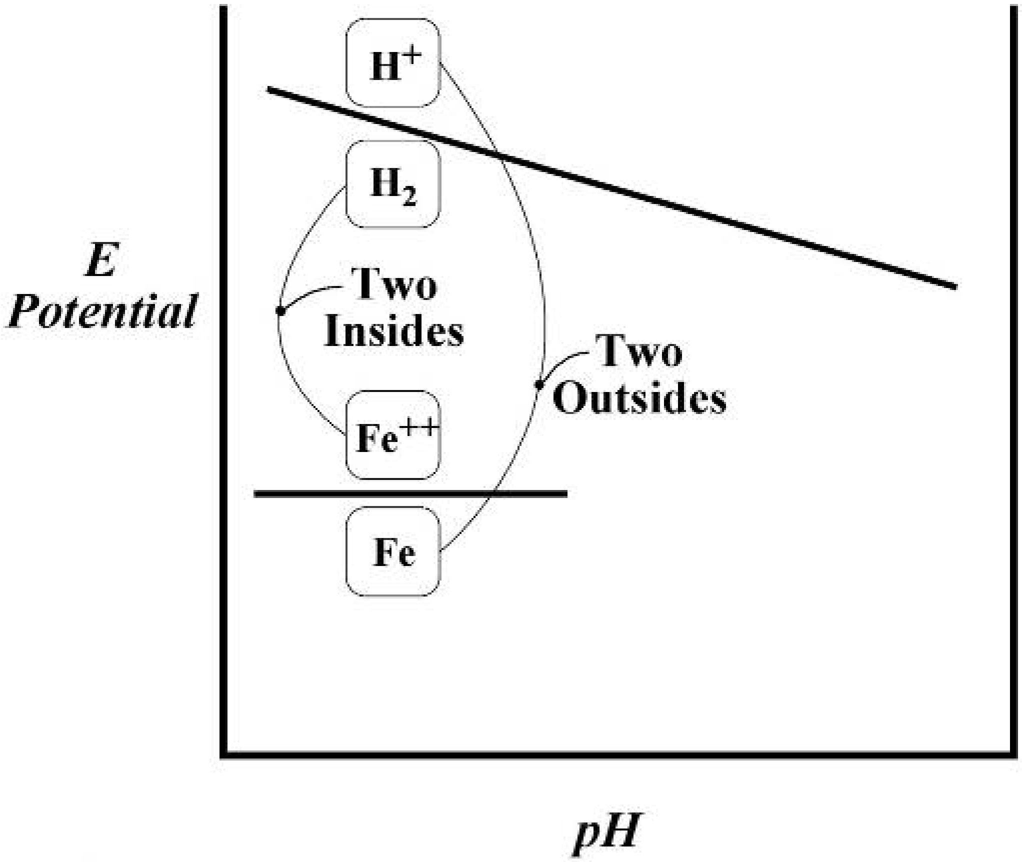

Since:

$$Fe + 2H^+ \longrightarrow Fe^{++} + H_2$$

Then:

The two outside species combine to produce two inside

Combining the water and metal equilibria gives boundaries of aerated and deaerated solutions. No potentials can exist outside these boundaries.

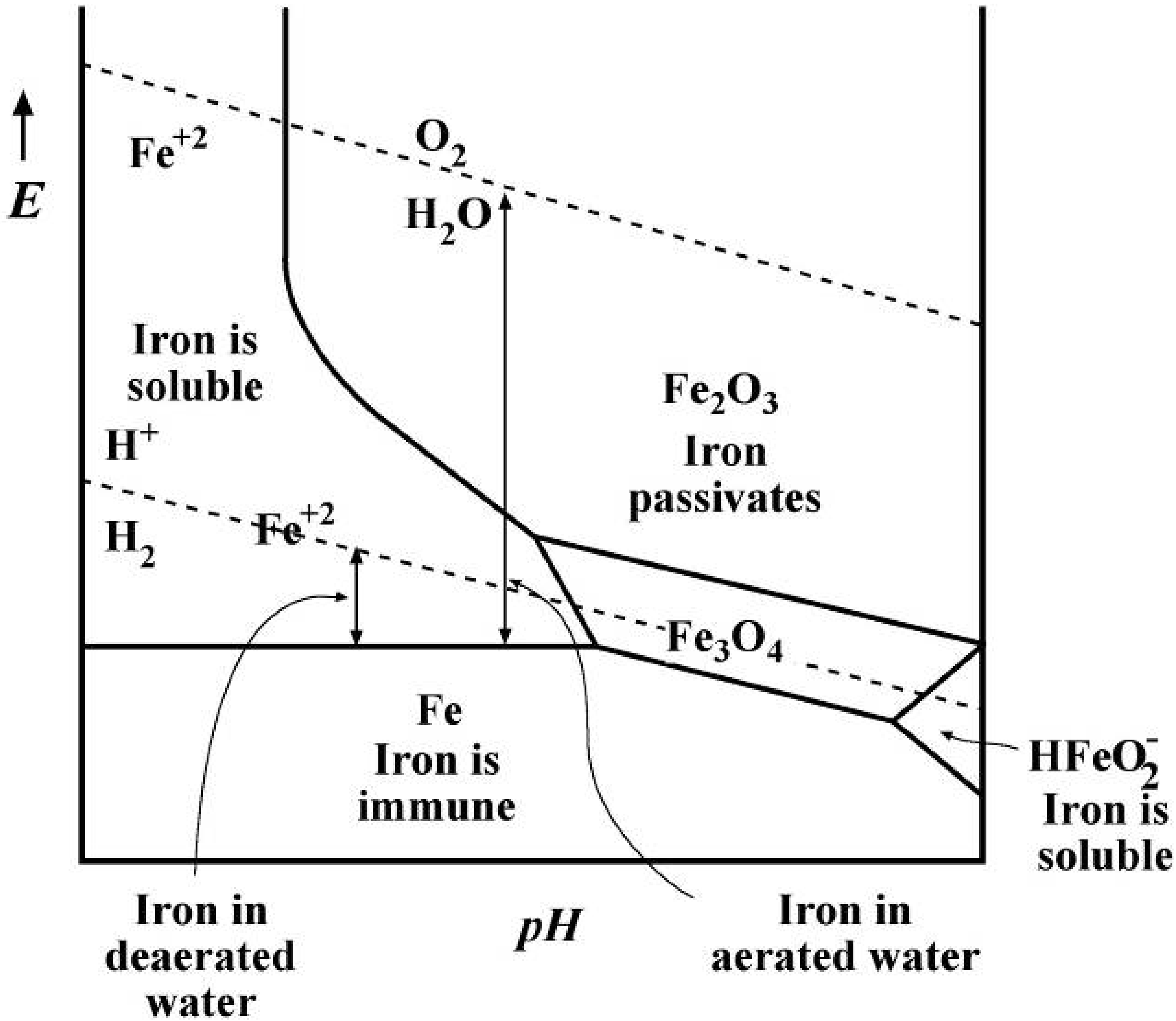

Hydrogen is added to the primary system where no boiling occurs and is stripped out in the secondary system by boiling; these changes produce important effects on the potentials and the corresponding corrosion of these two system.

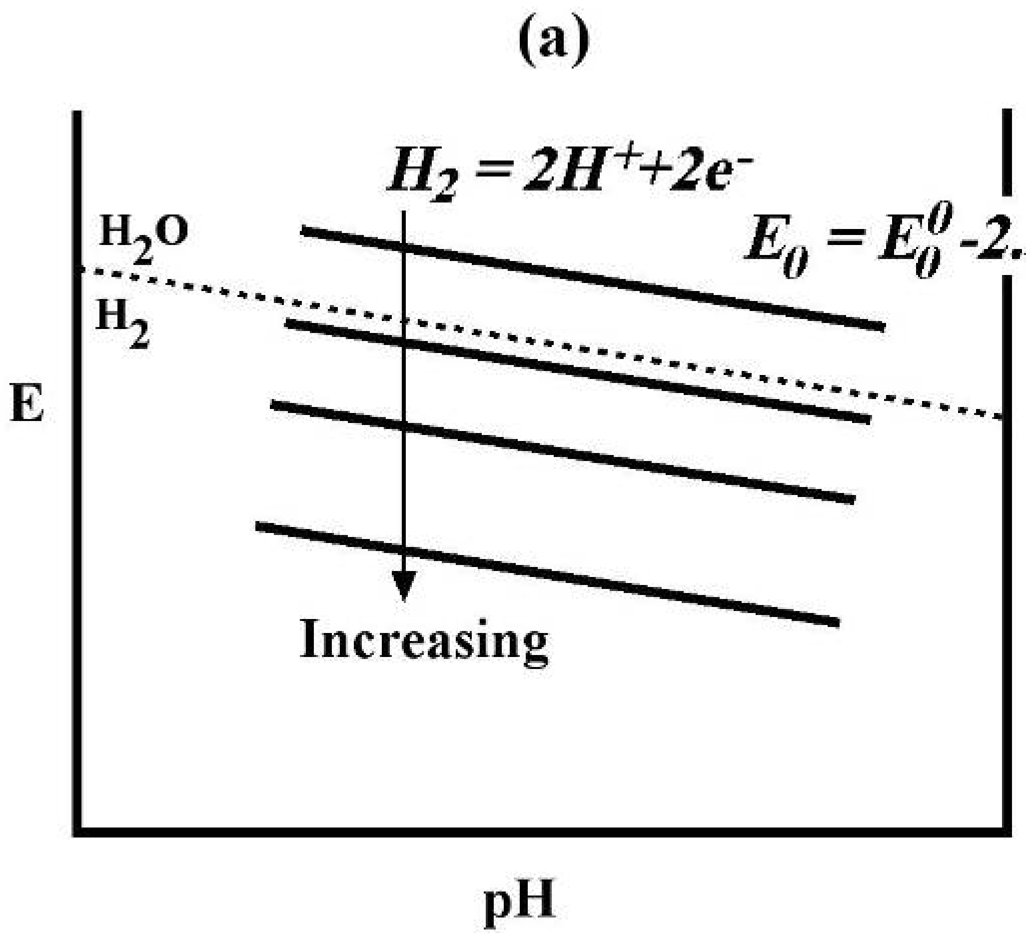

$$E_0 = E_0^0 - 2.3\frac{RT}{nF}pH - 2.3\frac{RT}{nF}\log P_{H_2}$$

Increasing hydrogen lowers potential

Put Both Half Cells on a Map of Potential and pH

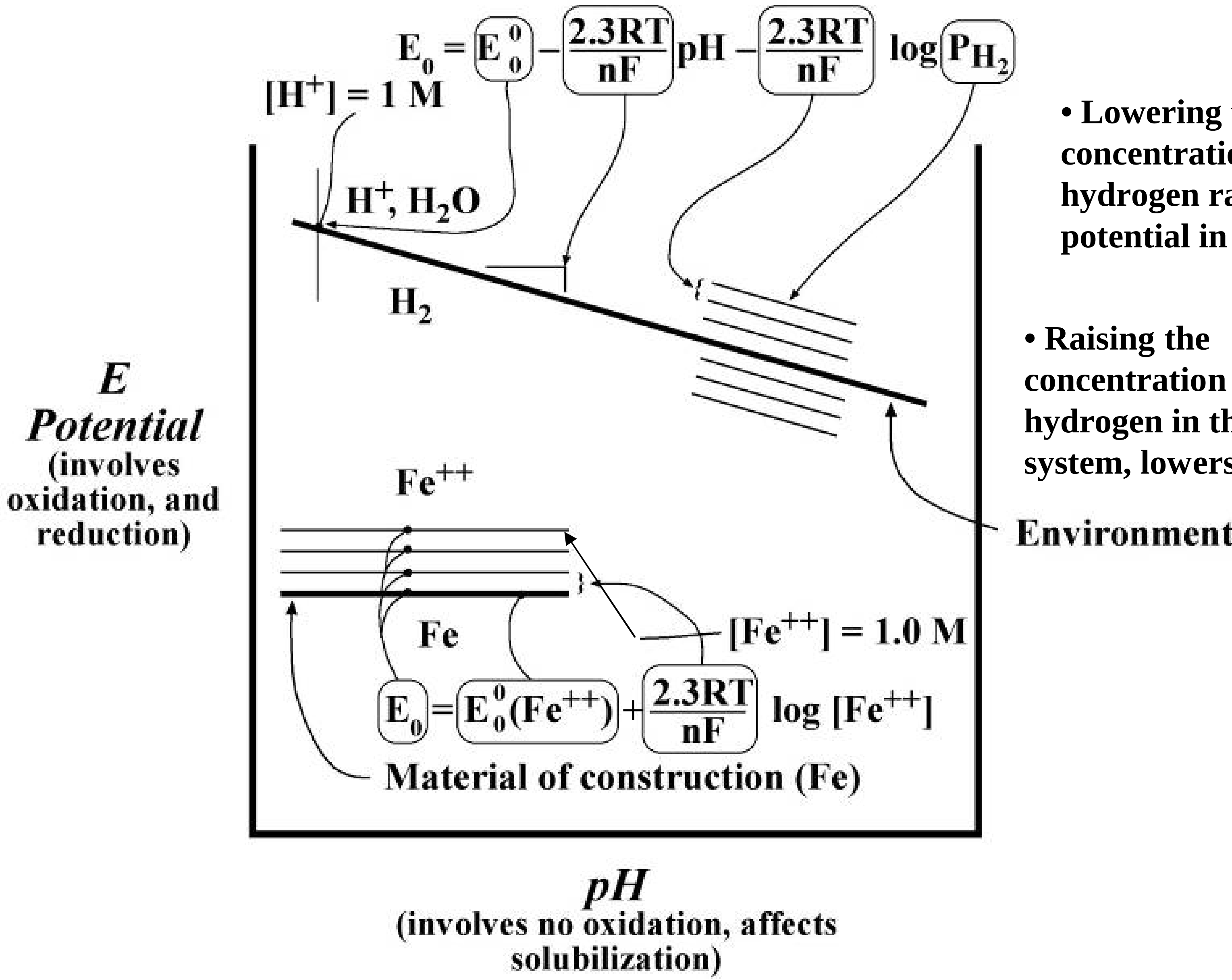

- Lowering the concentration of hydrogen raises the potential in SGs.

- Raising the concentration of hydrogen in the primary system, lowers the potential

E-pH for iron from RT to 300°C

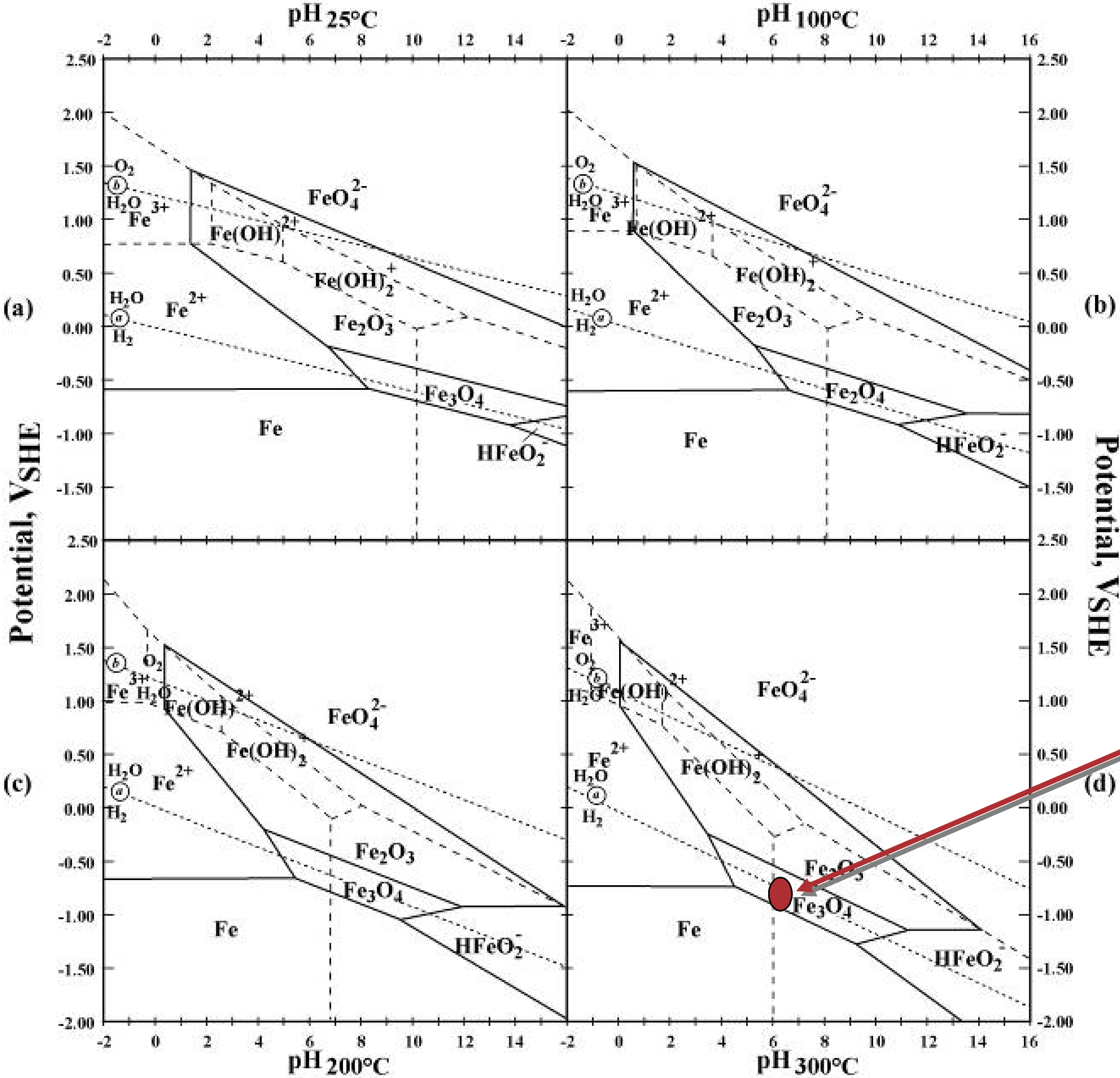

About the primary system

Potential Affects Environmental Reactions

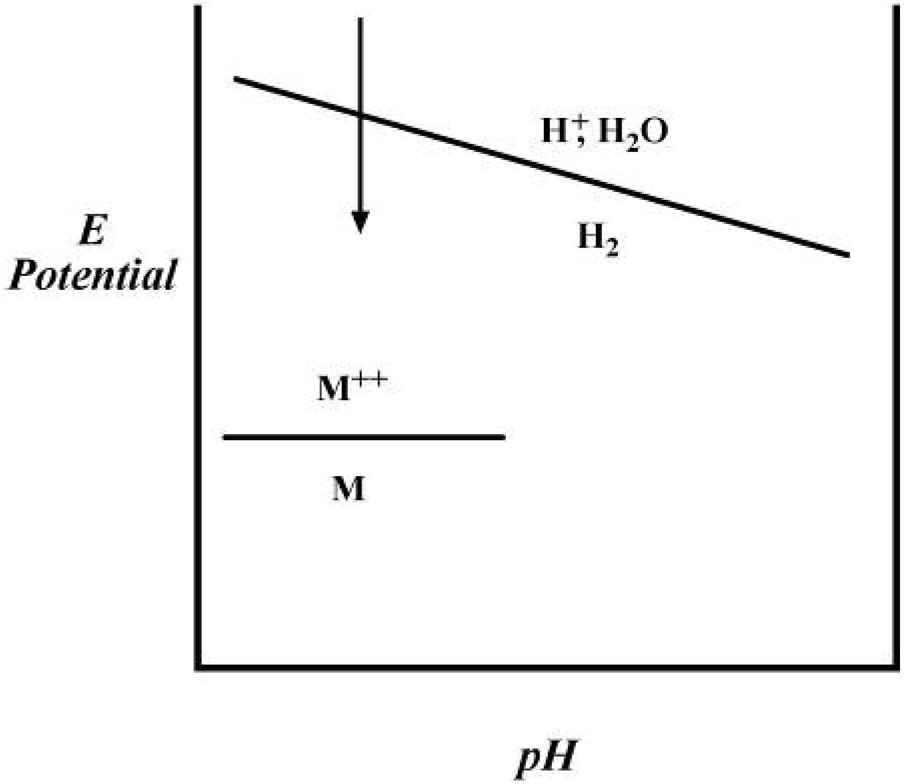

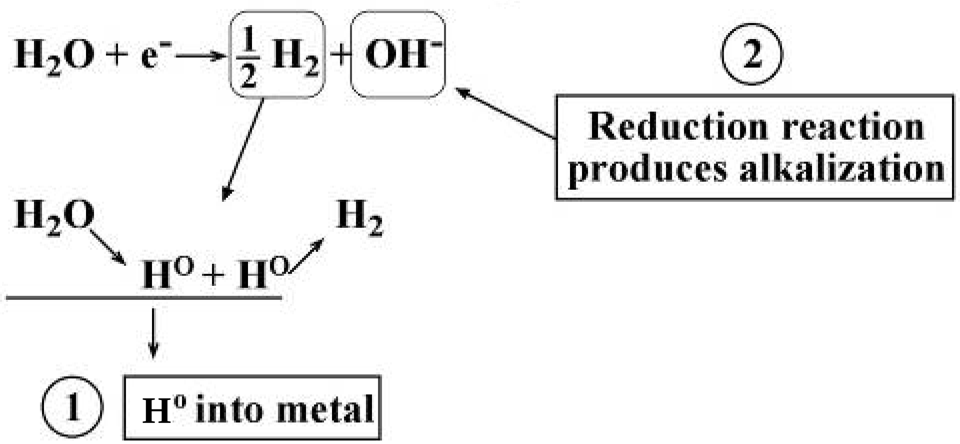

Equilibria at 300°C and $pH_{300°C}$ = 6

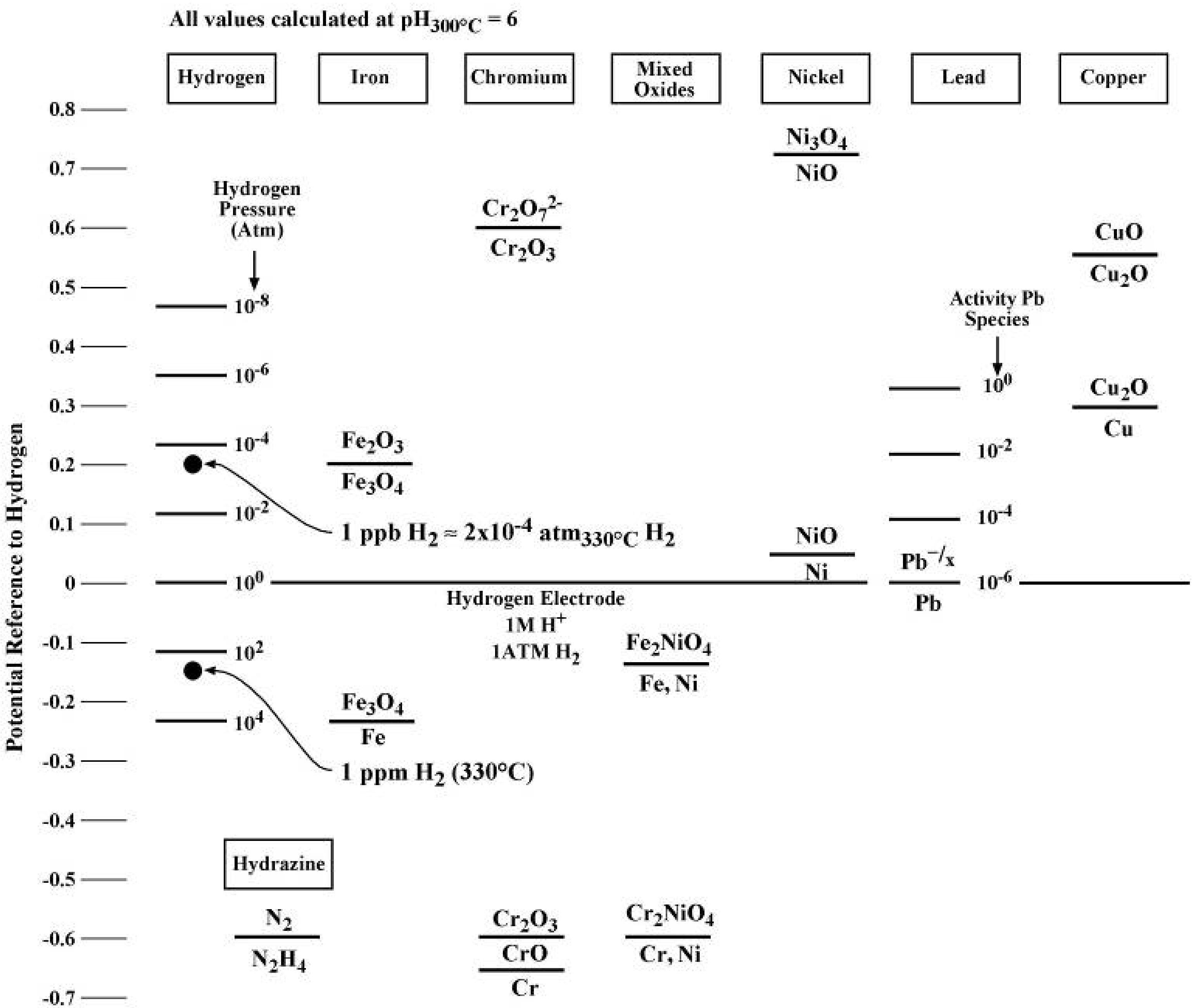

E-pH diagrams for water

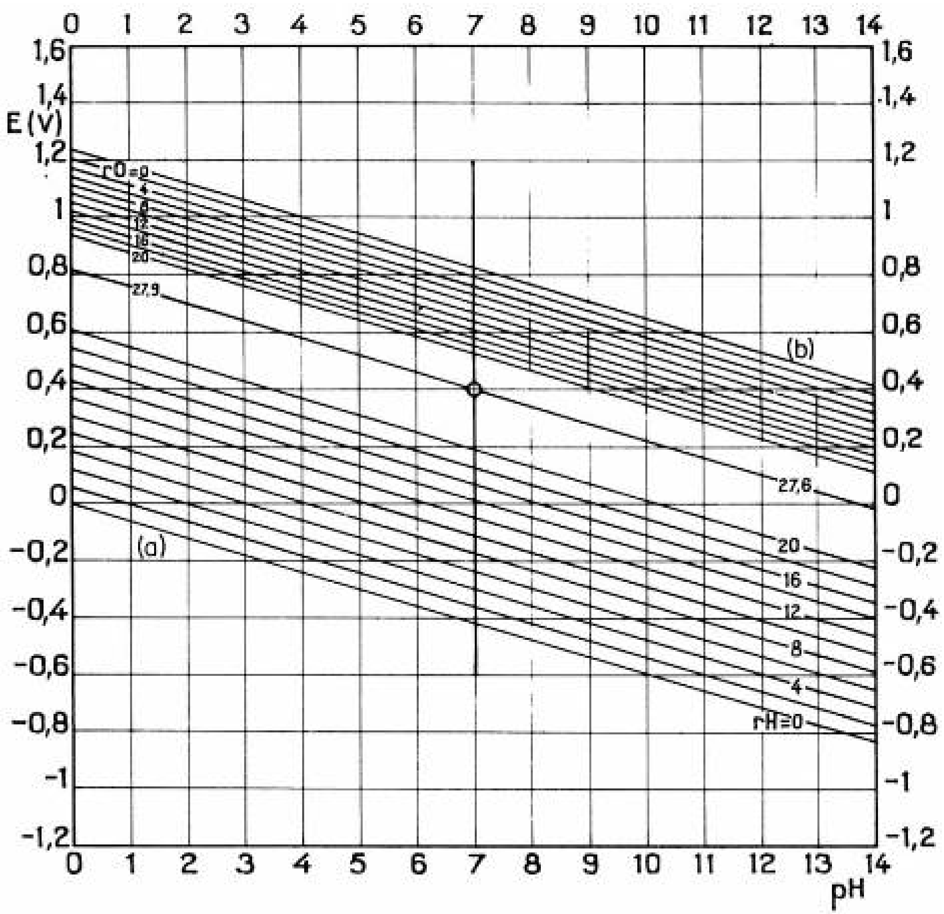

FIG. 5. rH and rO of aqueous solutions.

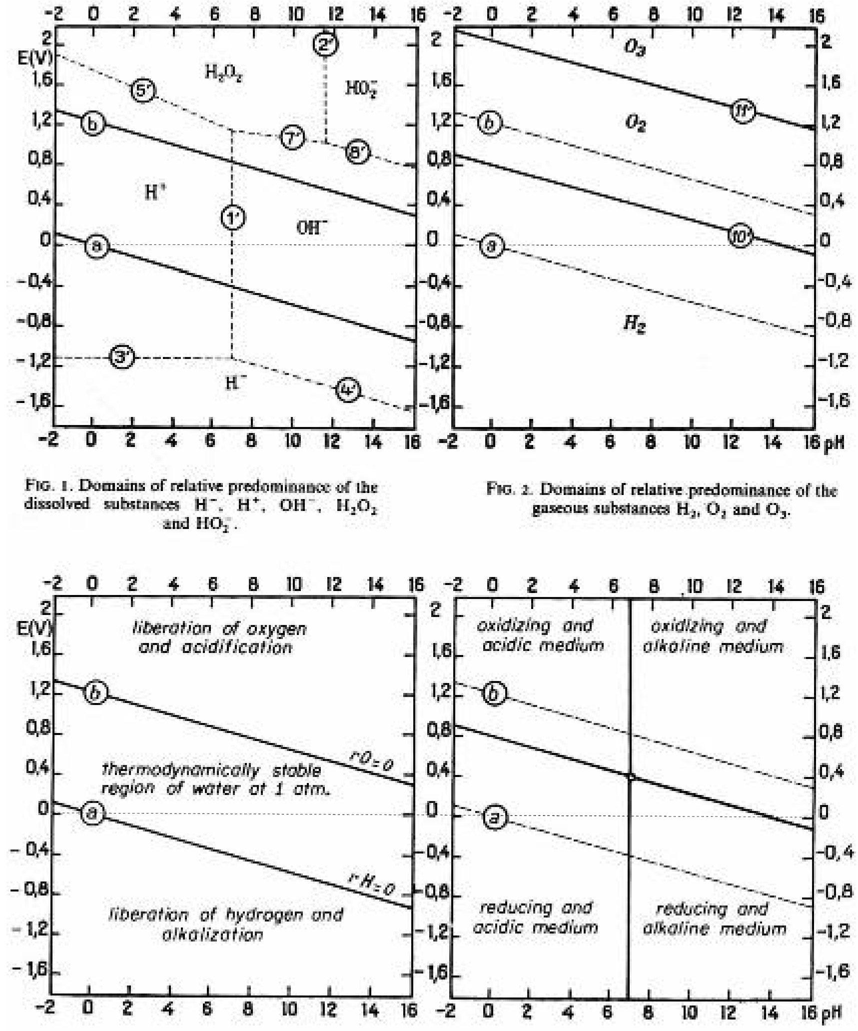

FIG. 1. Domains of relative predominance of the dissolved substances H^-, H^+, OH^-, H_2O_2 and HO_2^-.

FIG. 2. Domains of relative predominance of the gaseous substances H_2, O_2 and O_3.

FIG. 3. Domain of thermodynamic stability of water under 1 atm. pressure.

FIG. 4. Acid, alkaline, oxidizing and reducing media.

E-pH diagrams for important materials and their significance in LWRs

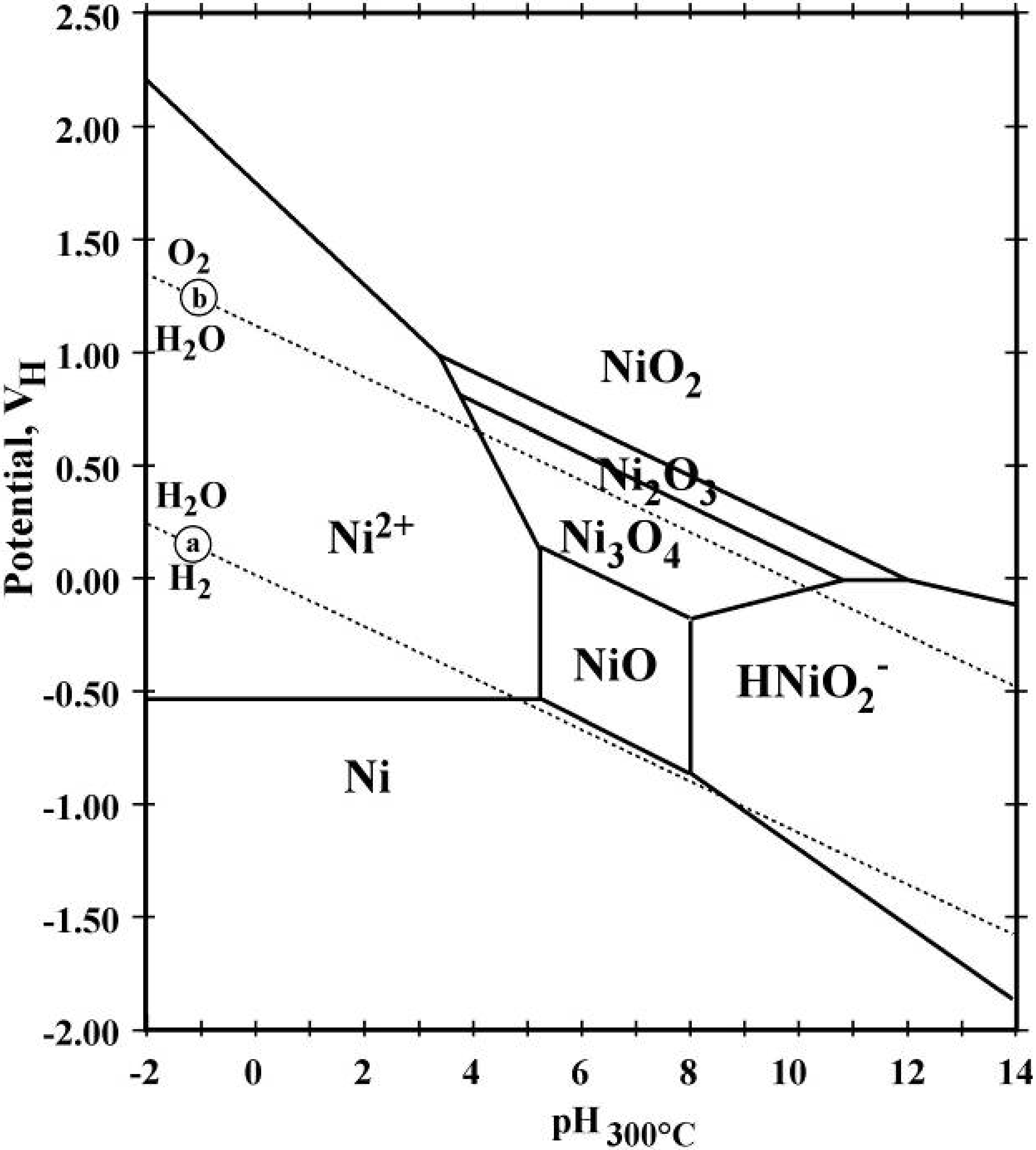

[Based on Chen and Miglin]

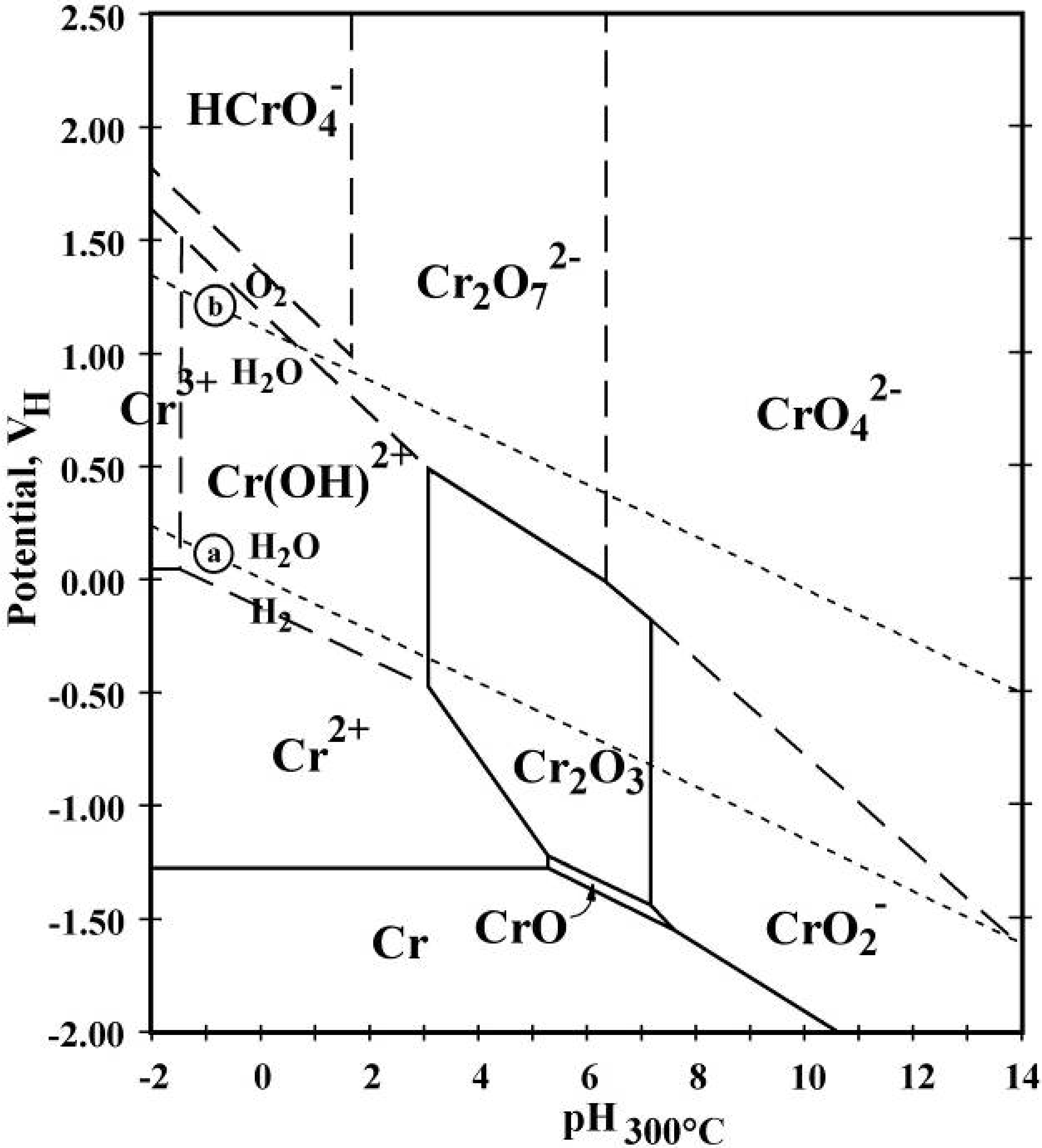

[Based on Chen and Miglin]

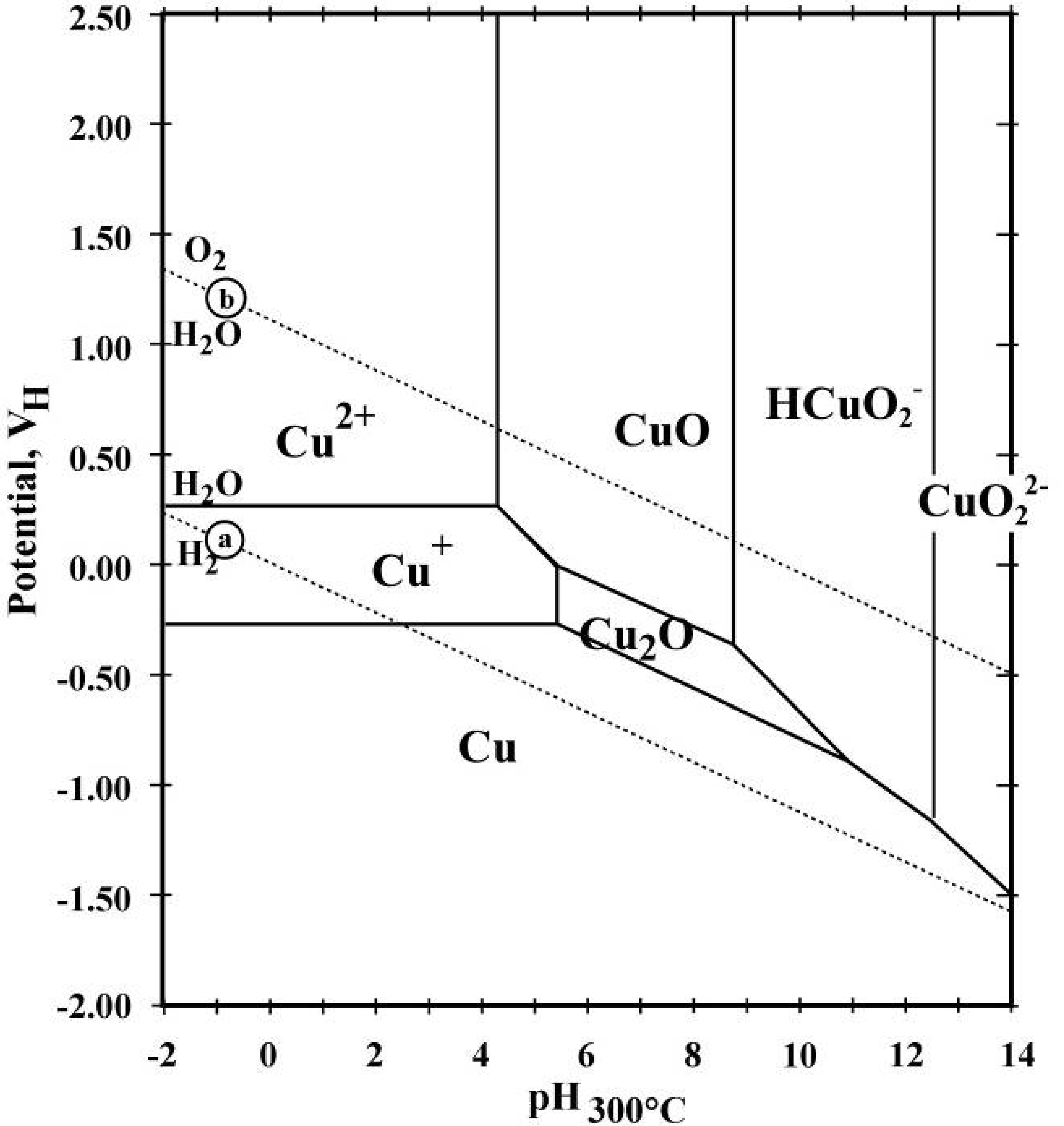

[Based on Chen and Miglin]

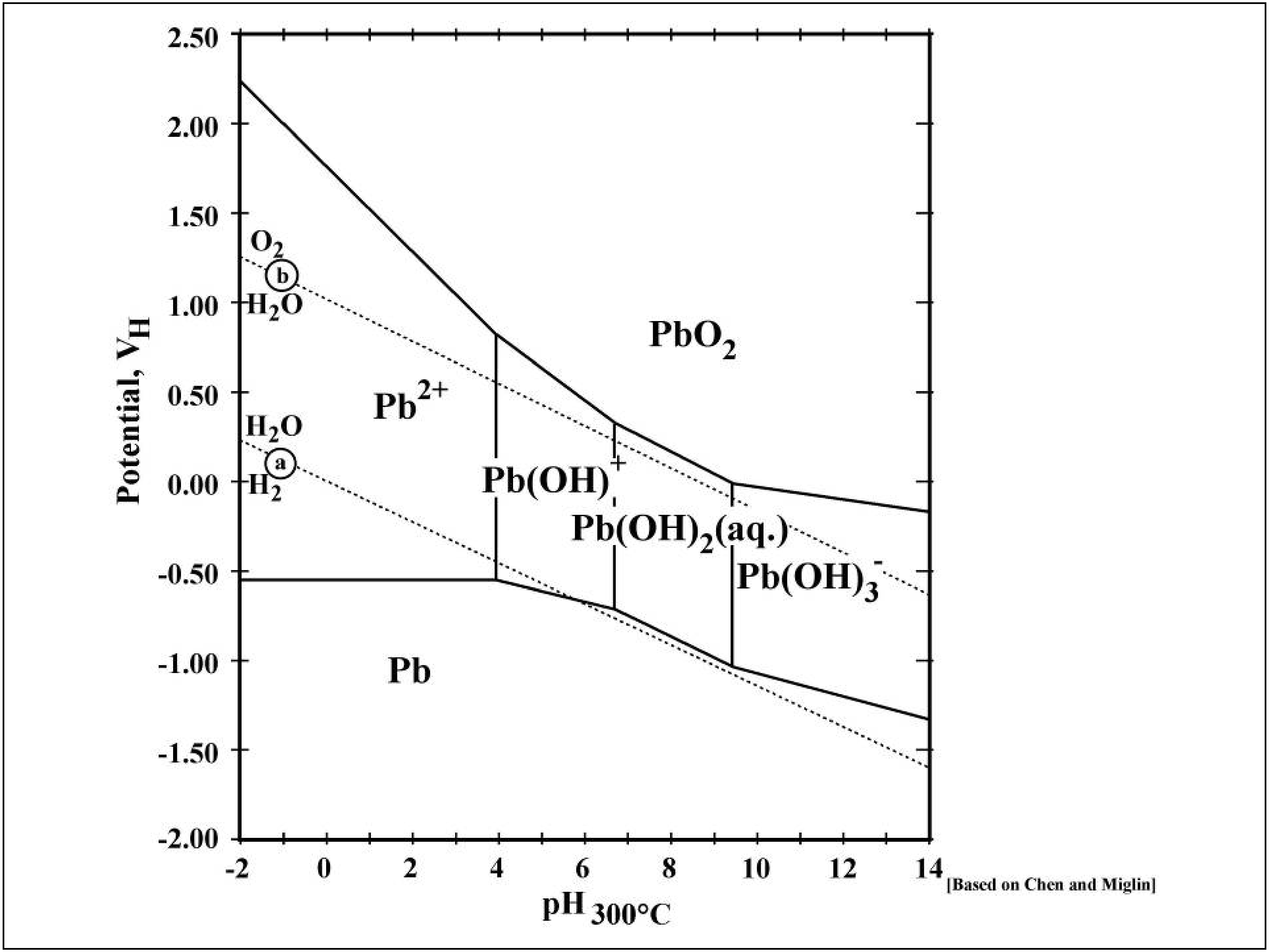

2.50
2.00
1.50
1.00
0.50
0.00
-0.50
-1.00
-1.50
-2.00
Potential, V_H
O_2
b
H_2O
H_2O
a
H_2
PbO_2
Pb^{2+}
$Pb(OH)^+$
$Pb(OH)_2$(aq.)
$Pb(OH)_3^-$
Pb
-2
0
2
4
6
8
10
12
14
pH 300°C
[Based on Chen and Miglin]

E-pH of titanium at RT and 300°C

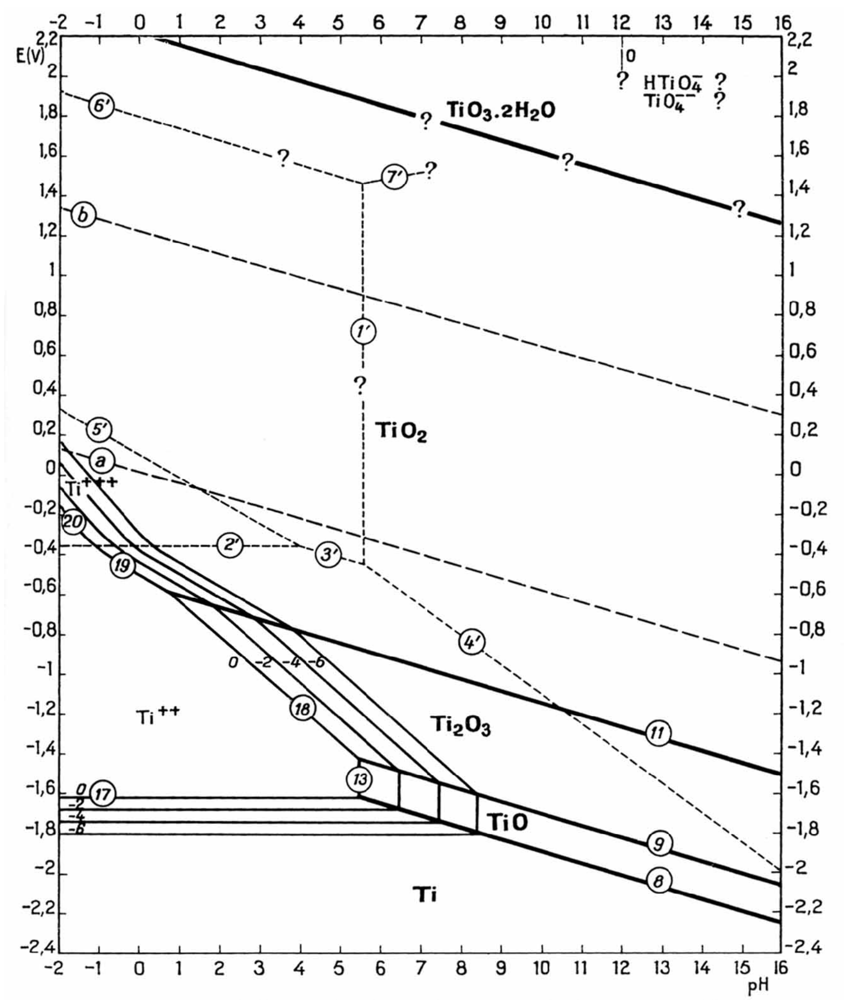

FIG. 1. Potential–pH equilibrium diagram for the system titanium–water, at 25°C. [Figure established by considering, as derivatives of tri- and tetravalent titanium, the anhydrous oxides Ti_2O_3 and TiO_2 (rutile).]

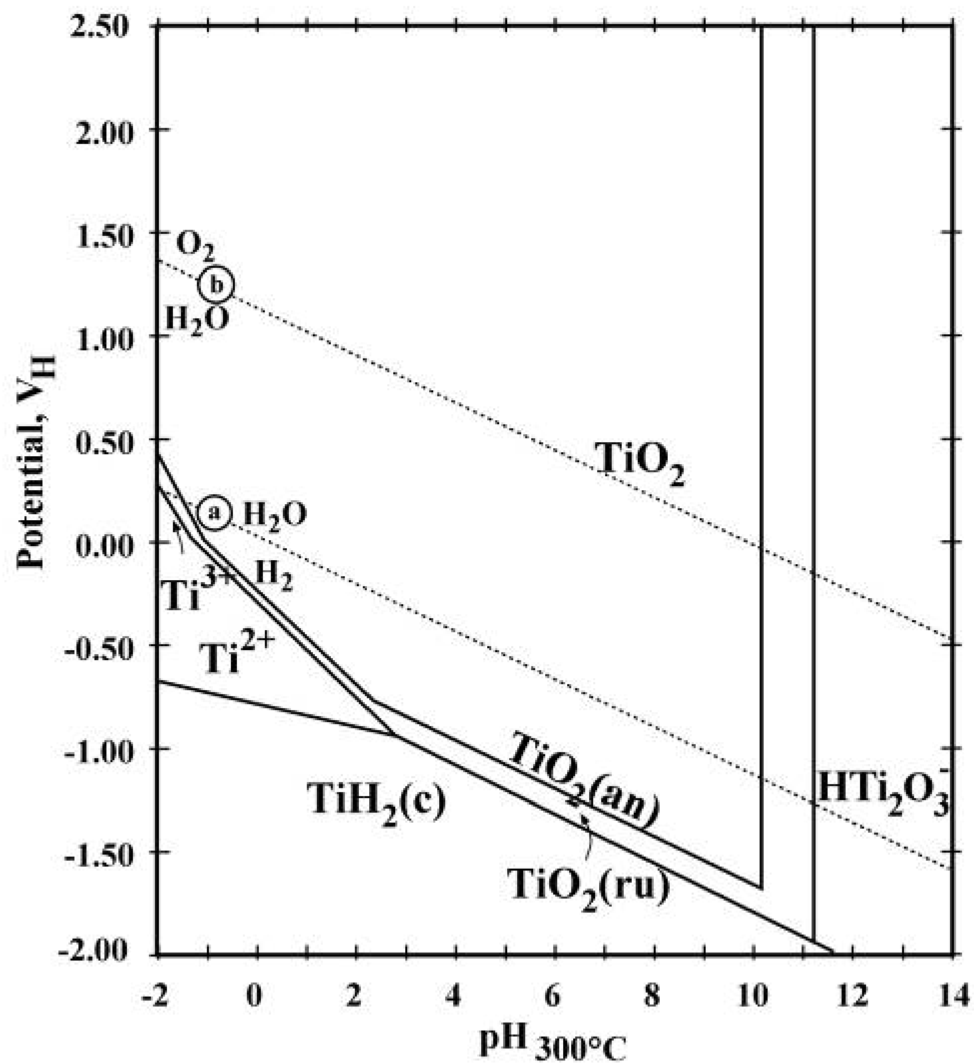

Chen and Miglin

Mo is totally soluble in practical ranges of pH and potential

Fuel cladding of Zr exhibits broad range of stability

E-pH diagrams for Mo and Zr at 25°C

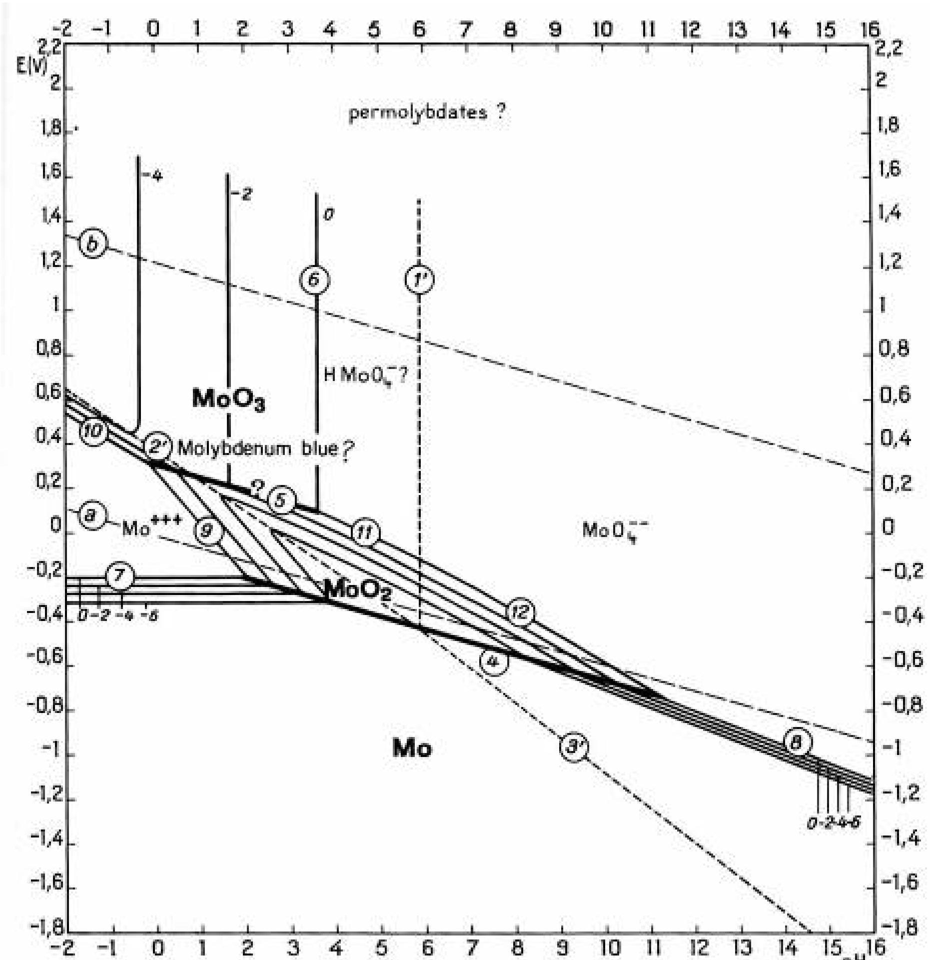

FIG. 1. Potential–pH equilibrium diagram for the system molybdenum–water, at 25°C.

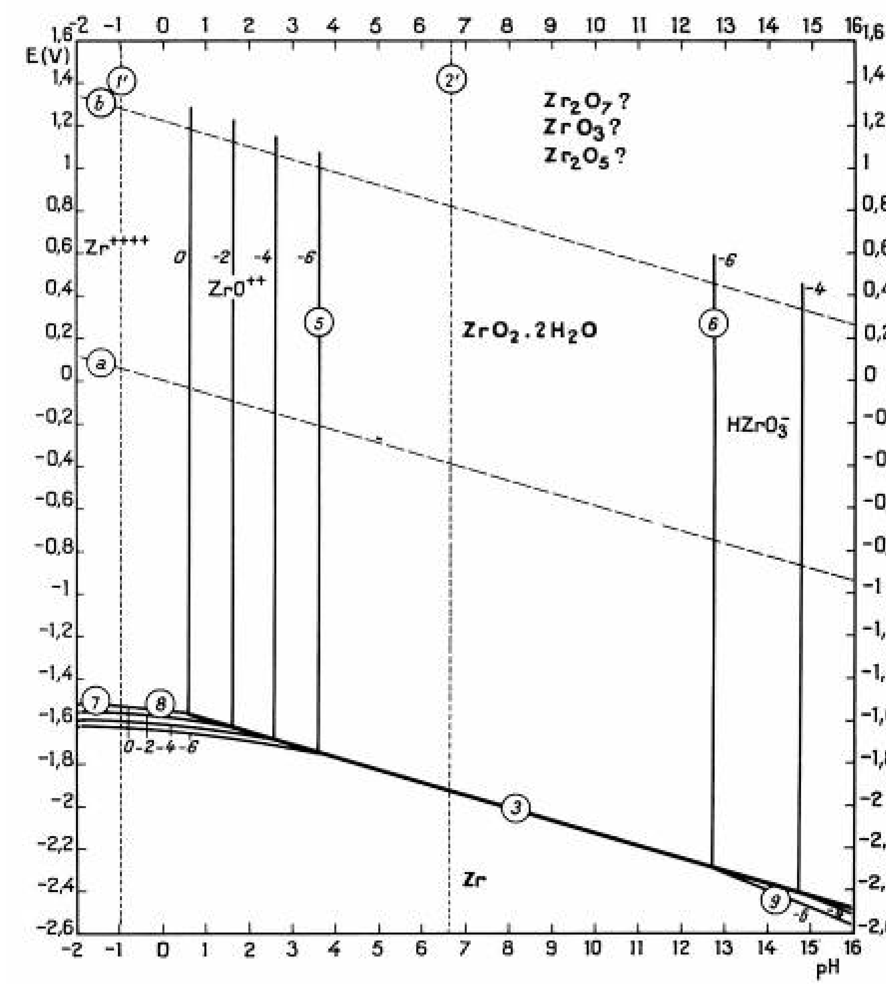

FIG. 1. Potential–pH equilibrium diagram for the system zirconium–water, at 25°C. (Considering $ZrO_2.2H_2O$.)

Comparison of E-pH diagrams for Al and Ti

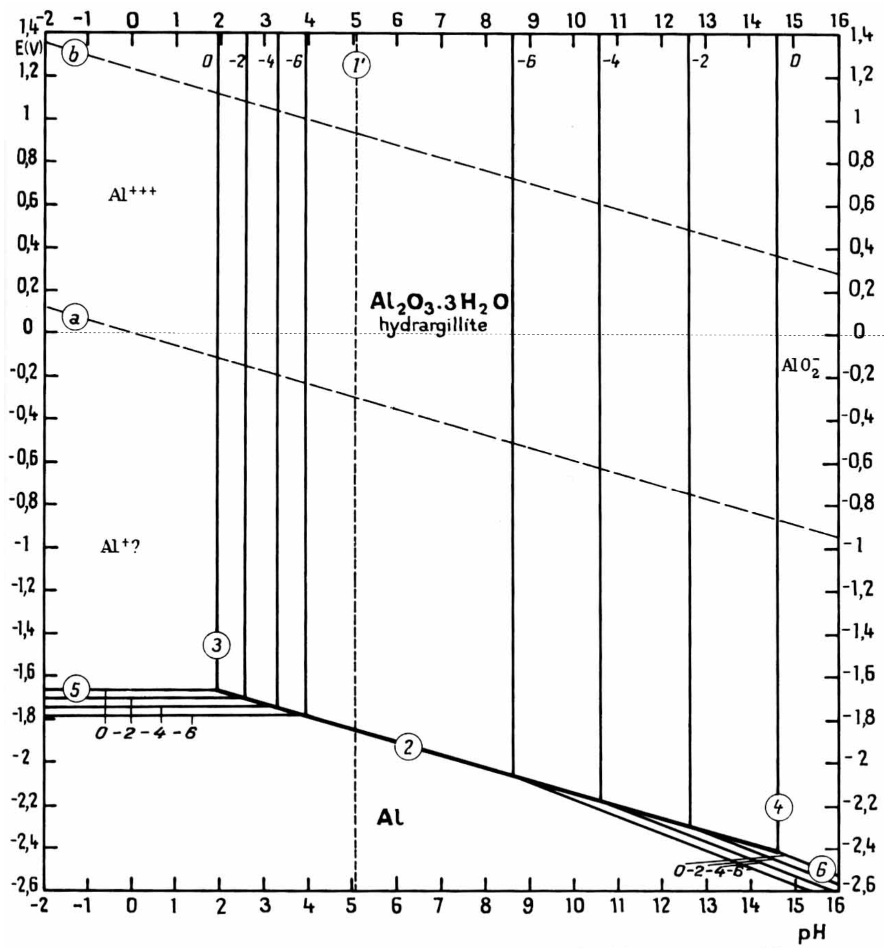

FIG. 1. Potential–pH equilibrium diagram for the system aluminium–water, at 25°C.

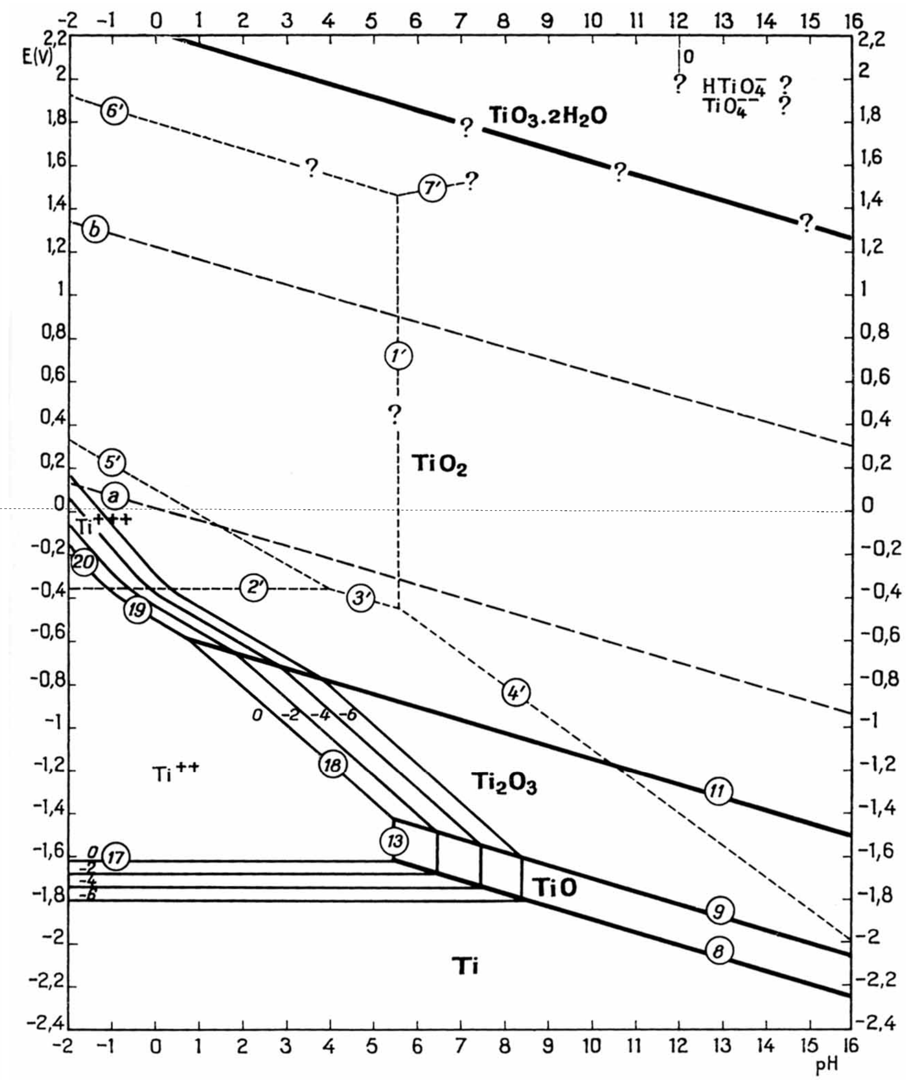

FIG. 1. Potential–pH equilibrium diagram for the system titanium–water, at 25°C. [Figure established by considering, as derivatives of tri- and tetravalent titanium, the anhydrous oxides Ti_2O_3 and TiO_2 (rutile).]

Comparison of E-pH of Al with main alloying elements

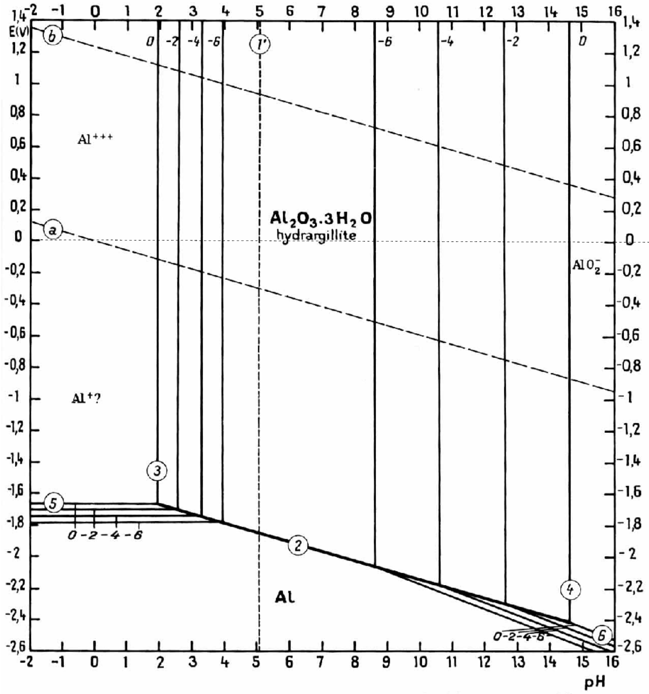

FIG. 1. Potential–pH equilibrium diagram for the system aluminium–water, at 25°C.

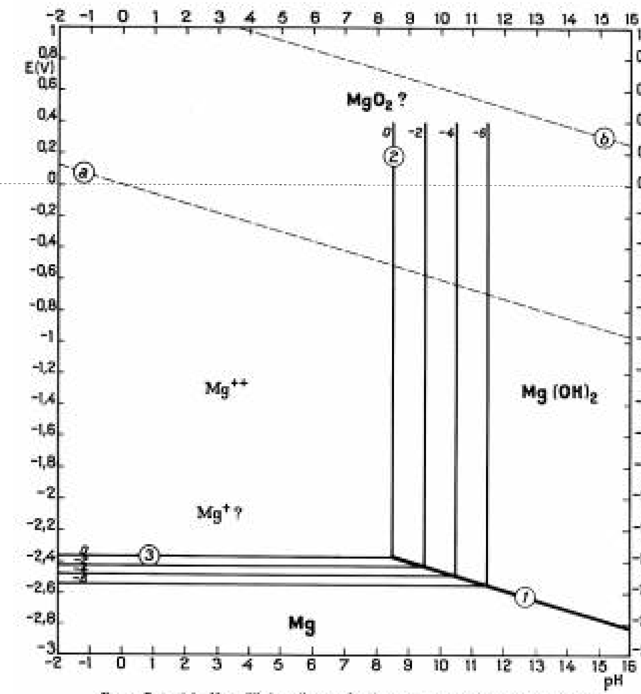

FIG. 1. Potential–pH equilibrium diagram for the system magnesium–water, at 25°C.

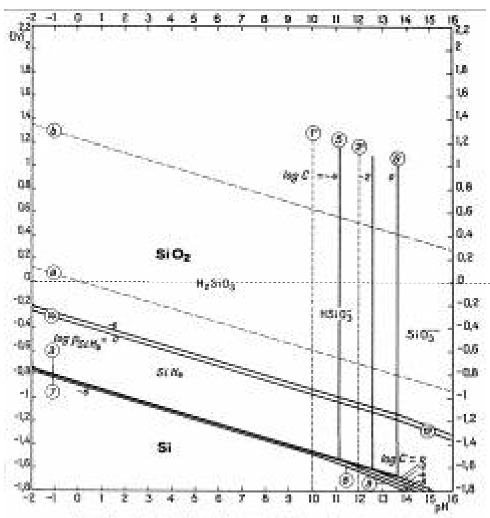

FIG. 1. Potential–pH equilibrium diagram for the system silicon–water, at 25°C. (Considering SiO_2 in the form of quartz. Approximate diagram.)

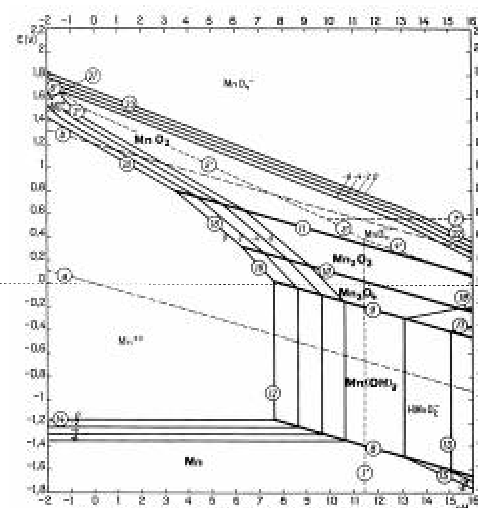

FIG. 1. Potential–pH equilibrium diagram for the system manganese–water, at 25°C. [Considering β-MnO_2 (pyrolusite).]

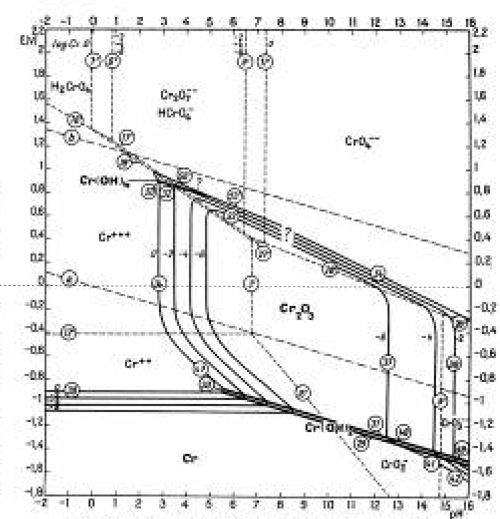

FIG. 5. Potential–pH equilibrium diagram for the system chromium–water, at 25°C. In solutions not containing chloride. (Figure established considering anhydrous Cr_2O_3.)

Comparison of E-pH diagrams of Al with Sn and Pb

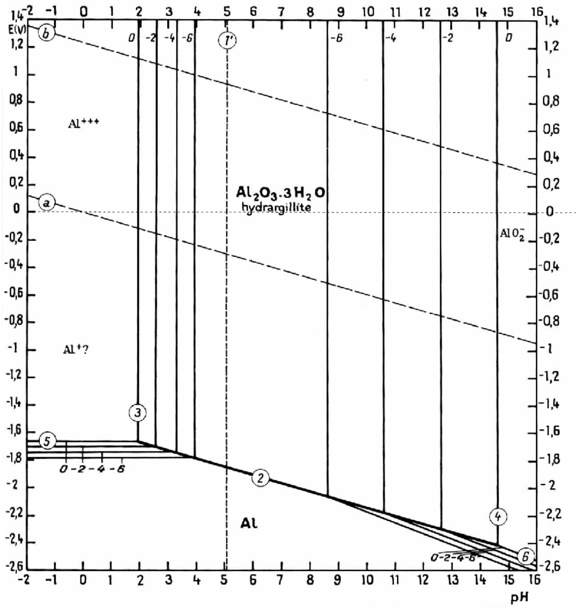

FIG. 1. Potential–pH equilibrium diagram for the system aluminium–water, at 25°C.

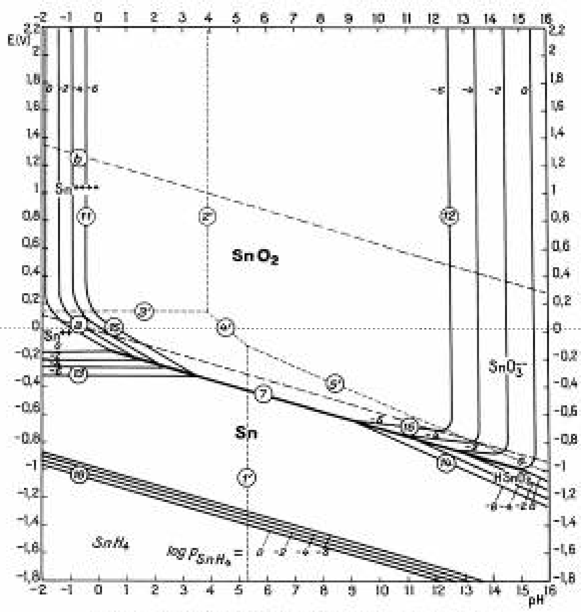

FIG. 1. Potential–pH equilibrium diagram for the system tin–water, at 25°C. (Considering the anhydrous oxides SnO and SnO_2.)

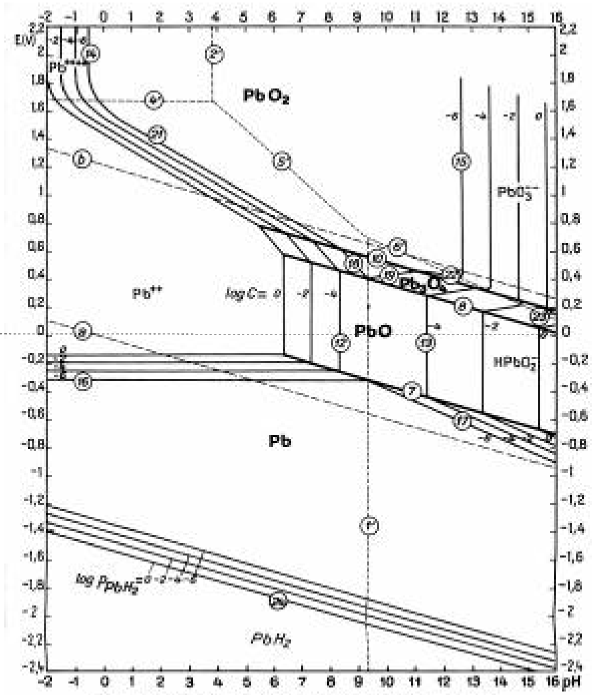

FIG. 1. Potential–pH equilibrium diagram for the system lead–water, at 25°C.

E-pH at 300°C compared

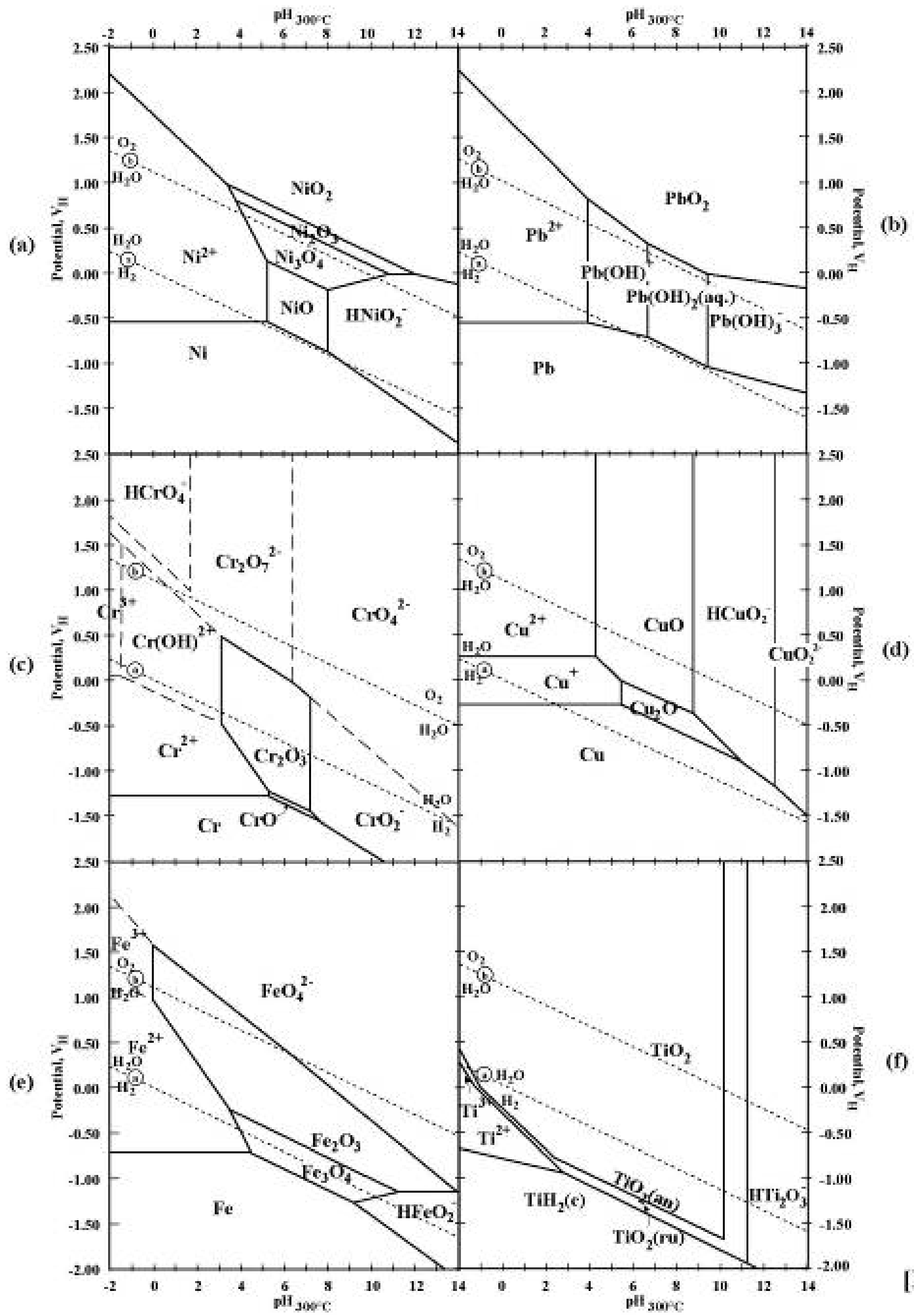

[Based on Chen and Miglin]

Conventions for E-pH in aqueous solutions

1. When metal is soluble, it is taken as corroding; when the metal is noble, it is taken as not corroding; when the metal forms an insoluble compound, it is taken as passive.

2. While the E-pH plots are constructed in terms of half cells, the chemical reactions are actually with respect to the hydrogen equilibrium with one atmosphere of gaseous hydrogen and unity H^+. A hydrogen reference cell is assumed although any equilibrium half cell can be used if properly calibrated.

3. The zones of corrosion, passivity, and nobility are taken at 10^{-6}M activity of relevant species.

4. Equilibria can be superimposed on a single diagram to assess whether reactions between the species might occur.

Kinetics and Mixed Electrodes

Equilibrium

1. Stability of materials defined by E, pH

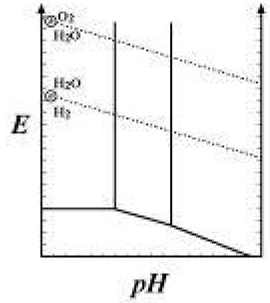

2. Equilibrium half cells can be manipulated

$$\frac{Al^{3+}}{Al} \quad \frac{Fe^{2+}}{Fe} \quad \frac{H^+}{H_2}$$

3. Environment at metal half cells define domain of corrosion

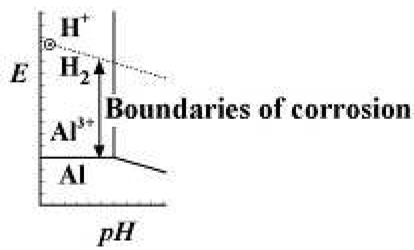

4. Equilibrium definition for kinetic reactions is knowable

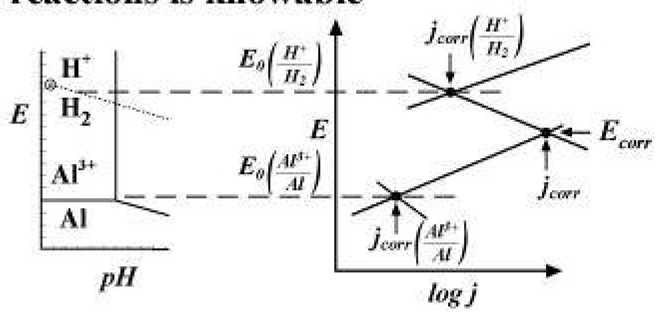

Kinetics

5. Algebraic sum of all current is zero

$$\Sigma\, i_a + \Sigma\, i_c = 0$$

6. Currents relate to areas and current densities

$$\Sigma\, s_a\, j_a + \Sigma\, s_c\, j_c = 0$$

7. # 5 and #6 gives mixed electrode including corrosion potential E_{corr} at corrosion current j_a

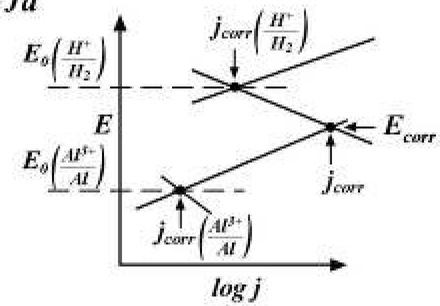

8. Separation of reaction rationalizes local cells

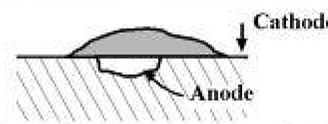

9. Electrochemical reaction includes flow

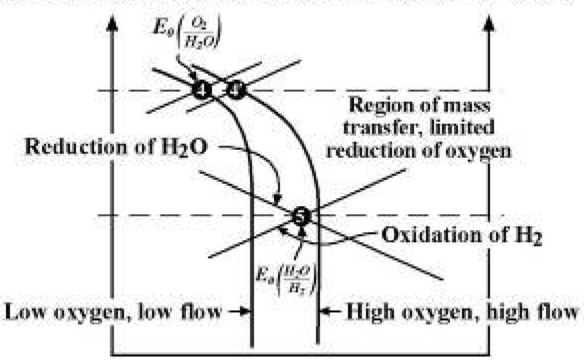

Connection of Electrical Current and Corrosion (Faraday's Law)

Current and weight loss penetration rate, $\dot{x}$ (cm/sec) =

$$\dot{x} = \frac{\underset{\substack{\text{current}\\ \text{coul/sec}}}{i} \quad \underset{\substack{\text{atomic weight}\\ \text{g/mol}}}{A}}{\underset{\substack{\text{surface area}\\ \text{cm}^2}}{s} \quad \underset{\substack{\text{equivalents}\\ \text{per molecular}\\ \text{weight}}}{n} \quad \underset{\substack{\text{Faraday}\\ \text{constant}\\ \text{coul/eq}}}{F} \quad \underset{\substack{\text{density}\\ \text{g/cm}^3}}{\rho}} = \frac{i \times A}{s \times n \times F \times \rho}$$

Corrosion tests verify "corrosion" region

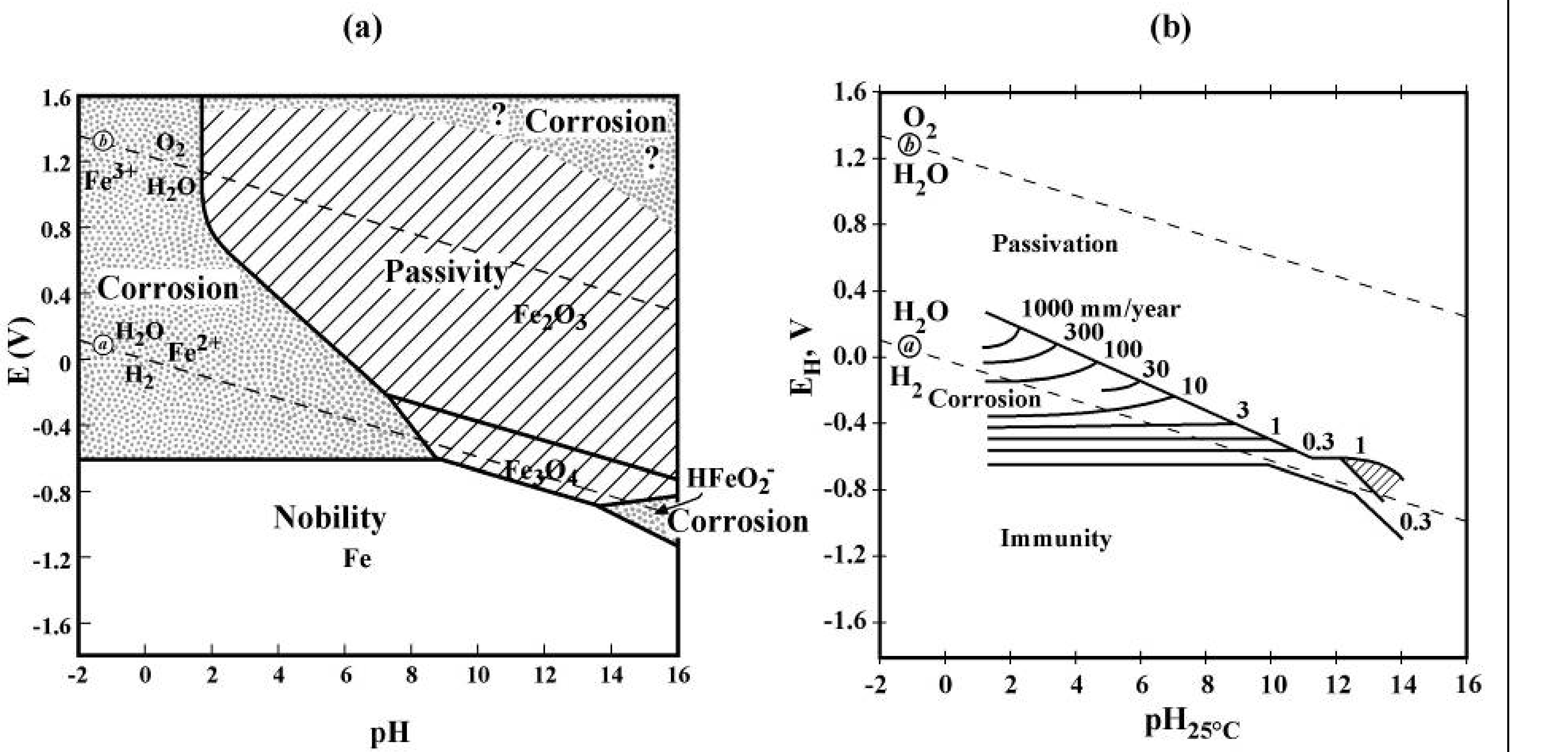

Terminology of Electrochemical Corrosion

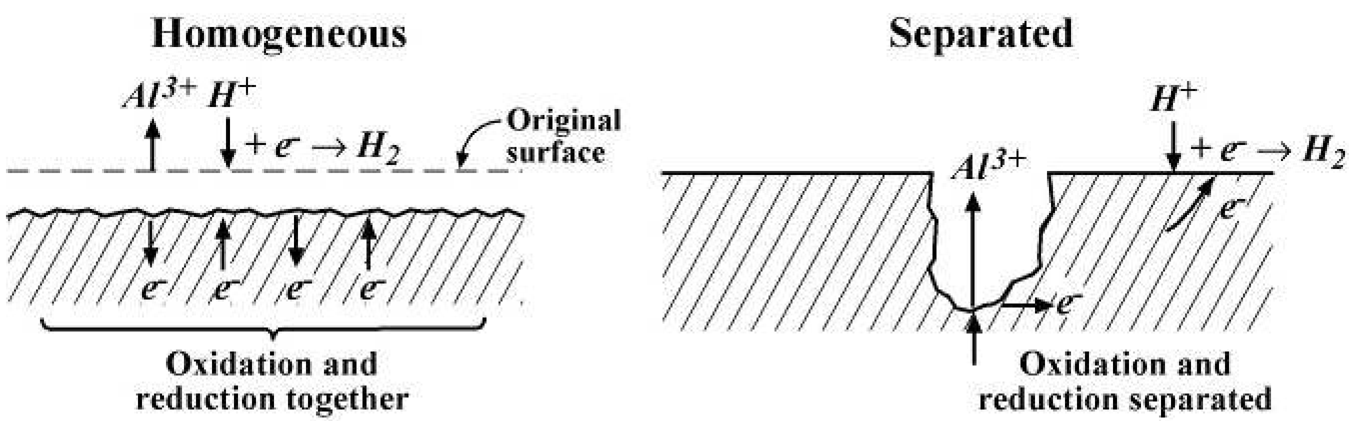

Anode		Cathode
Produce electrons		Absorb electrons
Number of electrons produced	=	Number of electrons absorbed
Oxidize (oxidation)		Reduce (reduction)
Acidify e.g., hydrolyze $2Al^{3+} + 3H_2O \rightarrow Al_2O_3 + 6H^+$		Alkalize e.g., $2H_2O + 2e^- \rightarrow 2OH^- + H_2$

Main Modes of Corrosion (general and separated)

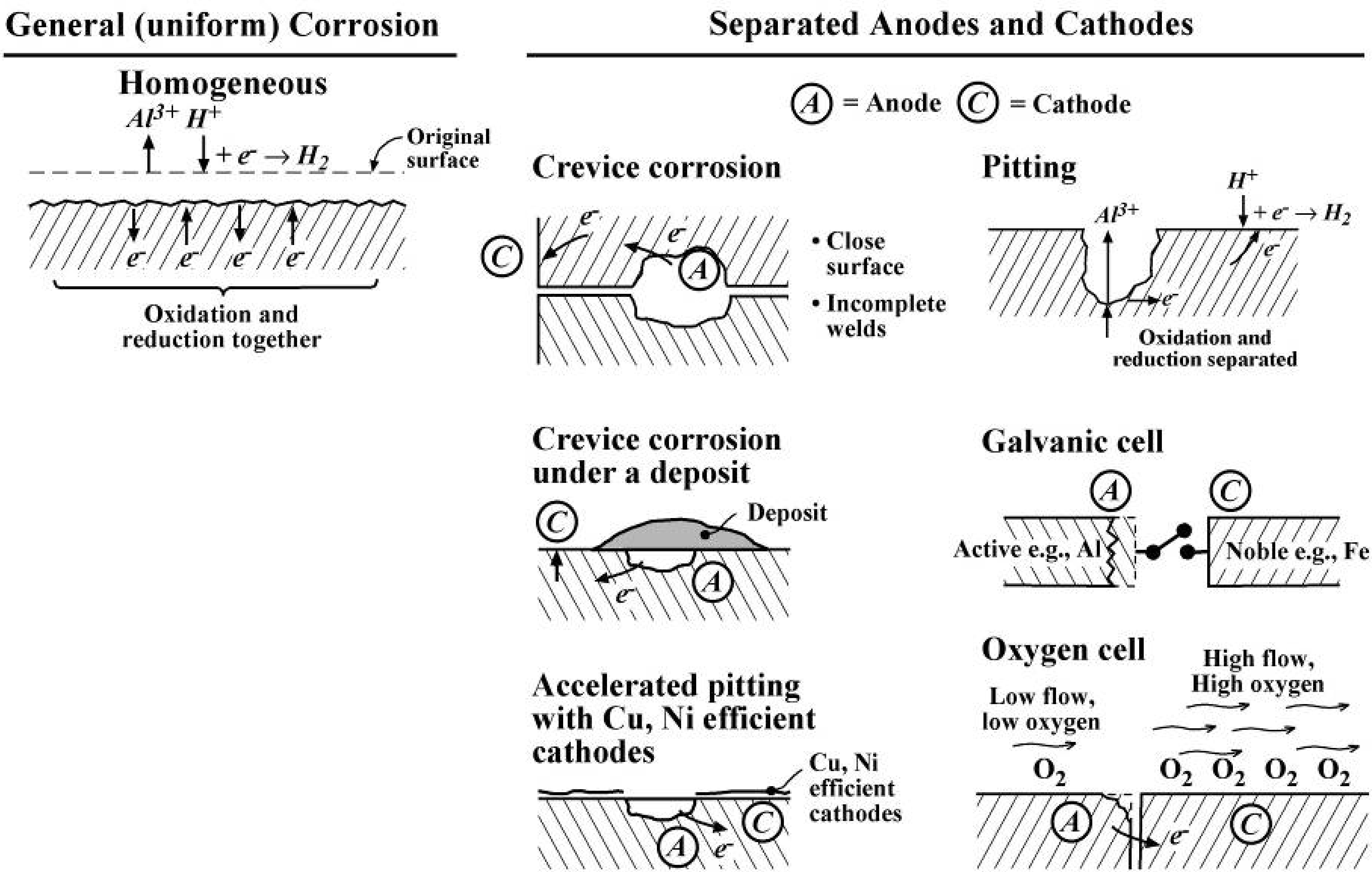

Configuration of chemical reactions and deposit before and after formation of deposit

(a) (b)

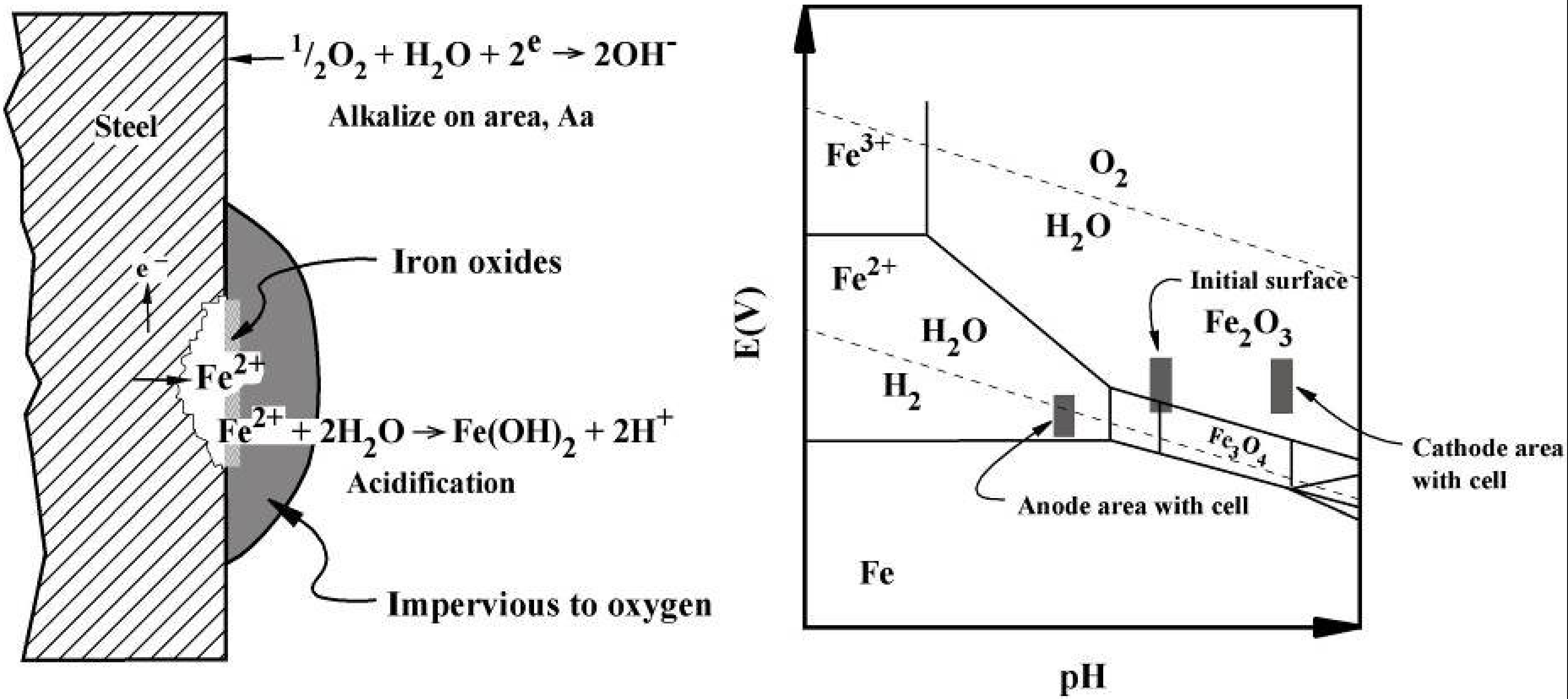

Dominant Dependencies of Electrochemical Reactions

(Not including flow)

A_2
Cu, Ni around pit

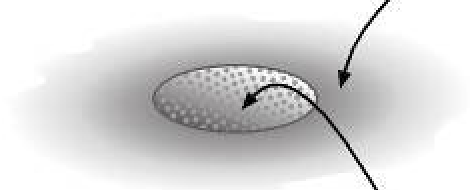

④
A_1
Separated local cells

$$i_{a,\,c} = A\, j_{a,\,c} = A\, j_0\, e^{\alpha \frac{-(E-E_0)}{RT}}$$

② E is potential ($\neq E_0$) - exponential

① A is area of electrons - geometrical, A_2/A_1 is area ratio

③ j_0 is exchange current density

$$\underbrace{10^{-12}\ A/cm^2\ (Pb, Sn) \rightarrow 10^{-5}\ (Fe) \rightarrow 10^{-3}\ (Cu, Ni)}_{H_2 = 2H^+ + 2e^-\ \text{half cell}}$$

1. Area effects are relatively modest
2. E - effects are more important, e.g., oxygen
3. Exchange current is most powerful. Range $10^{-12} \rightarrow 10^{-2}$. The deposition of Cu or Ni changes the efficiency around a pit relative to Al by at least 10^3
4. Separated local cells, A_2/A_1 is $\gg 1$

Thermodynamics bounds kinetics

- **Activated kinetics, film free**
- **Passivating kinetics**
- **Flow limited kinetics**

Equilibrium half cells from the E vs. pH plots define kinetics

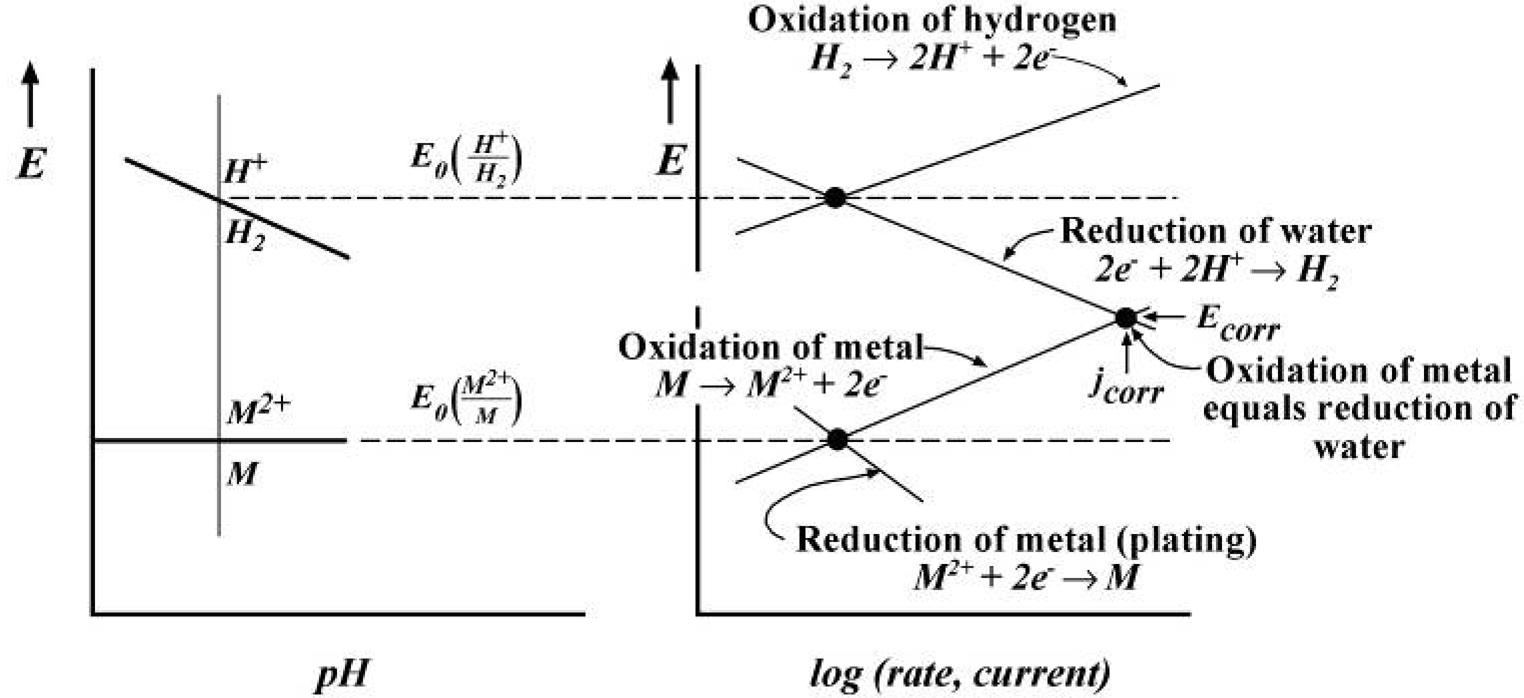

Corrosion Potential, E_c

1. Between two half cell equilibria
2. Defined when rate of electron production of oxidation equals rate of electron absorption by water
3. $E_0\left({}^{M^{++}}\!/\!_{M}\right) < E_c < E_0\left({}^{H^+}\!/\!_{H_2}\right)$

The actual current cannot be measured directly but can be found by extrapolating to E_{corr} from either or both of the anodic or cathodic elements

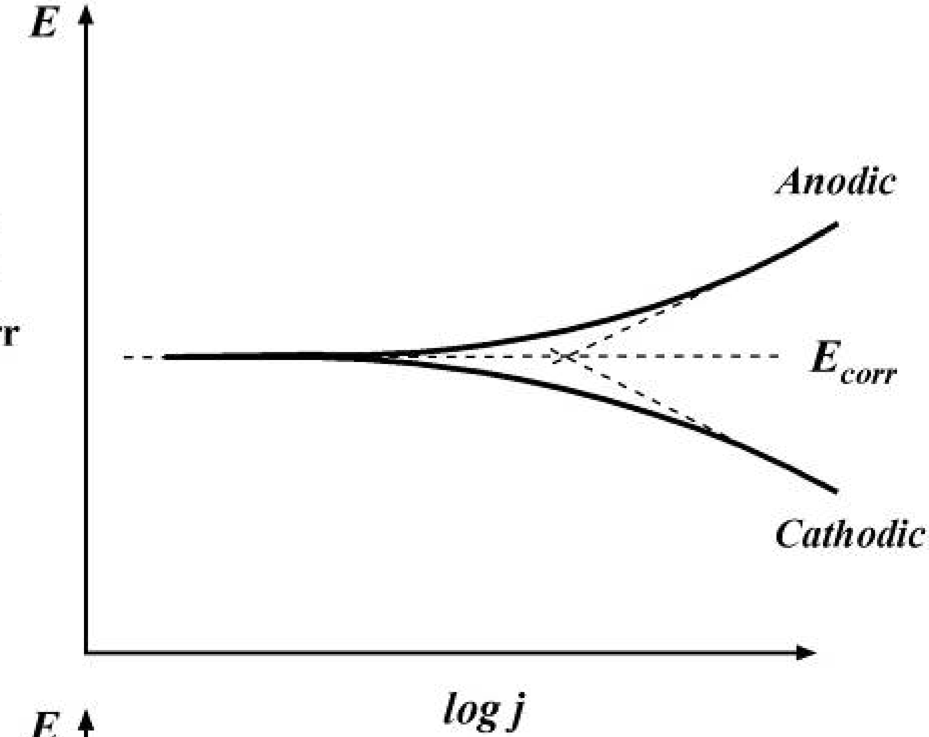

Another apporach is to use the method of "linear polarization" with an extent less than about 10 mV

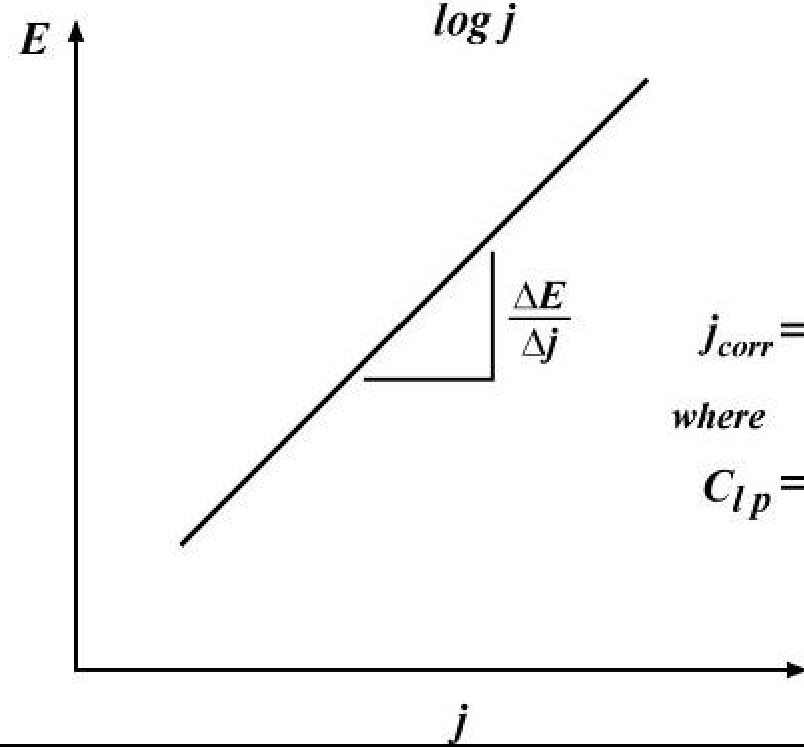

$$j_{corr} = C_{lp} \frac{\Delta E}{\Delta j}$$

where

$$C_{lp} = \frac{1}{\left(\frac{1}{\beta_a} + \frac{1}{\beta_c}\right)}$$

The net current is seen in the system of external measurement and is the difference in current between that produced by the anodic and cathodic reactions

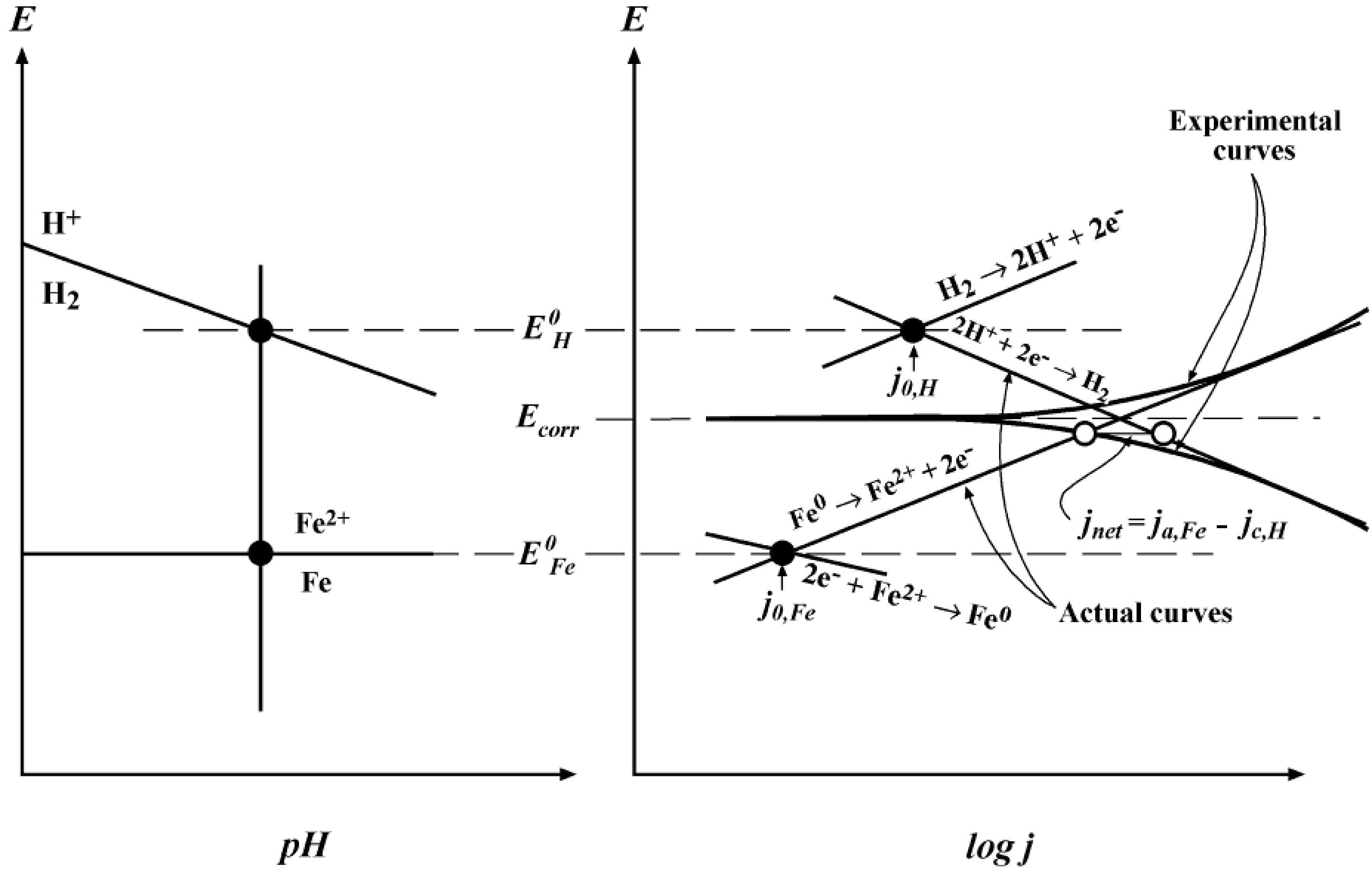

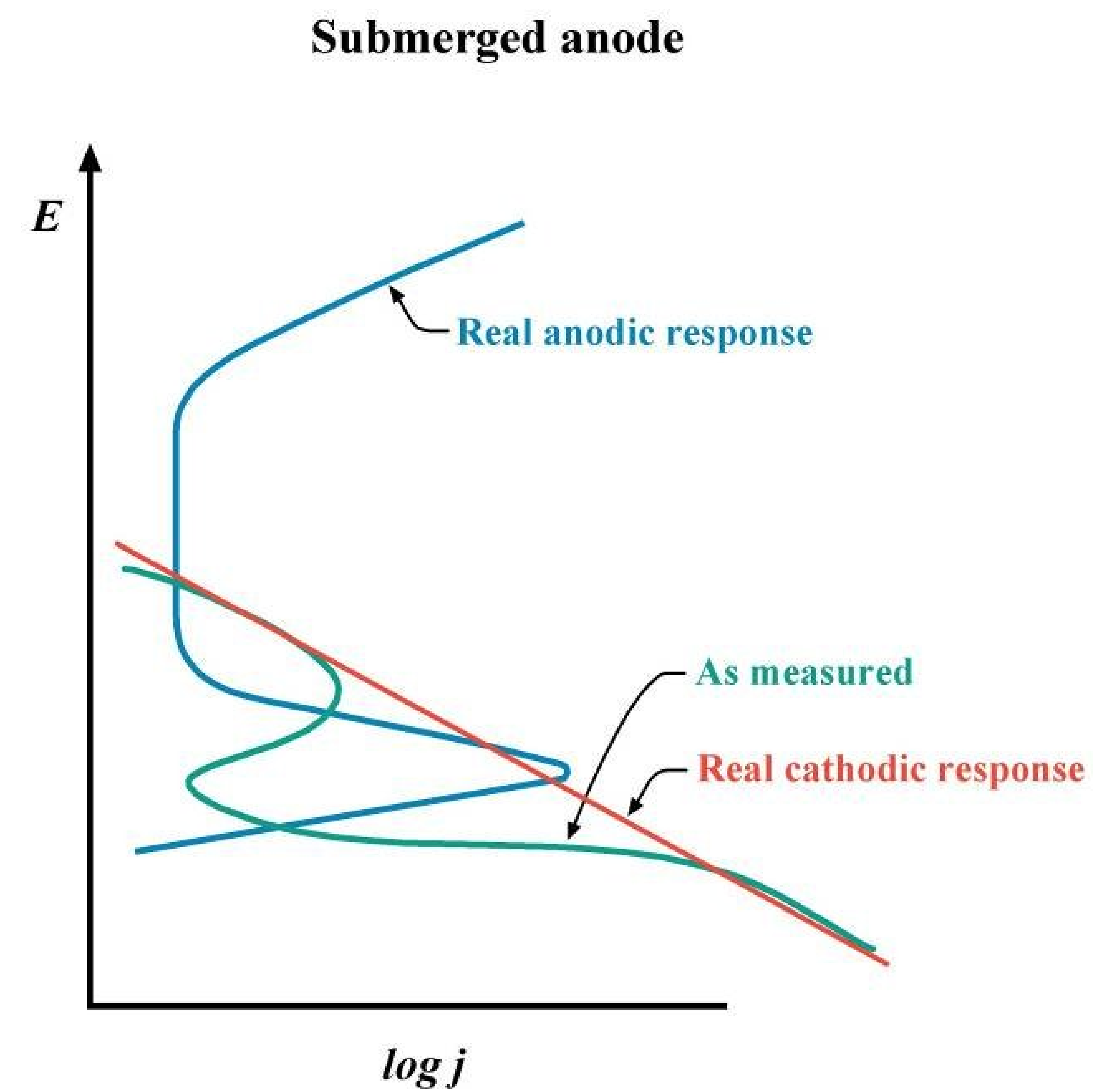
Submerged anode
E
Real anodic response
As measured
Real cathodic response
log j

Activated and passivating kinetics combined "active-passive" behavior

Potential and pH Affect Reactivity and Nature of Surface

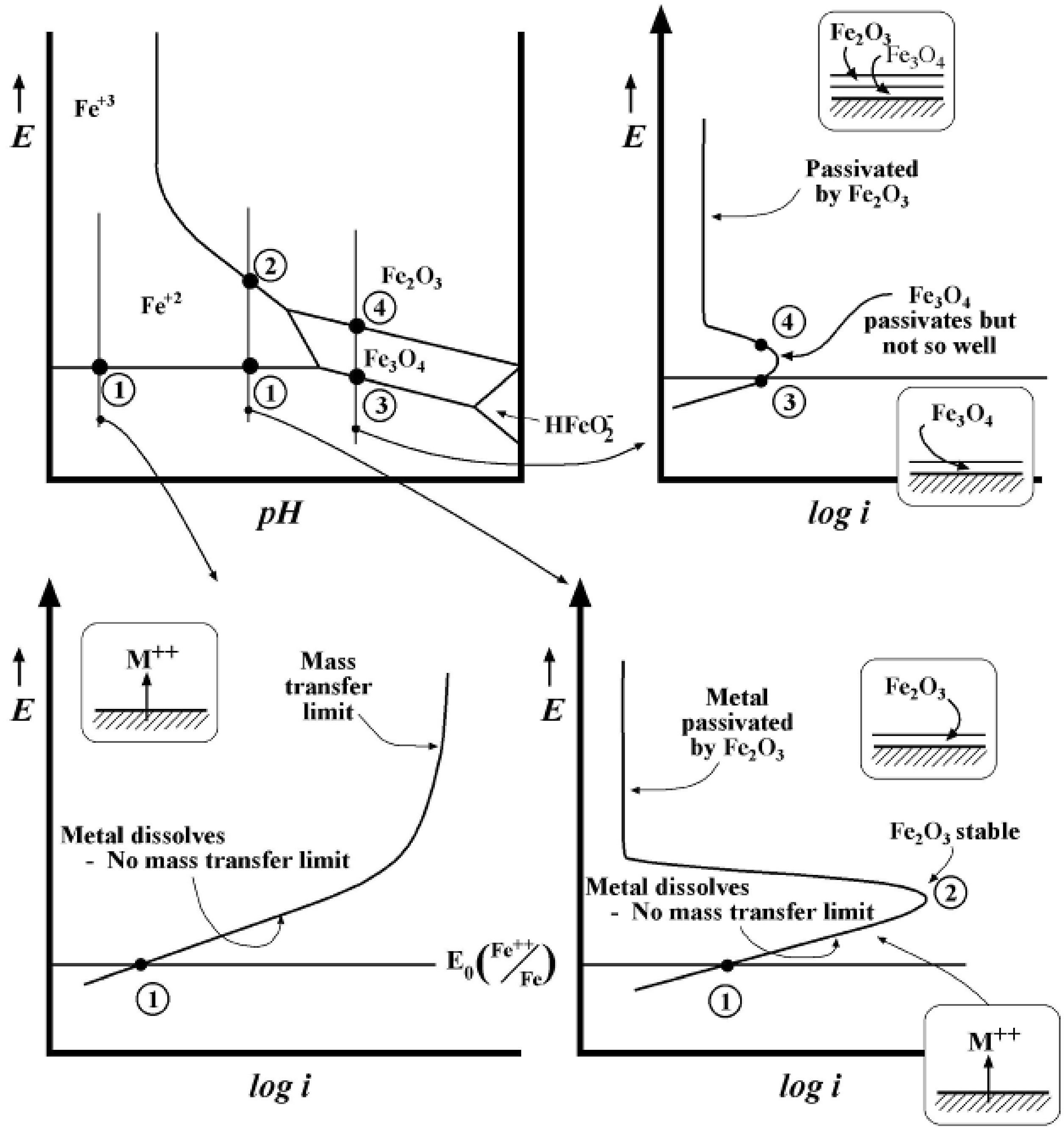

Potential Affects Rates of Electrochemical Reactions

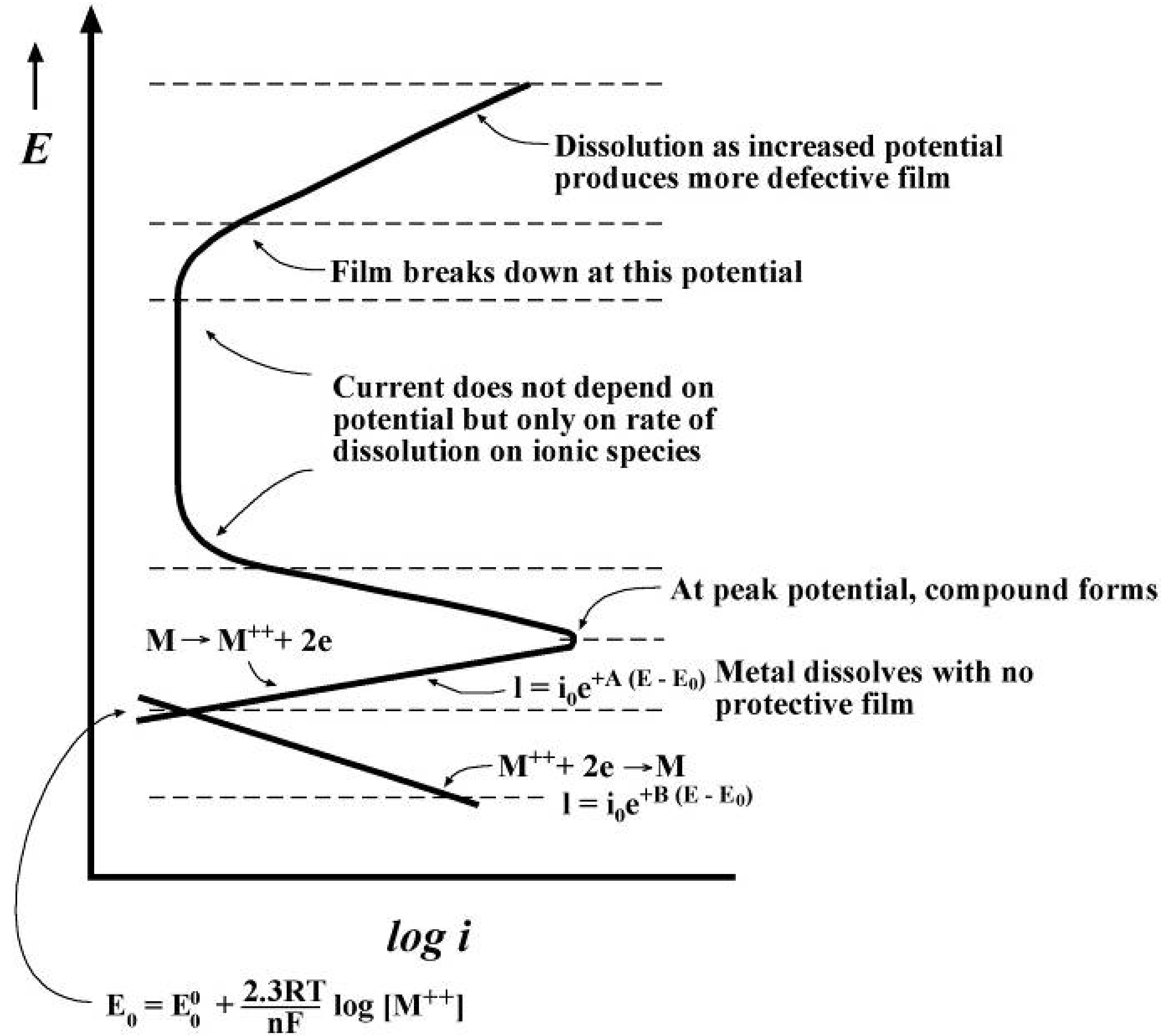

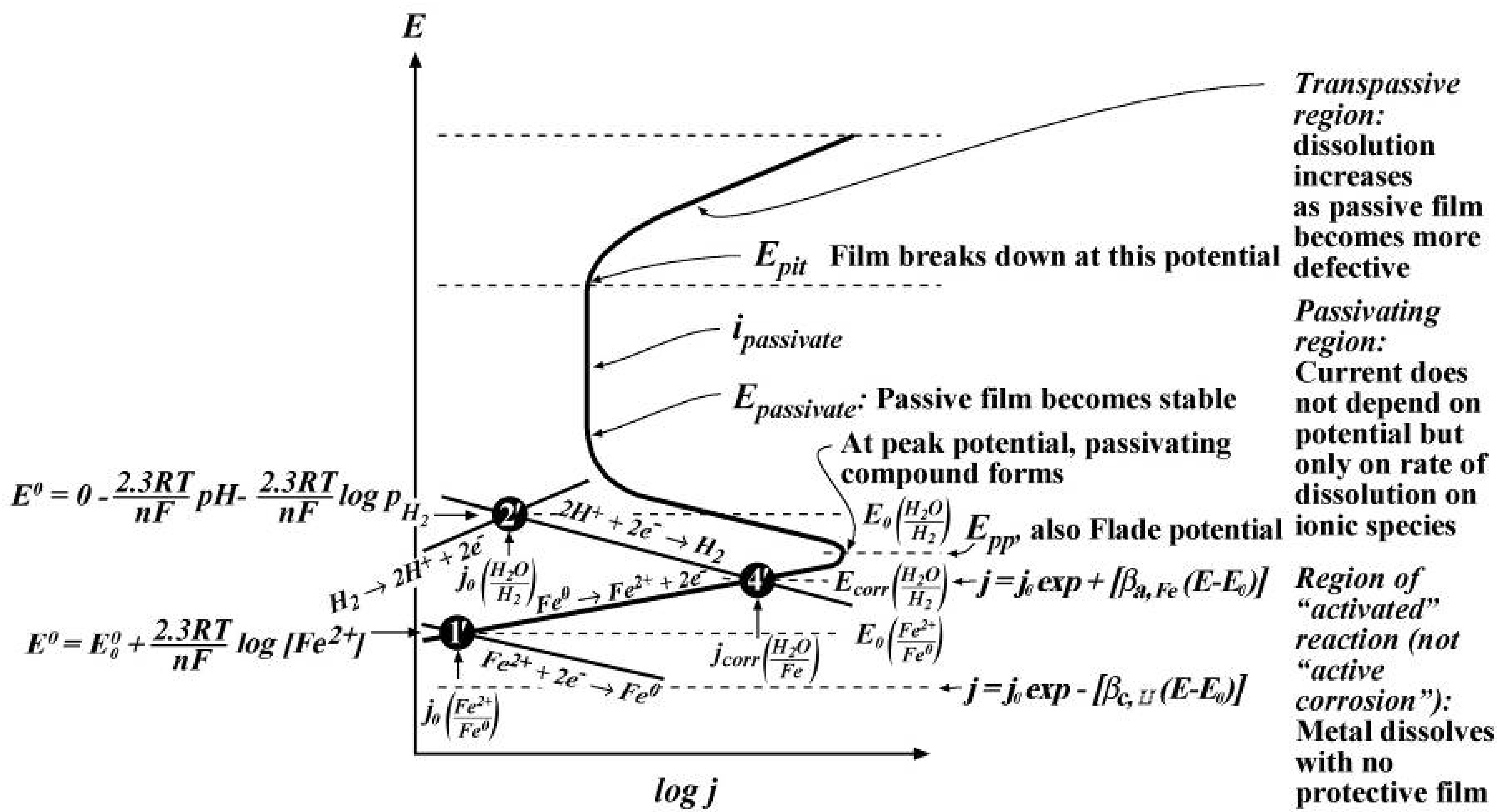

E
log j
Transpassive region: dissolution increases as passive film becomes more defective
E_{pit} Film breaks down at this potential
$i_{passivate}$
$E_{passivate}$: Passive film becomes stable
Passivating region: Current does not depend on potential but only on rate of dissolution on ionic species
At peak potential, passivating compound forms
E_{pp}, also Flade potential
$E^0 = 0 - \frac{2.3RT}{nF} pH - \frac{2.3RT}{nF} \log p_{H_2}$
2'
$2H^+ + 2e^- \rightarrow H_2$
$E_0\left(\frac{H_2O}{H_2}\right)$
$H_2 \rightarrow 2H^+ + 2e^-$
$j_0\left(\frac{H_2O}{H_2}\right)$
$Fe^0 \rightarrow Fe^{2+} + 2e^-$
4'
$E_{corr}\left(\frac{H_2O}{H_2}\right)$
$j = j_0 \exp + [\beta_{a,Fe}(E-E_0)]$
Region of "activated" reaction (not "active corrosion"): Metal dissolves with no protective film
$E^0 = E_0^0 + \frac{2.3RT}{nF} \log [Fe^{2+}]$
1'
$E_0\left(\frac{Fe^{2+}}{Fe^0}\right)$
$j_{corr}\left(\frac{H_2O}{Fe}\right)$
$Fe^{2+} + 2e^- \rightarrow Fe^0$
$j = j_0 \exp - [\beta_{c,H}(E-E_0)]$
$j_0\left(\frac{Fe^{2+}}{Fe^0}\right)$

Combined reduction reactions based on oxygen and water

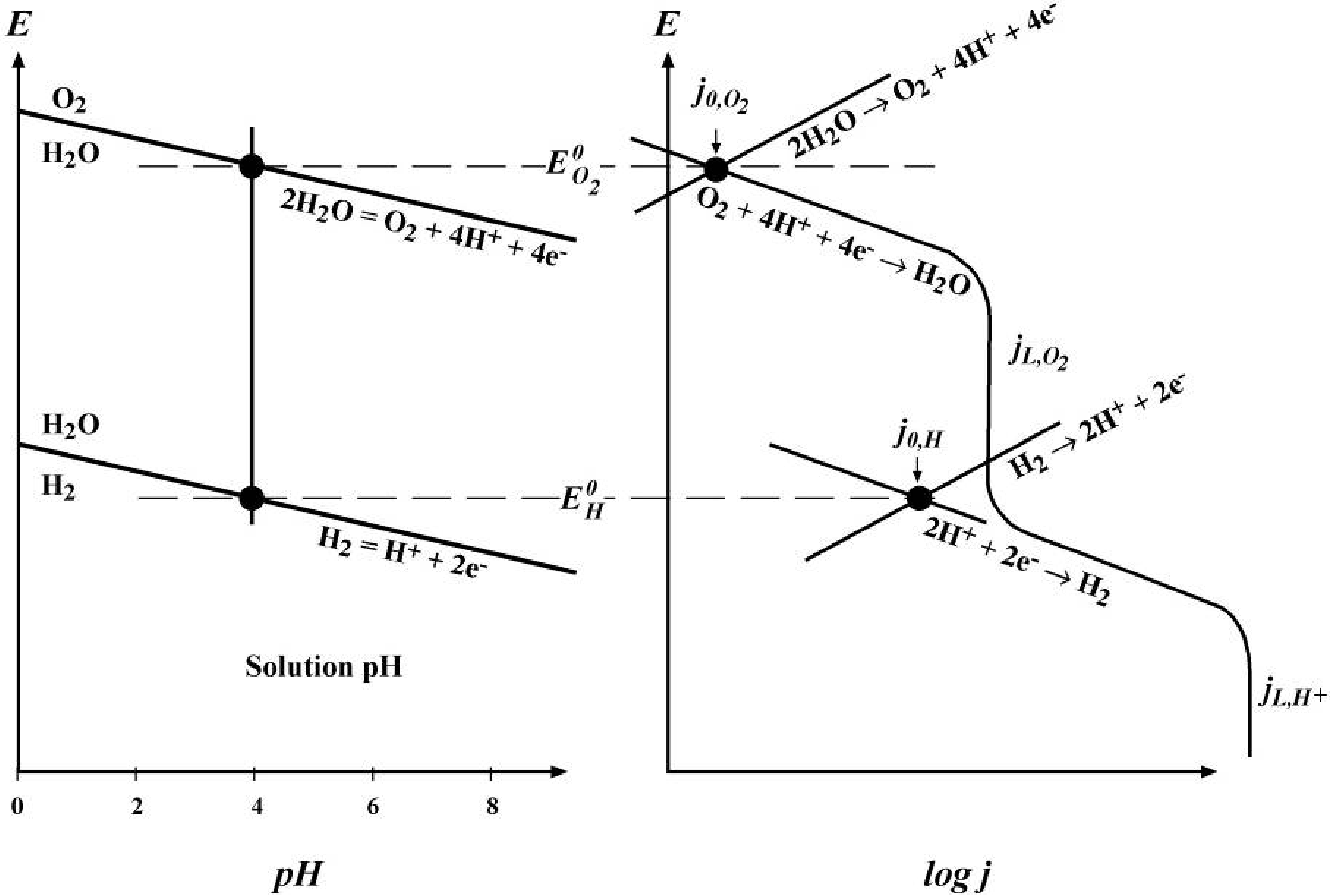

Response of Polarization Current Density for Regions of Corrosion and Passivity

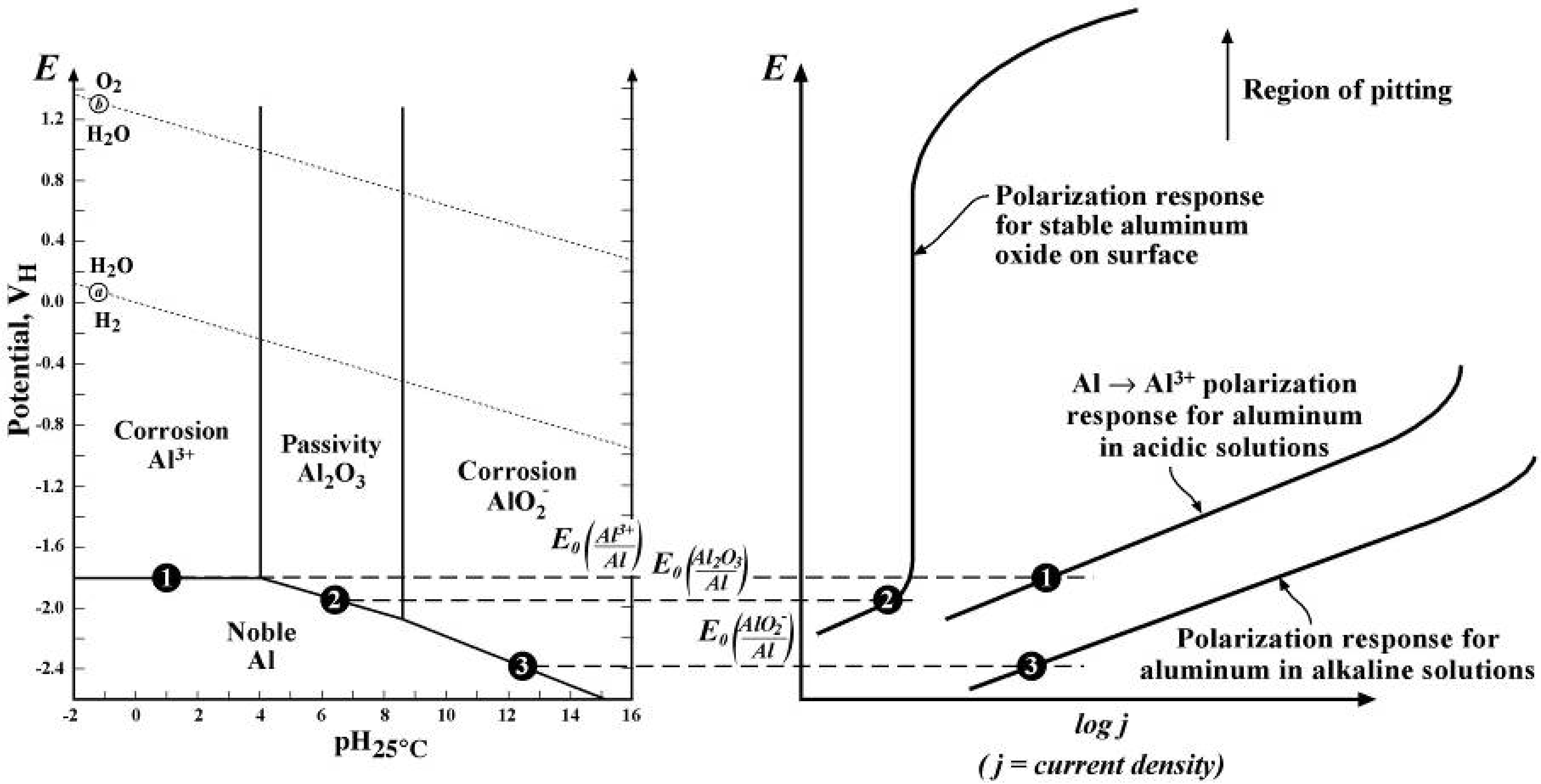

Polarization curves for Alloy 600 exposed to concentrated solutions of NaOH at various concentrations

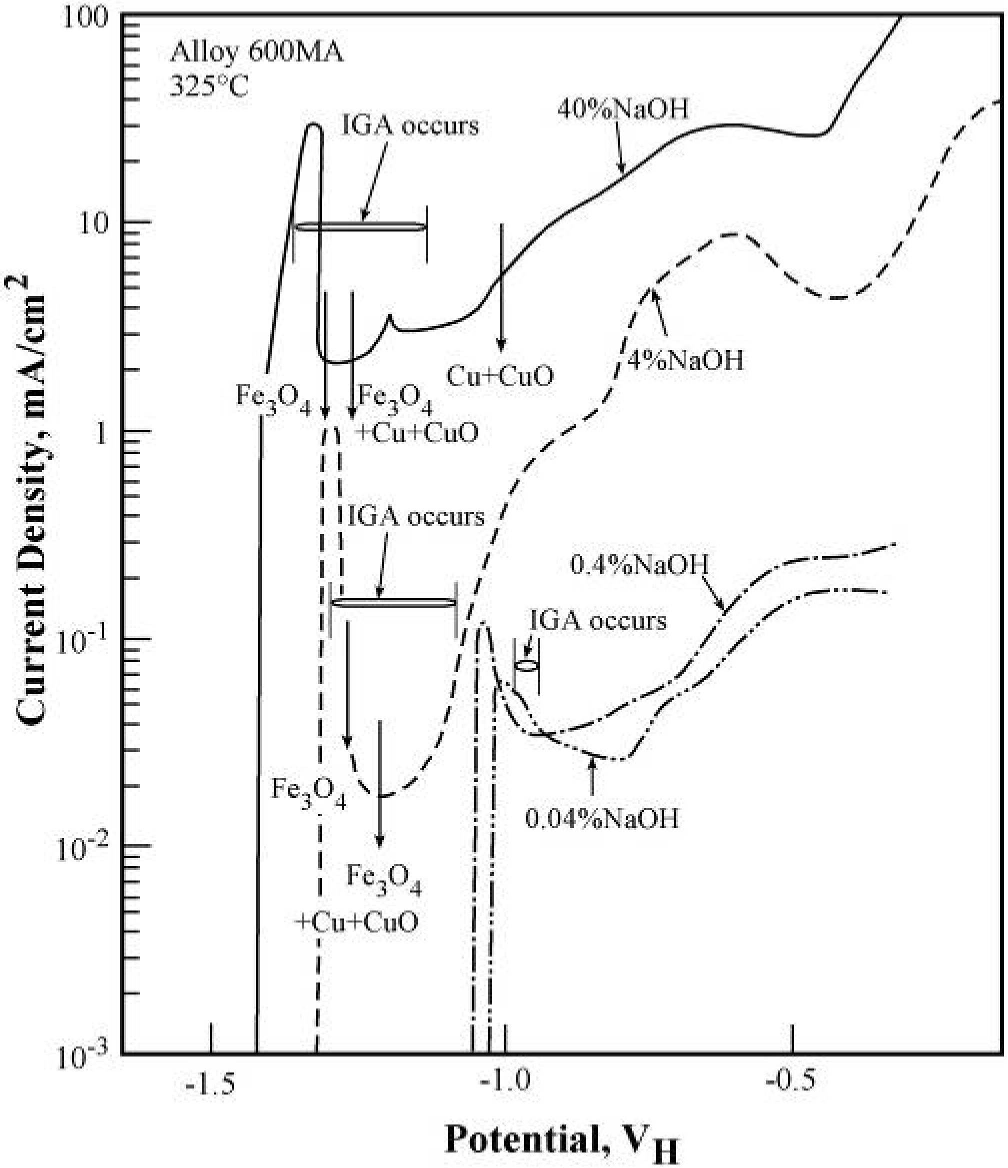

Comparison of reduction of nitrates (oxidizing) and non-oxidizing acid

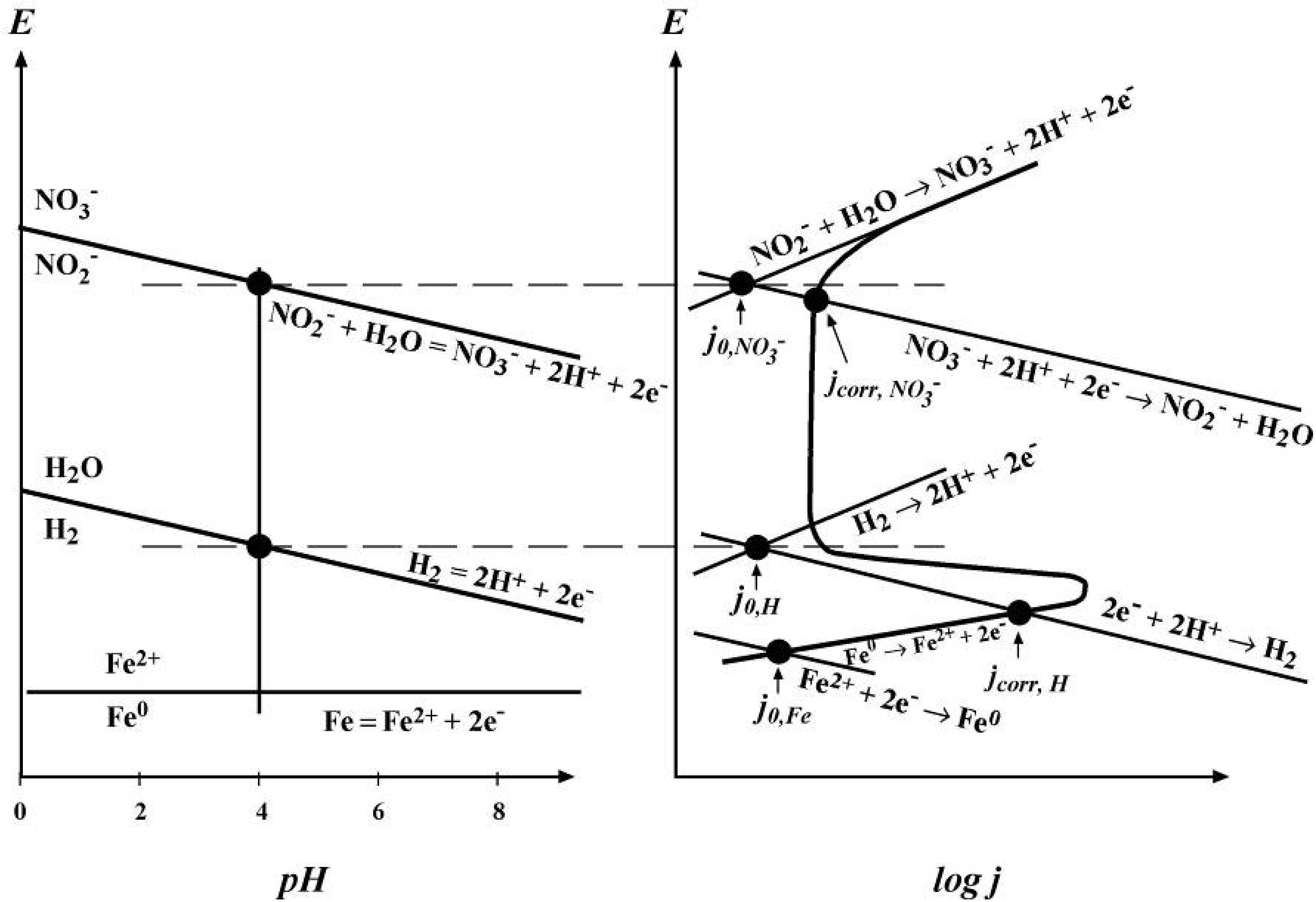

Implications of rate of repassivation on the corrosion at high potentials in nitrate solutions.

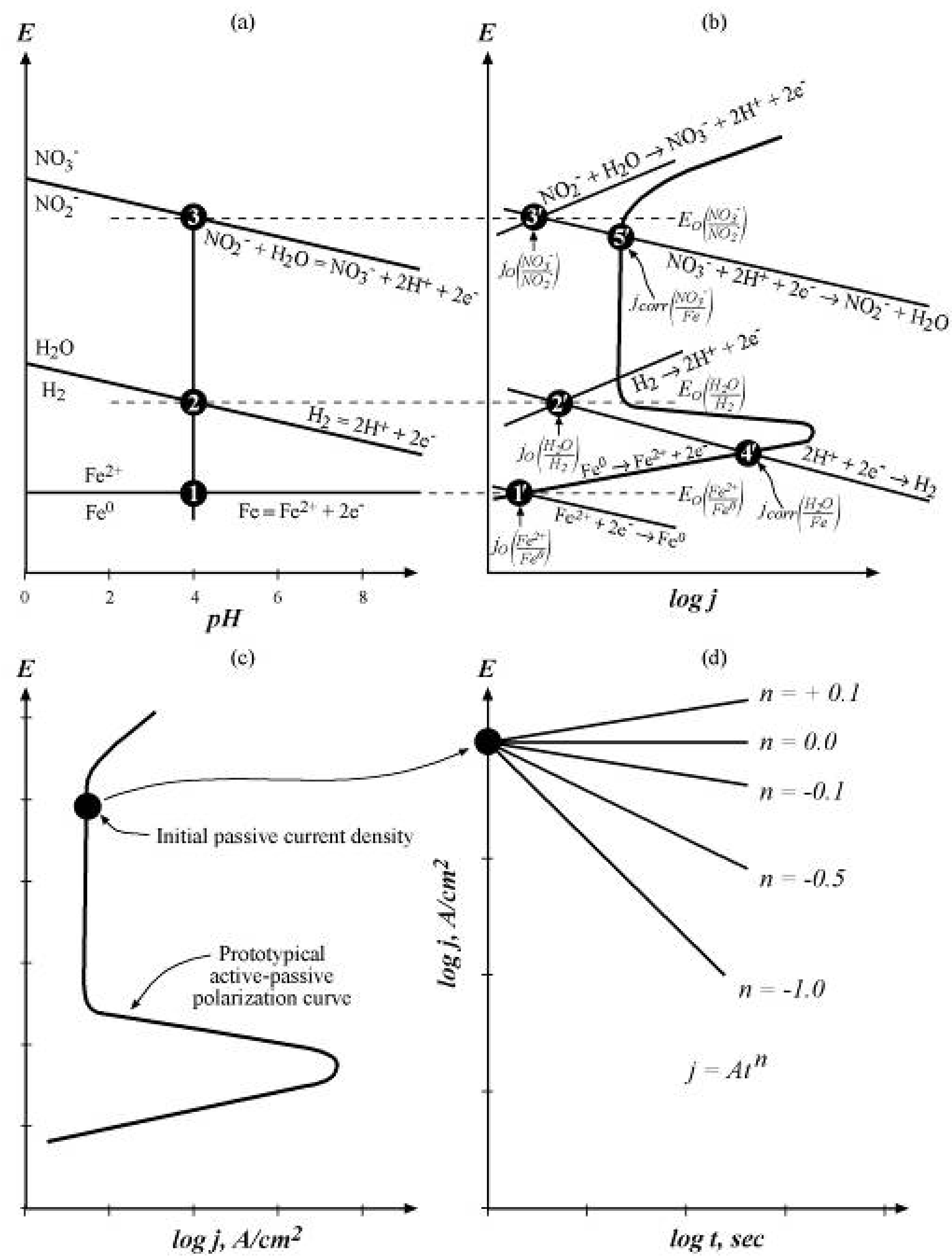

Comparison of the reduction processes for Fe and Ti in chloride solutions

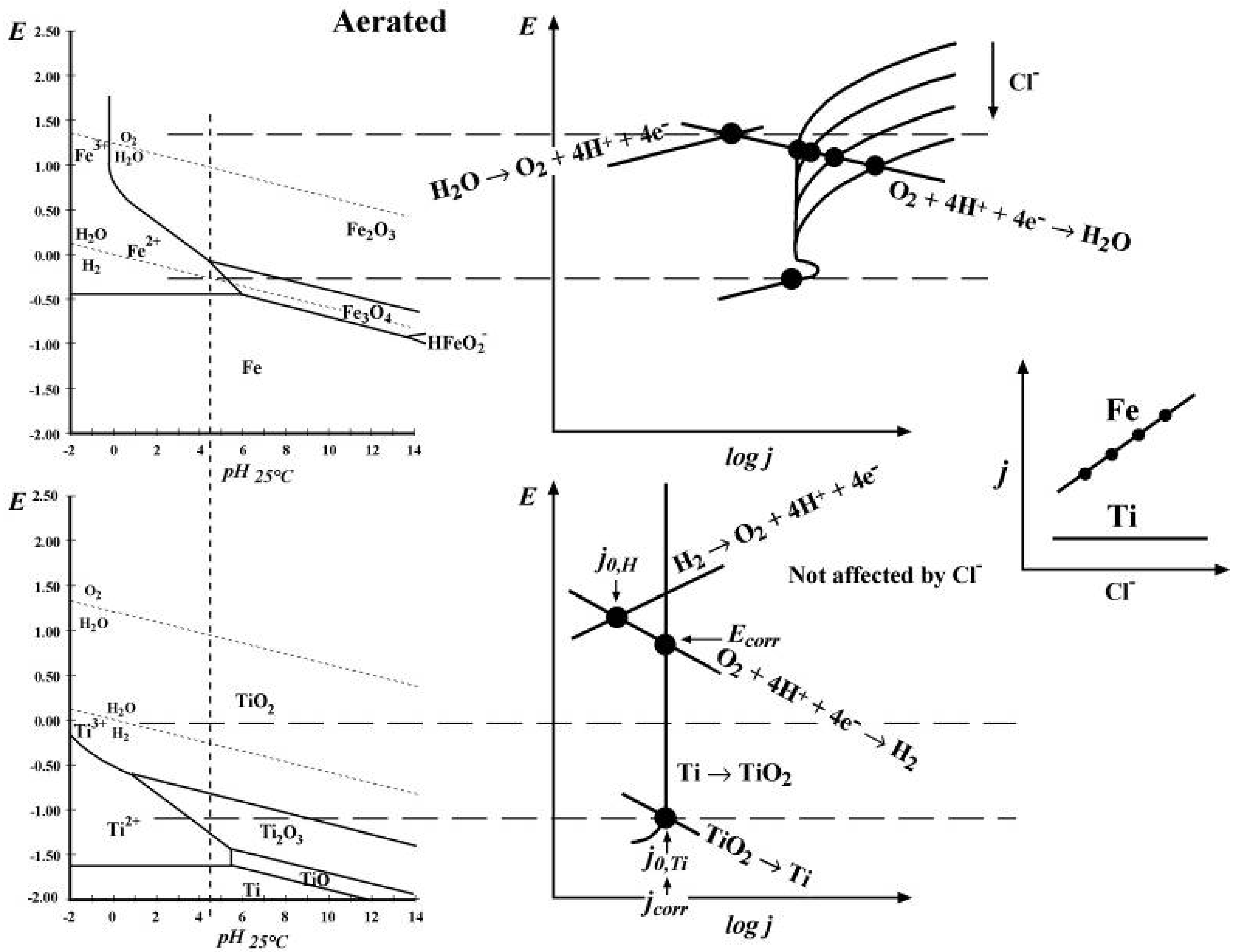

Effects of multiple anodes

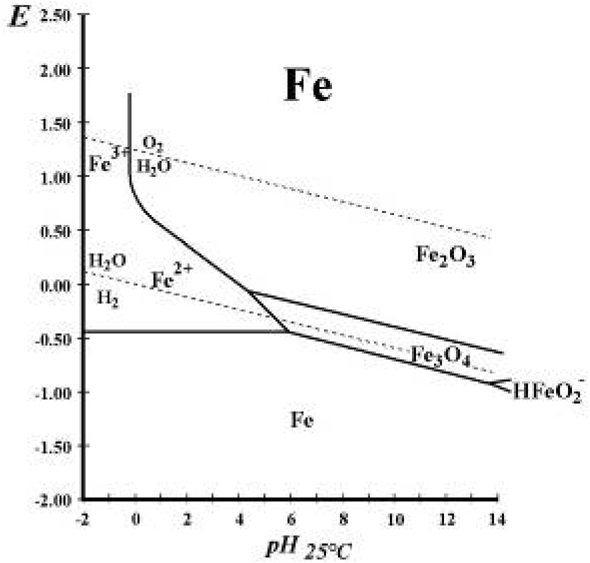

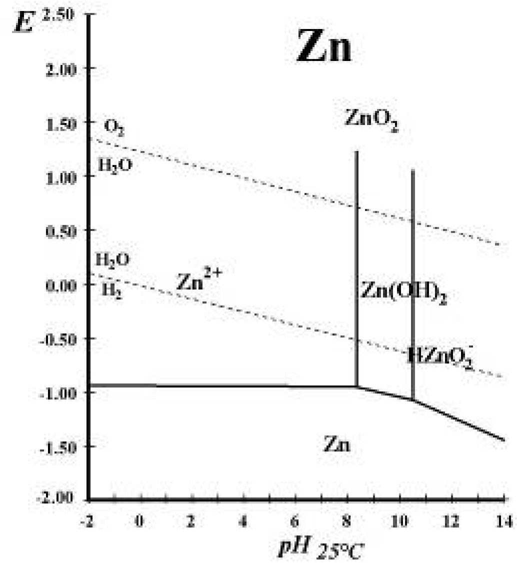

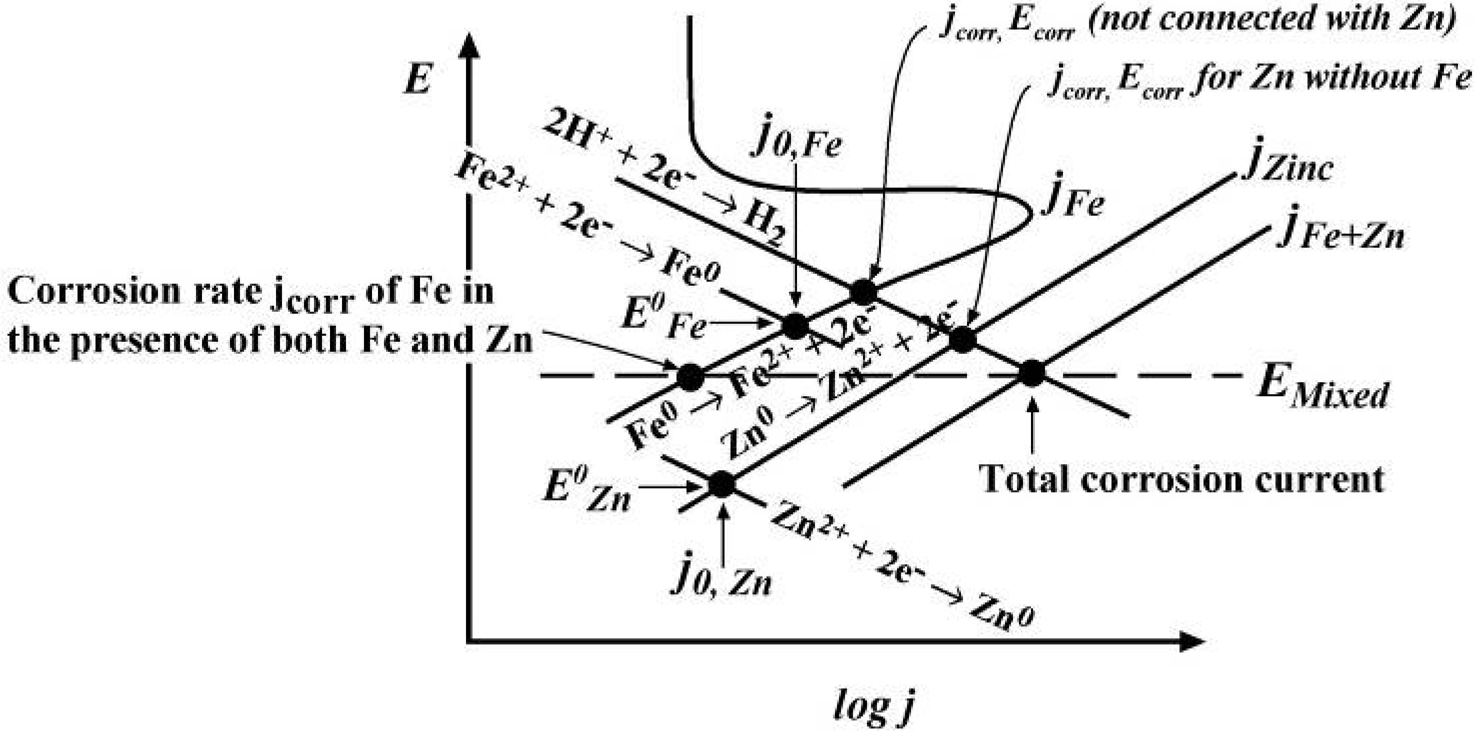

Schematic view of the effects of flow on the corrosion current density in an oxygenated solution

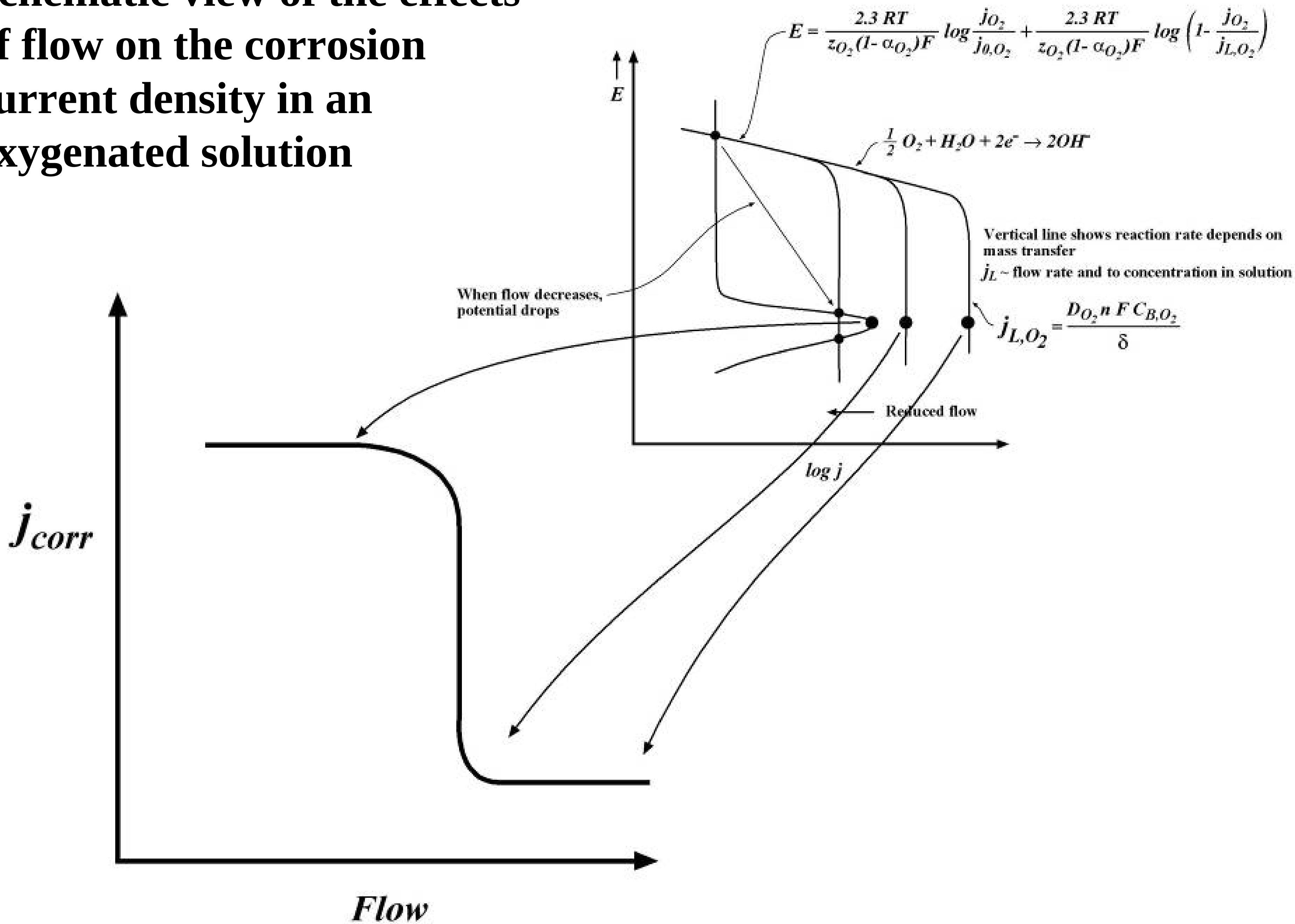

Effects of oxygen concentration on the flow limited oxidation of Fe

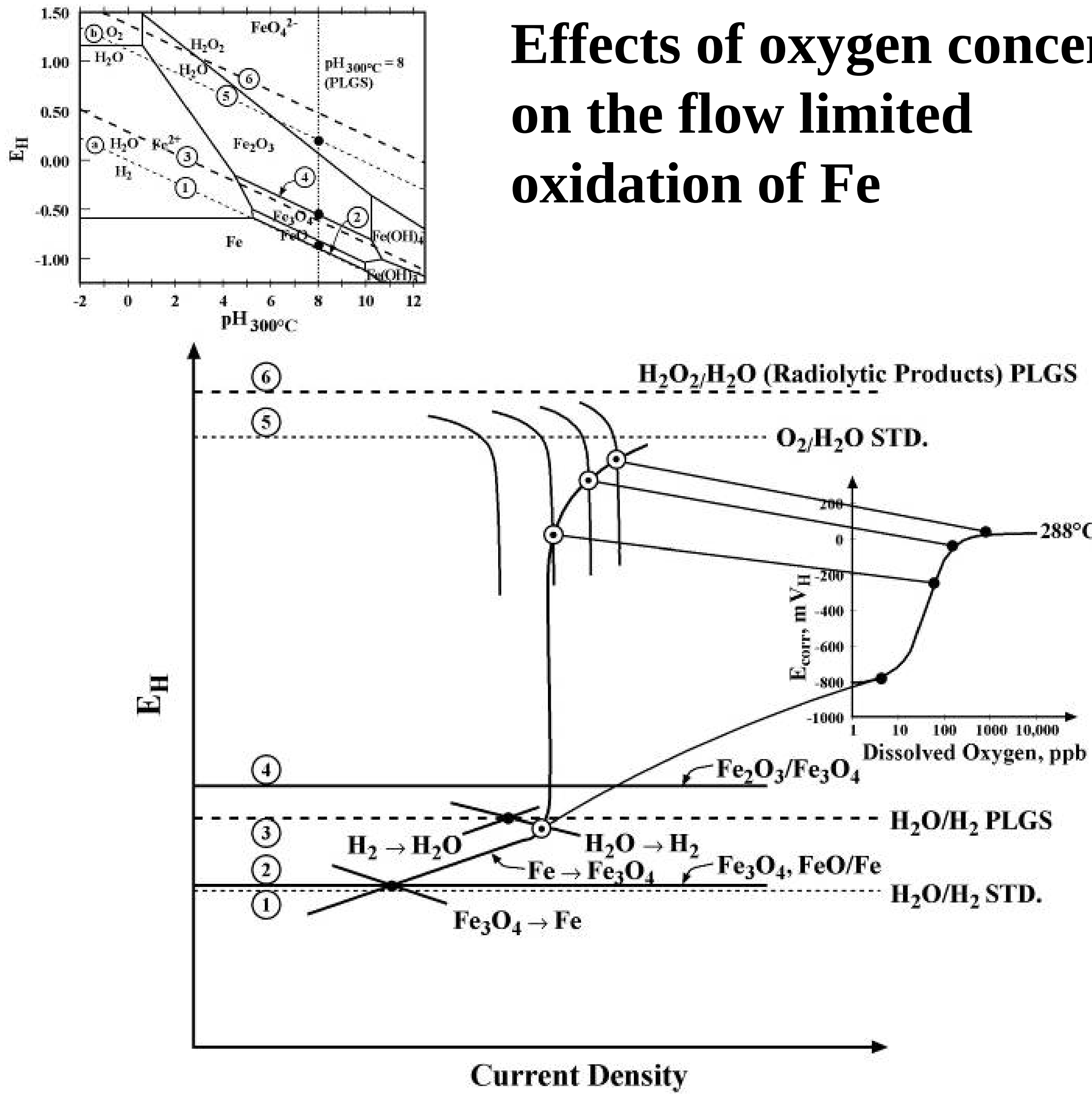

Direct polarization measurements on passivity of iron

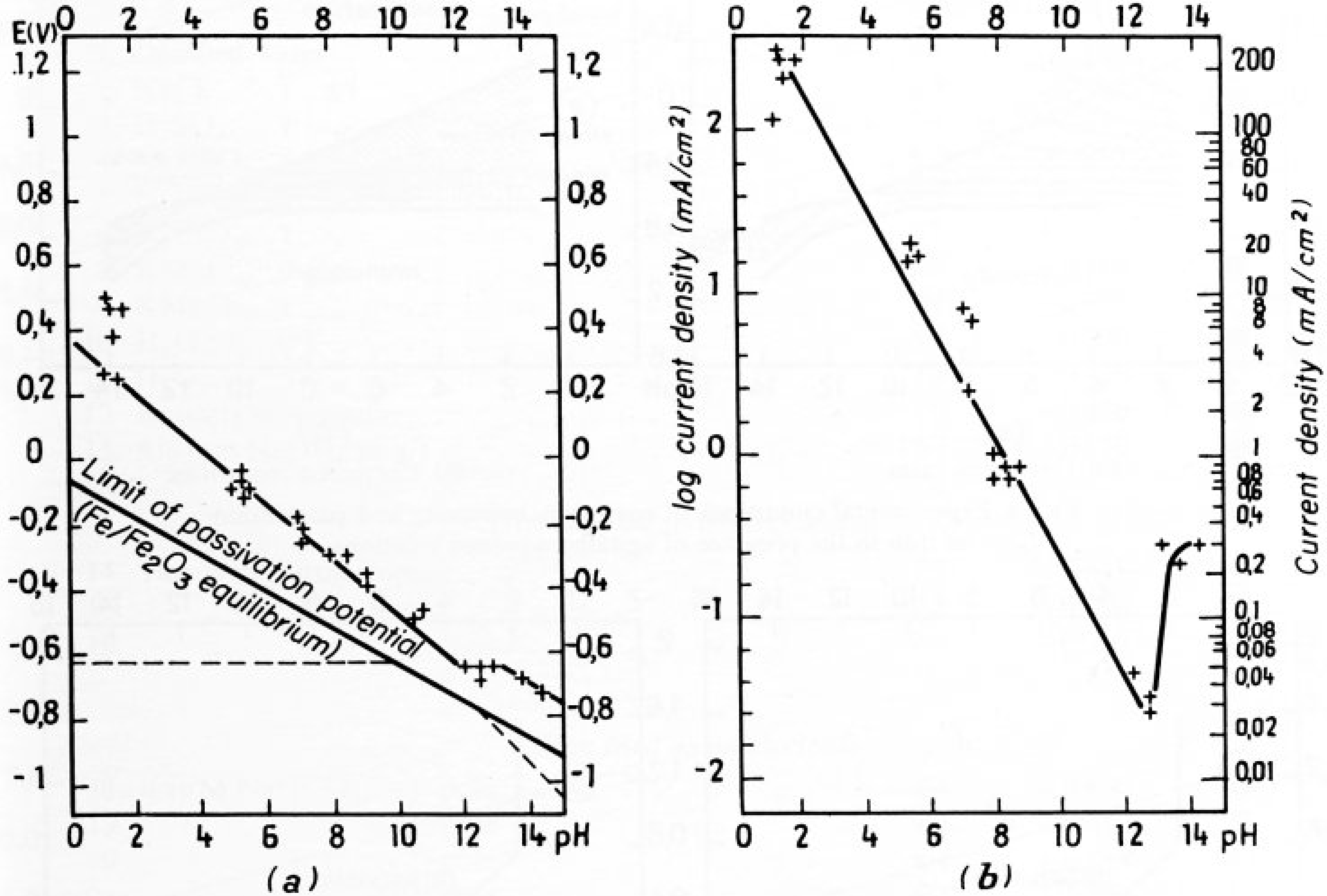

(*a*) Passivation potentials. (*b*) Passivation current densities.

FIG. 8. Influence of pH on the conditions of anodic passivation of iron.

Pourbaix

Thermodynamics bounds kinetics in electrochemistry and metallurgy

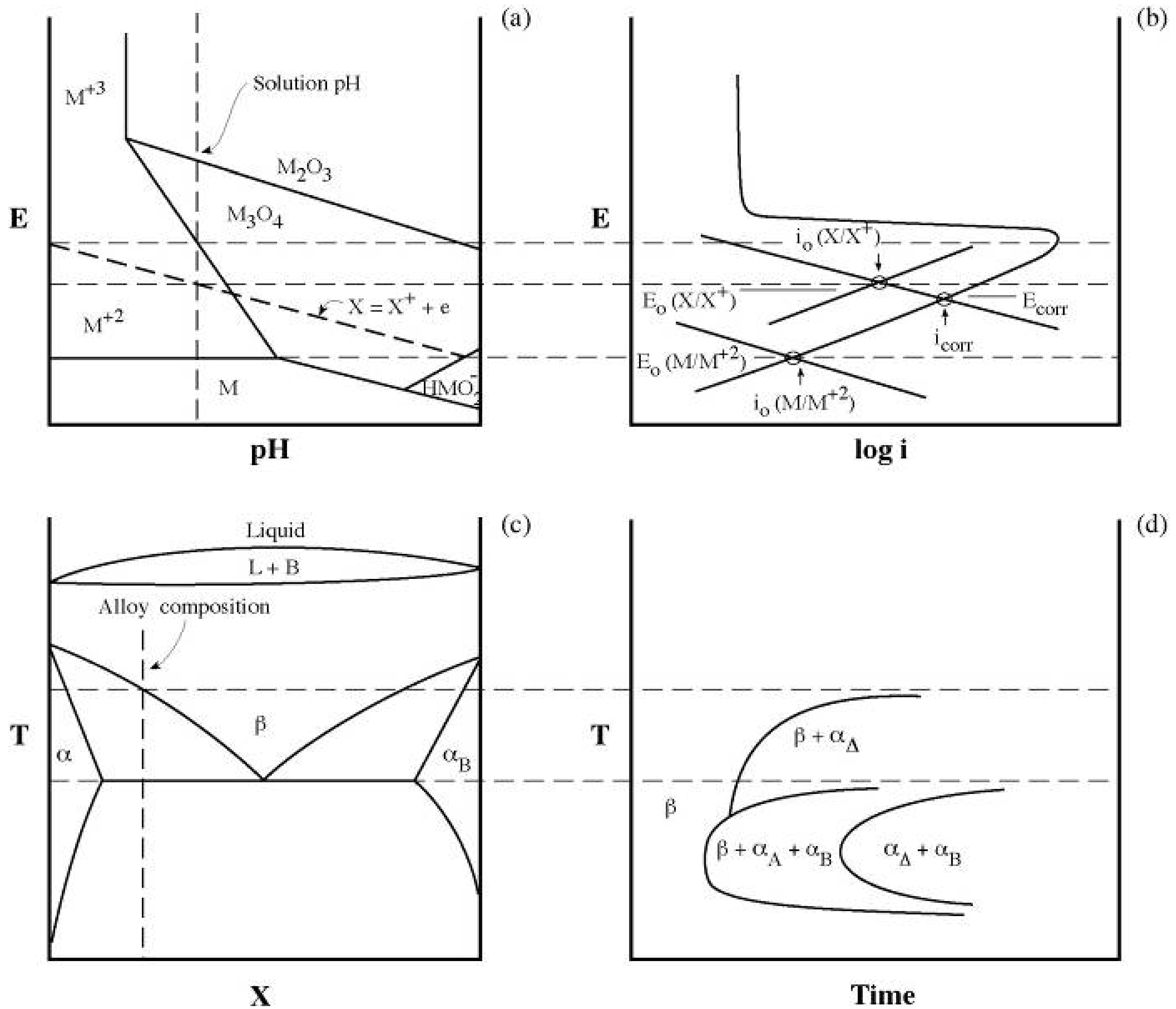

Factors Affecting Potential:
pH

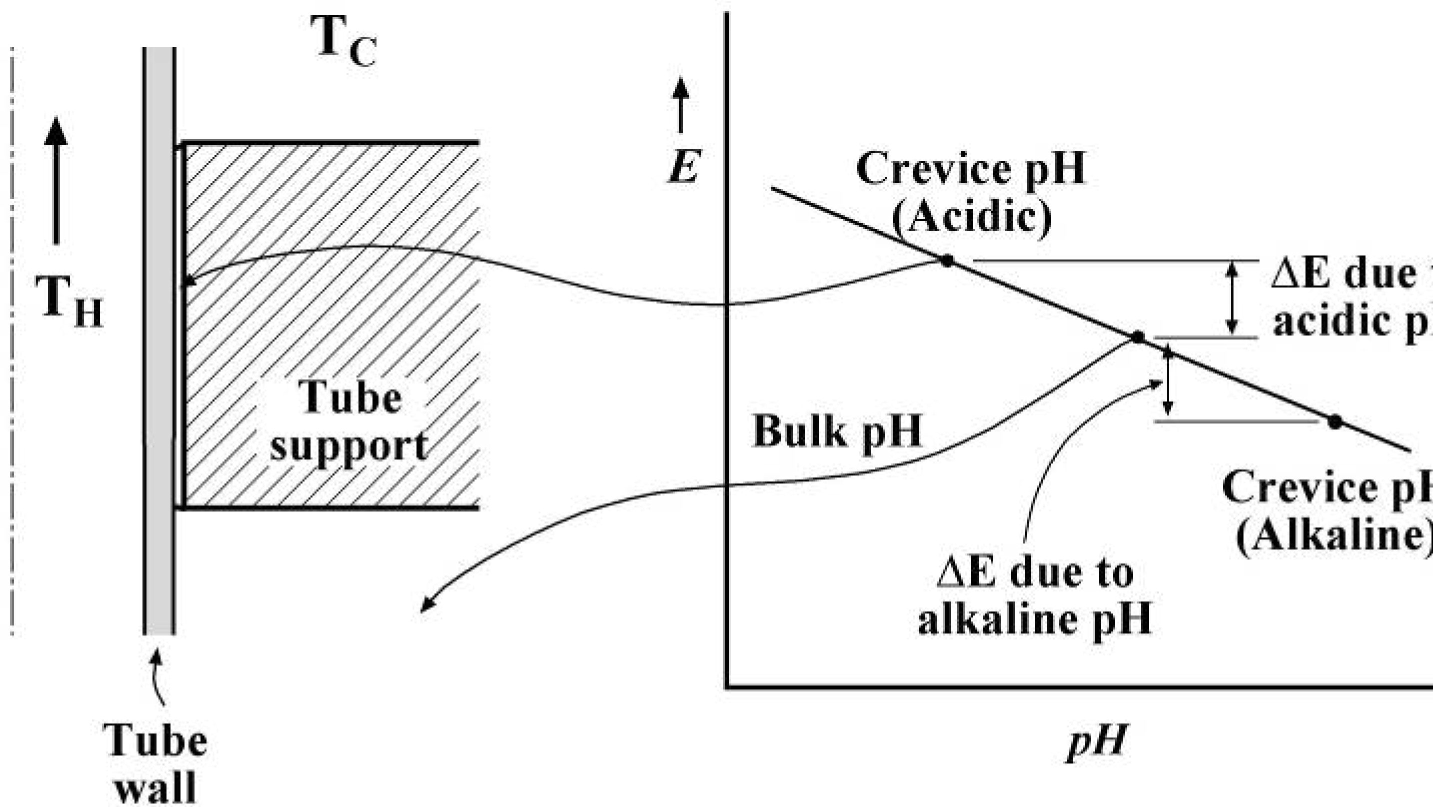

Comparison of SG conditions with static autoclaves in terms of hydrogen half cell equilibrium

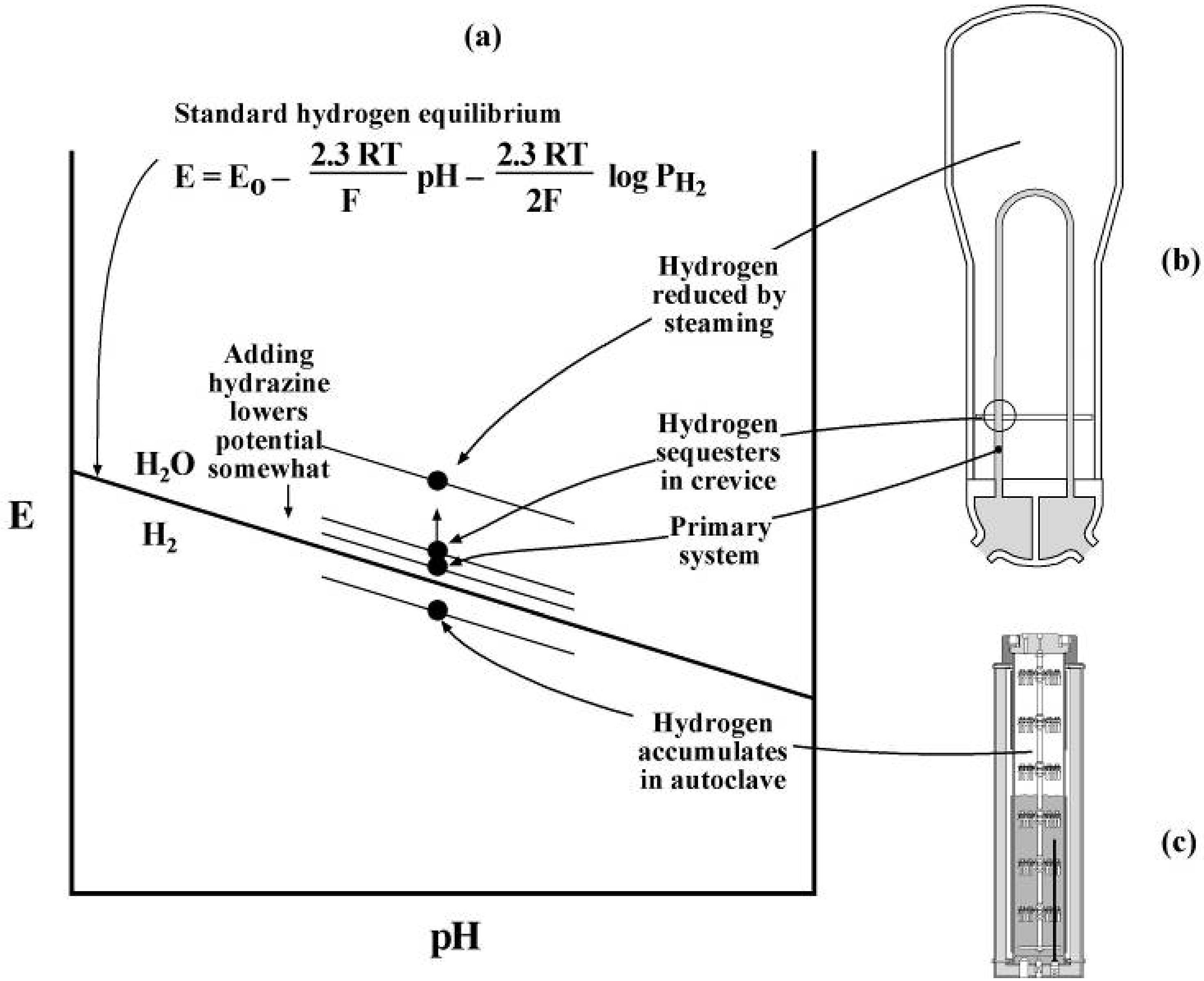

Corrosion in Superheated Regions

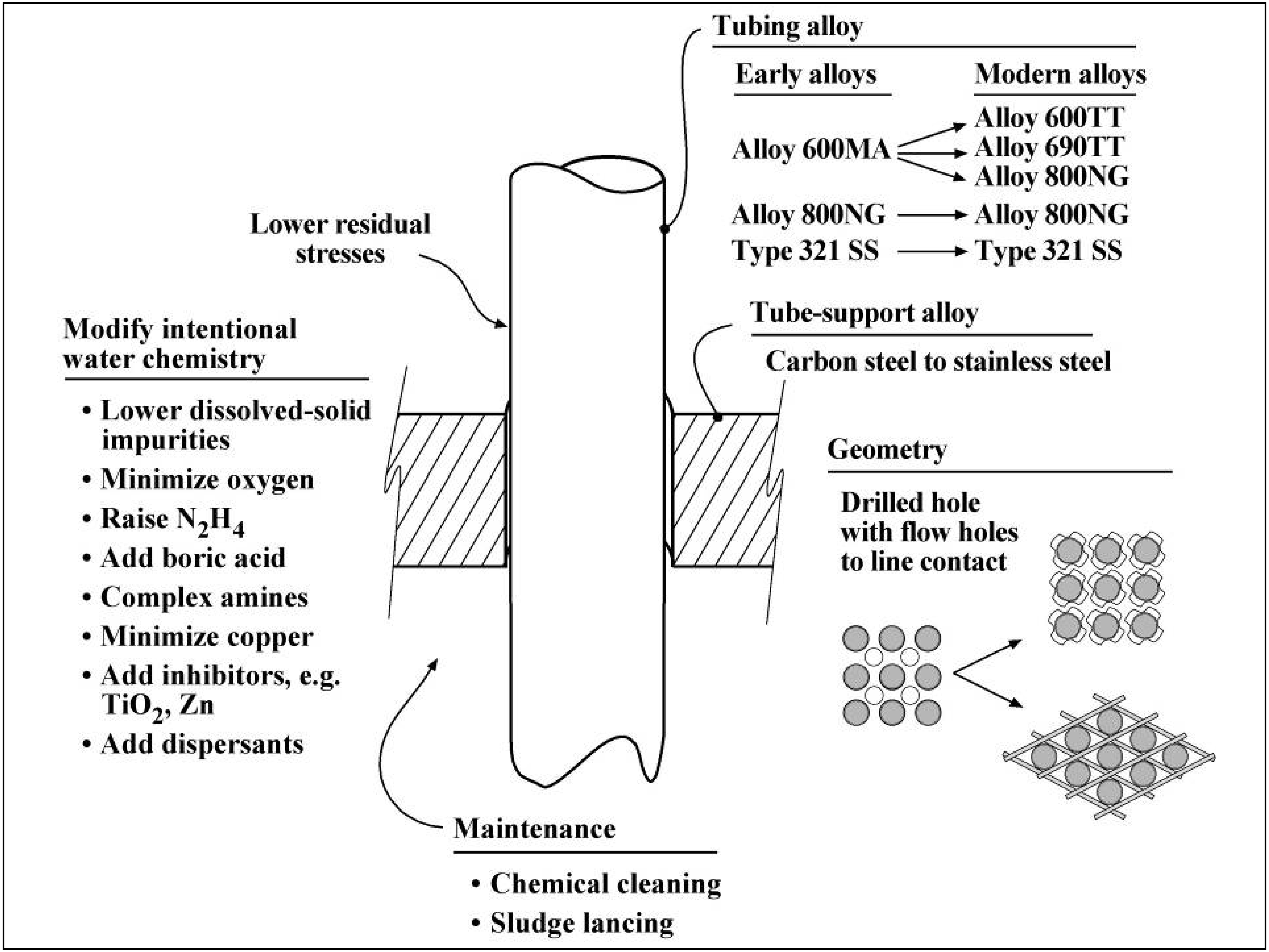
Tubing alloy
Early alloys
Modern alloys
Alloy 600MA
Alloy 600TT
Alloy 690TT
Alloy 800NG
Alloy 800NG
Alloy 800NG
Type 321 SS
Type 321 SS
Lower residual stresses
Tube-support alloy
Carbon steel to stainless steel
Modify intentional water chemistry
• Lower dissolved-solid impurities
• Minimize oxygen
• Raise N_2H_4
• Add boric acid
• Complex amines
• Minimize copper
• Add inhibitors, e.g. TiO_2, Zn
• Add dispersants
Geometry
Drilled hole with flow holes to line contact
Maintenance
• Chemical cleaning
• Sludge lancing

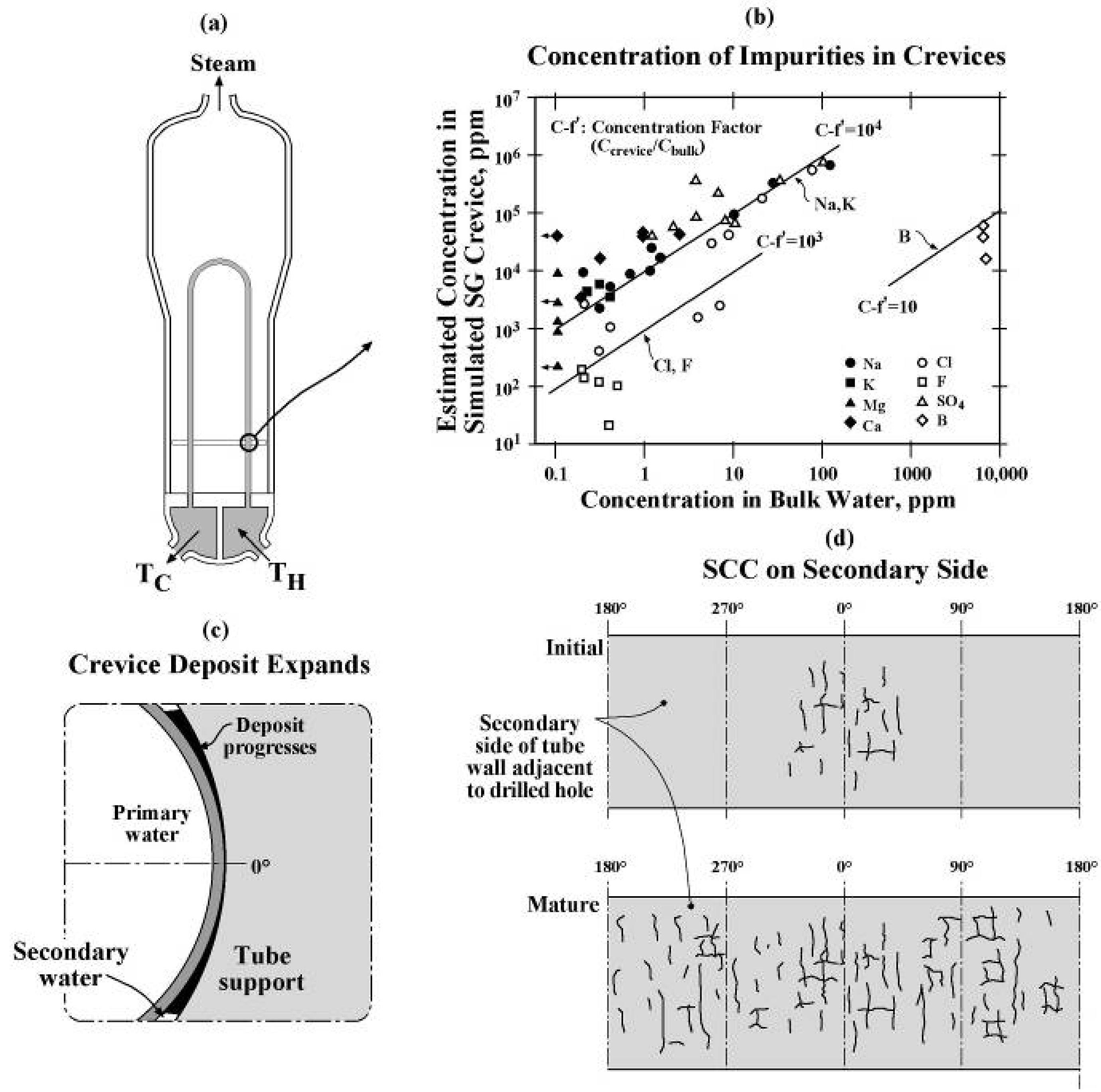
(a)
Steam
T_C
T_H
(b)
Concentration of Impurities in Crevices
Estimated Concentration in Simulated SG Crevice, ppm
Concentration in Bulk Water, ppm
C-f': Concentration Factor ($C_{crevice}/C_{bulk}$)
C-f'=10^4
C-f'=10^3
C-f'=10
Na,K
Cl, F
B
Na
K
Mg
Ca
Cl
F
SO_4
B
(c)
Crevice Deposit Expands
Deposit progresses
Primary water
0°
Secondary water
Tube support
(d)
SCC on Secondary Side
180° 270° 0° 90° 180°
Initial
Secondary side of tube wall adjacent to drilled hole
Mature

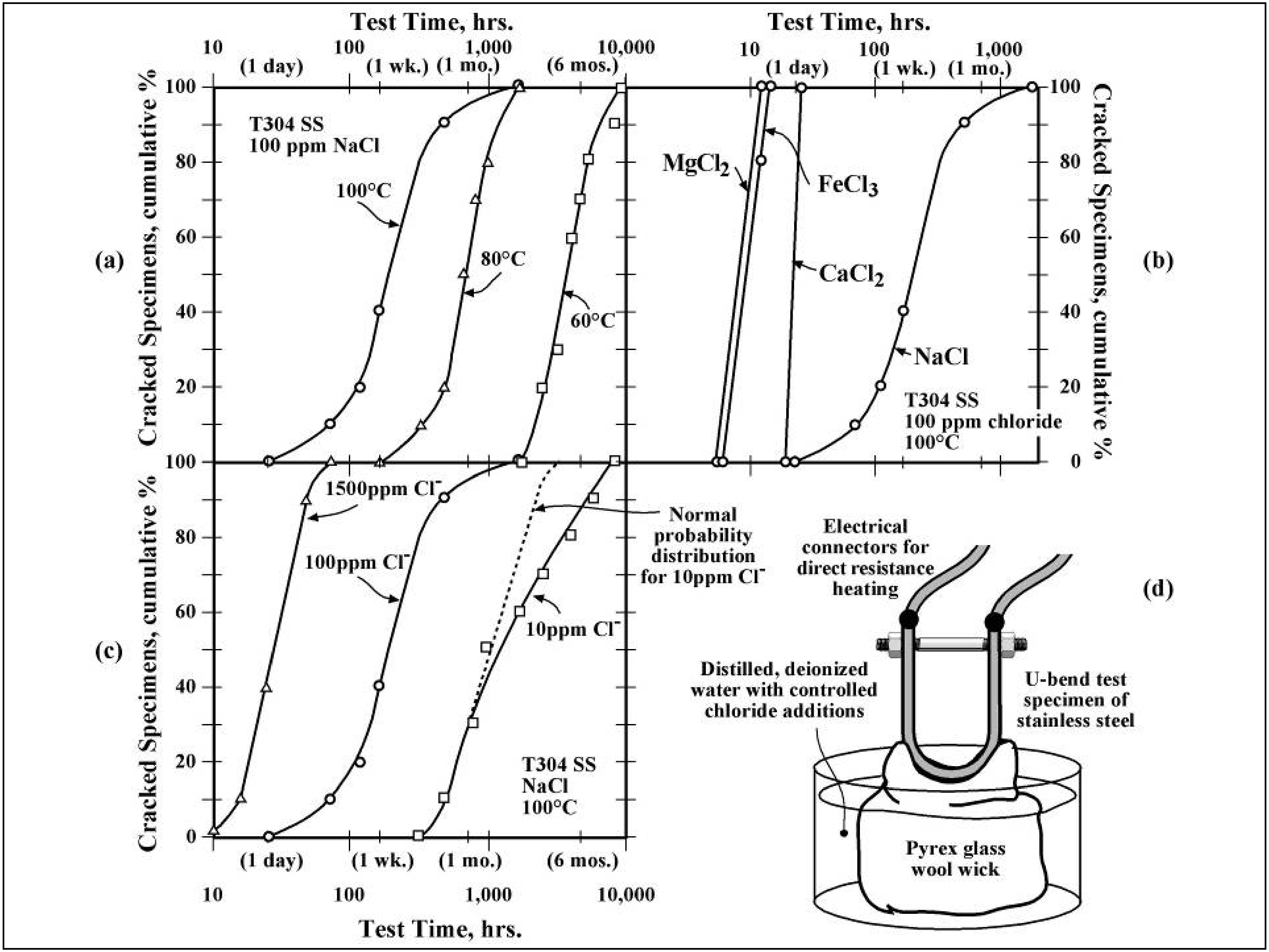

Test Time, hrs.
10
100
1,000
10,000
(1 day)
(1 wk.)
(1 mo.)
(6 mos.)
Cracked Specimens, cumulative %
T304 SS
100 ppm NaCl
100°C
80°C
60°C
(a)
MgCl$_2$
FeCl$_3$
CaCl$_2$
NaCl
T304 SS
100 ppm chloride
100°C
(b)
1500ppm Cl$^-$
100ppm Cl$^-$
10ppm Cl$^-$
Normal probability distribution for 10ppm Cl$^-$
T304 SS
NaCl
100°C
(c)
Electrical connectors for direct resistance heating
Distilled, deionized water with controlled chloride additions
U-bend test specimen of stainless steel
Pyrex glass wool wick
(d)

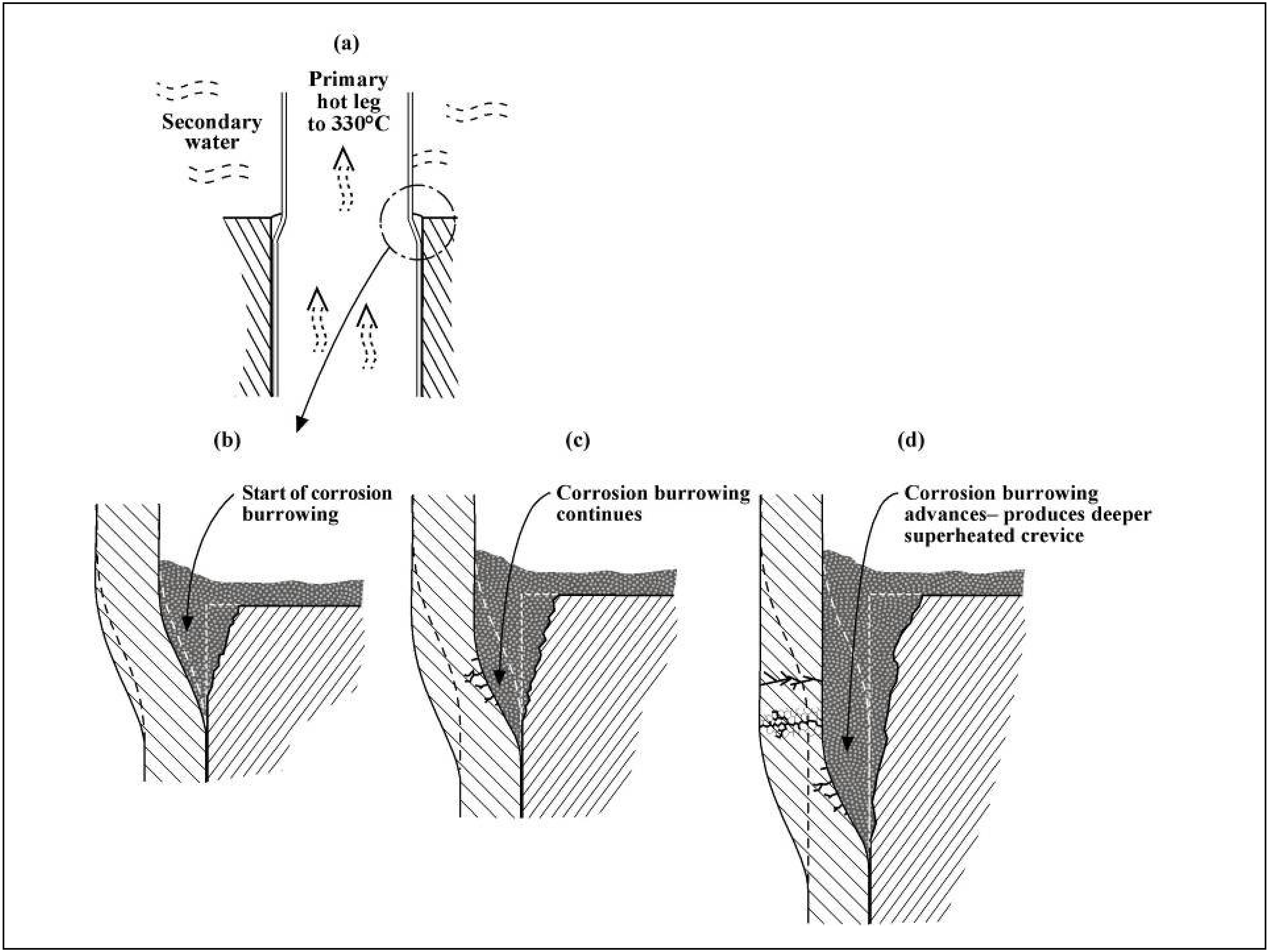
(a)
Primary
hot leg
to 330°C
Secondary
water
(b)
(c)
(d)
Start of corrosion
burrowing
Corrosion burrowing
continues
Corrosion burrowing
advances– produces deeper
superheated crevice

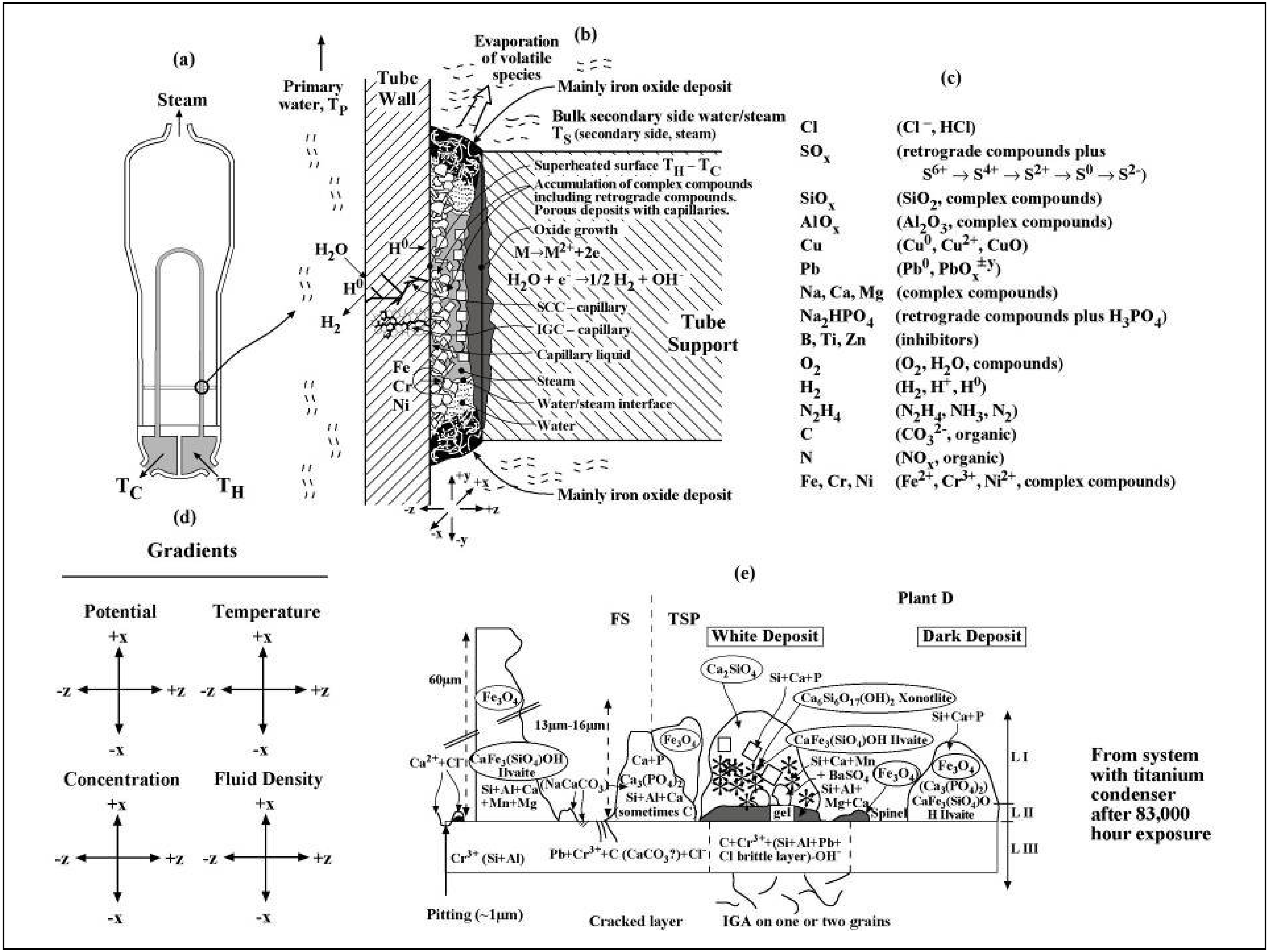

(a)
Steam
T_C
T_H
(b)
Primary water, T_P
Tube Wall
Evaporation of volatile species
Mainly iron oxide deposit
Bulk secondary side water/steam
T_S (secondary side, steam)
Superheated surface $T_H - T_C$
Accumulation of complex compounds including retrograde compounds. Porous deposits with capillaries.
Oxide growth
$M \rightarrow M^{2+} + 2e$
$H_2O + e^- \rightarrow 1/2\ H_2 + OH^-$
SCC – capillary
IGC – capillary
Capillary liquid
Steam
Water/steam interface
Water
Tube Support
H_2O
H^0
H_2
Fe
Cr
Ni
Mainly iron oxide deposit
+y +x -z +z -x -y
(c)
Cl (Cl^-, HCl)
SO_x (retrograde compounds plus $S^{6+} \rightarrow S^{4+} \rightarrow S^{2+} \rightarrow S^0 \rightarrow S^{2-}$)
SiO_x (SiO_2, complex compounds)
AlO_x (Al_2O_3, complex compounds)
Cu (Cu^0, Cu^{2+}, CuO)
Pb $(Pb^0, PbO_x^{\pm y})$
Na, Ca, Mg (complex compounds)
Na_2HPO_4 (retrograde compounds plus H_3PO_4)
B, Ti, Zn (inhibitors)
O_2 (O_2, H_2O, compounds)
H_2 (H_2, H^+, H^0)
N_2H_4 (N_2H_4, NH_3, N_2)
C (CO_3^{2-}, organic)
N (NO_x, organic)
Fe, Cr, Ni (Fe^{2+}, Cr^{3+}, Ni^{2+}, complex compounds)
(d)
Gradients
Potential
Temperature
Concentration
Fluid Density
+x -x -z +z
(e)
Plant D
FS
TSP
White Deposit
Dark Deposit
60μm
13μm-16μm
Fe_3O_4
$Ca^{2+}+Cl^-$
$CaFe_3(SiO_4)OH$ Ilvaite
Si+Al+Ca +Mn+Mg
$(NaCaCO_3)$
Ca+P
$Ca_3(PO_4)_2$
Si+Al+Ca (sometimes C)
Ca_2SiO_4
Si+Ca+P
$Ca_6Si_6O_{17}(OH)_2$ Xonotlite
$CaFe_3(SiO_4)OH$ Ilvaite
Si+Ca+Mn + $BaSO_4$
Si+Al+ Mg+Ca
gel
Spinel
$(Ca_3(PO_4)_2)$
$CaFe_3(SiO_4)OH$ Ilvaite
L I
L II
L III
Cr^{3+} (Si+Al)
Pb+Cr^{3+}+C ($CaCO_3$?)+Cl^-
C+Cr^{3+}+(Si+Al+Pb+ Cl brittle layer)-OH^-
Pitting (~1μm)
Cracked layer
IGA on one or two grains
From system with titanium condenser after 83,000 hour exposure

Chemical inside the superheated region and outside composition of surfaces of steam generator tube

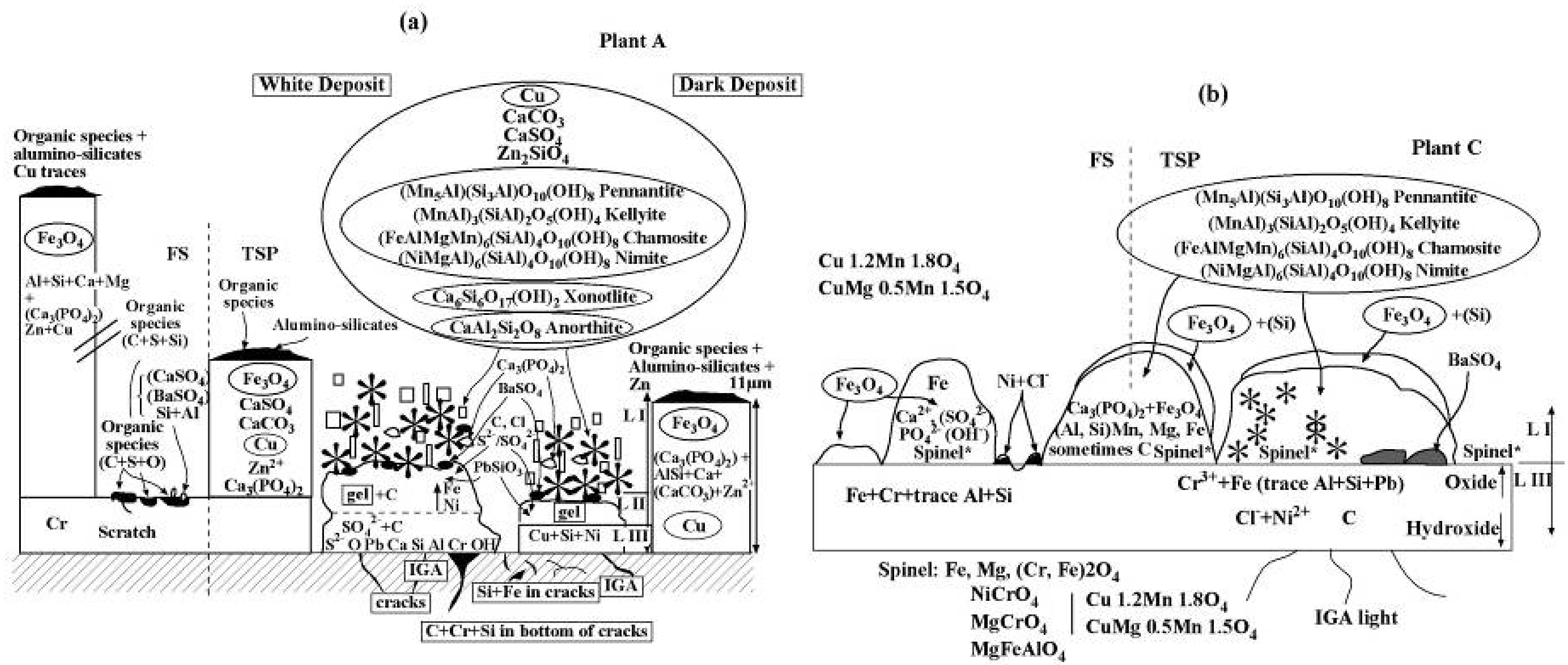

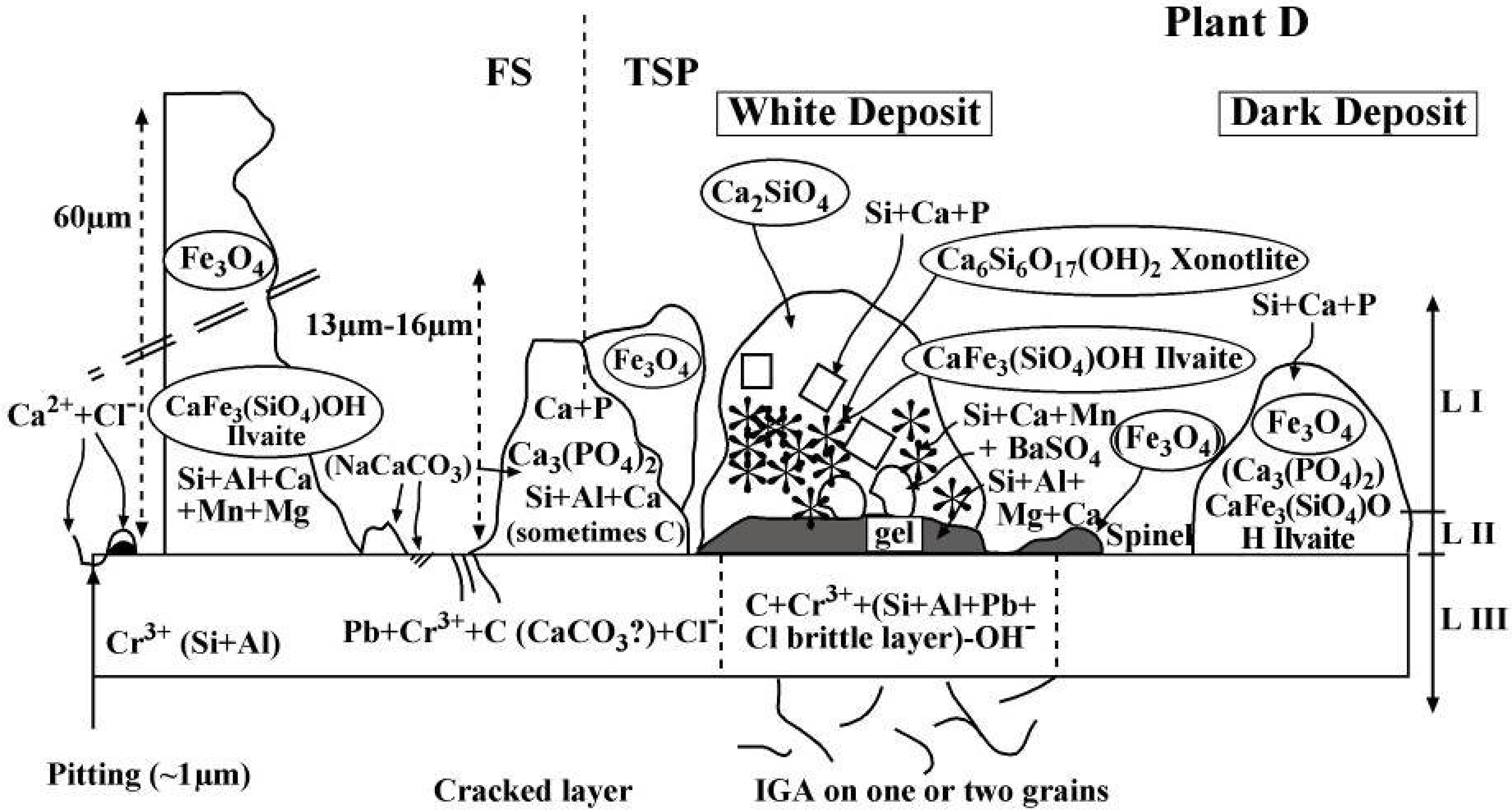

Plant D
FS
TSP
White Deposit
Dark Deposit
60µm
13µm-16µm
Fe3O4
CaFe3(SiO4)OH
Ilvaite
Ca2++Cl-
Si+Al+Ca
+Mn+Mg
(NaCaCO3)
Ca+P
Ca3(PO4)2
Si+Al+Ca
(sometimes C)
Fe3O4
Ca2SiO4
Si+Ca+P
Ca6Si6O17(OH)2 Xonotlite
CaFe3(SiO4)OH Ilvaite
Si+Ca+Mn
+ BaSO4
Si+Al+
Mg+Ca
gel
Fe3O4
Spinel
Si+Ca+P
Fe3O4
(Ca3(PO4)2)
CaFe3(SiO4)O
H Ilvaite
L I
L II
L III
Cr3+ (Si+Al)
Pb+Cr3++C (CaCO3?)+Cl-
C+Cr3++(Si+Al+Pb+
Cl brittle layer)-OH-
Pitting (~1µm)
Cracked layer
IGA on one or two grains

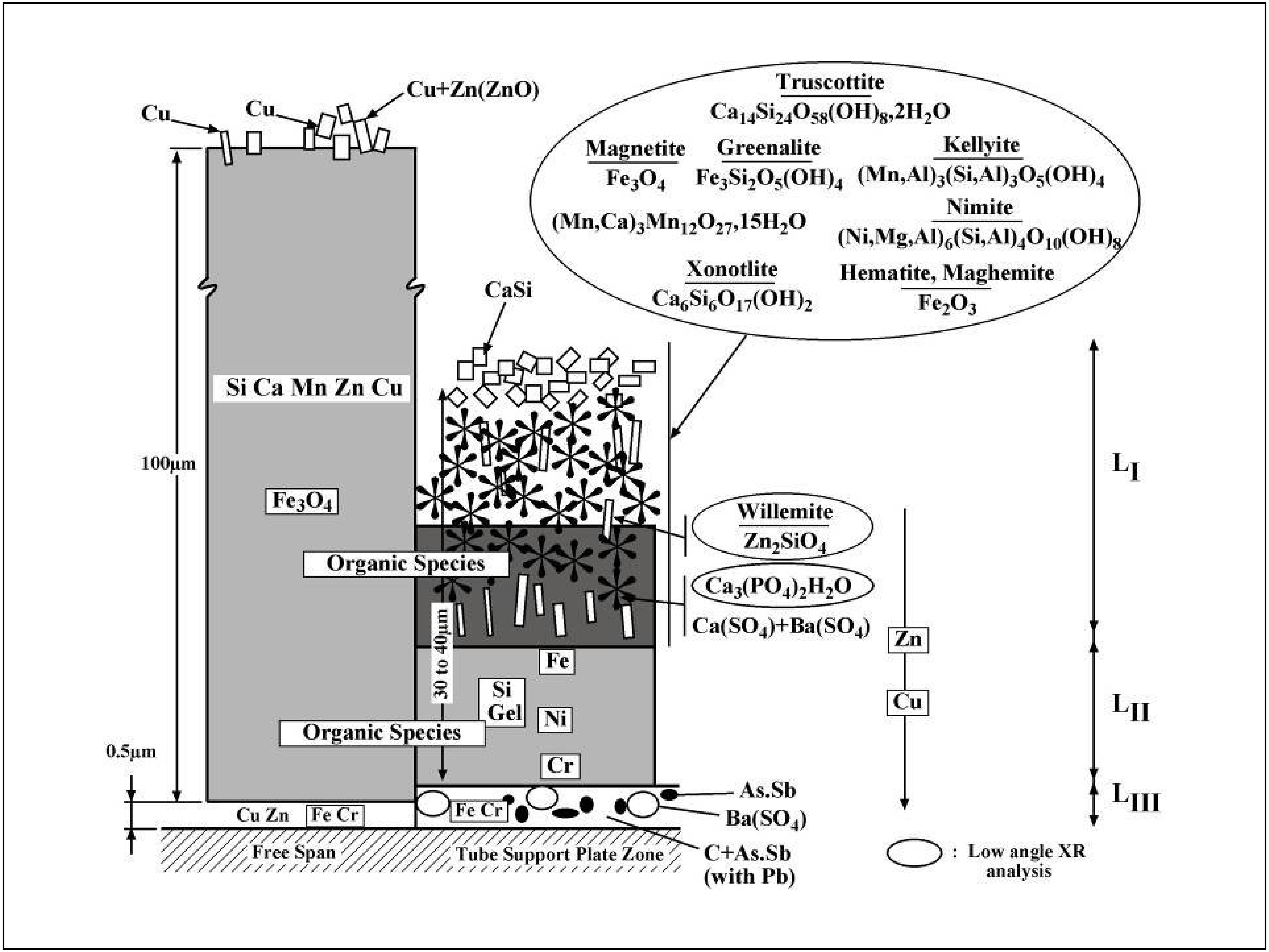

Cu
Cu
Cu+Zn(ZnO)
Truscottite
Ca14Si24O58(OH)8,2H2O
Magnetite
Fe3O4
Greenalite
Fe3Si2O5(OH)4
Kellyite
(Mn,Al)3(Si,Al)3O5(OH)4
(Mn,Ca)3Mn12O27,15H2O
Nimite
(Ni,Mg,Al)6(Si,Al)4O10(OH)8
Xonotlite
Ca6Si6O17(OH)2
Hematite, Maghemite
Fe2O3
CaSi
Si Ca Mn Zn Cu
100µm
Fe3O4
LI
Willemite
Zn2SiO4
Organic Species
Ca3(PO4)2H2O
Ca(SO4)+Ba(SO4)
Zn
Fe
30 to 40µm
Si
Gel
Cu
LII
Ni
Organic Species
0.5µm
Cr
As.Sb
LIII
Cu Zn
Fe Cr
Fe Cr
Ba(SO4)
Free Span
Tube Support Plate Zone
C+As.Sb
(with Pb)
: Low angle XR analysis

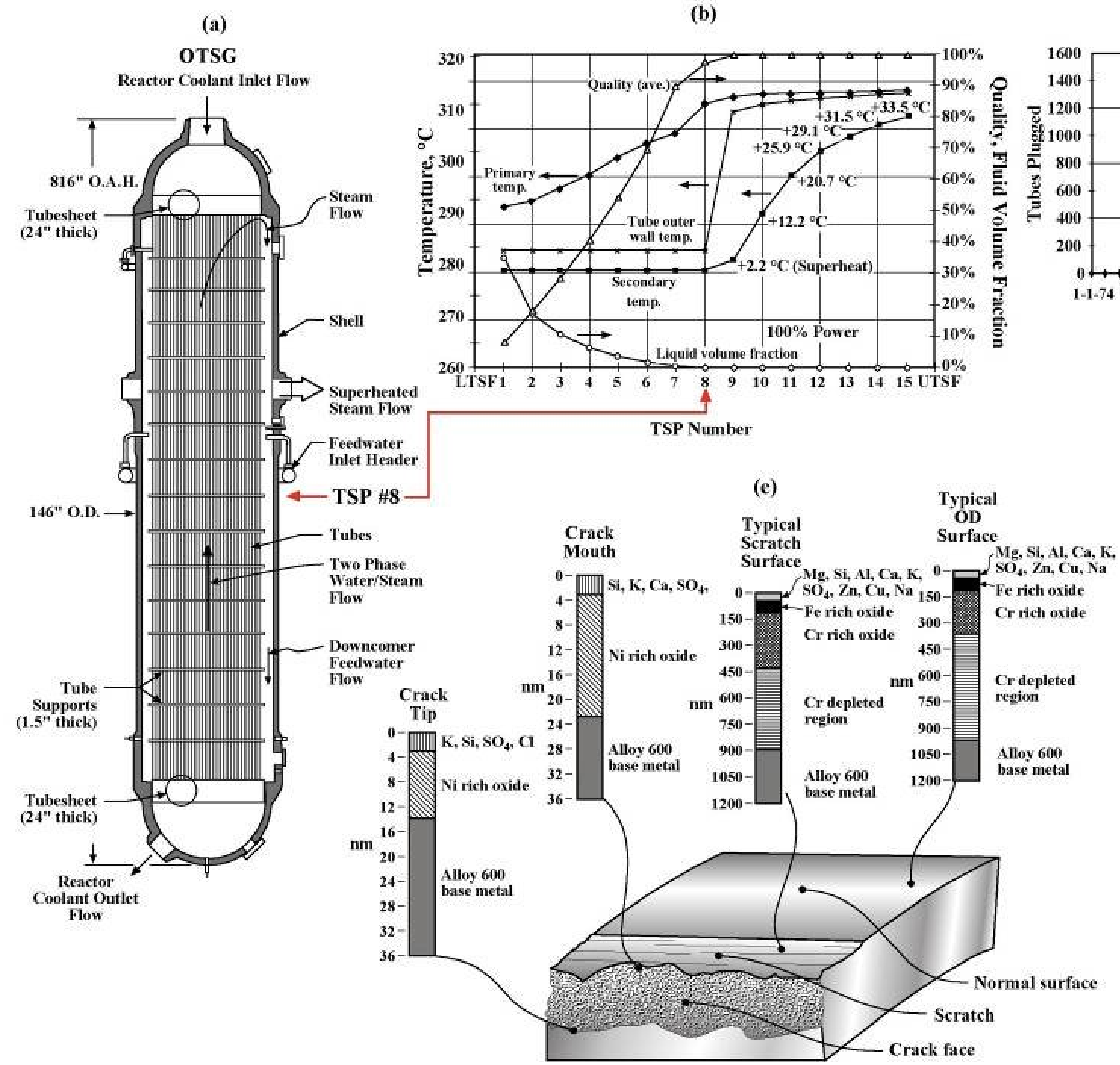

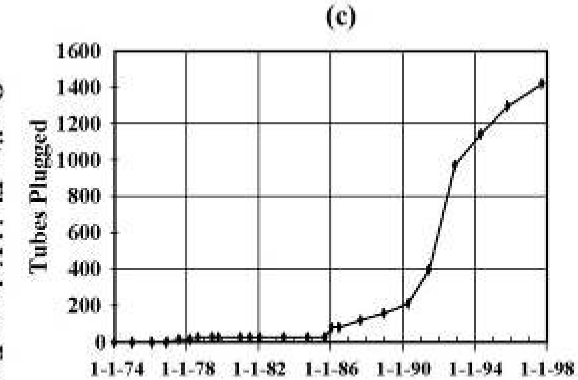

(d)

SG	Total Plugged	Total Percent Plugged
1A	451	2.90
1B	1453	9.36
Total	1904	6.13
2A	501	3.23
2B	676	4.35
Total	1177	3.79
3A	643	4.16
3B	483	3.11
Total	1126	3.63

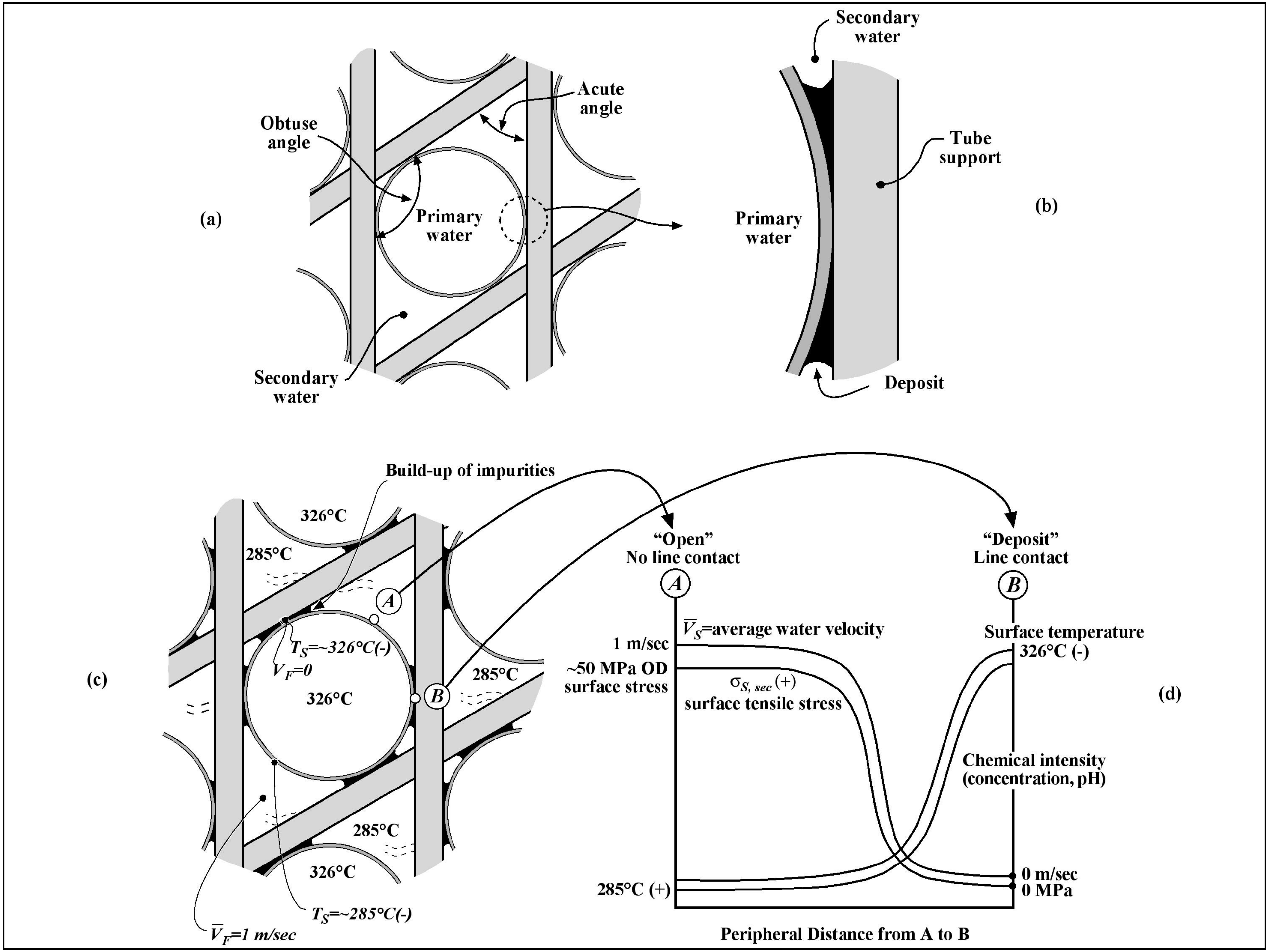

Secondary water
Acute angle
Obtuse angle
Primary water
Tube support
(a)
(b)
Primary water
Secondary water
Deposit
Build-up of impurities
326°C
285°C
T_S=~326°C(-)
V_F=0
326°C
285°C
(c)
285°C
326°C
T_S=~285°C(-)
$\overline{V}_F$=1 m/sec
"Open"
No line contact
"Deposit"
Line contact
A
B
$\overline{V}_S$=average water velocity
Surface temperature
1 m/sec
326°C (-)
~50 MPa OD surface stress
$\sigma_{S,\ sec}$ (+) surface tensile stress
(d)
Chemical intensity (concentration, pH)
0 m/sec
285°C (+)
0 MPa
Peripheral Distance from A to B

SCC due to Pb at line contact crevices

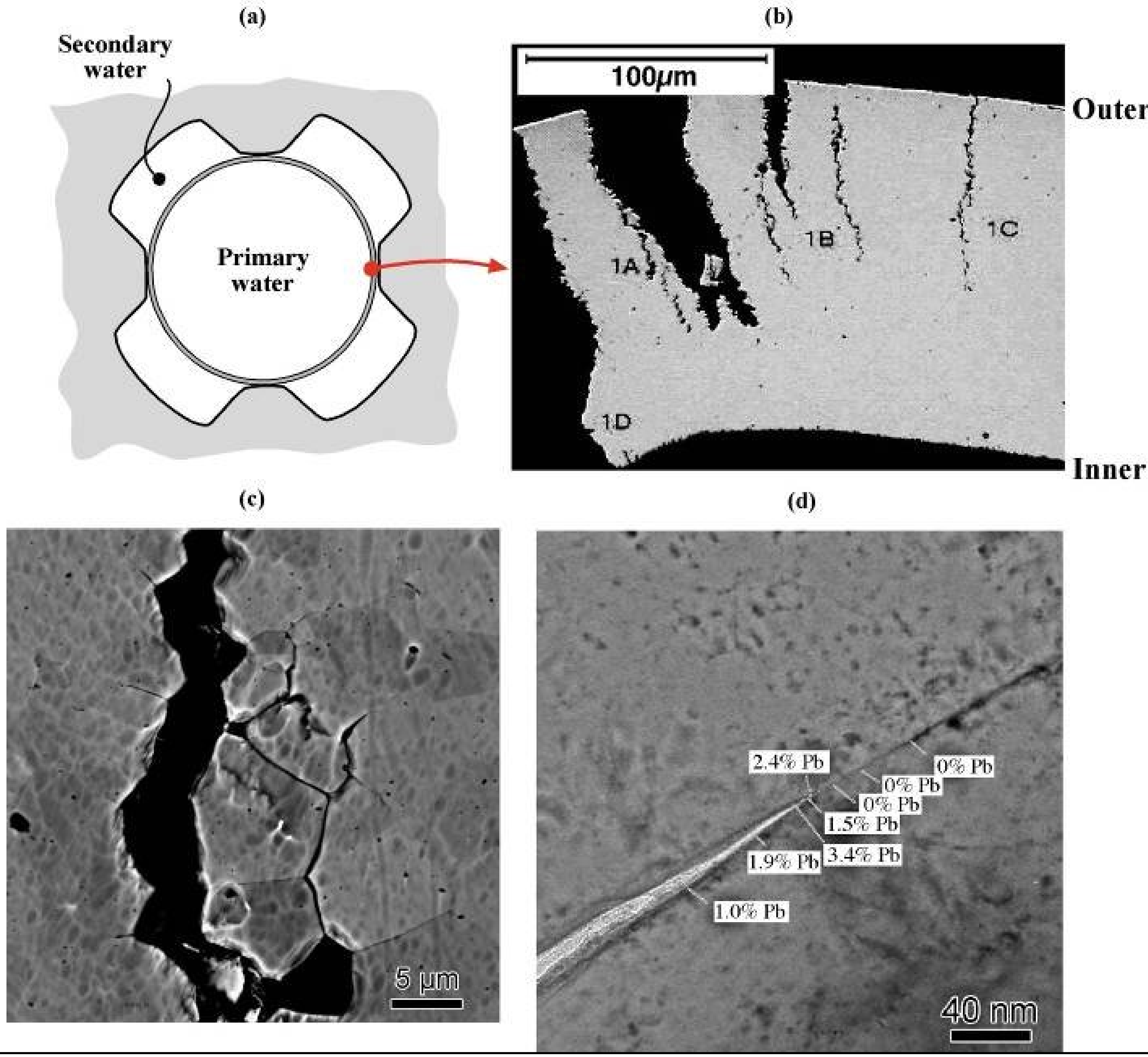

Dependences on Potential

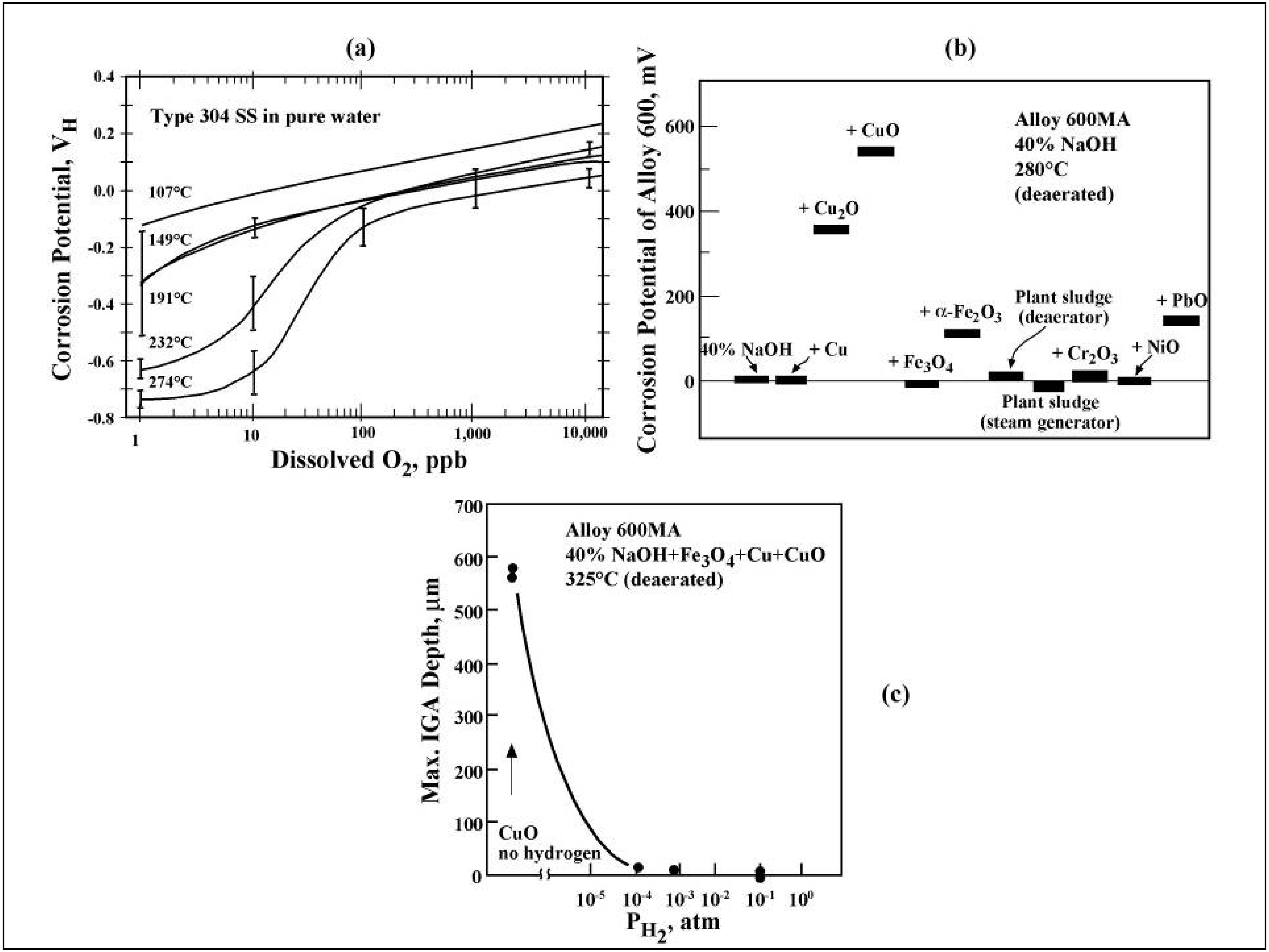
(a)
Type 304 SS in pure water
107°C
149°C
191°C
232°C
274°C
Corrosion Potential, V_H
Dissolved O_2, ppb
(b)
Alloy 600MA
40% NaOH
280°C
(deaerated)
+ CuO
+ Cu_2O
+ α-Fe_2O_3
Plant sludge
(deaerator)
+ PbO
40% NaOH
+ Cu
+ Fe_3O_4
+ Cr_2O_3
+ NiO
Plant sludge
(steam generator)
Corrosion Potential of Alloy 600, mV
Alloy 600MA
40% NaOH+Fe_3O_4+Cu+CuO
325°C (deaerated)
CuO
no hydrogen
Max. IGA Depth, µm
P_{H_2}, atm
(c)

Correlate with Potential and pH

Dynamic polarization as a means for determining stability of protective film

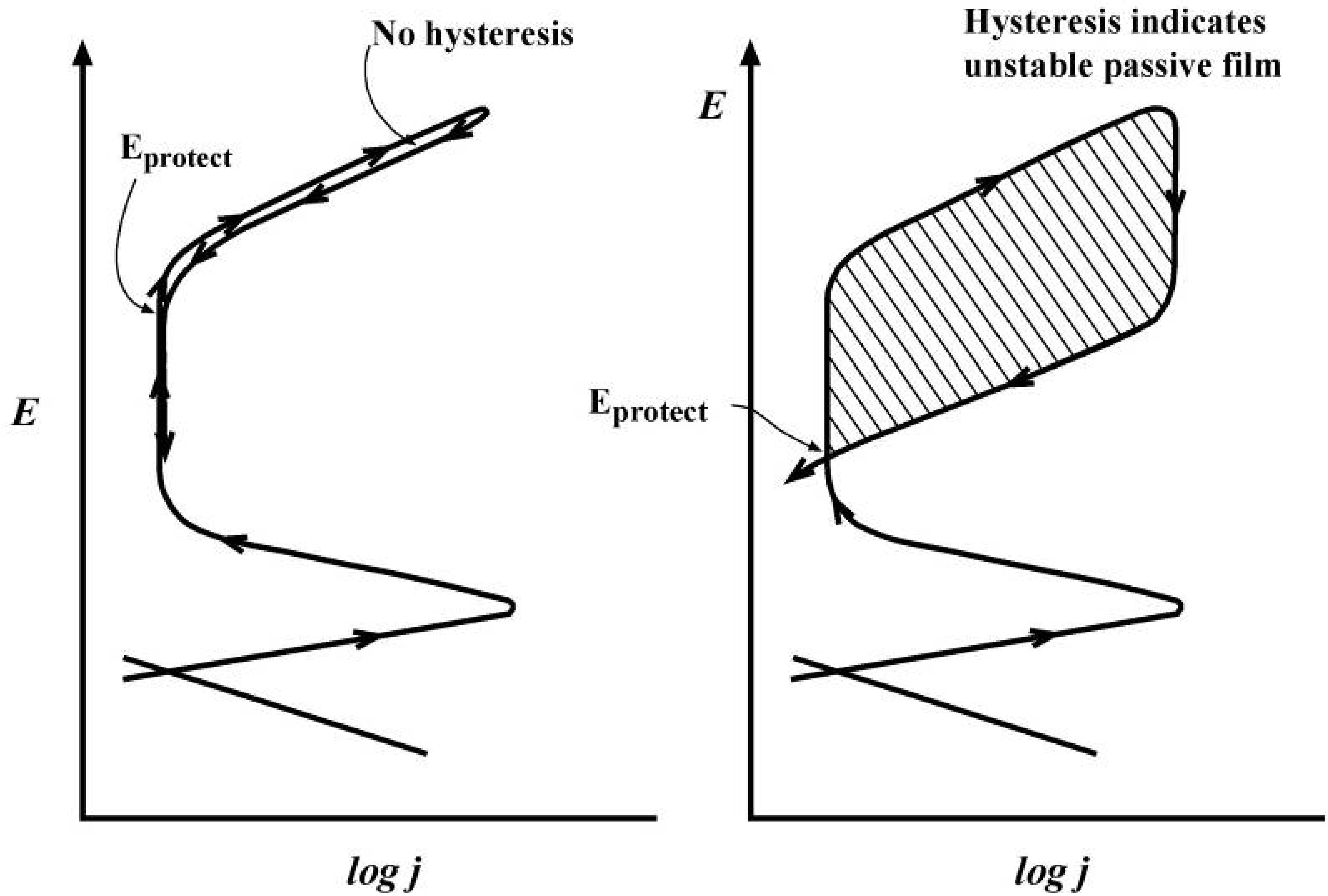

Measuring effects of chloride on pitting occurrence and imperfect passivation

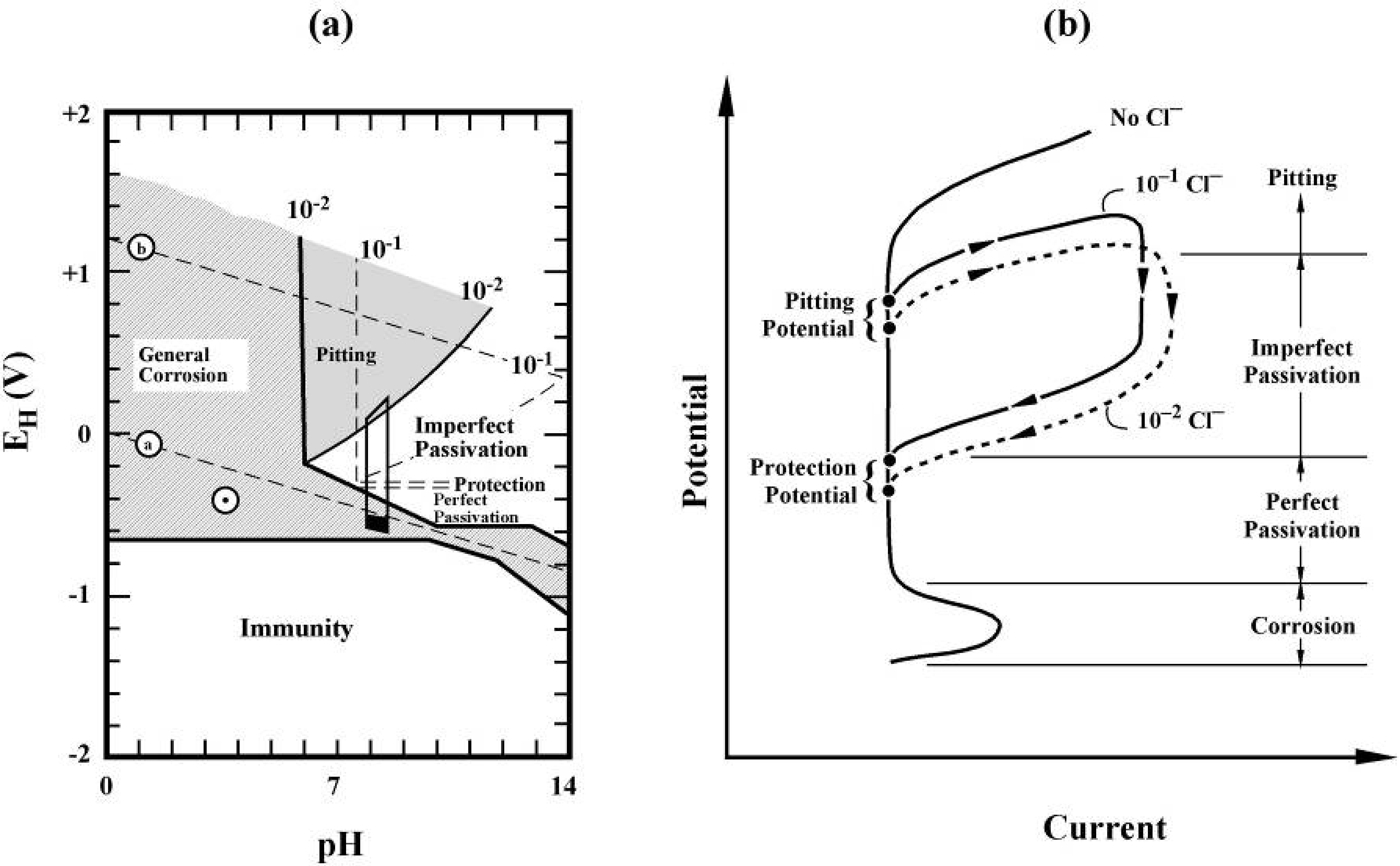

Outside surfaces compared with sequestered conditions with res
to E-pH diagram for Ni

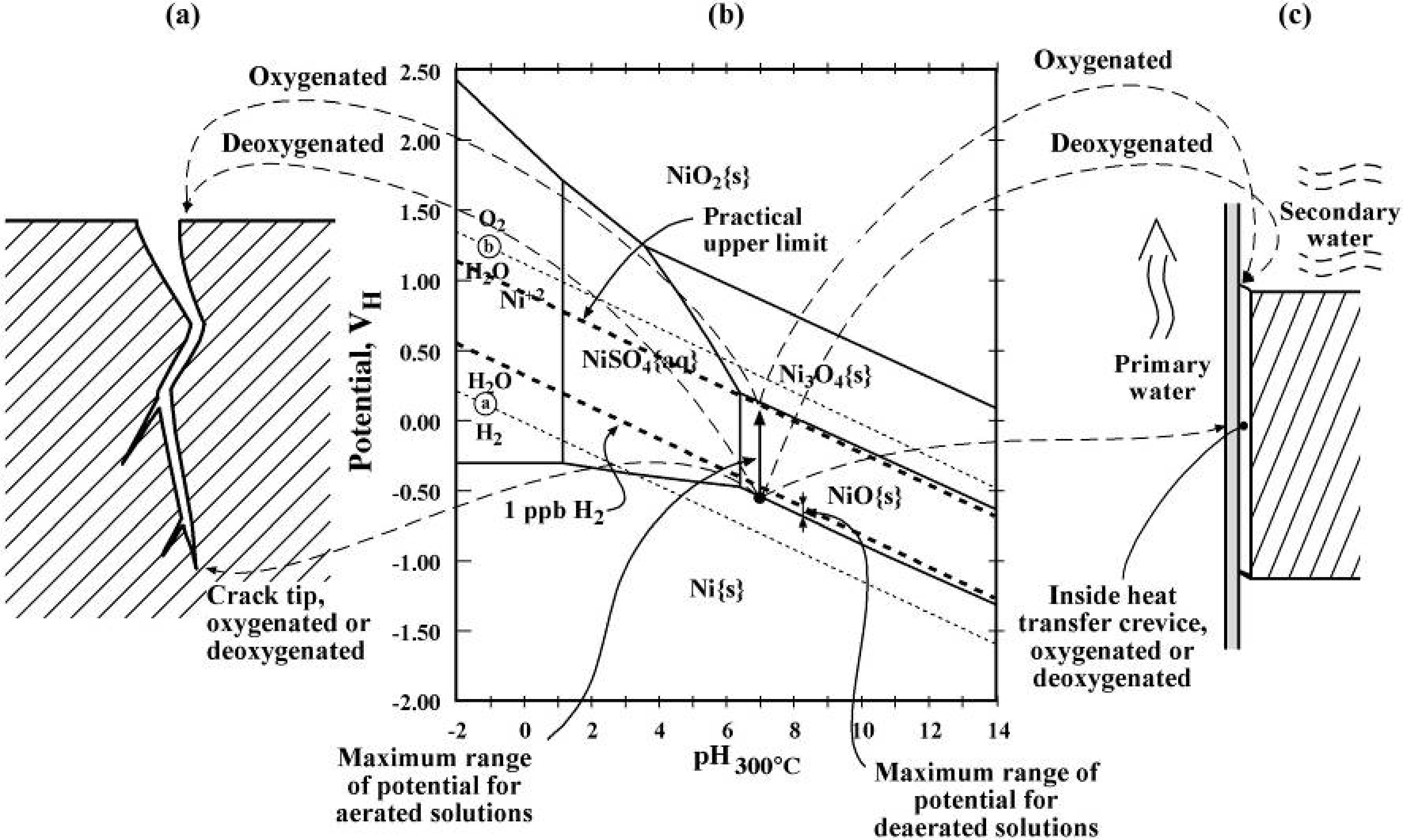

Crack tip as a deaerated mixed electrode

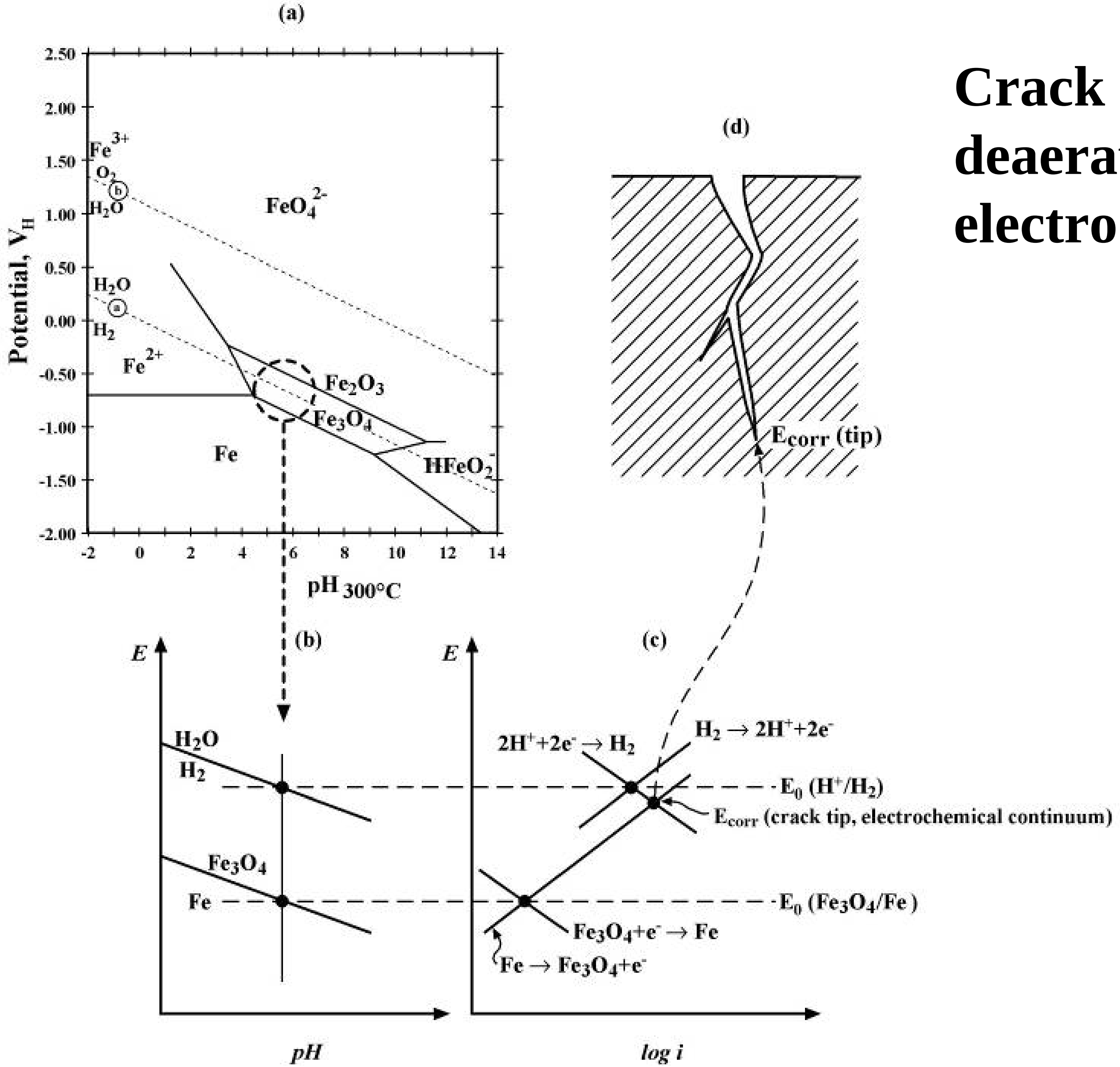

SCC zones for Fe in room temperature solutions

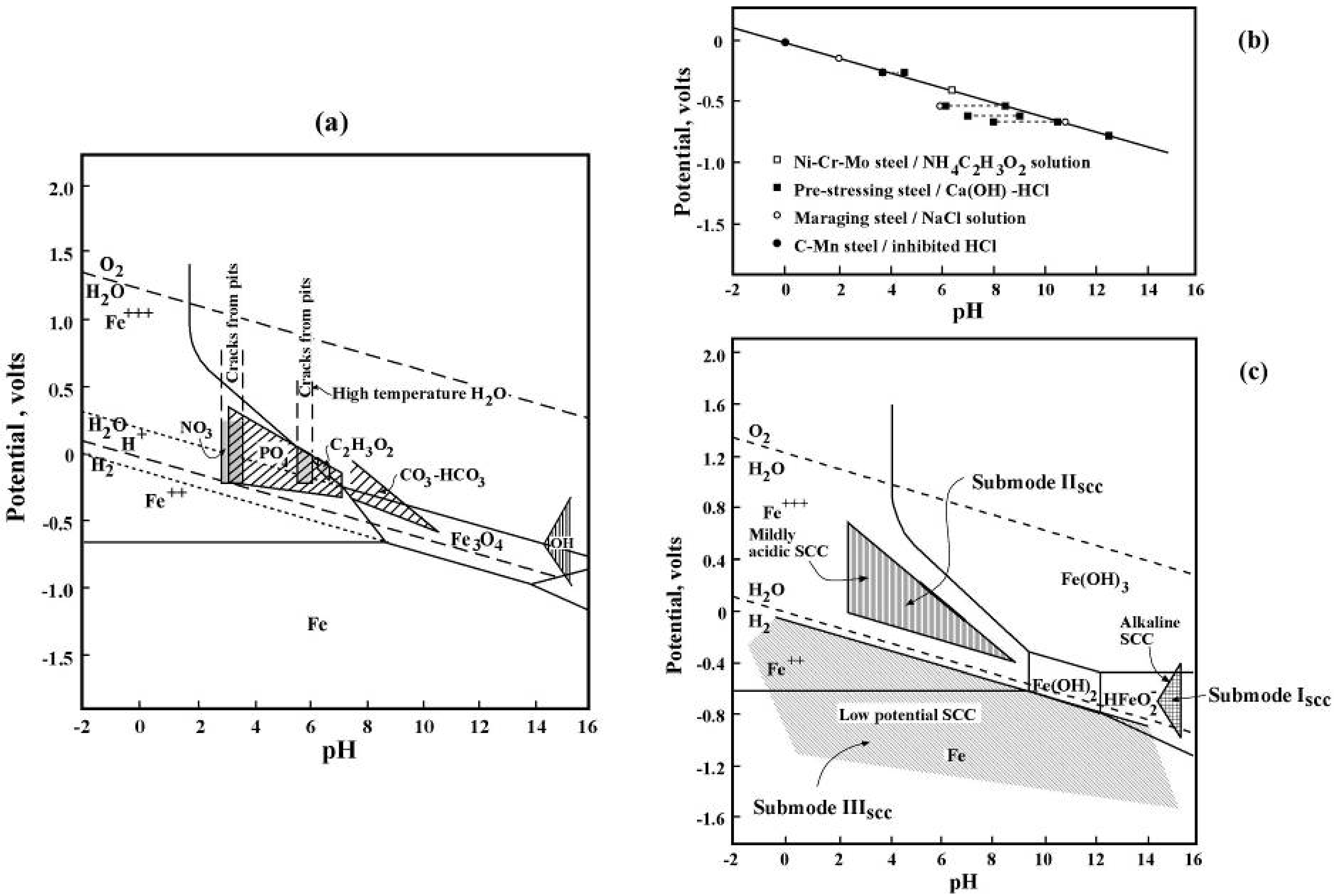

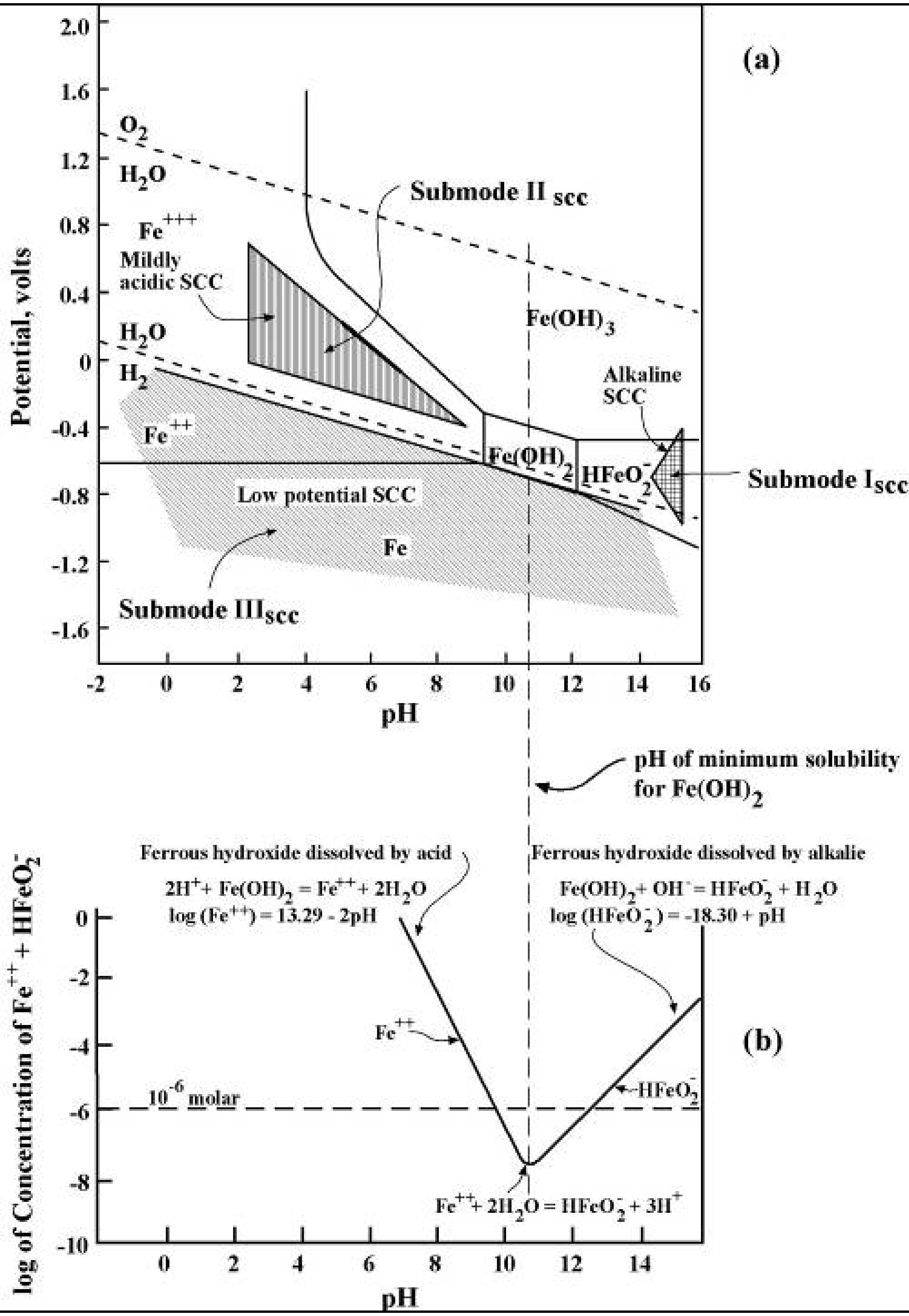

Occurrence of SCC for steel with respect to solubility of Fe

Modes of corrosion of iron and steel compared with E-pH

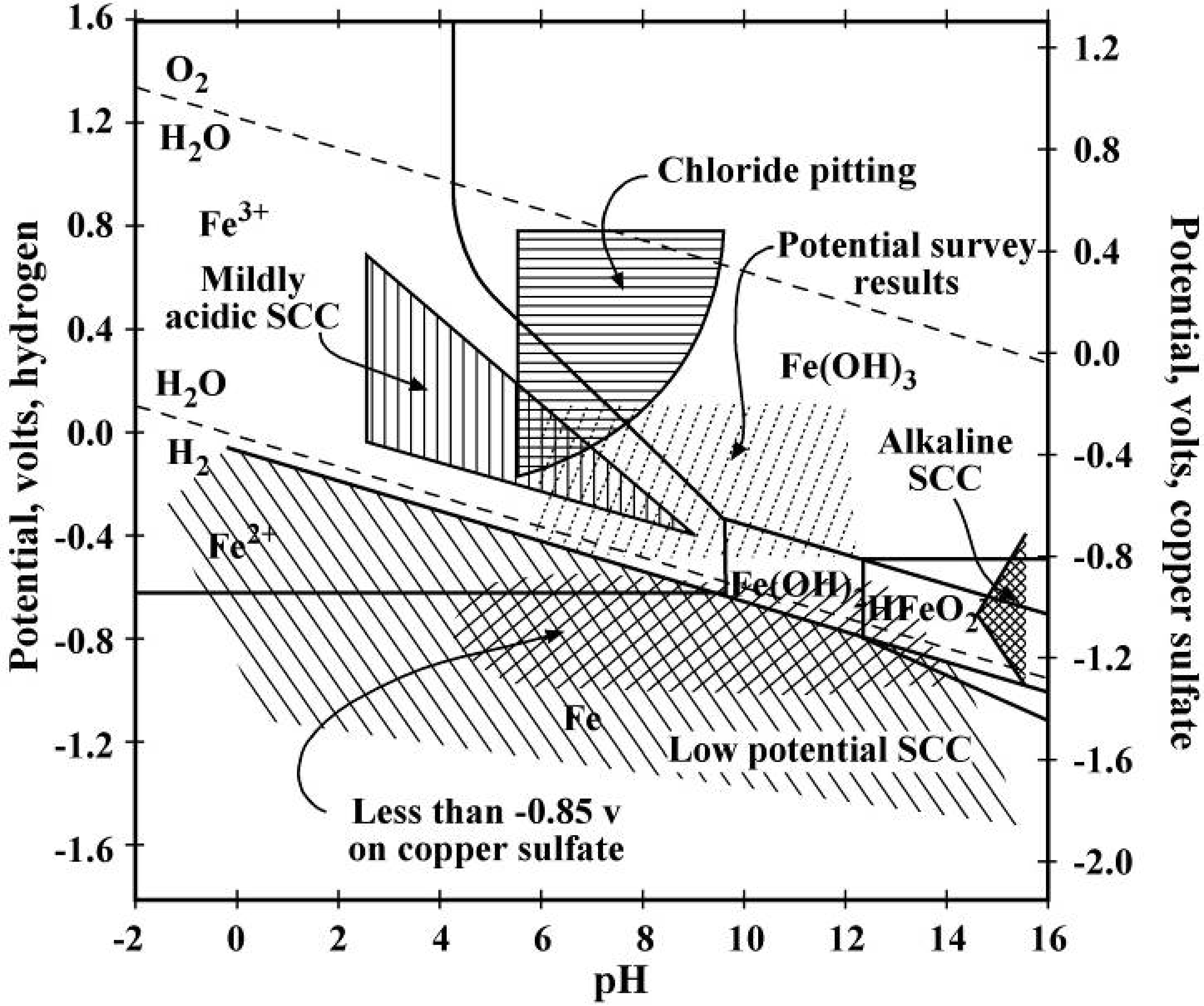

Submodes of SCC for Alloy 600MA in high-temperature water (>300°C)

Other contributors to the "mode diagram" concept

- **Parkins**
- **Pourbaix**
- **Combrade**
- **Tsujikawa**
- **Nagano**

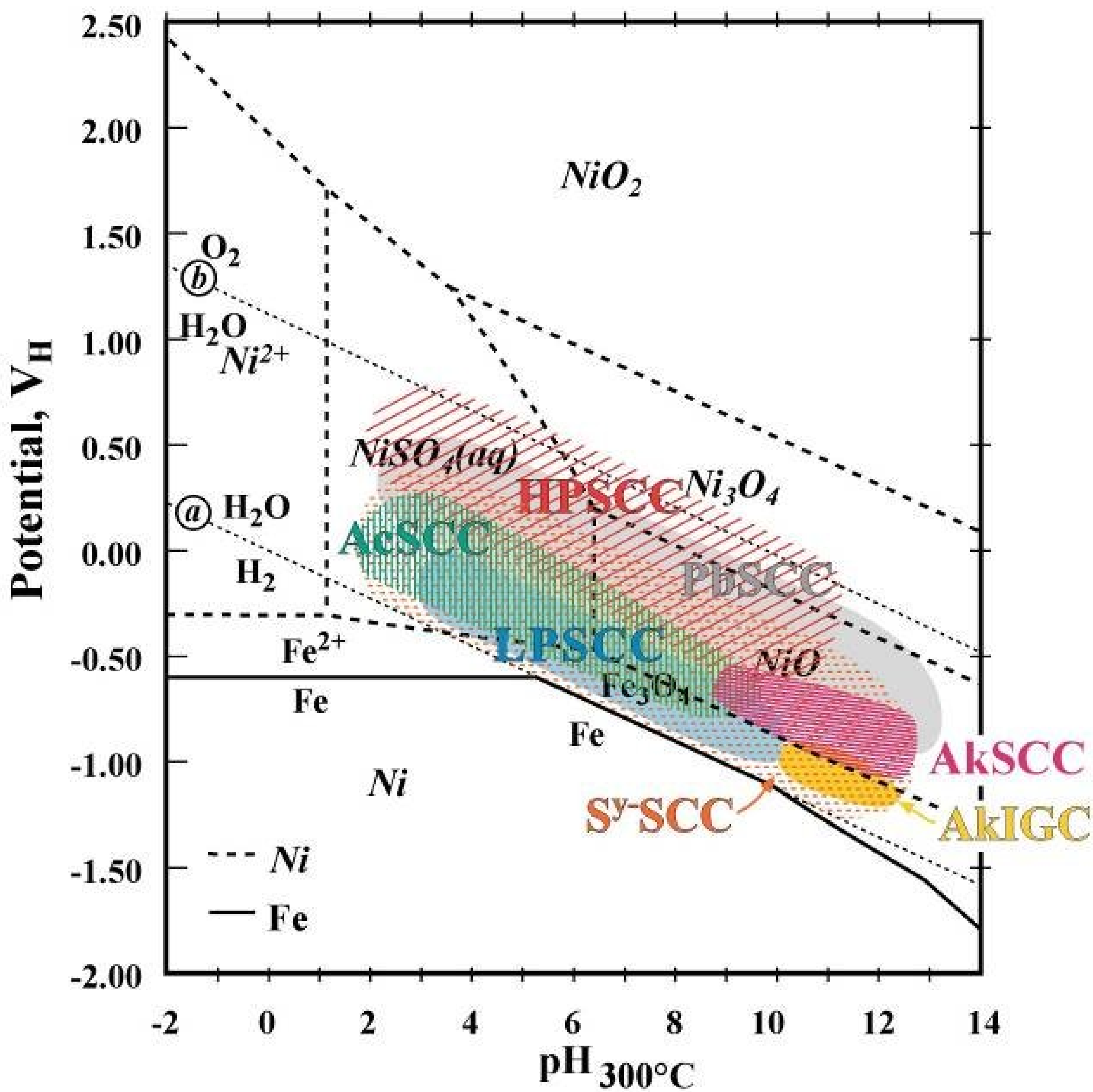

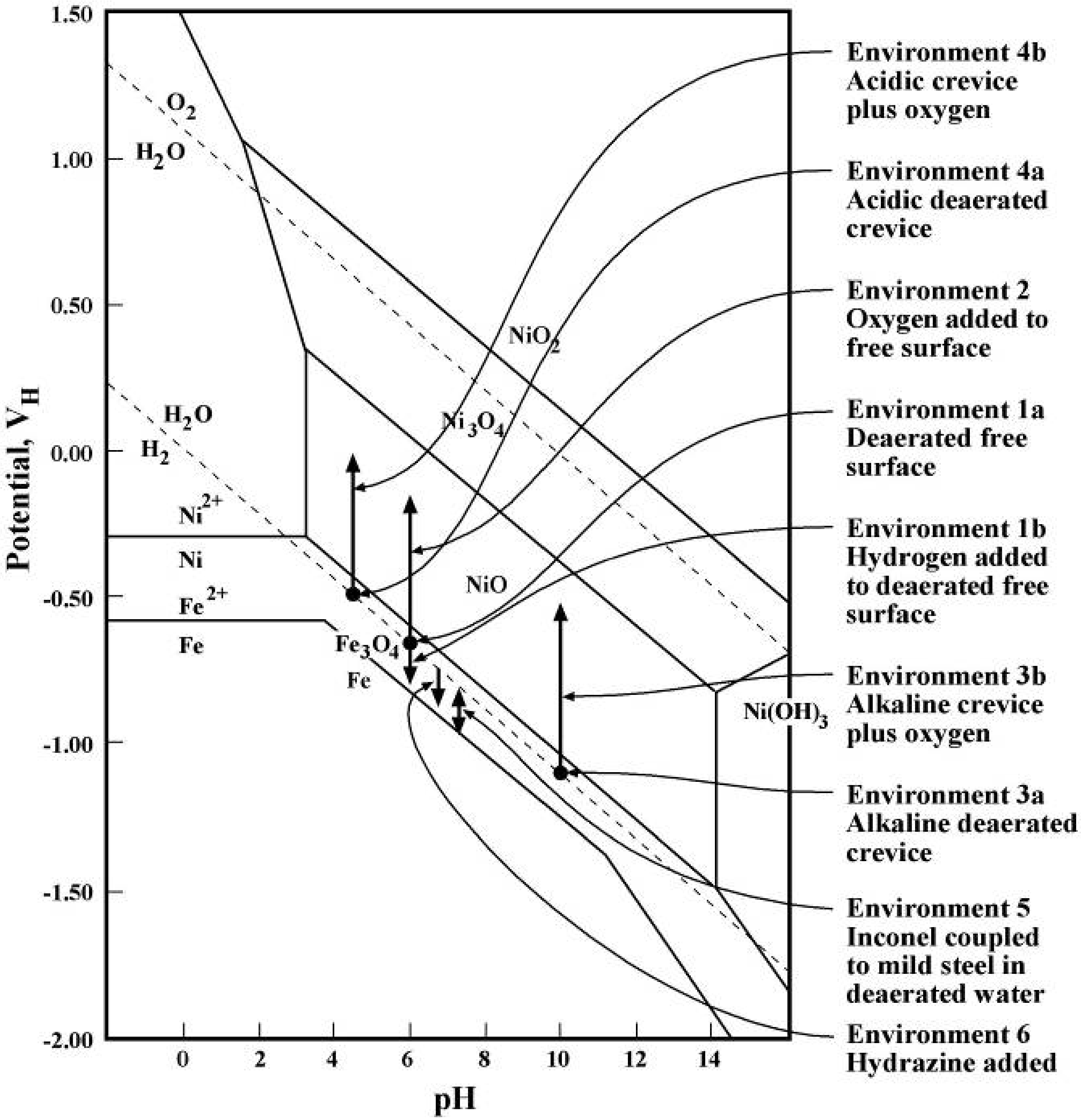

Patterns for electrochemical processes with respect to Ni E-pH diagram

SCC and other modes with respect to active-passive polarization

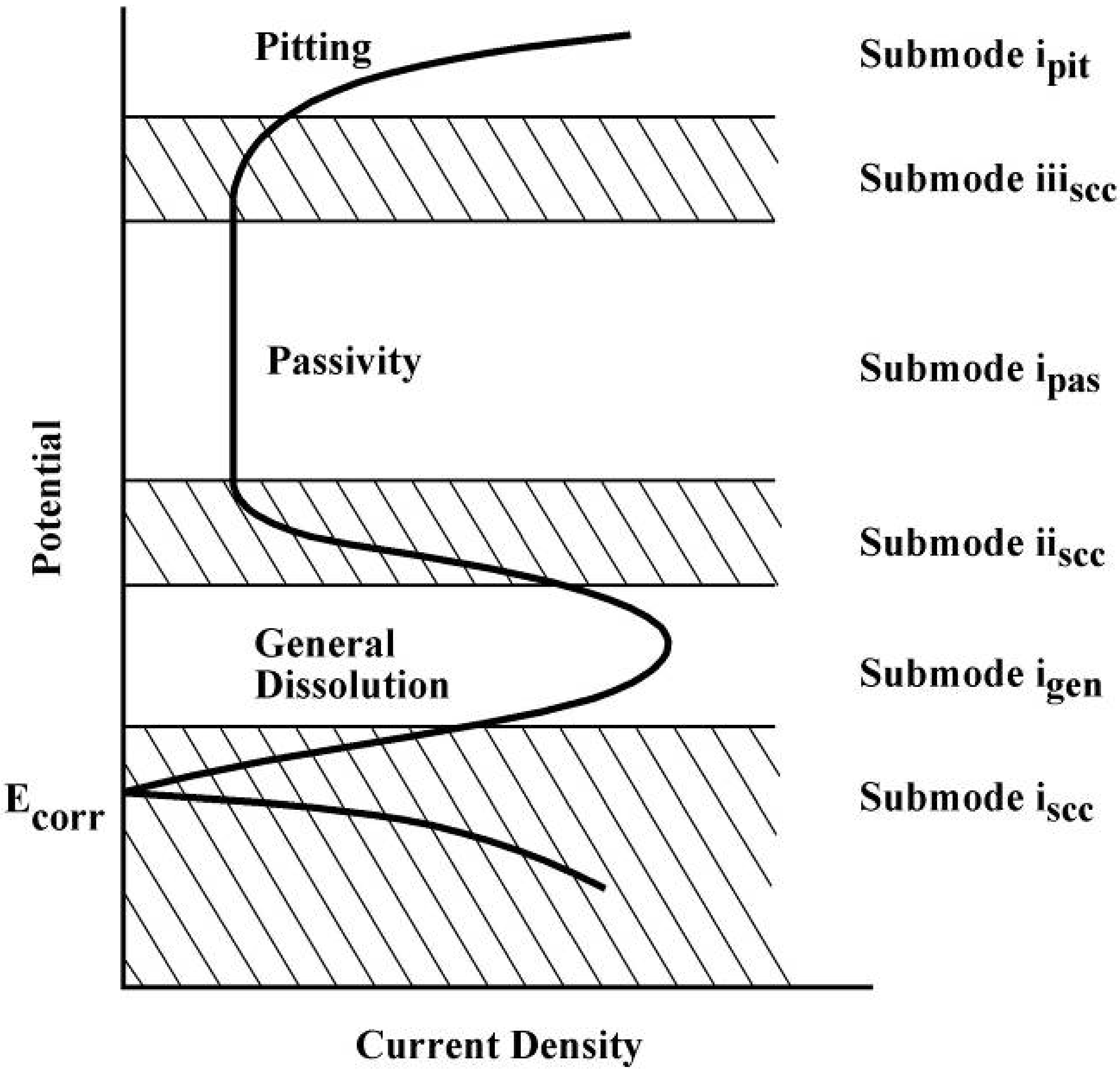

Lead and Impurities

Mass balance for Pb in SGG

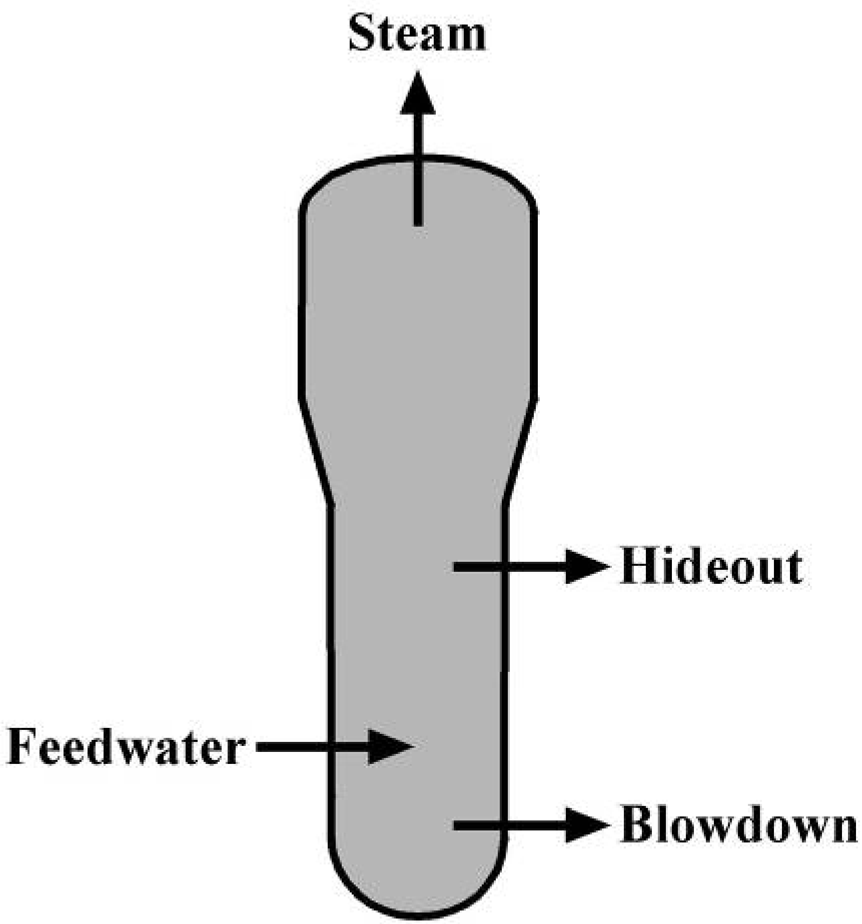

- Feedwater transport
  - Order of 10ppt
  - ~200 - 500 g/yr
- Blowdown transport
  - Order of 100ppt
  - BD = 1% FW
  - ~20 - 50 g/yr
- Steam transport
  - Assume ~0 g/yr
- Hideout
  - Still order of 200 - 500 g/yr
- Average yearly accumulation on SG tubes at TSPs ~500 monolayers/yr based on 200 g/yr hideout

PbSCC as function of pH and potential

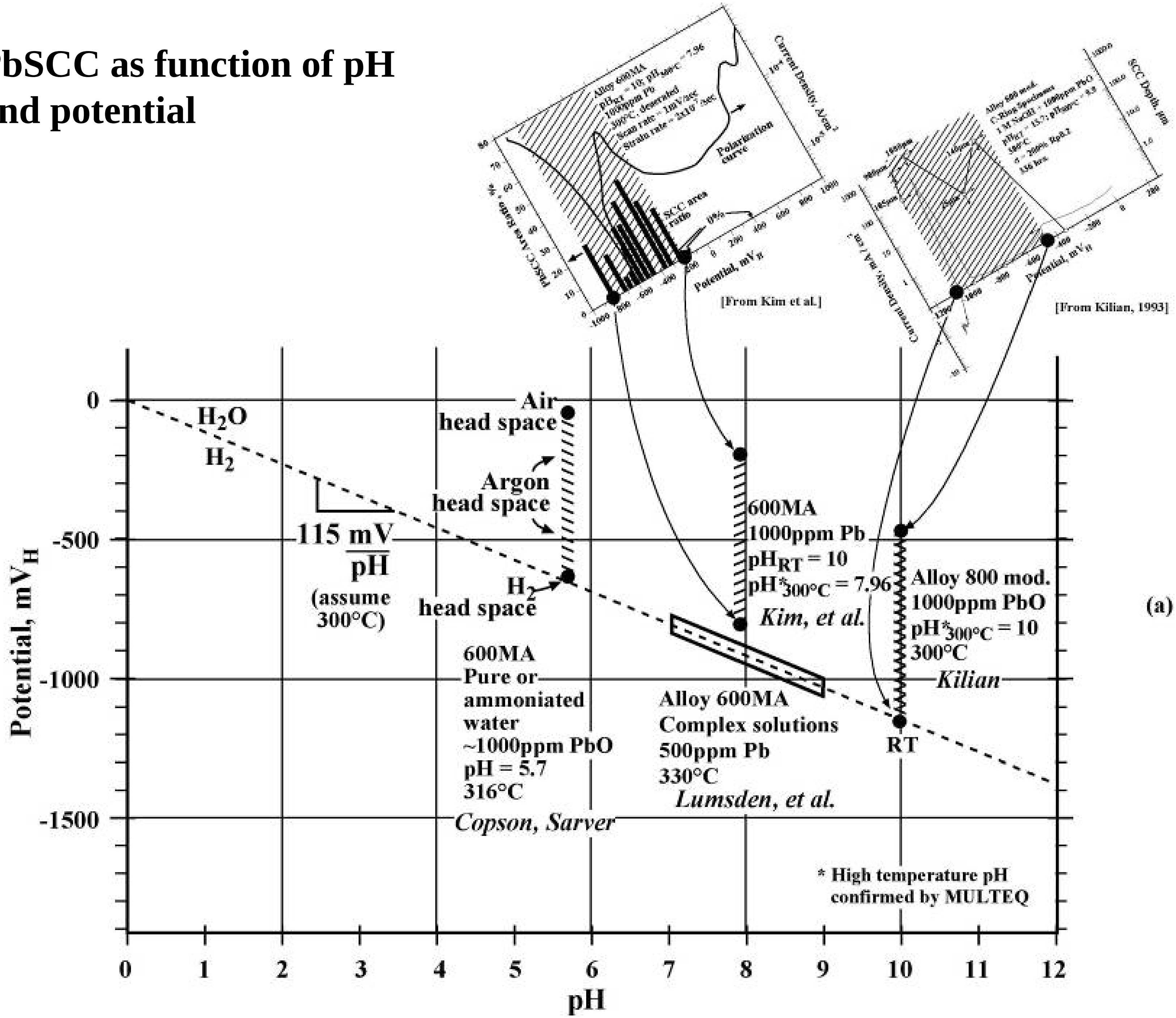

SCC and spalling of Fe-Cr-Ni alloys in Pb solutions

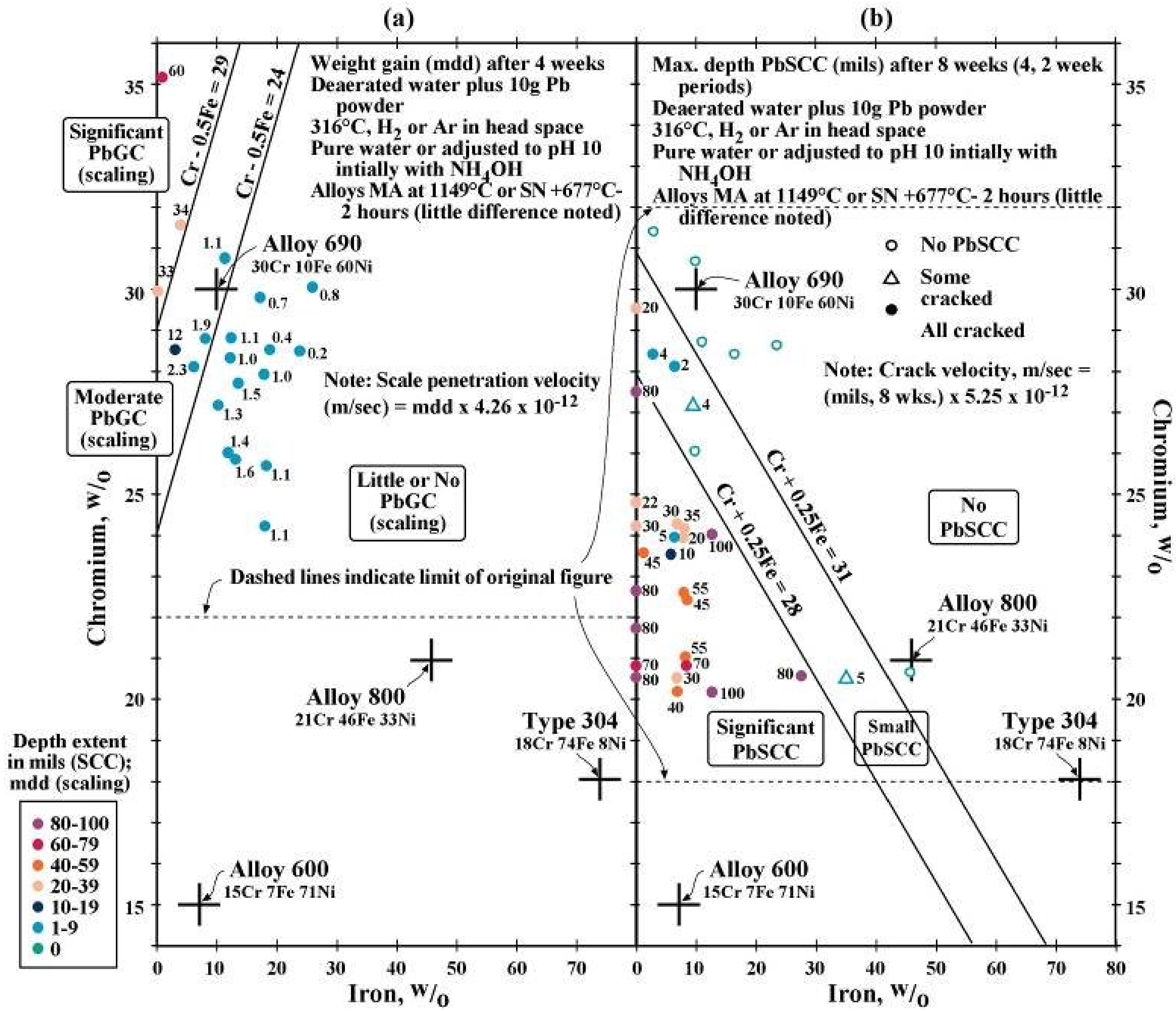

Alloy 600, E_{corr}, 500ppm Pb, simulated upper bundle pore chemistry

$0.01mFe_3O_4+0.05mAl_2O_3+0.3mSiO_2+0.15mKOH+0.04mHCl$
$+1.5m\ Na_2SO_4$, 500ppm as $PbO+6ppm\ H_2$, $pH_{330°C}=9$

(a)	(b)	(c)
Alloy 600 MA; tested 840 hours; as rec'd; mod Huey=15 mdd	Alloy 600 TT; tested 2770 hours; 1300°F/15h; mod Huey=32 mdd	Alloy 600 SN; tested 1150 hours; 1100F/18h; mod Huey=1052 mdd

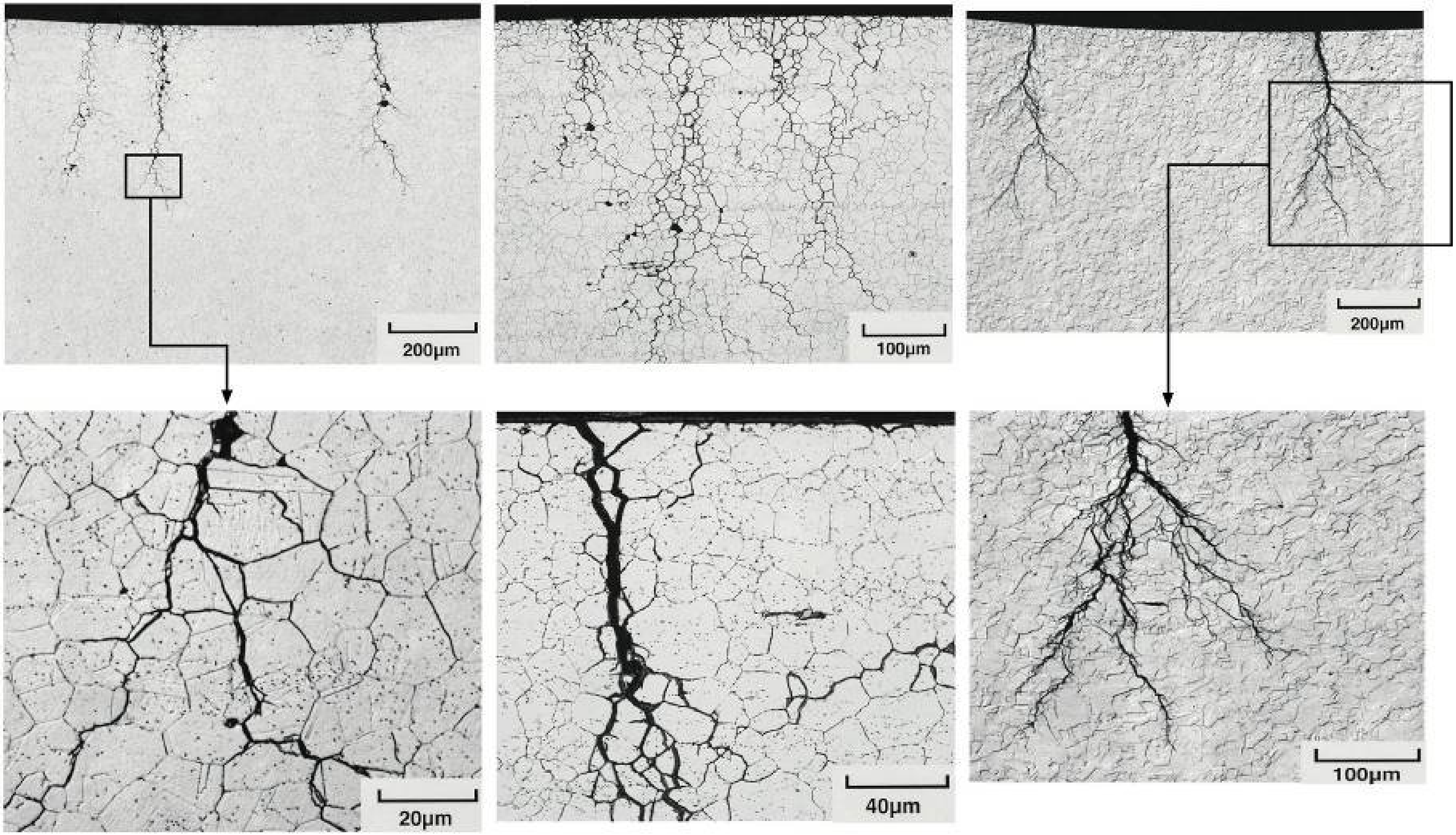

Scaling of Alloy 800 at elevated potential due to Pb

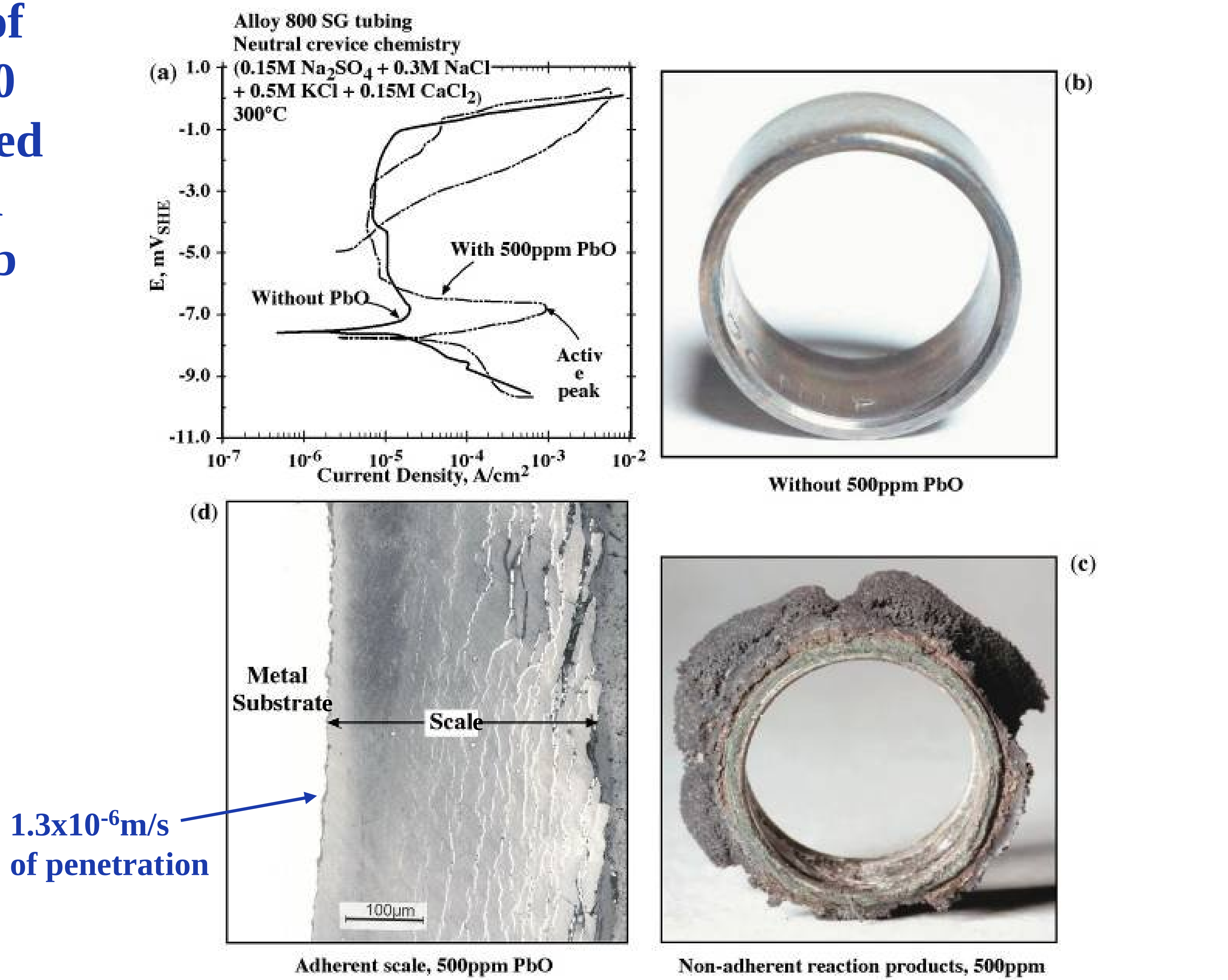

Alloy 800 SG tubing samples, near active peak for 24 hrs.
Neutral crevice chemistry (0.15M Na_2SO_4 + 0.3M NaCl + 0.5M KCl + 0.15M $CaCl_2$), at 300°C [From Lu, 2005]

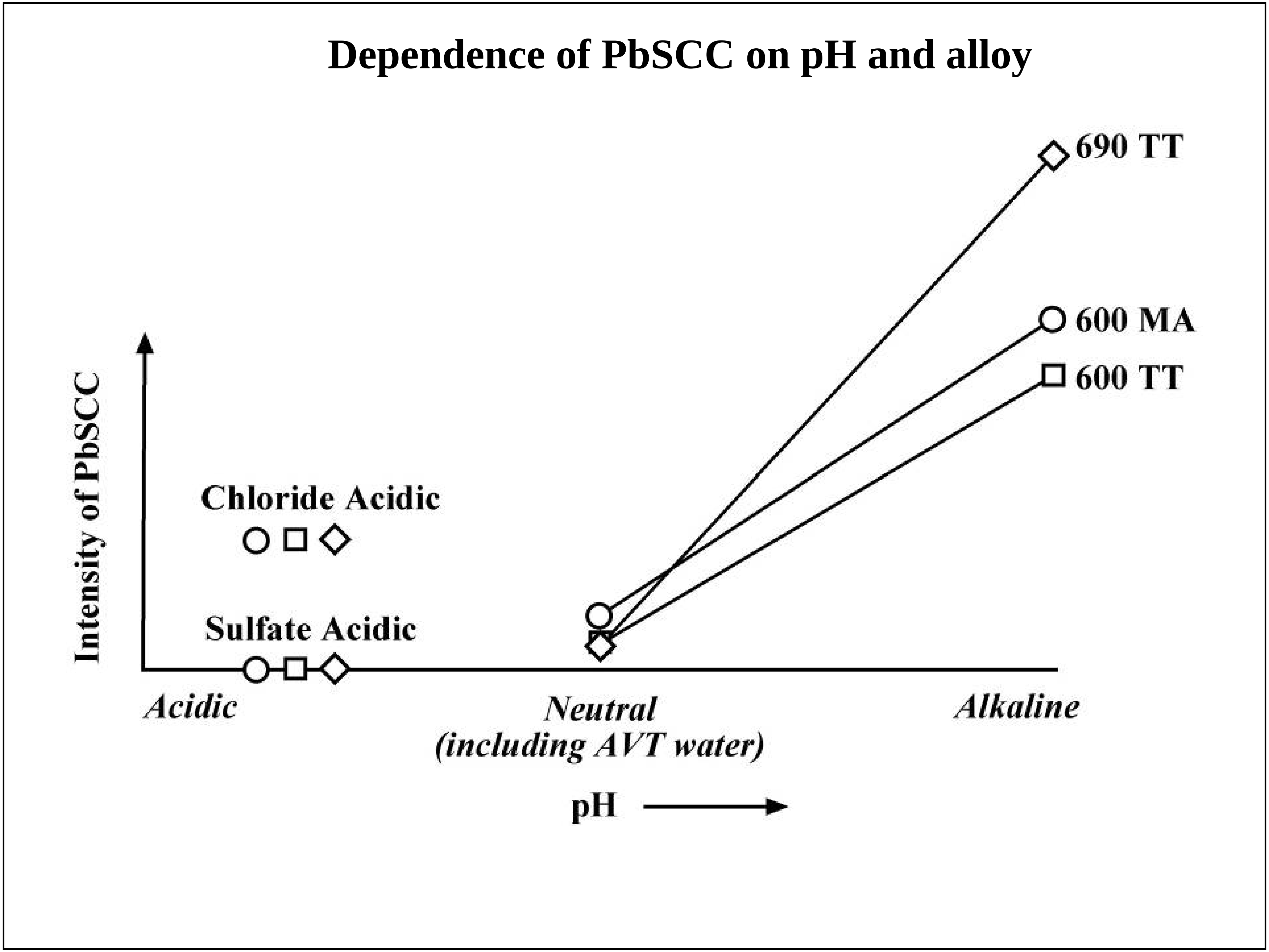
Dependence of PbSCC on pH and alloy
690 TT
600 MA
600 TT
Intensity of PbSCC
Chloride Acidic
Sulfate Acidic
Acidic
Neutral
(including AVT water)
Alkaline
pH

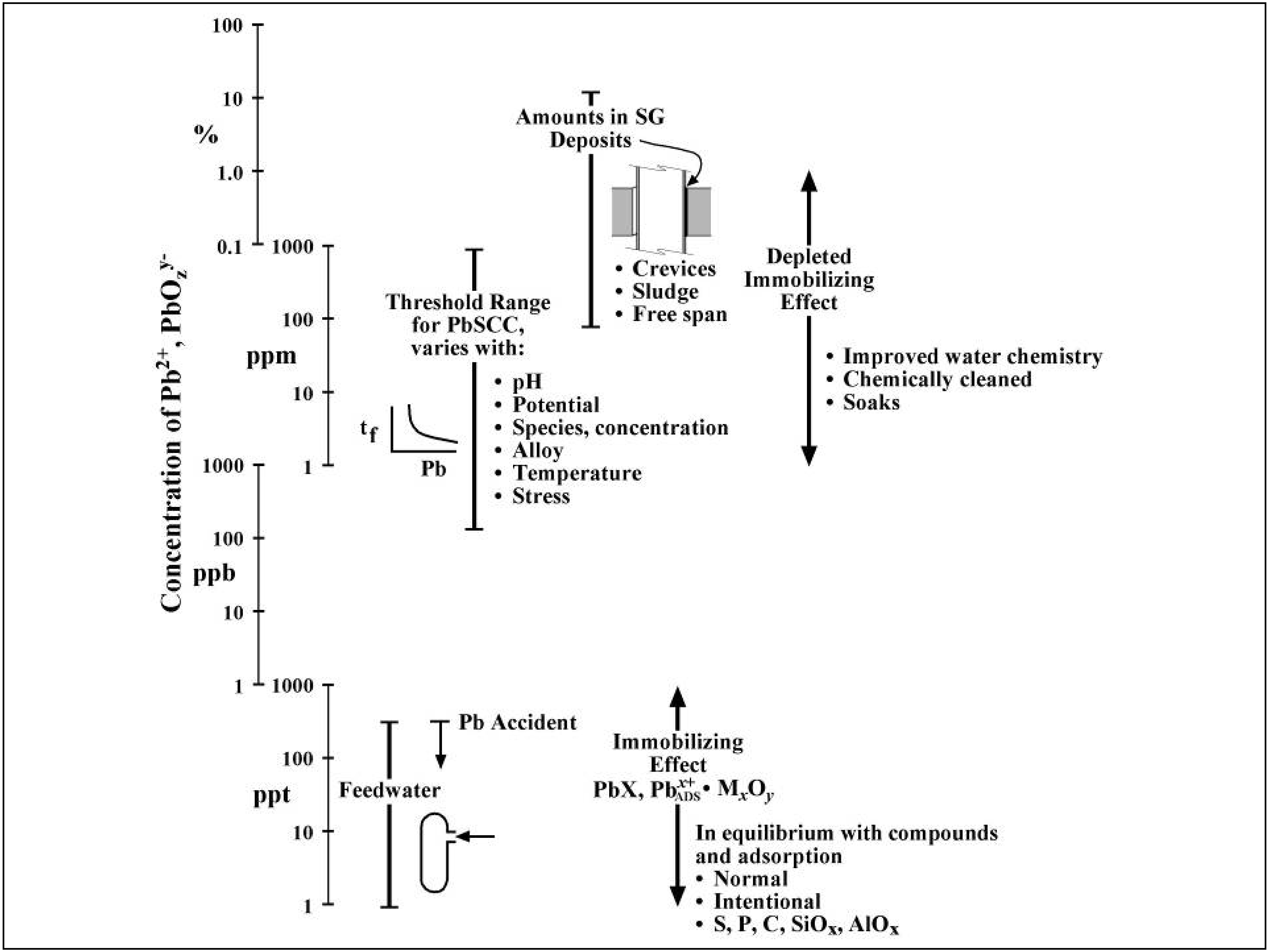

Concentration of Pb^{2+}, PbO_z^{y-}
%
100
10
1.0
0.1
ppm
1000
100
10
1
ppb
1000
100
10
1
ppt
1000
100
10
1
Amounts in SG Deposits
• Crevices
• Sludge
• Free span
Threshold Range for PbSCC, varies with:
• pH
• Potential
• Species, concentration
• Alloy
• Temperature
• Stress
t_f
Pb
Depleted Immobilizing Effect
• Improved water chemistry
• Chemically cleaned
• Soaks
Pb Accident
Feedwater
Immobilizing Effect
PbX, $Pb^{x+}_{ADS} \cdot M_xO_y$
In equilibrium with compounds and adsorption
• Normal
• Intentional
• S, P, C, SiO_x, AlO_x

Generation of low valence sulfur in SGs by reaction with hydrazine

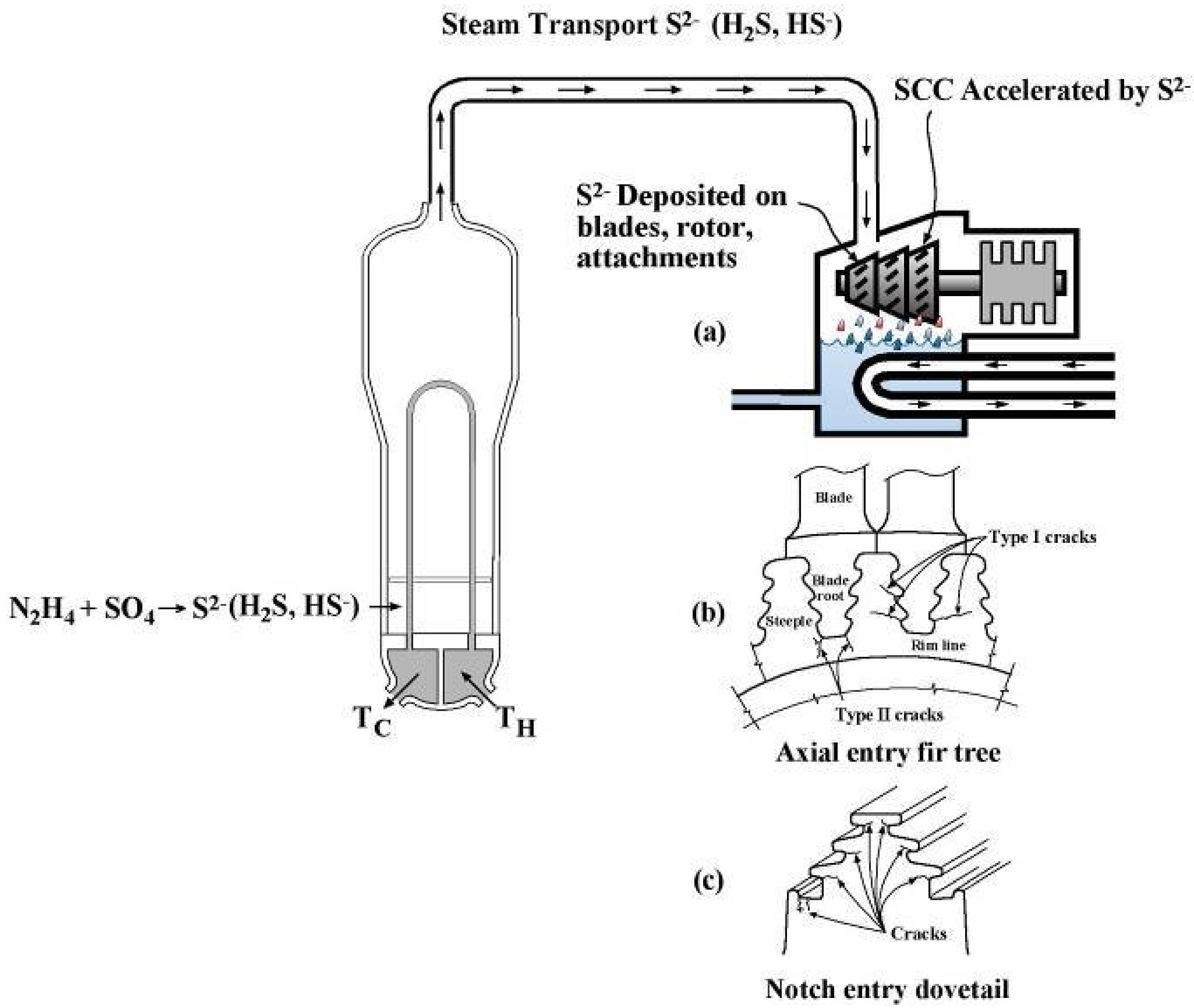

Flow Velocity

FAC and mitigations: oxidizing, Cr in alloy, raise pH

Oxidation reduction proportional to flow

Intersection with active-passive character

Flow assisted corrosion, Mihama-3, 2004

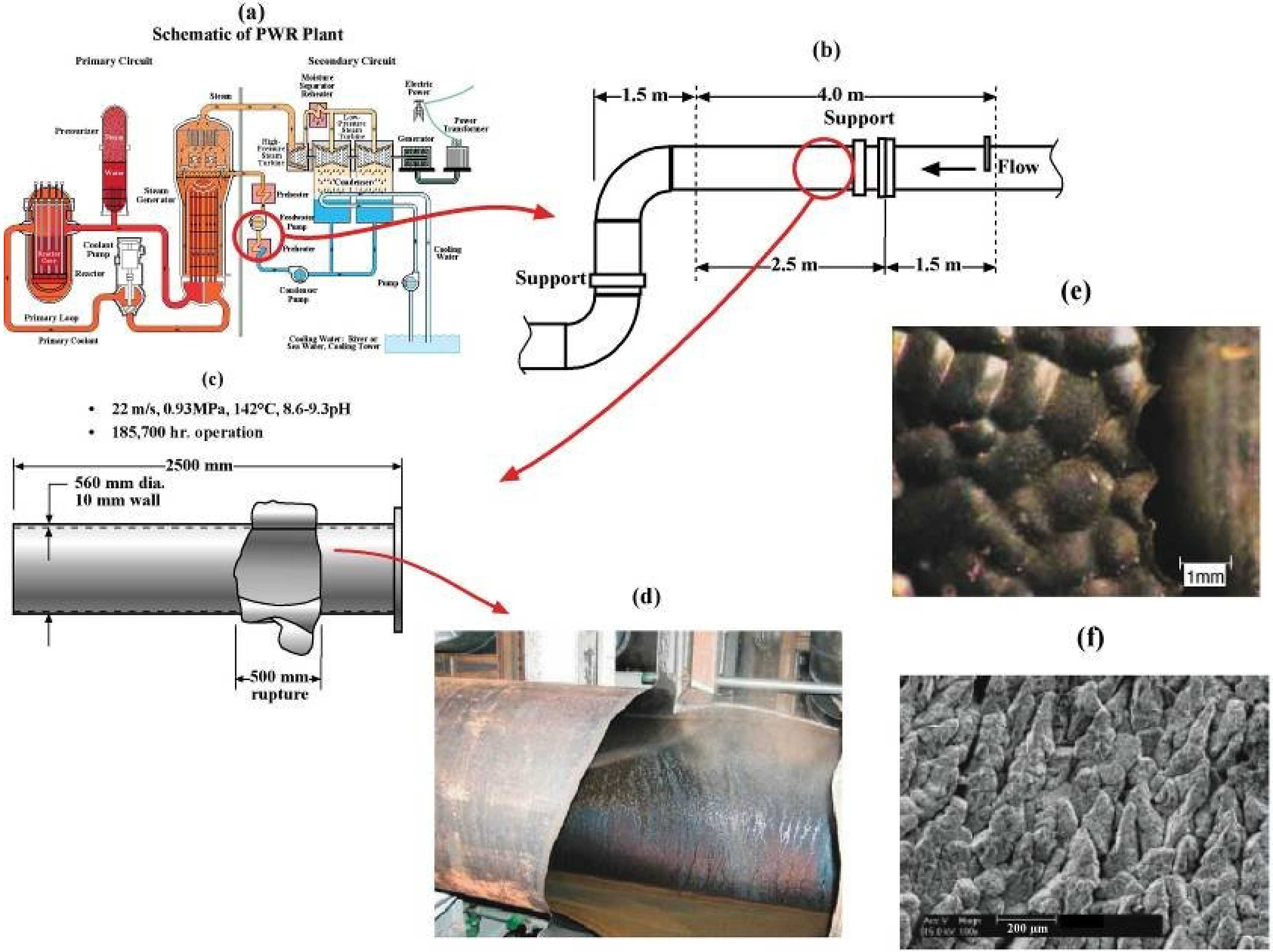

FAC

Loss vs. flow and temperature

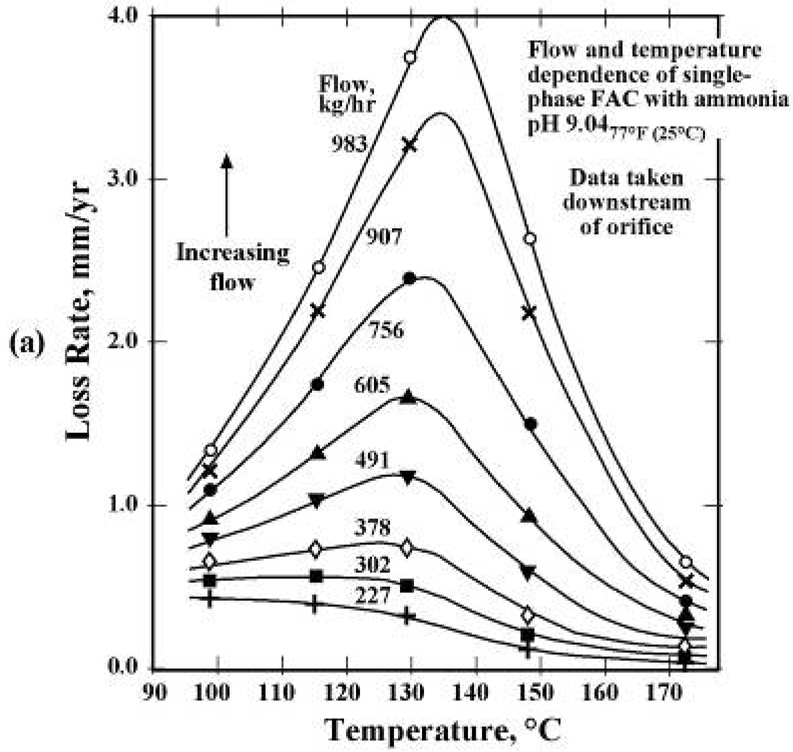

Loss vs. flow and pH

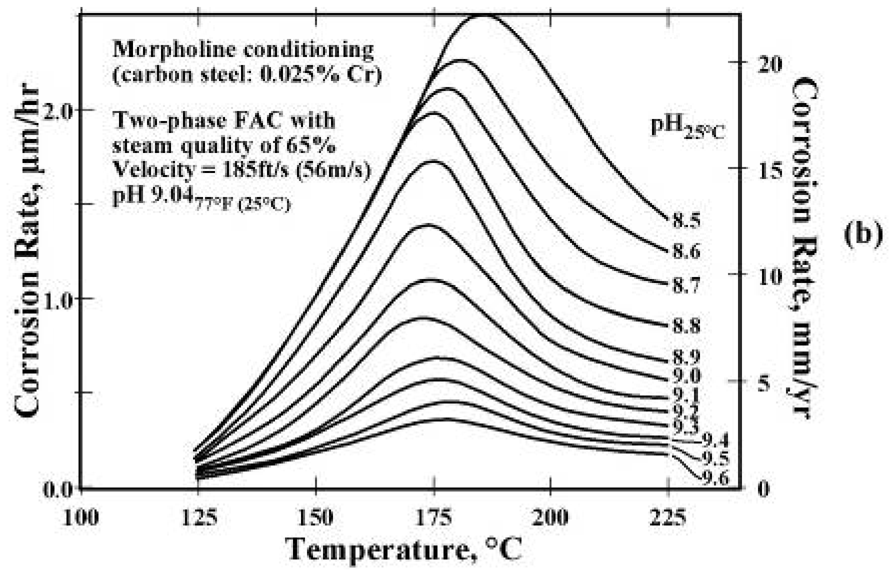

from Tapping

Relative thinning rate
vs. concentration of Cr in alloy

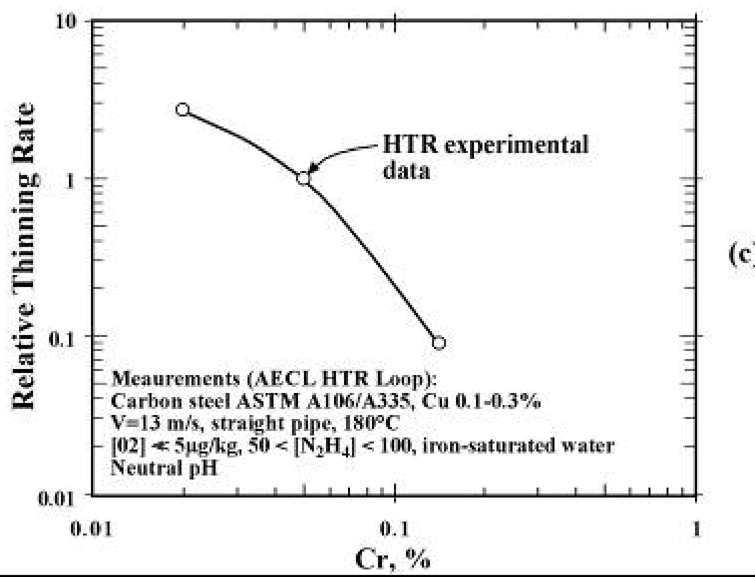

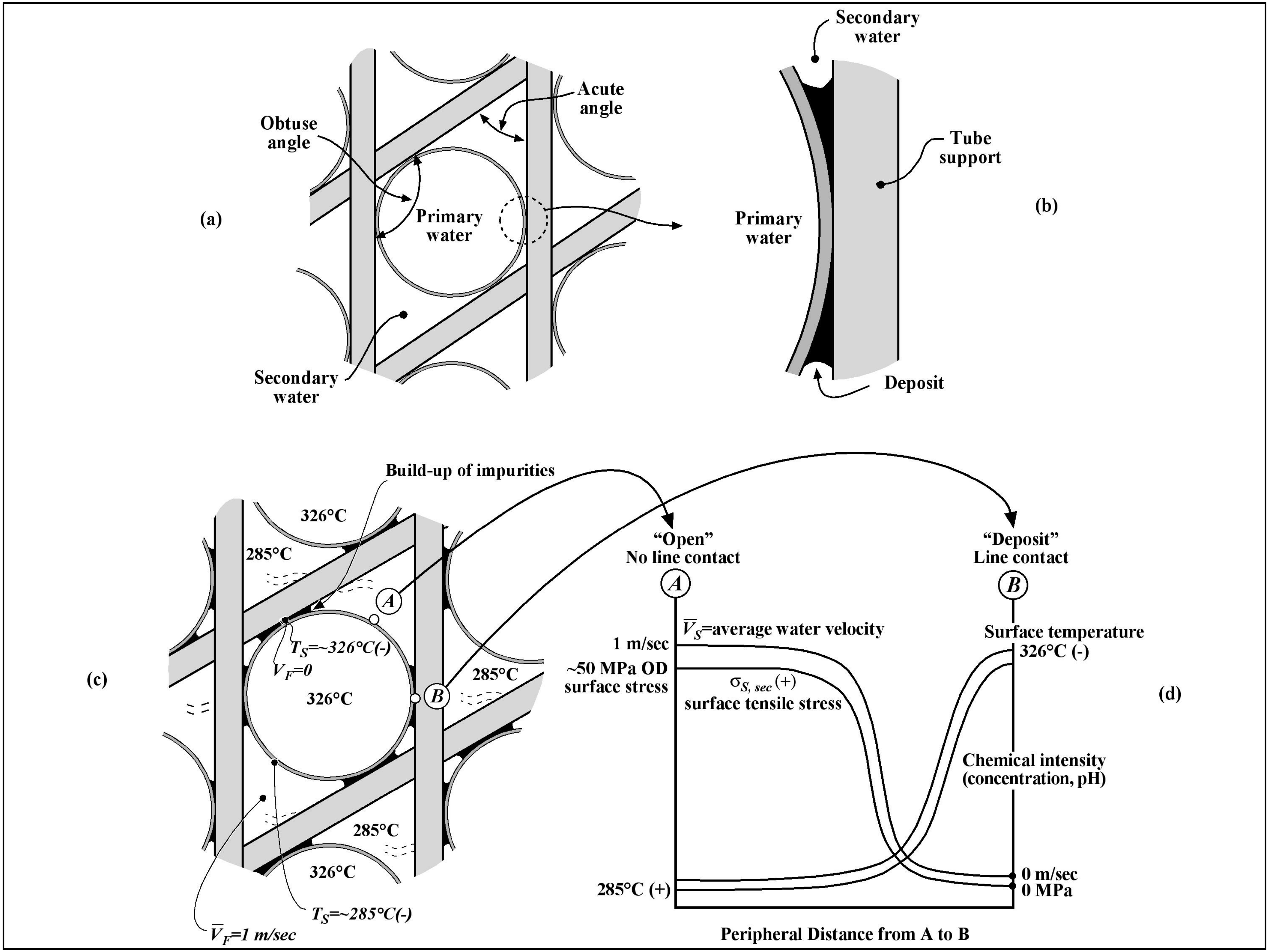

Obtuse angle
Acute angle
Primary water
Secondary water
(a)
Secondary water
Tube support
Primary water
Deposit
(b)
Build-up of impurities
326°C
285°C
A
T_S=~326°C(-)
V_F=0
326°C
B
285°C
285°C
326°C
T_S=~285°C(-)
$\overline{V}_F$=1 m/sec
(c)
"Open"
No line contact
"Deposit"
Line contact
A
B
$\overline{V}_S$=average water velocity
1 m/sec
~50 MPa OD surface stress
$\sigma_{S,\ sec}$ (+) surface tensile stress
Surface temperature
326°C (-)
Chemical intensity (concentration, pH)
285°C (+)
0 m/sec
0 MPa
Peripheral Distance from A to B
(d)

Gradients in Potential

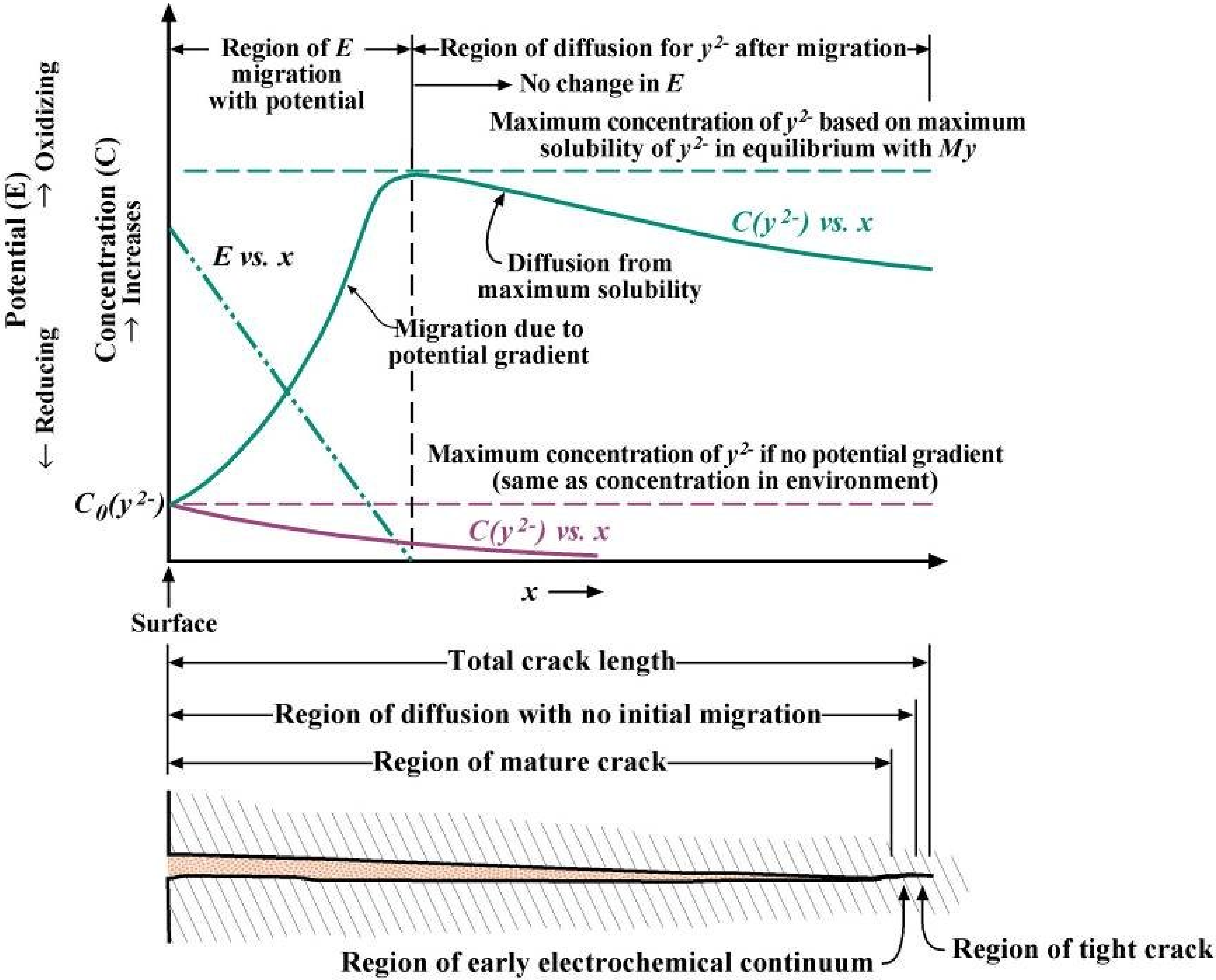

Region of E migration with potential
Region of diffusion for y^{2-} after migration
No change in E
Maximum concentration of y^{2-} based on maximum solubility of y^{2-} in equilibrium with My
Potential (E) ← Reducing → Oxidizing
Concentration (C) → Increases
E vs. x
$C(y^{2-})$ vs. x
Diffusion from maximum solubility
Migration due to potential gradient
Maximum concentration of y^{2-} if no potential gradient (same as concentration in environment)
$C_0(y^{2-})$
$C(y^{2-})$ vs. x
x
Surface
Total crack length
Region of diffusion with no initial migration
Region of mature crack
Region of early electrochemical continuum
Region of tight crack

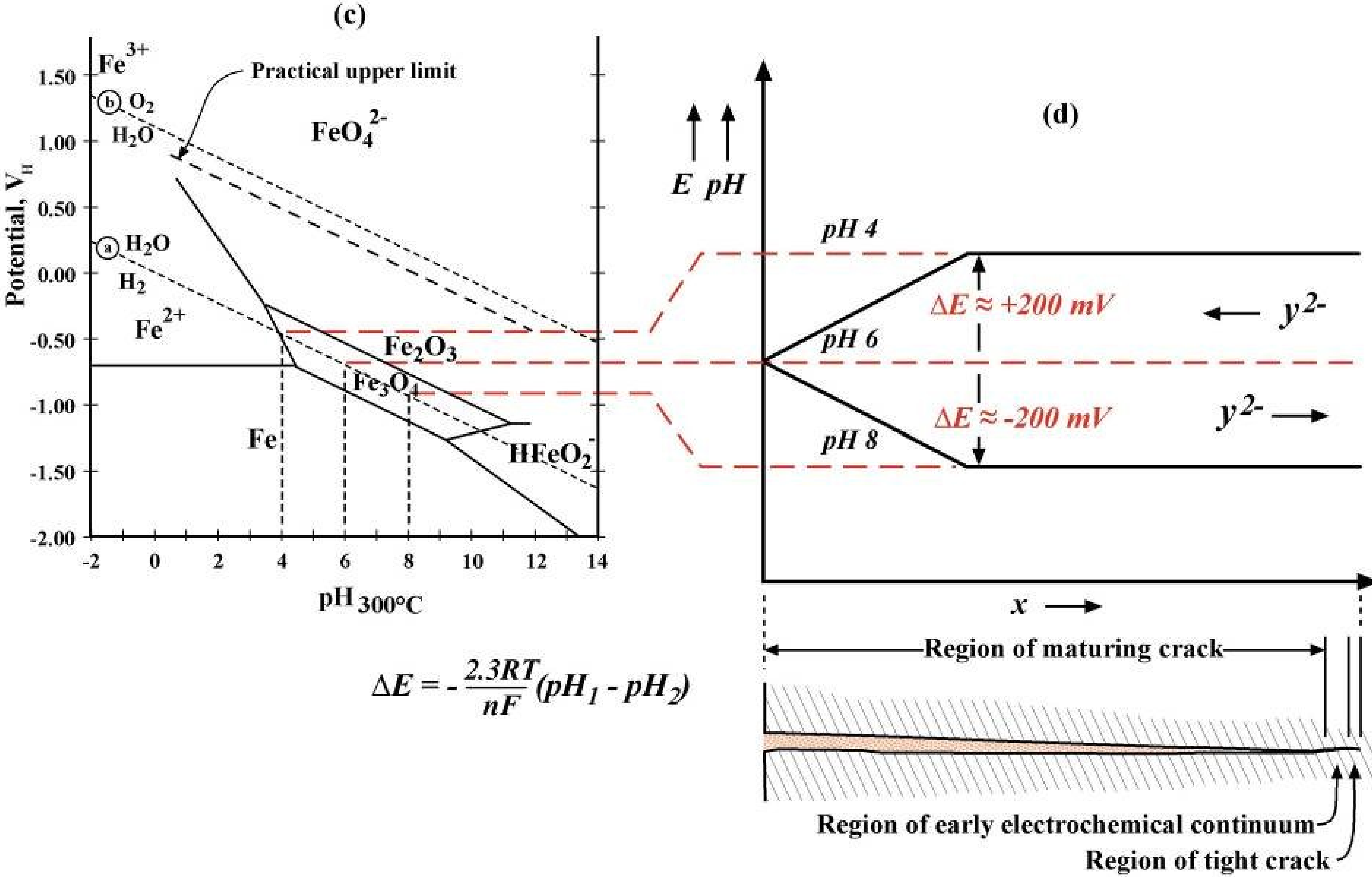
(c)
Practical upper limit
Fe3+
FeO4 2-
O2
H2O
H2O
H2
Fe2+
Fe2O3
Fe3O4
Fe
HFeO2-
Potential, VH
1.50
1.00
0.50
0.00
-0.50
-1.00
-1.50
-2.00
-2
0
2
4
6
8
10
12
14
pH 300°C
ΔE = - 2.3RT/nF (pH1 - pH2)
(d)
E pH
pH 4
pH 6
pH 8
ΔE ≈ +200 mV
ΔE ≈ -200 mV
y2-
y2-
x
Region of maturing crack
Region of early electrochemical continuum
Region of tight crack

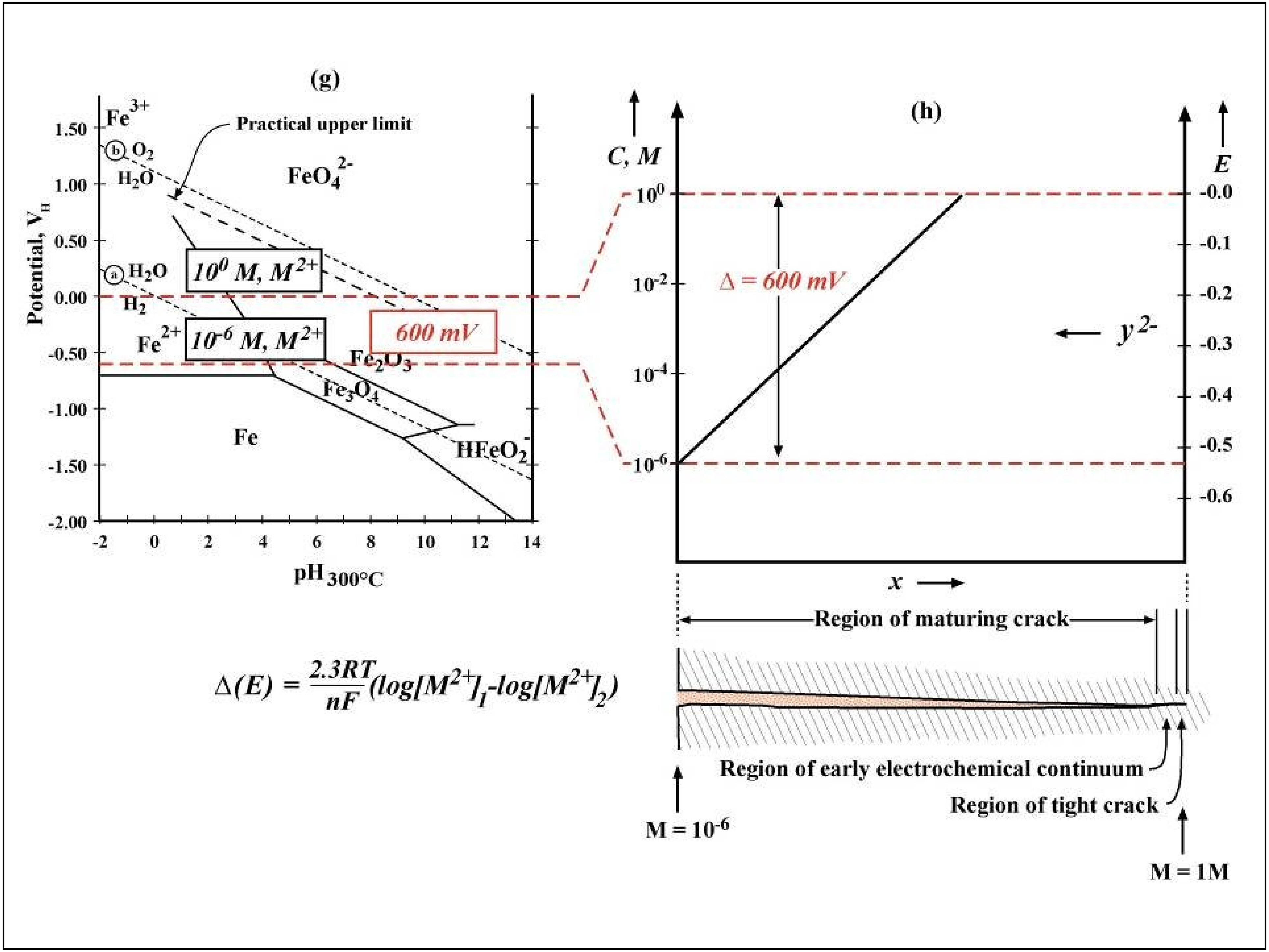

(g)
Fe3+
Practical upper limit
b O2
H2O
FeO4 2-
a H2O
H2
10^0 M, M2+
10^-6 M, M2+
Fe2+
600 mV
Fe2O3
Fe3O4
Fe
HFeO2-
Potential, VH
1.50
1.00
0.50
0.00
-0.50
-1.00
-1.50
-2.00
-2
0
2
4
6
8
10
12
14
pH 300°C
Δ(E) = 2.3RT/nF (log[M2+]1-log[M2+]2)
(h)
C, M
E
10^0
10^-2
10^-4
10^-6
Δ = 600 mV
y2-
-0.0
-0.1
-0.2
-0.3
-0.4
-0.5
-0.6
x
Region of maturing crack
Region of early electrochemical continuum
Region of tight crack
M = 10^-6
M = 1M

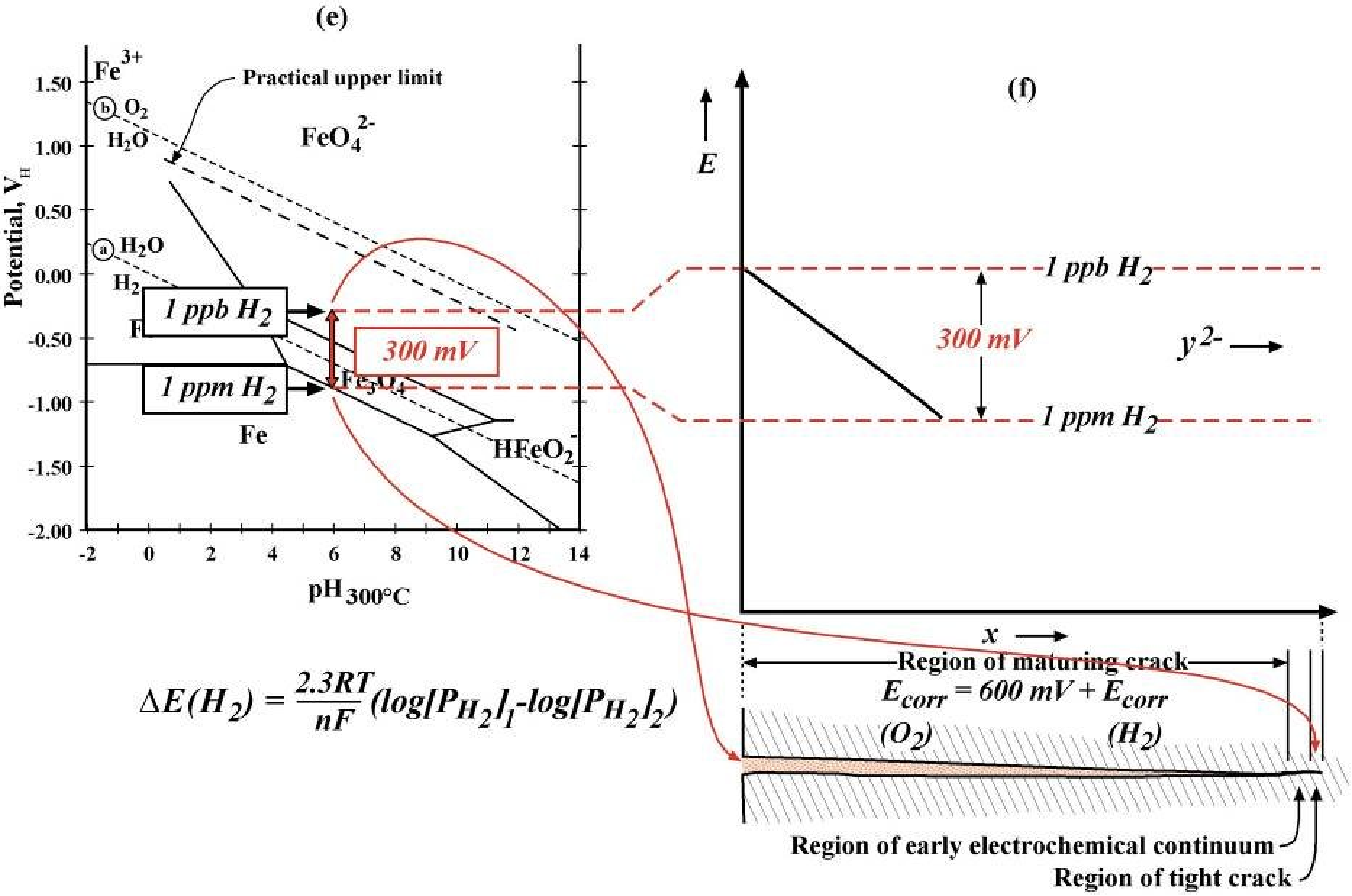

$$\Delta E(H_2) = \frac{2.3RT}{nF}(\log[P_{H_2}]_1 - \log[P_{H_2}]_2)$$

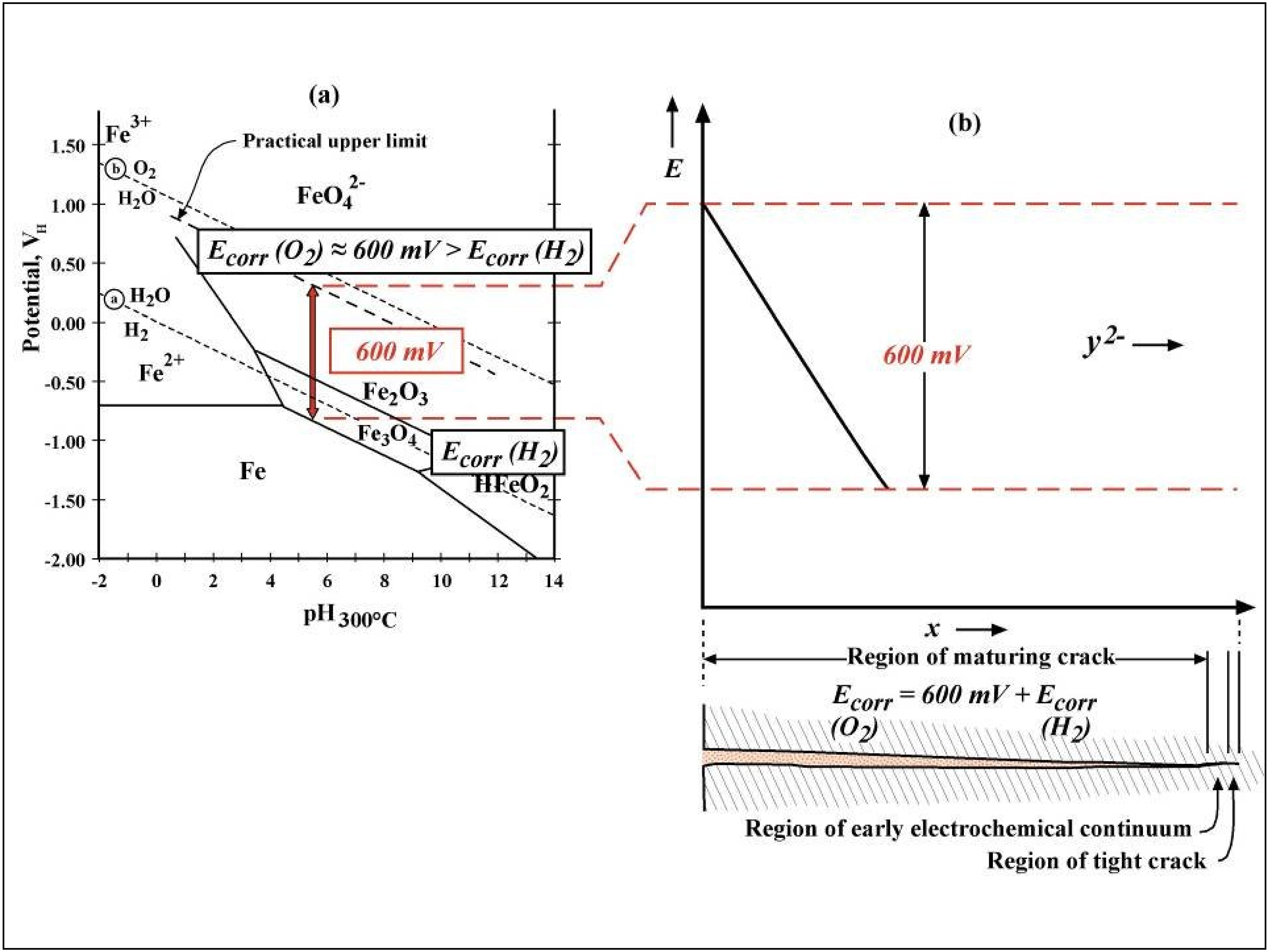
(a)
Practical upper limit
Potential, V_H
1.50
1.00
0.50
0.00
-0.50
-1.00
-1.50
-2.00
-2
0
2
4
6
8
10
12
14
$pH_{300°C}$
Fe^{3+}
O_2
H_2O
FeO_4^{2-}
H_2O
H_2
Fe^{2+}
$E_{corr}\,(O_2) \approx 600\ mV > E_{corr}\,(H_2)$
600 mV
Fe_2O_3
Fe_3O_4
$E_{corr}\,(H_2)$
$HFeO_2^-$
Fe
(b)
E
600 mV
y^{2-}
x
Region of maturing crack
$E_{corr}\,(O_2) = 600\ mV + E_{corr}\,(H_2)$
Region of early electrochemical continuum
Region of tight crack

Tight Cracks

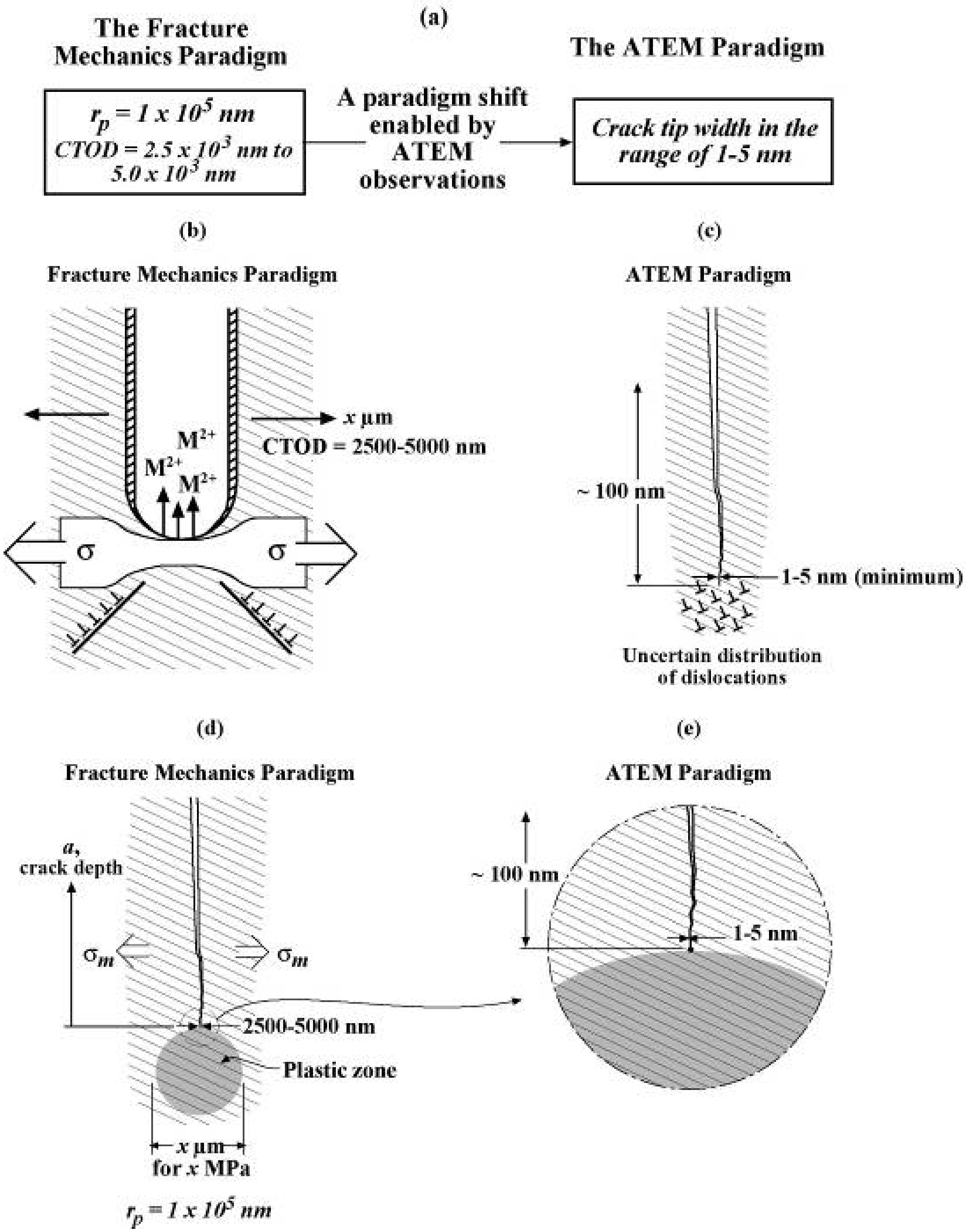
(a)
The Fracture Mechanics Paradigm
$r_p = 1 \times 10^5$ nm
CTOD = 2.5×10^3 nm to 5.0×10^3 nm
A paradigm shift enabled by ATEM observations
The ATEM Paradigm
Crack tip width in the range of 1-5 nm
(b)
Fracture Mechanics Paradigm
x µm
CTOD = 2500-5000 nm
M^{2+}
M^{2+}
M^{2+}
σ
σ
(c)
ATEM Paradigm
~ 100 nm
1-5 nm (minimum)
Uncertain distribution of dislocations
(d)
Fracture Mechanics Paradigm
a, crack depth
σ_m
σ_m
2500-5000 nm
Plastic zone
x µm for x MPa
$r_p = 1 \times 10^5$ nm
(e)
ATEM Paradigm
~ 100 nm
1-5 nm

Meanings of 1 nm width of SCC crack tip

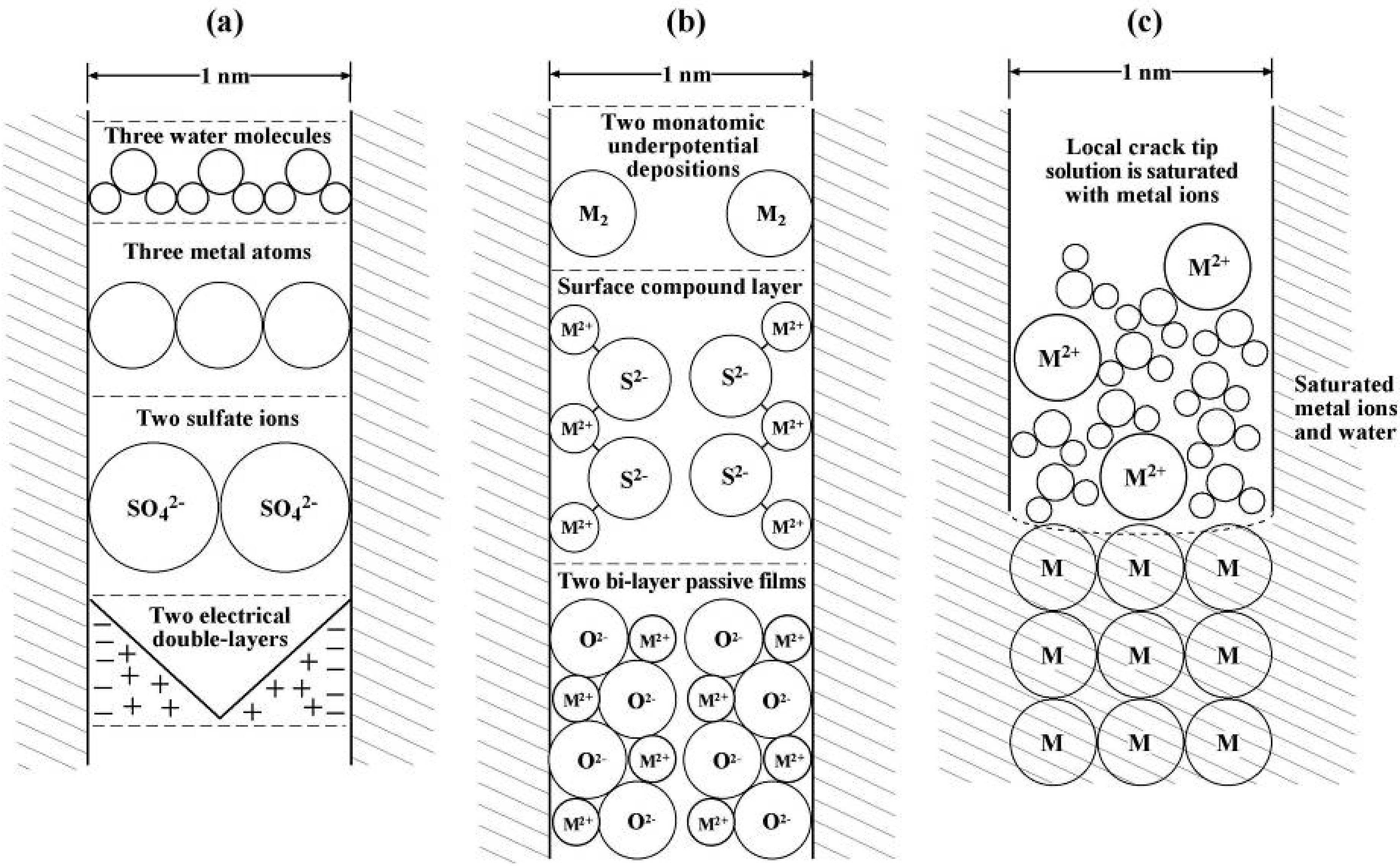

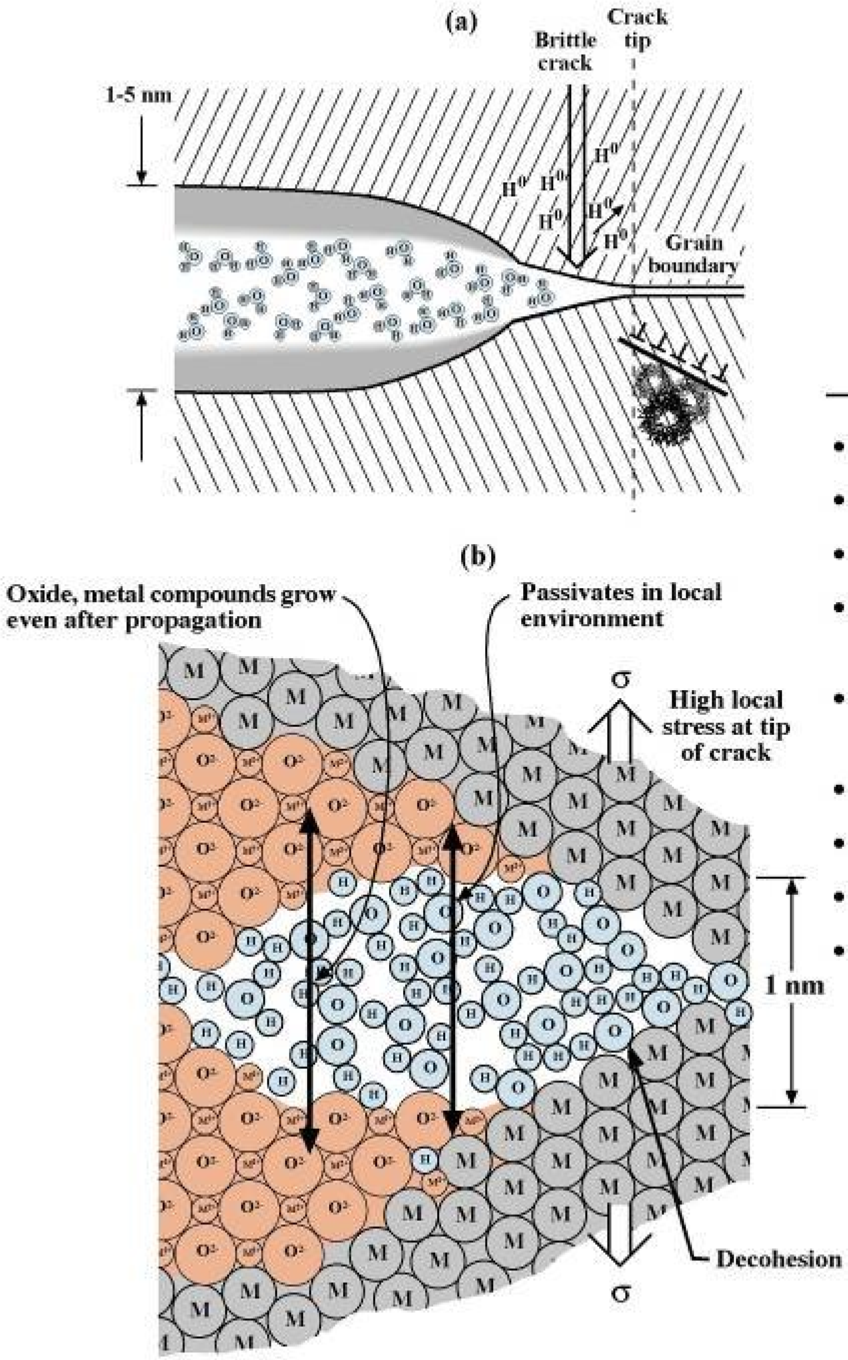

(c)

Apparent Options for Crack Advance

- Surface energy lowering embrittles
- Brittle films due to dealloying
- Oxygen diffusion in grain boundary
- Hydrogen facilitates movement of dislocations which causes barriers to fail
- Cold-work embrittled layer at edge of plastic zone–further embrittled by hydrogen
- Vacancy from dissolution produce crack nucleus
- Brittleness due to surface-film formation
- Film break and repassivation
- Film thinning and increased reactivity

Primary and Secondary Deposits

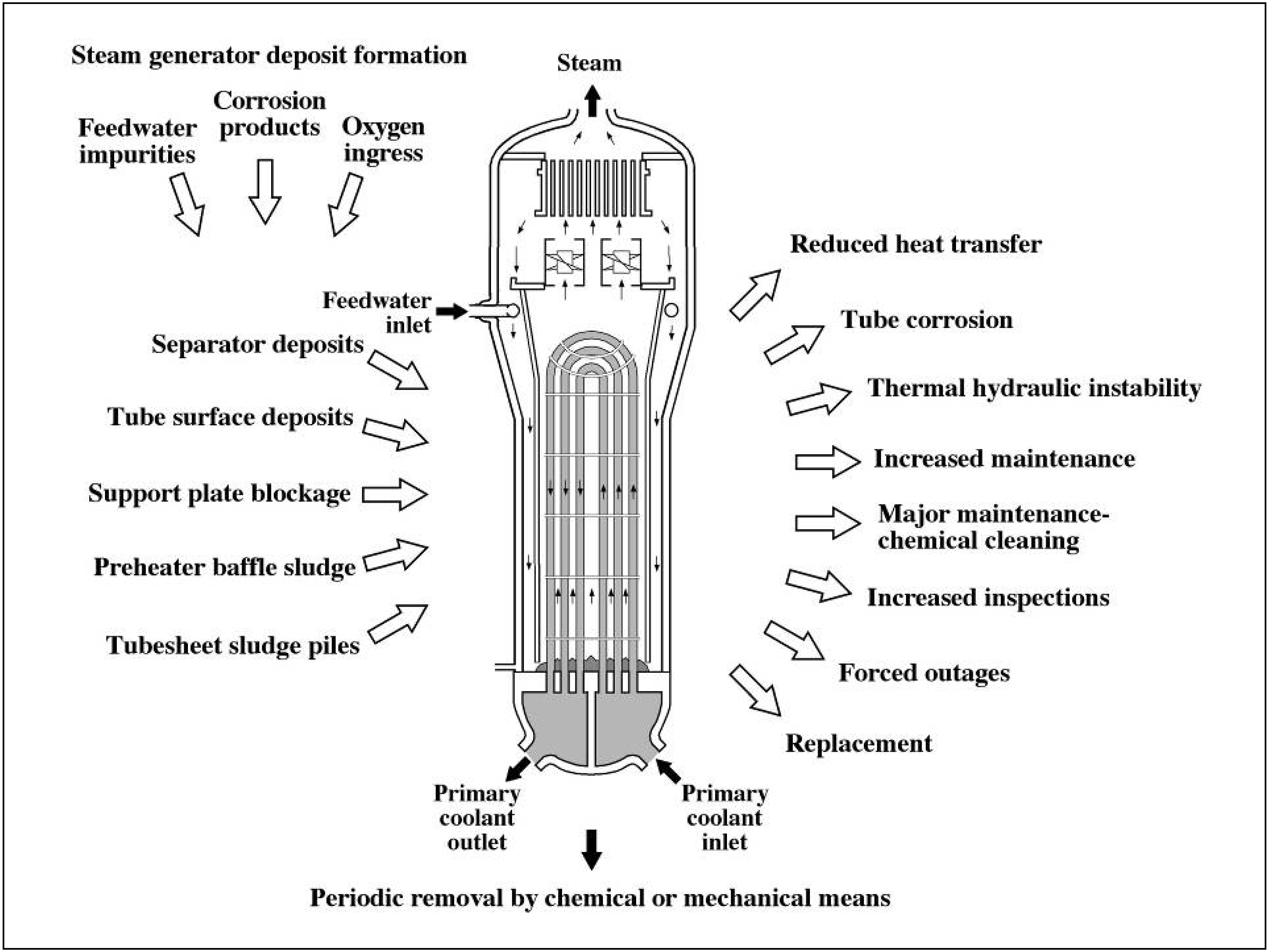

Steam generator deposit formation
Feedwater impurities
Corrosion products
Oxygen ingress
Steam
Feedwater inlet
Separator deposits
Tube surface deposits
Support plate blockage
Preheater baffle sludge
Tubesheet sludge piles
Reduced heat transfer
Tube corrosion
Thermal hydraulic instability
Increased maintenance
Major maintenance-chemical cleaning
Increased inspections
Forced outages
Replacement
Primary coolant outlet
Primary coolant inlet
Periodic removal by chemical or mechanical means

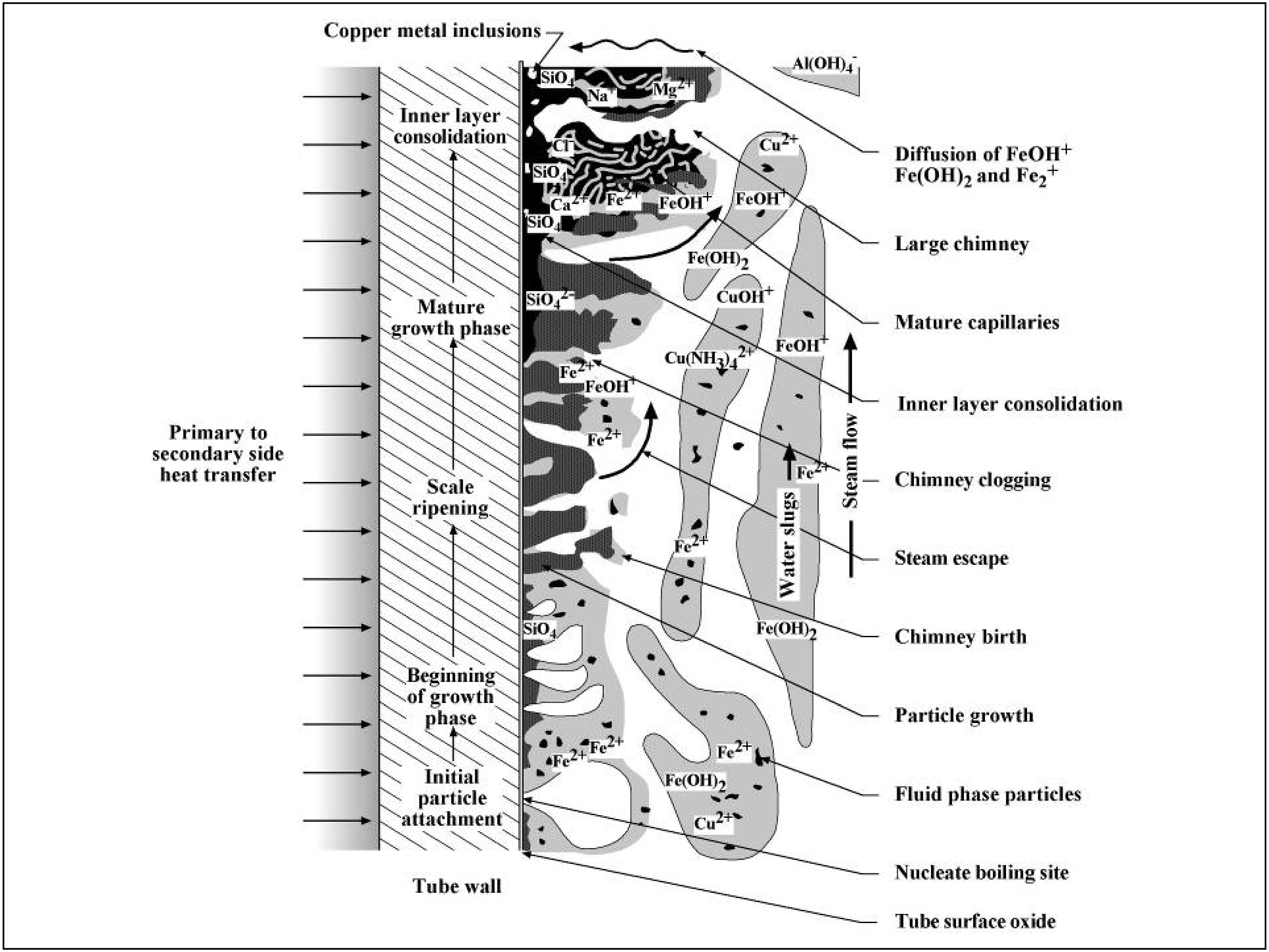
Copper metal inclusions
Al(OH)4-
SiO4
Na+
Mg2+
Inner layer consolidation
Cl-
SiO4
Cu2+
Ca2+
Fe2+
FeOH+
FeOH+
SiO4
Diffusion of FeOH+ Fe(OH)2 and Fe2+
Large chimney
Fe(OH)2
Mature growth phase
SiO4 2-
CuOH+
Mature capillaries
FeOH+
Cu(NH3)4 2+
Fe2+
FeOH+
Inner layer consolidation
Primary to secondary side heat transfer
Fe2+
Steam flow
Fe2+
Chimney clogging
Scale ripening
Water slugs
Fe2+
Steam escape
Chimney birth
SiO4
Fe(OH)2
Beginning of growth phase
Particle growth
Fe2+
Fe2+
Fe2+
Fluid phase particles
Initial particle attachment
Fe(OH)2
Cu2+
Nucleate boiling site
Tube wall
Tube surface oxide

Deposits on fuel and acceleration of oxide growth and perforation

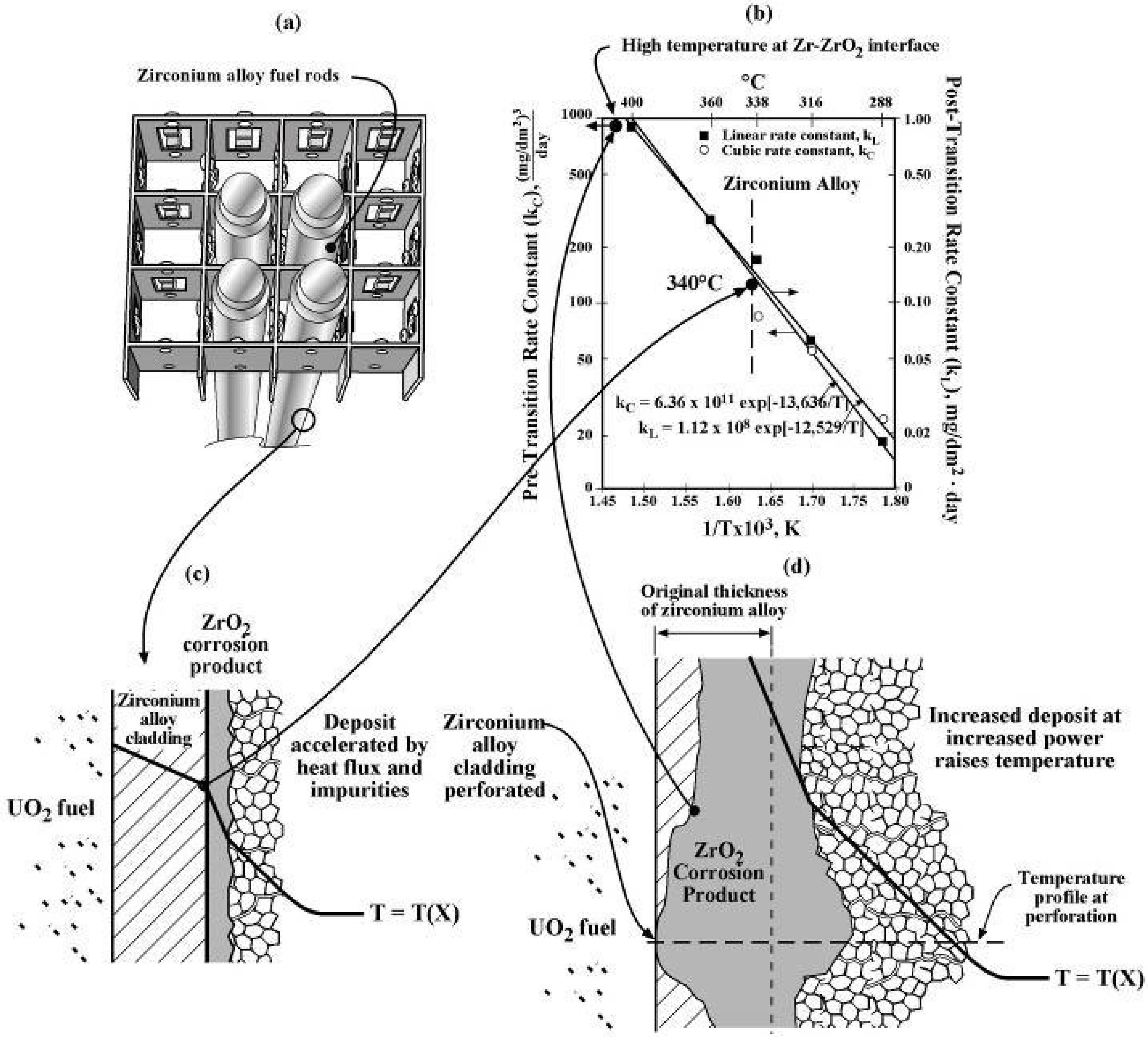

Deposits containing boron on fuel surfaces: produces local variations in neutron flux.

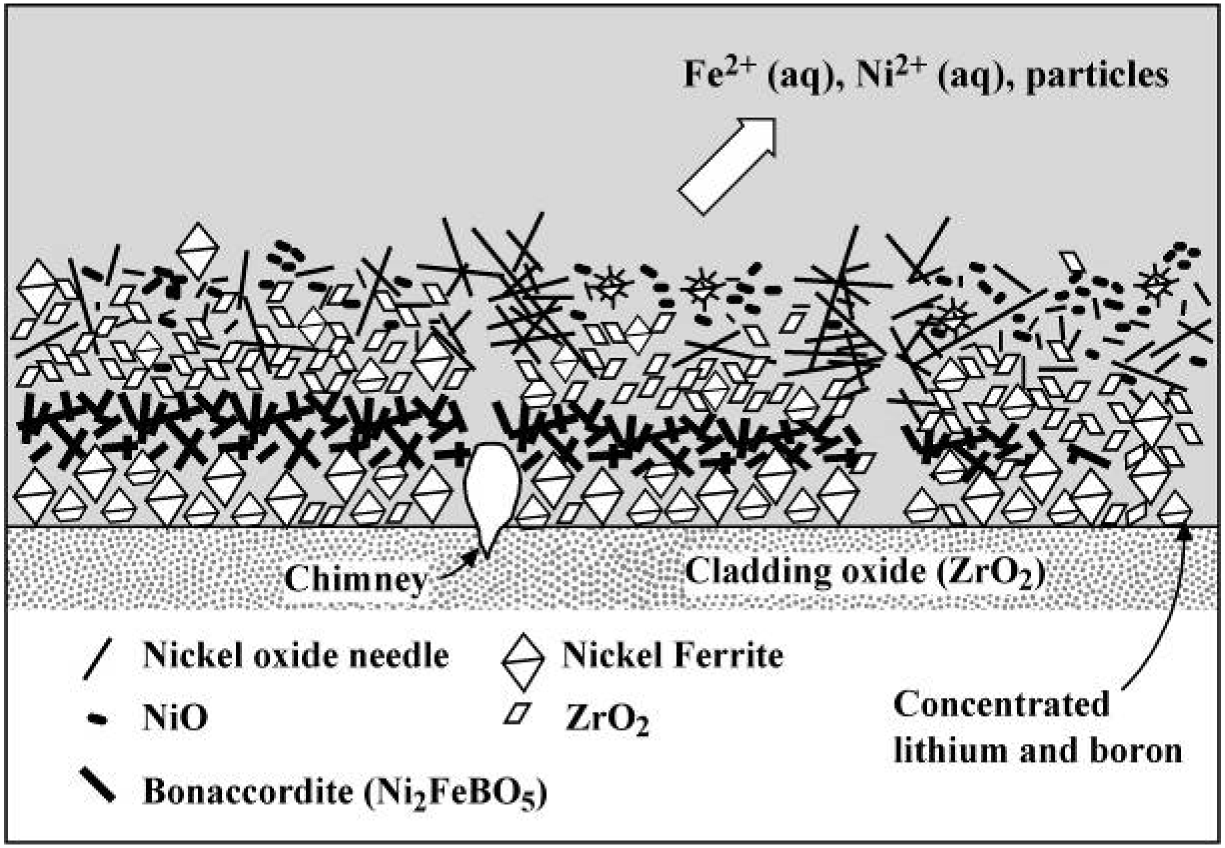

Deposit formed on fuel surfaces including boron to give "axial offset anamoly"

from Byers

Surface Mechanical Reactions Depend on Potential

Kinetics of film breaking and repassivation

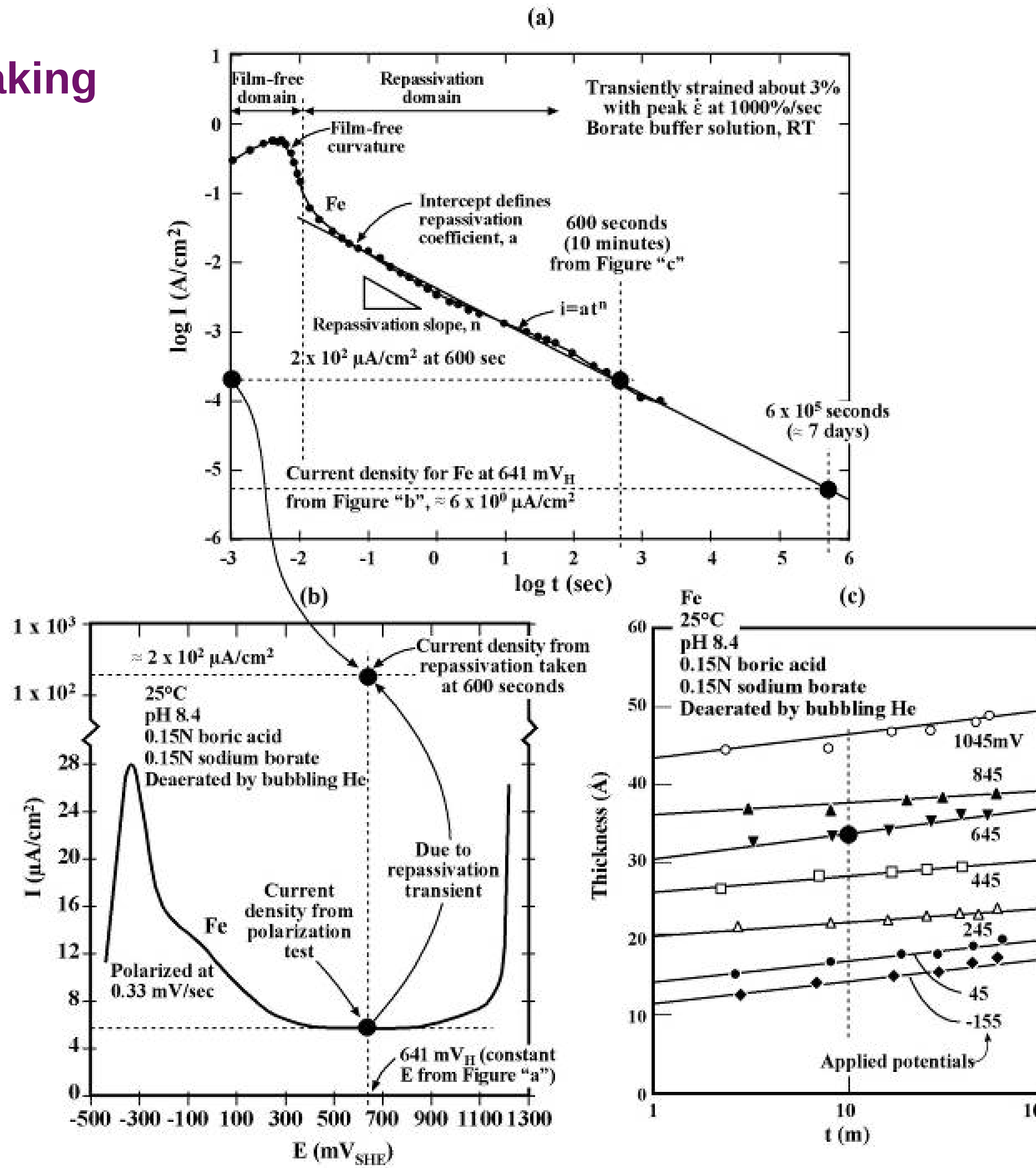

Dislocations at films: surface slip interacts with electrochemical state

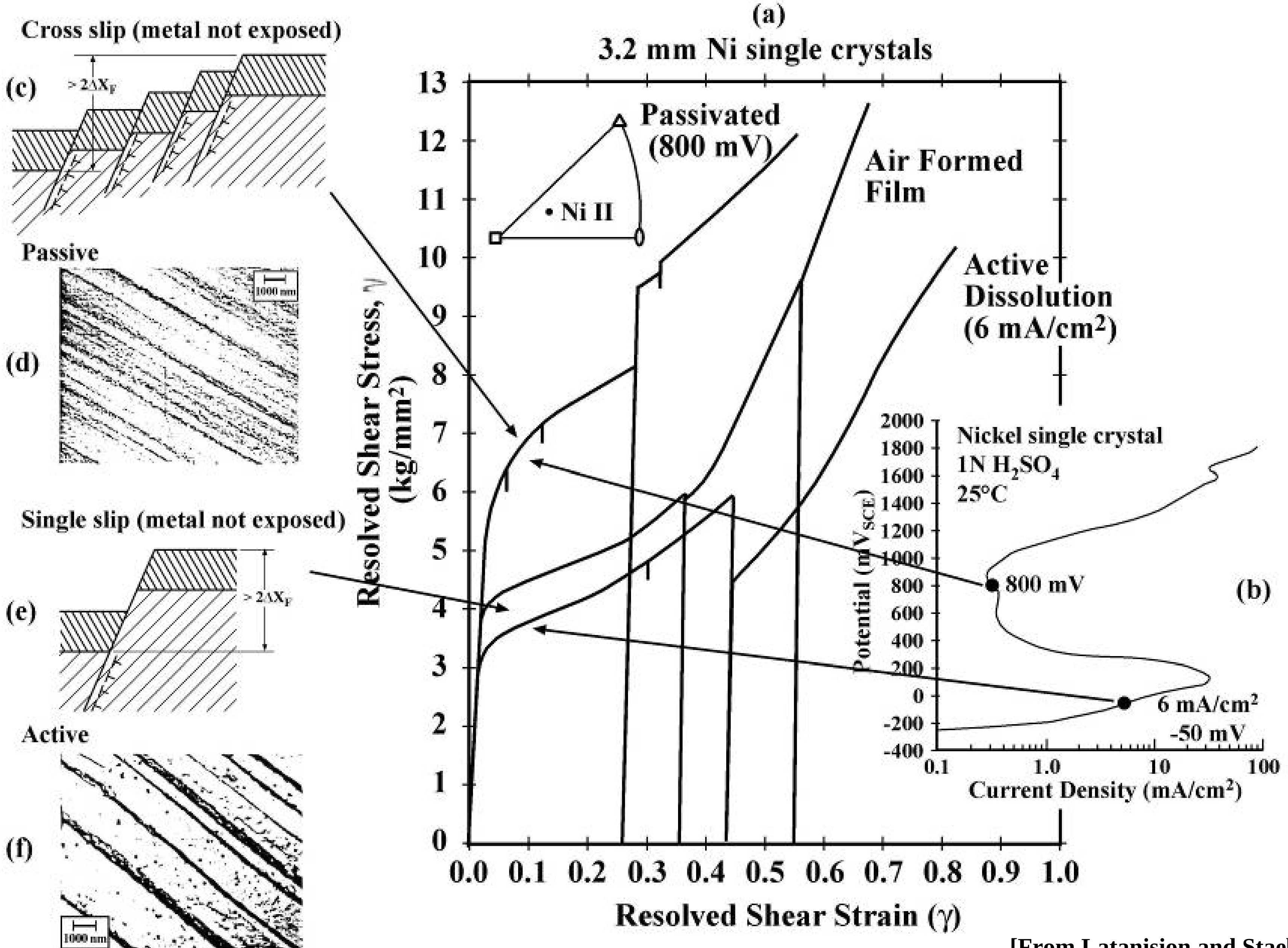

[From Latanision and Staehle]

SCC in Carbon and Low Alloy Steels Depend on Potential

SCC of LAS

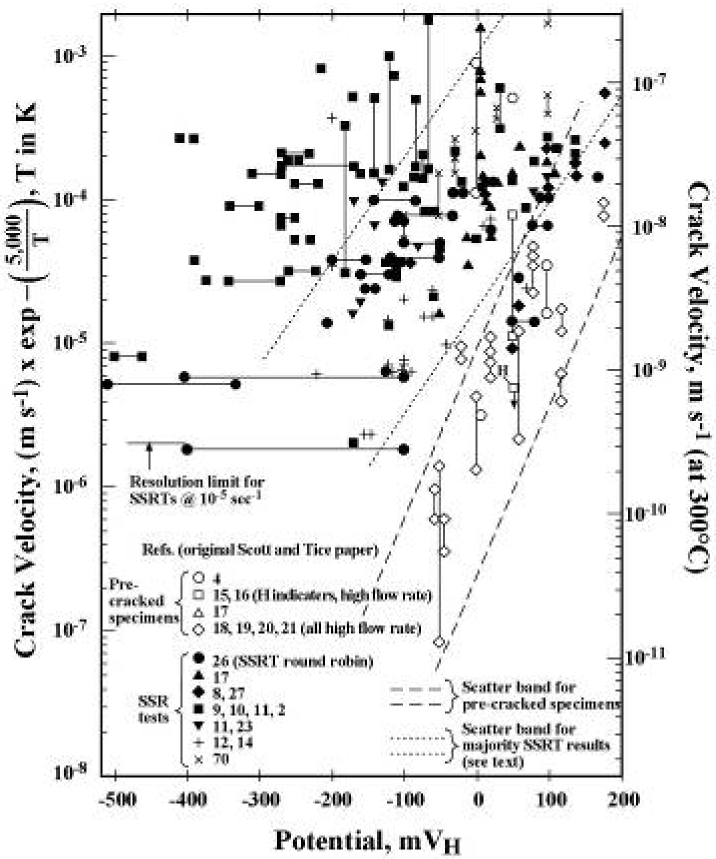

From Scott and Tice

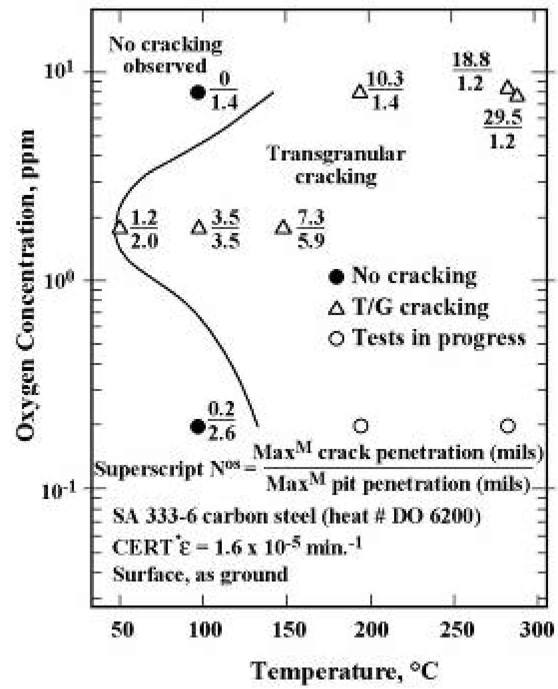

From Kowaka

(f)

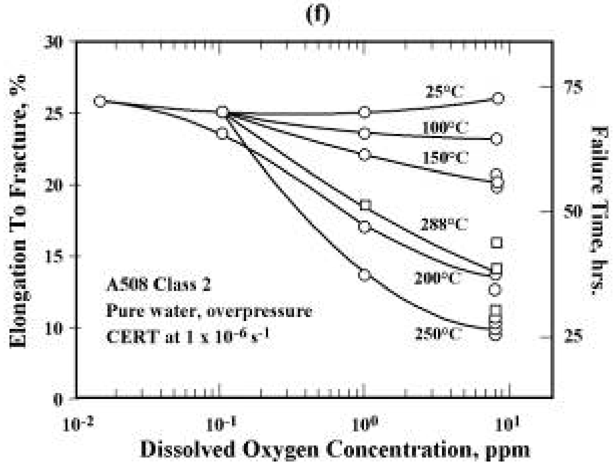

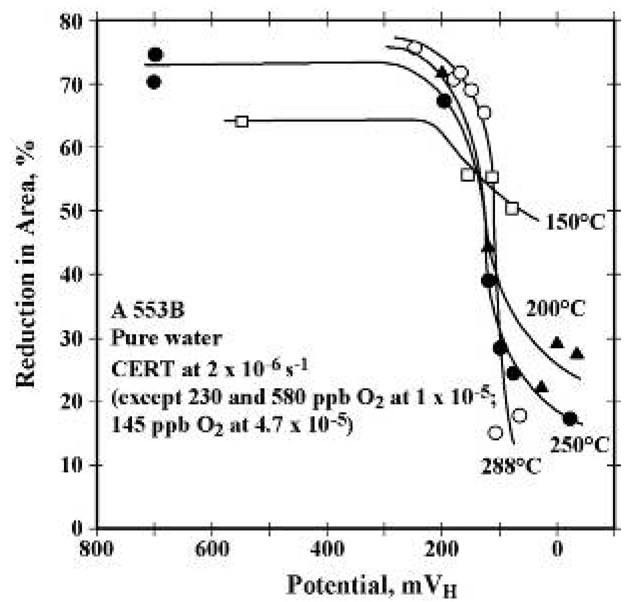

SCC of LAS

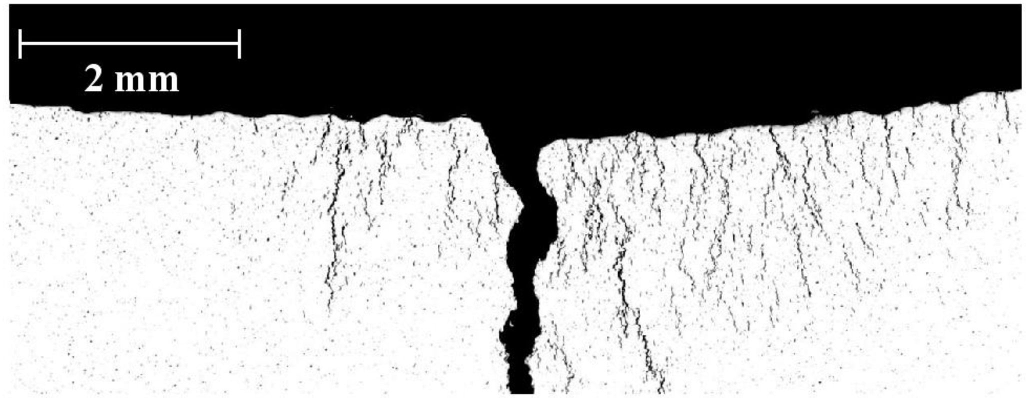

SCC of LAS feeder tube
at Pt. LePreau

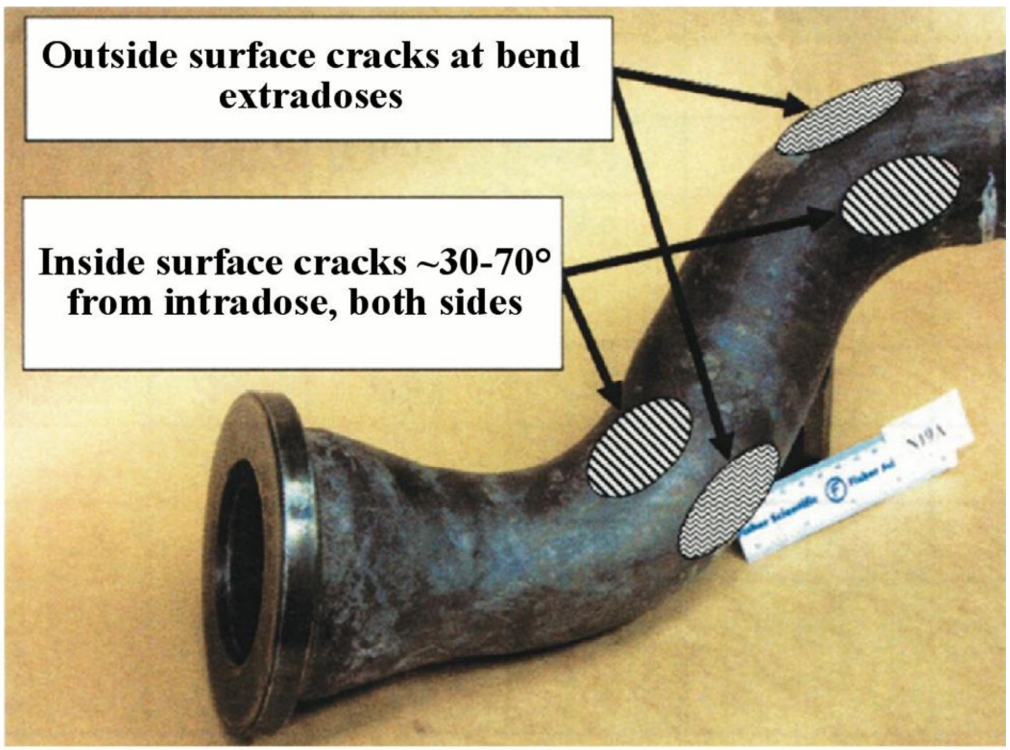

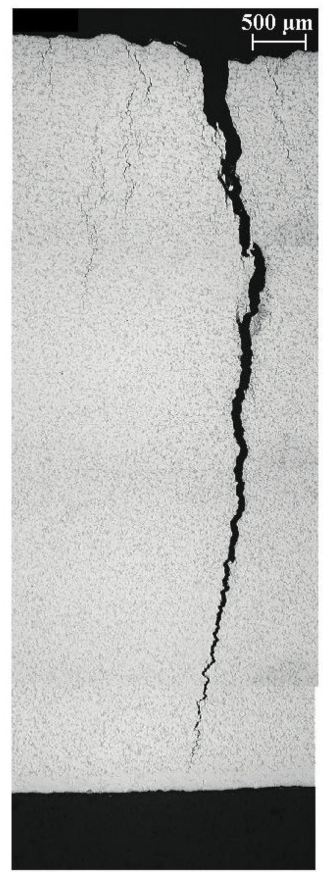

Inside surface

Cheek crack
Outside surface

From Wright

Creep

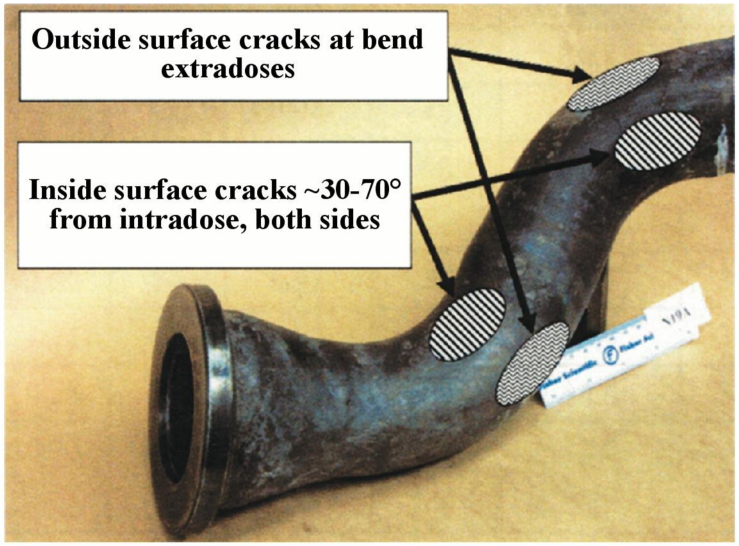

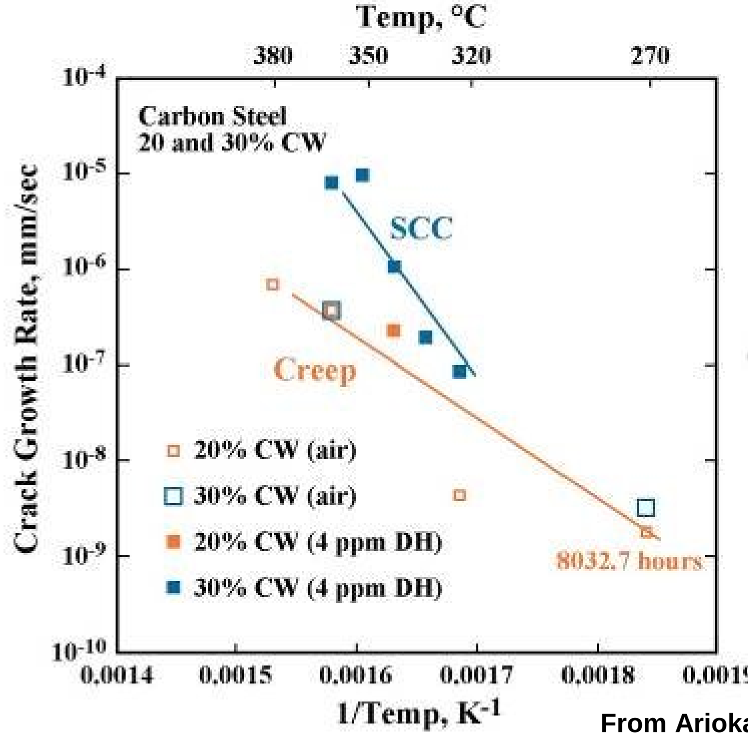

Crack growth rate vs. temperature for creep and SCC for carbon steel

From Arioka

Creep crack from outside surface in feeder tube at Pt Lepreau

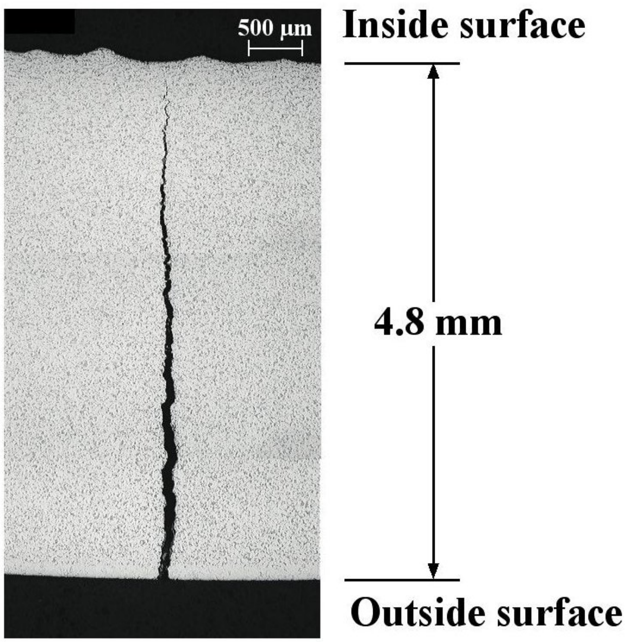

Extrados crack

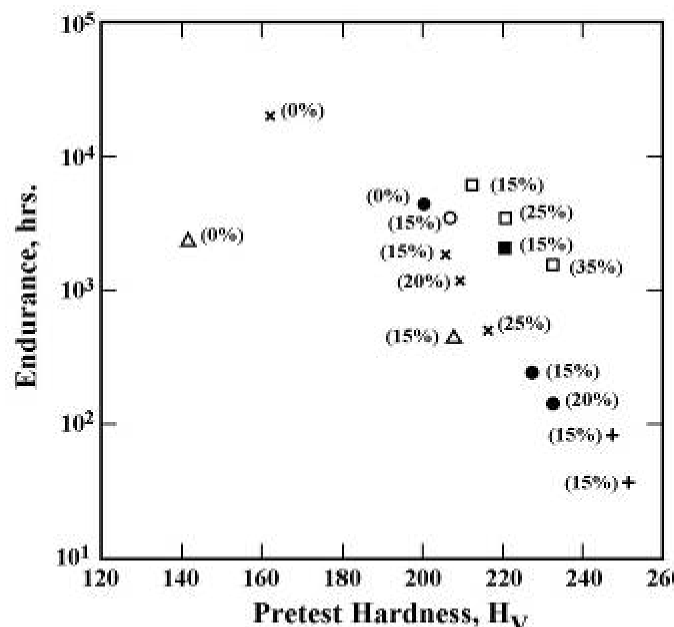

Endurance vs. pretest hardness

from Shibli

Expanding corrosion products

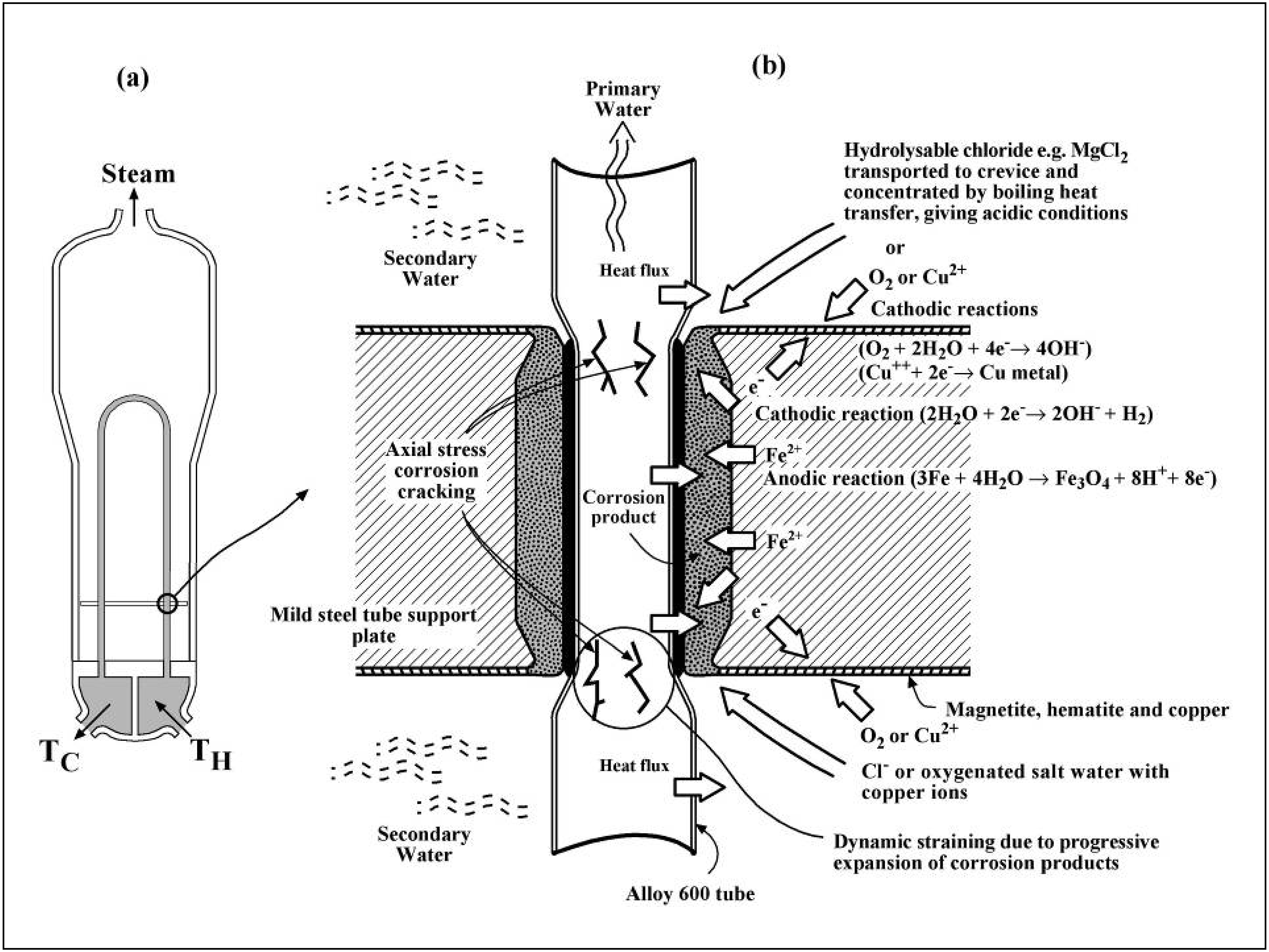

(a)
Steam
T_C
T_H
(b)
Primary Water
Secondary Water
Heat flux
Hydrolysable chloride e.g. $MgCl_2$ transported to crevice and concentrated by boiling heat transfer, giving acidic conditions
or
O_2 or Cu^{2+}
Cathodic reactions
($O_2 + 2H_2O + 4e^- \rightarrow 4OH^-$)
($Cu^{++} + 2e^- \rightarrow$ Cu metal)
e^-
Cathodic reaction ($2H_2O + 2e^- \rightarrow 2OH^- + H_2$)
Fe^{2+}
Anodic reaction ($3Fe + 4H_2O \rightarrow Fe_3O_4 + 8H^+ + 8e^-$)
Axial stress corrosion cracking
Corrosion product
Fe^{2+}
Mild steel tube support plate
e^-
Magnetite, hematite and copper
O_2 or Cu^{2+}
Heat flux
Cl^- or oxygenated salt water with copper ions
Secondary Water
Dynamic straining due to progressive expansion of corrosion products
Alloy 600 tube

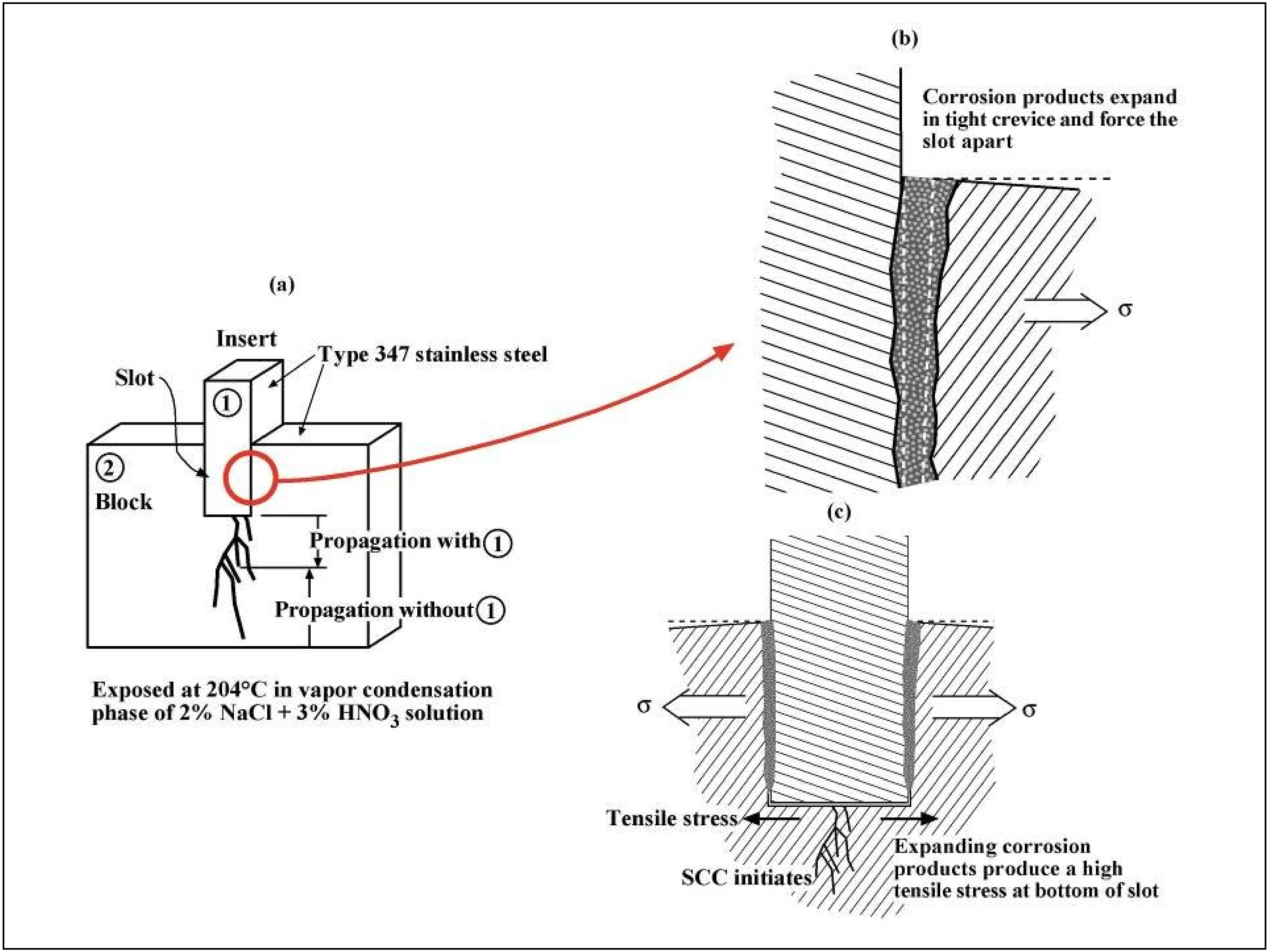
(a)
Insert
Type 347 stainless steel
Slot
1
2
Block
Propagation with 1
Propagation without 1
Exposed at 204°C in vapor condensation phase of 2% NaCl + 3% HNO_3 solution
(b)
Corrosion products expand in tight crevice and force the slot apart
σ
(c)
σ
σ
Tensile stress
SCC initiates
Expanding corrosion products produce a high tensile stress at bottom of slot

SCC in RPV Welds and Boric Acid Concentrated

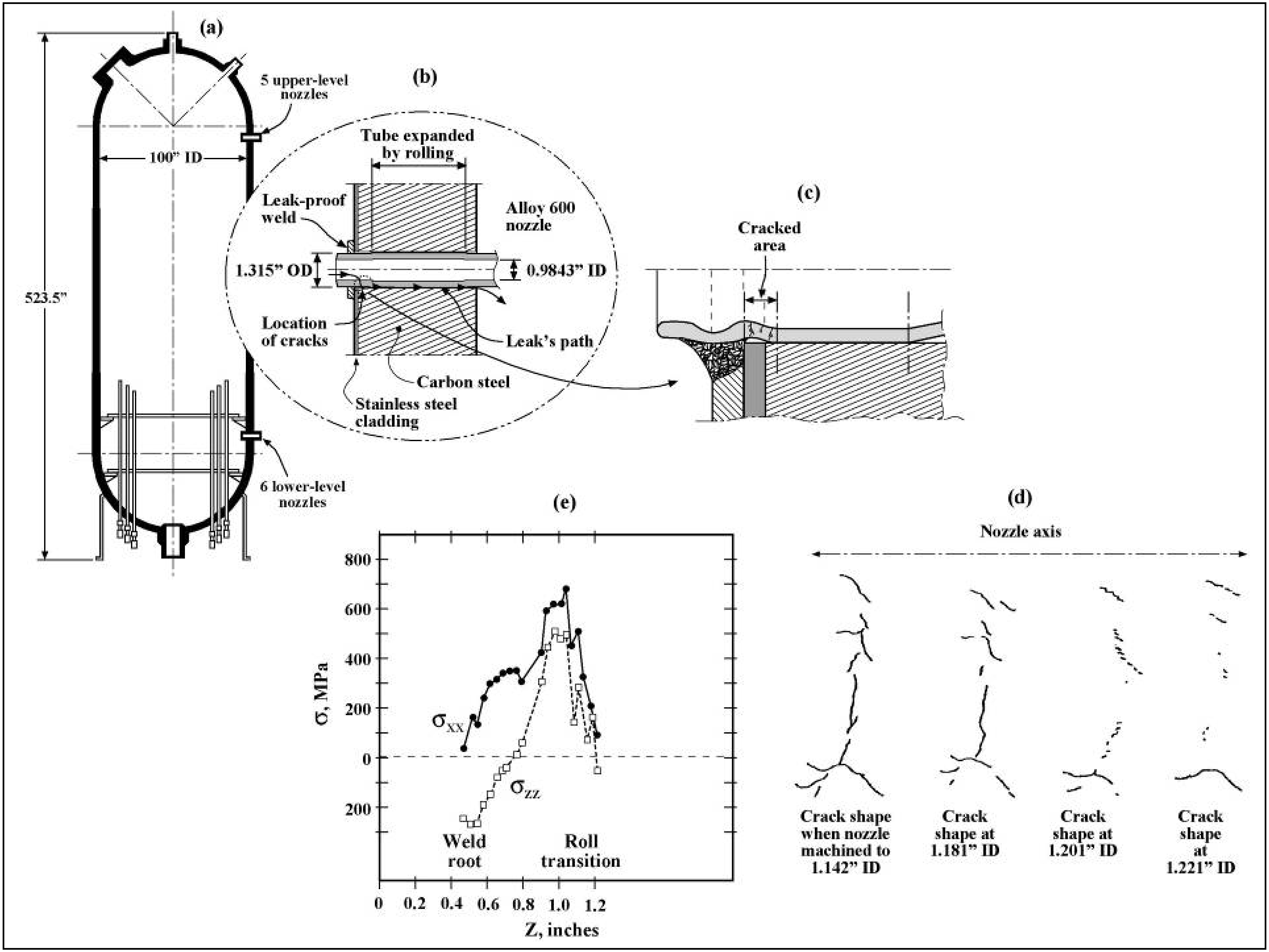

(a)
5 upper-level nozzles
100" ID
523.5"
6 lower-level nozzles
(b)
Tube expanded by rolling
Leak-proof weld
Alloy 600 nozzle
1.315" OD
0.9843" ID
Location of cracks
Leak's path
Carbon steel
Stainless steel cladding
(c)
Cracked area
(e)
σ, MPa
800
600
400
200
0
200
σXX
σZZ
Weld root
Roll transition
0
0.2
0.4
0.6
0.8
1.0
1.2
Z, inches
(d)
Nozzle axis
Crack shape when nozzle machined to 1.142" ID
Crack shape at 1.181" ID
Crack shape at 1.201" ID
Crack shape at 1.221" ID

(a)
Oconee, Unit 1

(b)
Oconee, Unit 3

(c)
Houston Light & Power, Unit 1

(d)
Houston Light & Power, Unit 1

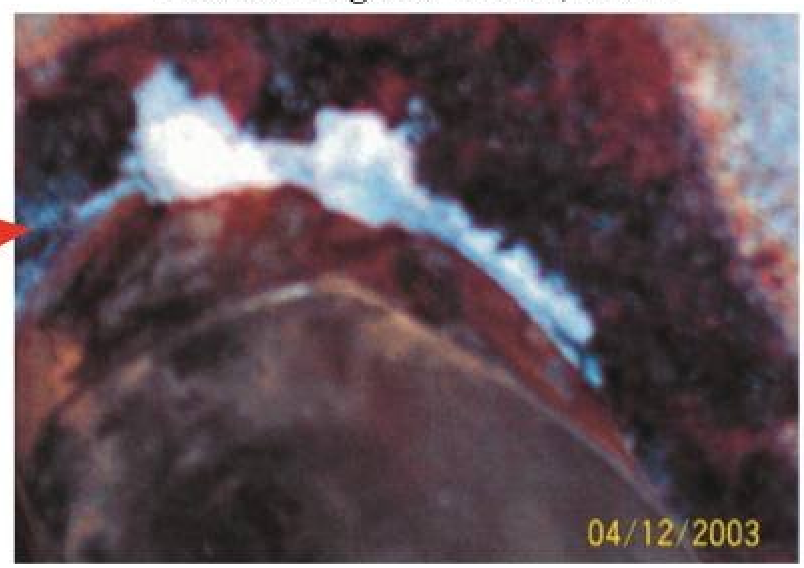

Conclusions

1. pH and potential dominate the corrosion behavior of metals in LWR systems.

2. Findings based on pH and potential provide the best means for predicting and assuring the reliable behavior of metals in nuclear plants.

3. Experimental work based on frameworks of potential and pH have the most credible bases for correlations with findings in operating plants where such measurements have also been taken. Also, such frameworks provide credible bases for comparing with experiments among the world laboratories.

4. Considerations of materials of constructions as chemicals should be compared with configurational designs with equal emphasis to provide the most credible bases for assuring reliable performance.

References

1. **The two major references by Pourbaix, his Atlas and his Lectures, provide the most coherent and useful references for beginners and for mature professionals to understand the thermodynamic bases for the discussions in this presentation.**

2. **The text by Kaesche, translated into English by Rapp, is the best text for understanding the kinetics of corrosion processes. Most others are severely deficient.**

3. **The best overall text for understanding the electrochemistry in aqueous solutions is the most recent one by Bockris and co-workers.**

4. **The best engineering text on corrosion engineering is the most recent one by Fontana.**

5. **Useful texts on the properties of compounds produced in corrosion are found in the geochemical literature.**